Formulation and Analysis of an Optimization-Based Atomistic-to-Continuum Coupling Algorithm

A THESIS
SUBMITTED TO THE FACULTY OF THE GRADUATE SCHOOL
OF THE UNIVERSITY OF MINNESOTA
BY

Derek Olson

IN PARTIAL FULFILLMENT OF THE REQUIREMENTS
FOR THE DEGREE OF
Doctor of Philosophy

Mitchell Luskin

September, 2015

Acknowledgements

I have had the great fortune of working with many amazing people over the past five years. My deepest thanks go to my advisor, Mitchell Luskin, who invited me to his group meetings on my first day of orientation and has whisked me off to many exotic conference locations. He has imparted much mathematical wisdom and professional guidance upon me.

I am indebted to Pavel Bochev for having me as an intern at Sandia National labs over four years ago and introducing me to the idea of optimization-based coupling algorithms. It has been privilege working with him. I thank Christoph Ortner for hosting me on a visit to Warwick and giving me many new insights into the world of atomistic-to-continuum coupling. I thank Xingji Li for her patience working with me over the last couple years and for graciously inviting me to visit her at Brown. Special thanks are also reserved for my committee members, Professors Daniel Spirn, Bernardo Cockburn, and Yoichiro Mori for taking the time be on my committee.

This thesis would not be possible without the efforts and contributions of Alexander Shapeev who was gracious enough to share many of his ideas with me and take the time to meet with me whenever asked. I have thoroughly enjoyed all of our discussions (mathematical or not) and learned a tremendous amount from him.

Finally, I would like to acknowledge my fellow graduate students for making Minnesota such a pleasure to be at. In particular, the many games of trivial pursuit shared with Joe Benson and Denis Bashkirov will be a lasting memory.

Much of Chapters 4 and 5 has been accepted for publication as [48]. The numerical algorithm of Chapter 6 has been published in [47]. This was joint work with Alexander Shapeev, Pavel Bochev, and Mitchell Luskin. The idea of using equivalence classes in Chapters 4 and 5 is due to Alex as is the idea of using a proof by contradiction to prove

the norm equivalence in Chapter 5. Alex also helped simplify the proof of Lemma 5.4.7. The original idea of an optimization-based atomistic-to-continuum coupling algorithm was due to Pavel, and I developed this into the virtual control framework/algorithm discussed in this thesis.

Dedication

To my family and friends, especially my mother.

Abstract

Atomistic-to-continuum (AtC) methods are multiphysics models of materials used to simulate atomistic systems on a size scale unreachable on even the largest modern computers. A cornucopia of AtC algorithms has been designed and implemented, but the core feature among them is the decomposition of the computational domain into an atomistic region modeled using an atomistic model and a continuum region modeled according to some continuum mechanics formulation such as nonlinear elasticity. Though much information can be gleaned from the individual atomistic and continuum models, the mathematical analysis of the errors involved in the coupled approximations are just now beginning to be understood. Such an analysis is vital to both guide the choice of AtC method and optimize its efficiency.

A convenient model problem for comparing the errors of various AtC methods has been simulating a single defect embedded in an infinite crystalline environment in Euclidean space [36, 42]. This allows the error to be generically decomposed into a far-field error resulting from truncating the problem to a finite domain, a coarsening error due to efficiently solving the continuum problem (e.g. using finite elements), and a coupling error arising from coupling the two models.

This work presents the optimization-based AtC algorithm of [48] in the context of a point defect in an infinite lattice and provides error estimates for the three aforementioned errors in two and three dimensions. The method relies on overlapping atomistic and continuum regions with individual atomistic and continuum subproblems. These two problems are coupled together using a virtual control technique originally developed in [26] to couple advection-diffusion PDEs. A cost functional consisting of the H^1 seminorm of the difference between atomistic and continuum states is minimized subject to the constraints that the atomistic and continuum equilibrium equations hold on each subdomain.

Contents

List of Tables

List of Figures

Chapter 1

Introduction

Atomistic-to-continuum (AtC) methods are a class of multiphysics solvers of increasing use in physics and engineering designed to overcome the computational intractability of atomistic (molecular statics or molecular dynamics) simulations. These methods are ideally suited for determining the effects that *defects* have on the mechanical and electrical properties of crystalline materials because defects cause both highly localized stress and strain fields near the defect, which cannot be captured by traditional continuum theories, and long range elastic fields which, on the other hand, can be modeled extremely efficiently and accurately by continuum theories such as elasticity or plasticity [49,63]. The goal of atomistic-to-continuum coupling is then to combine the accuracy of the atomistic model with the efficiency of a continuum model suitably discretized by a numerical method. Very generically, this is accomplished by dividing the computational domain, Ω, into an atomistic domain, Ω_{a}, where the atomistic model is used, and a continuum domain, Ω_{c}, where the continuum model is employed. The central issues of how to *couple* the two models and choose the domains and discretization in an optimal manner have sparked the interests of engineers, physicists, and material scientists seeking to model new phenomena and new materials and mathematicians seeking to understand and quantify the errors committed in the coupling.

This thesis is devoted to the development of a new, optimization-based atomistic-to-continuum coupling and a thorough numerical analysis of the errors involved. The method is defined by selecting overlapping atomistic and continuum regions with individual atomistic and continuum subproblems posed on each subdomain. These two

problems are coupled by minimizing a "mismatch" energy (defined as the H^1 seminorm of the difference between atomistic and continuum states) subject to the constraints that the atomistic and continuum equilibrium equations hold on each subdomain. We introduce the optimization-based AtC algorithm using virtual controls in the terminology of [26]. This is based on the author's work [46–48] and was one of the first two AtC methods to have a rigorous error estimate established for defects valid in both two and three dimensions [48] for *simple lattices*, or those of the form $\mathsf{F}\mathbb{Z}^d$ where F is a nonsingular $d \times d$ matrix. Specifically, we show that the error can be bounded in terms of the degrees of freedom, and the error is bounded by $(\#\text{DoF})^{-(d/2-1)/2}$ where d is the dimension of the space ($d = 2, 3$).

The history of AtC methods can be traced back all the way to Cauchy in his formulation of the Cauchy-Born rule [11], but the watershed moment in the development of AtC methods was the advent of the quasicontinuum (QC) method [49], which coupled empirical atomistic potentials with the Cauchy-Born rule [8,11], a nonlinear elastic model. The Cauchy-Born rule provided a mechanism to link the atomistic response of a material with the continuum deformation and has been widely used in many AtC methods including the optimization-based approach described herein. Meanwhile, the quasicontinuum method itself is an energy based coupling where a global, hybrid energy is defined as a sum of atomistic and continuum energies, and this energy is then minimized to find local minima corresponding to defect configurations [49]. As pointed out in the original quasicontinuum method [49] and subsequent works [45,51,68,70], the quasicontinuum method and many energy based methods suffered from non-physical forces dubbed "ghost forces." They arise from coupling an inherently local continuum model, whose energy is given by a strain energy density functional at each point, with a nonlocal atomistic model where the energy computation of an atom requires the positions of atoms in a (possibly large) neighborhood of the atom. Moreover, the ghost forces have the drastic effect that in a perfect lattice with no defects and no external forces, the perfect lattice is *no* longer an equilibrium of the QC energy because atoms near the atomistic and continuum interface will relax resulting in a lower energy [22, 49, 68].

Attempting to solve the ghost force problem led to many important new AtC methods, many of which have been thoroughly analyzed in one or two dimensions. Several notable methods are the ghost-force correction method [68], where the ghost forces were

explicitly computed and removed as a dead load; the force-based QC methods [19, 69], where forces were defined on each degree of freedom and then equilibrated; the quasinonlocal (QNL) type methods [22, 38, 54, 58, 67, 70] which took geometry into account to design special energies free of ghost forces; and the blending methods [3–5, 33, 35, 76] which attempt to smoothly blend either energies or forces over a blending region.

Owing to their simplicity to implement, the force based QC methods are among the most popular AtC methods in practice. A standard way to define an AtC method using forces is to compute the forces on atoms in Ω_{a} as if the entire domain is being modeled with an atomistic model and forces on atoms in Ω_c as if the entire domain is being modeled with a continuum model. By design, these methods are often free of ghost forces; however, the stability of these methods is difficult to establish (and may in fact fail) meaning that the linearized operator corresponding to the force-balance equations may not be positive definite even when the Hessian of the fully atomistic energy is positive definite [20, 21]. Moreover, the force fields are provably non-conservative [19], thus precluding the use of any minimization algorithm that requires an energy. To date, there remains no general theory on the stability of purely force-based couplings in more than one dimension.

The quasinonlocal methods operate by creating a third region apart from the atomistic and continuum region typically called the interface region, Ω_I. Atoms in the interface region have a specially assigned energy which is neither purely nonlocal (as in the atomistic region) nor purely local (as in the continuum region) resulting in the name quasinonlocal [70]. However, the design and implementation of these methods is extremely difficult, is often restricted to only one and two dimensional lattices, and includes severe restrictions on the types of interactions allowed between atoms. For example, the original quasinonlocal method [70] is valid only in one dimension while the geometric reconstruction technique [22] is valid in two dimensions but the atomistic and continuum domains must meet in very simple geometries such as a line. The method [59] allows for corners in the interface but only allows atoms to interact with their nearest neighbors (or atoms located closest to themselves). Meanwhile, the recent extension [61] of the geometric reconstruction is notable in that it is valid in three dimension for arbitrary interfaces but requires the numerical solution of a large system of overdetermined nonlinear equations (the original geometric construction required an

analytic solution). A very novel approach is the consistent energy based method of [67]. This, however, is only valid for pairwise interactions between atoms in one and two dimensions. Similarly, the work of [43,66] produces an energy-based method that works in three dimensions but is still limited to pair potentials.

One of the most promising solutions to the ghost force problem of the energy based methods and the stability problem of the force based methods has been the development of the blended methods. The blended energy methods, including [5, 33, 76], rely not on eliminating the ghost forces but instead on smearing the ghost forces out over a blending region to reduce their effects. In these methods, the atomistic and continuum regions are allowed to overlap in a handshake or overlap region, Ω_o, and the goal is to smoothly transition between the atomistic and continuum models. Likewise, in the force-based blending methods [3, 4, 35], the forces are smoothly blended over Ω_o. Recently, the blended force (BQCF) and blended energy (BQCE) quasicontinuum methods have been completely analyzed in two and three dimensions in [37], and this is valid for general finite-range interactions with minimal restrictions on the interface geometry. The BQCE method has also been recently combined with the ghost force correction method [68] to yield a method which may be suitable to the application of multilattices [60].

The idea of the optimization based AtC method, introduced in [46–48], is to couple the atomistic and continuum models via a constrained minimization problem. The objective function to be minimized is the difference between atomistic and continuum states defined over a common overlap region with the constraints being the variational form of the force balance equations on each individual atomistic and continuum subdomain. The norm we use to measure the difference between atomistic and continuum states is the H^1 semi-norm. The origins of the method date to the least squares conjugate gradient algorithms of [28] but were later introduced in the context of virtual controls in [26, 39–41]. Interestingly, the virtual control approach can be applied to a wide variety of coupling problems arising from PDEs or other physical models. Given any two models to be coupled, they rely on formulating individual subproblems on domains that either overlap (as in the AtC case) or simply have a shared boundary. The difference between the solutions to the two subproblems is then minimized over the shared domain of definition subject to the constraints that the subproblems are satisfied. In fact, virtual controls were first used to couple advection-diffusion PDEs where

advection dominated in one domain and diffusion in the other [26]. They have also recently been applied to the coupling of various fluid flow problems [17,18] and coupling a local and nonlocal diffusion model [15]. Finally, virtual controls have also been used in coupling stochastic PDEs [13].

The remainder of this thesis is organized as follows. Chapter 2 describes the problem of the defect embedded in an infinite lattice and the basic assumptions needed for the existence of an atomistic solution. This is followed by the introduction of the Cauchy-Born continuum model in Chapter 3. Each of these contains necessary background material to provide a well-posed formulation of the optimization-based AtC method given in Chapter 4. We end Chapter 4 by stating the essential existence and error result for the optimization-based method, and we prove this result in Chapter 5. Chapter 6 describes how the algorithm may be implemented, finalizes the $(\#\text{DoF})^{-(d/2-1)/2}$ error bound, and details some simple numerical experiments in one dimension validating the bounds. We conclude the thesis and provide a discussion of future work and outstanding problems with the optimization-based AtC in Chapter 7. For the convenience of the reader, we have added a list of notation used in Appendix B.

Chapter 2

Atomistic Model

2.1 Chapter Overview

In this chapter, we discuss the necessary preliminaries to define the true atomistic problem that we wish to approximate by our AtC algorithm. This will be the problem of a point defect embedded in an infinite lattice. We will introduce the concepts of a lattice, site energy, and atomistic energy functional and also define the appropriate function spaces over which we will define the atomistic minimization problem whose local minima correspond to defect configurations. We end the chapter with a discussion of regularity results concerning decay of the defect and an introduction to the types of error estimates we expect for an atomistic-to-continuum method.

2.2 Lattice Preliminaries

We are interested in modeling crystalline materials which are materials whose atoms are arranged in a lattice. A lattice in $\mathbb{R}^d$ is merely the range of a nonsingular linear transformation, F, when the domain is taken to be $\mathbb{Z}^d$. We denote the lattice by $\mathcal{L}$:

$$\mathcal{L} := \{\mathsf{F}\boldsymbol{z} \mid \boldsymbol{z} \in \mathbb{Z}^d\}. \tag{2.2.1}$$

The columns of F are called the lattice basis vectors. At each site of the lattice, a set of N_b basis atoms is attached. Each atom is offset from the lattice site by a shift vector $\boldsymbol{p}_i$ for $i = 0, \ldots, N_b - 1$. The result of attaching a set of atoms to a lattice site is a

crystal. When $N_b = 1$, there is a single species of atom located at each site, and the crystal can be taken to be synonymous with the lattice by taking $\boldsymbol{p}_0 = \mathbf{0}$ without loss of generality. In this case, the terms simple lattice or *Bravais* lattice are used to describe the material. Copper is an example of a material that is described by a simple lattice (a face-centered cubic lattice). When $N_b > 1$, the material is often called a multilattice or complex crystal. Many technologically important materials such as diamond, silicon, and graphene are complex crystals. Unfortunately, the optimization-based AtC method has not yet been extended to complex crystals so we focus entirely on Bravais lattices.

We will assume that the potential energy of a crystal is given by a *site potential* which associates an energy to each atom in the lattice. The total internal potential energy is then a sum over site energies minus the site energy at the reference state, and the equilibrium configurations of the material correspond to local minima of the lattice.[1]

The site potential is denoted by V_ξ where $\xi \in \mathcal{L}$. From the axiom of material frame indifference, V_ξ can only depend upon distances between atoms, e.g. vectors in the lattice. We will further assume the site potential only depends on distances between atoms within a finite cut-off distance, r_{cut}. Thus, there is a finite interaction range, $\mathcal{R} \subset \mathcal{L}$, that can be used to describe all interactions: given a fixed $\xi \in \mathcal{L}$, the positions of other atoms needed to compute V_ξ is $\xi + \mathcal{R}$ where

$$\mathcal{R} \subset \big\{\rho \in \mathcal{L} : 0 < |\rho| \leq r_{\text{cut}}\big\}.$$

We require that $\mathcal{R}$ satisfies the symmetry condition $\mathcal{R} = -\mathcal{R}$. An example interaction range is shown in two dimensions below.

We denote displacements of an atom ξ by $u(\xi)$ and write differences between atoms' displacements using finite difference operators, D_ρ, where $\rho \in \mathcal{R}$:

$$D_\rho u(\xi) := u(\xi + \rho) - u(\xi).$$

The set of all finite differences for $\rho \in \mathcal{R}$ is a stencil in $(\mathbb{R}^d)^{\mathcal{R}}$ denoted by

$$Du(\xi) := \big(D_\rho u(\xi)\big)_{\rho \in \mathcal{R}}.$$

Since $Du(\xi)$ incorporates all of the vectors needed to compute the site energy at ξ, the site energy can be defined as a mapping of finite difference stencils to $\mathbb{R}$, and thus V_ξ is

[1] This means any empirical potential may be used, and it has recently been shown that even tight binding methods may also be cast in this framework [12].

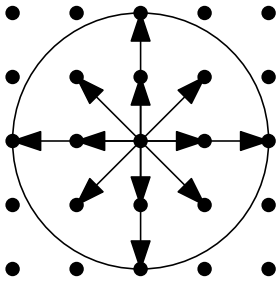

Figure 2.1: A possible interaction range with $r_{\text{cut}} = 2$ in $\mathbb{R}^2$. The atom, ξ, is at the center, and the interaction range, $\mathcal{R}$, consists of all vectors shown.

a function of $Du(\xi)$. We will often evaluate the site potential at the undeformed lattice in which case $u(\xi) = 0$ (the zero vector) so that $D_\rho u(\xi) = 0$. In lieu of introducing more notation, we will simply adopt the convention that $D(0) = 0$. Deformations of atoms are simply denoted by $y(\xi) := u(\xi) + \xi$ for $\xi \in \mathcal{L}$. We impose the following requirements on the site potential V_ξ:

V.1 (Regularity) The site potential, V_ξ, is $\mathrm{C}^4((\mathbb{R}^d)^{\mathcal{R}})$, and for $k \in \{1, 2, 3, 4\}$, there exists M_k such that for all multiindices $\alpha, |\alpha| \leq k$

$$|\partial^\alpha V_\xi(\boldsymbol{g})| \leq M_k \quad \forall \xi \in \mathbb{Z}^d, \boldsymbol{g} \in (\mathbb{R}^d)^{\mathcal{R}},$$

where ∂^α represents the partial derivative.

V.2 (Homogeneity) There exists an integer $M > 0$ and a potential $V : (\mathbb{R}^d)^{\mathcal{R}} \to \mathbb{R}^d$ such that $V_\xi \equiv V$ for all $|\xi| \geq M$.

V.3 (Symmetry) For $(g_\rho)_{\rho\in\mathcal{R}} \in (\mathbb{R}^d)^{\mathcal{R}}$, $V\Big((g_\rho)_{\rho\in\mathcal{R}}\Big) = V\Big(-(g_\rho)_{-\rho\in\mathcal{R}}\Big)$.

We will always evaluate the site potential at displacements which means we must encode the reference configuration inside the site potential. Thus, we use the notation $V_\xi(Du(\xi)) \equiv V_\xi(\mathsf{F} + Du(\xi)) = V_\xi\left((\mathsf{F}\rho + D_\rho u(\xi))_{\rho\in\mathcal{R}}\right)$ from here on.

Remark 2.2.1. *The regularity requirement* $\boldsymbol{V}.1$ *is not a property possessed by many realistic potentials since the site potential should be singular at any displacements which may cause atoms to occupy the same point in space. However, it greatly simplifies the notation used to define the atomistic energy functional in the proceeding section, and*

furthermore, since the fundamental existence result we prove is a local result formulated in a neighborhood of an a priori known atomistic solution, we fully expect the site potential to be C^4 *in this neighborhood. Alternatively, one can take great care to define the domains of definition of* V_ξ *to be sufficiently far away from any "improper" displacements as is the case in [23].*

The Homogeneity requirement is a completely natural assumption in modeling defects located at the origin in an infinite lattice since this says all atoms far away from the defect experience the same environment. Likewise, the symmetry condition is also physically motivated and can be shown to hold provided the atomistic energy functional is invariant under reflection of the atoms and permutation of the atoms [34].

2.3 Atomistic Energy Difference Functional

At first glance, it may seem that the total potential energy of the lattice is simply the sum over all site energies: $\sum_{\xi\in\mathcal{L}} V_\xi(Du(\xi))$. In reality, this is not well-defined since, in particular, the potential energy of the reference state $u(\xi)\equiv 0$ has infinite energy unless $V(0)=0$. This means we should consider an atomistic energy difference functional:

$$\mathcal{E}^{\mathrm{a}}(u) := \sum_{\xi\in\mathcal{L}} V_\xi(Du) - V(0).$$

However, without loss of generality, we further assume

V.4 (Zero) V(0) = 0.

This assumption is further justified because we will eventually be carrying out a finite dimensional optimization problem in which the addition of a constant will not affect the displacement at which the minimum is achieved (see Section 2.5). The atomistic energy is then given by

$$\mathcal{E}^{\mathrm{a}}(u) := \sum_{\xi\in\mathcal{L}} V_\xi(Du). \tag{2.3.1}$$

Our next task is to define the appropriate function spaces on which $\mathcal{E}^{\mathrm{a}}$ may be defined. To that end, we employ the homogeneous Sobolev space approach of [53, 55] and introduce a continuous representation of a discrete displacement via interpolation.

Let $\mathcal{T}_{\mathrm{a}}$ be a partition of $\mathbb{Z}^d$ into simplices (triangles in $2D$ and tetrahedra in $3D$) such that (i) ξ is a node of $\mathcal{T}_{\mathrm{a}}$ if and only if $\xi\in\mathcal{L}$, (ii) for each $\rho\in\mathcal{L}$ and each $\tau\in\mathcal{T}_{\mathrm{a}}$,

$\rho + \tau \in \mathcal{T}_\mathrm{a}$, and (iii) if ξ and η are nodes of the same simplex, $\tau \in \mathcal{T}_\mathrm{a}$, then $\eta - \xi \in \mathcal{R}$. (The last assumption states that the edges of $\mathcal{T}_\mathrm{a}$ correspond to vectors in the interaction range.) We refer to this as the atomistic triangulation; see Figure 2.2 for an example in two dimensions. In $\mathbb{Z}^3$, this triangulation can be constructed by first dividing a cube in half and then dividing each half cube into three tetrahedra [37, 53].

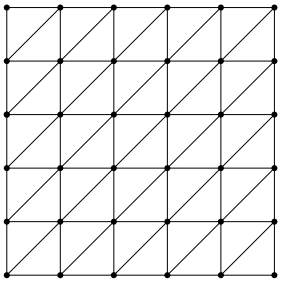

Figure 2.2: An atomistic triangulation of $\mathbb{Z}^2$.

Let $\mathcal{P}^1(\mathcal{T}_\mathrm{a}) = \left\{u \in \mathrm{C}^0(\mathbb{R}^d) : u|_T \in \mathcal{P}^1(T)\right\}$ be the standard finite element space of continuous piecewise linear functions with respect to $\mathcal{T}_\mathrm{a}$. The nodal interpolant, $Iu \in \mathcal{P}^1(\mathcal{T}_\mathrm{a})$, of a lattice function u is defined by setting

$$Iu(\xi) = u(\xi) \quad \forall \xi \in \mathcal{L}.$$

Using this interpolant, we define the function space of displacements to be

$$\mathcal{U} := \left\{u : \mathcal{L} \to \mathbb{R}^d : \nabla Iu \in L^2(\mathbb{R}^d)\right\}$$

and endow it with a semi-norm, $\|\nabla Iu\|_{L^2(\mathbb{R}^d)}$. A space of test functions whose gradients have compact support is defined by

$$\mathcal{U}_0 := \left\{u : \mathcal{L} \to \mathbb{R}^d : \mathrm{supp}(\nabla Iu) \,\text{is compact}\right\}.$$

The kernel of the semi-norm is the space of constant functions, $\mathbb{R}^d$, and elements of the associated quotient space, $\boldsymbol{\mathcal{U}} := \mathcal{U}/\mathbb{R}^d$, are equivalence classes that we denote by bold-faced font:

$$\boldsymbol{u} = \left\{v \in \mathcal{U} : \exists\, c \in \mathbb{R}^d, v - u = c\right\}.$$

Since the interpolation operator maps constants to constants, it is well defined on $\boldsymbol{\mathcal{U}}$. Consequently, $\|\nabla Iu\|_{L^2(\mathbb{R}^d)}$ is also a norm on $\boldsymbol{\mathcal{U}}$. Likewise, if $\boldsymbol{\mathcal{U}}_0$ is the quotient space of $\mathcal{W}_0$, we have

Proposition 2.3.1. *The quotient space $\boldsymbol{\mathcal{U}}$ with norm $\|\nabla Iu\|_{L^2(\mathbb{R}^d)}$ is a Hilbert space, and $\boldsymbol{\mathcal{U}}_0$ is dense in $\boldsymbol{\mathcal{U}}$.*

The proof is essentially contained in [55][Theorem 2.1 and Proposition 2.1] but requires slight modifications to handle the discrete setting we are employing. The proposition is also stated but not proven in [37].

Proof. We recall the definition of a homogeneous type Sobolev spaces [55]:

$$\dot{W}^{1,2}(\mathbb{R}^d) := \Big\{ f \in W^{1,2}_{\mathrm{loc}}(\mathbb{R}^d) : \nabla f \in L^2(\mathbb{R}^d) \Big\}$$

and its quotient space modulo constant functions,

$$\boldsymbol{W}^{1,2}(\mathbb{R}^d) := \dot{W}^{1,2}(\mathbb{R}^d)/\mathbb{R}^d.$$

Let $\boldsymbol{u}_n$ be a Cauchy sequence. Then $I\boldsymbol{u}_n$ belongs to $\boldsymbol{W}^{1,2}(\mathbb{R}^d)$, and by [55][Proposition 2.1], this space is complete so $I\boldsymbol{u}_n$ has some limit $\boldsymbol{u}_0 \in \dot{W}^{1,2}(\mathbb{R}^d)/\mathbb{R}^d$.

It remains to show that $\boldsymbol{u}_0$ is in fact piecewise linear with respect to the mesh. We assume for contradiction that $\boldsymbol{u}_0$ is not piecewise linear with respect to the mesh. Then there is a finite domain Ω whose boundary may be taken to be a union of edges of $\mathcal{T}_{\mathrm{a}}$ (by taking Ω sufficiently large) such that $\boldsymbol{u}_0$ is not piecewise linear on Ω. However, since $I\boldsymbol{u}_n$ is Cauchy and the set of piecewise linear functions with respect to $\mathcal{T}_{\mathrm{a}}$ on Ω is a finite dimensional normed space, it is automatically complete. Thus $I\boldsymbol{u}_n$ must converge to a piecewise linear function on Ω, and by uniqueness of limits, this must be equal to $\boldsymbol{u}_0$, which yields a contradiction.

Next, we prove the density statement so fix $\boldsymbol{u} \in \boldsymbol{\mathcal{U}}$.[2] Let η be a smooth bump function with support in $B_1(0)$, the ball of radius one about zero, and equal to one on $B_{3/4}(0)$. Let $A_R := \mathrm{supp}(\nabla(I\eta(x/R)))$ and define

$$T_R\boldsymbol{u}(x) = \eta(x/R)\big(I\boldsymbol{u} - \frac{1}{|A_R|}\int_{A_R} I\boldsymbol{u}\, dx\big),$$

and note again that T_R is well defined on equivalence classes. Define $\Pi_R\boldsymbol{u} := I(T_R\boldsymbol{u})$, and observe $\nabla\Pi_R\boldsymbol{u}$ has support on $B_{2R}(0)$ (for large R) so $\Pi_R\boldsymbol{u} \in \boldsymbol{\mathcal{U}}_0$.

[2] See also Lemma 4.3.4 for a similar proof.

We show that $\Pi_R \boldsymbol{u} \to \boldsymbol{u}$. Let us set $B_R := B_{2R}(0)$, and note

$$\begin{aligned}
\|\nabla \Pi_R \boldsymbol{u} - \nabla I\boldsymbol{u}\|^2_{L^2(\mathbb{R}^d)} =& \ \|\nabla I T_R \boldsymbol{u} - \nabla I\boldsymbol{u}\|^2_{L^2(\mathbb{R}^d)} \\
=& \ \|\nabla I(\eta(x/R) I\boldsymbol{u}) - \frac{1}{|A_R|}\int_{A_R} I\boldsymbol{u}\, dx \otimes \nabla(I\eta(x/R)) - \nabla I\boldsymbol{u}\|^2_{L^2(\mathbb{R}^d)} \\
=& \ \|\nabla I(\eta(x/R) I\boldsymbol{u}) - \frac{1}{|A_R|}\int_{A_R} I\boldsymbol{u}\, dx \otimes \nabla(I\eta(x/R)) - \nabla I\boldsymbol{u}\|^2_{L^2(B_R)} \\
&+ \|\nabla I\boldsymbol{u}\|^2_{L^2(\mathbb{R}^d \setminus B_R)}.
\end{aligned} \tag{2.3.2}$$

Since $\nabla I\boldsymbol{u}$ is in $L^2(\mathbb{R}^d)$, it follows that $\|\nabla I\boldsymbol{u}\|_{L^2(\mathbb{R}^d\setminus B_R)}$ goes to zero as $R \to \infty$. Thus, we focus on the first term. Towards that goal, we write the first term in (2.3.2) as[3]

$$\begin{aligned}
&\|\nabla I(\eta(x/R) I\boldsymbol{u}) - I(\eta(x/R))\nabla I\boldsymbol{u} - I\boldsymbol{u} \otimes \nabla(I\eta(x/R)) + I\boldsymbol{u} \otimes \nabla(I\eta(x/R)) \\
&\qquad - \frac{1}{|A_R|}\int_{A_R} I\boldsymbol{u}\, dx \otimes \nabla(I\eta(x/R)) + I(\eta(x/R))\nabla I\boldsymbol{u} - \nabla I\boldsymbol{u}\|^2_{L^2(B_R)} \\
\lesssim& \ \|\nabla I(\eta(x/R) I\boldsymbol{u}) - I(\eta(x/R))\nabla I\boldsymbol{u} - I\boldsymbol{u} \otimes \nabla(I\eta(x/R))\|^2_{L^2(B_R)} \\
&+ \|(I\boldsymbol{u} - \frac{1}{|A_R|}\int_{A_R} I\boldsymbol{u}\, dx) \otimes \nabla(I\eta(x/R))\|^2_{L^2(B_R)} + \|(I(\eta(x/R)) - 1)\nabla I\boldsymbol{u}\|^2_{L^2(B_R)} \\
=& \ \|\nabla I(\eta(x/R) I\boldsymbol{u}) - \nabla(I(\eta(x/R)) I\boldsymbol{u})\|^2_{L^2(B_R)} \\
&+ \|(I\boldsymbol{u} - \frac{1}{|A_R|}\int_{A_R} I\boldsymbol{u}\, dx) \otimes \nabla(I\eta(x/R))\|^2_{L^2(A_R)} + \|(I(\eta(x/R)) - 1)\nabla I\boldsymbol{u}\|^2_{L^2(B_R)}.
\end{aligned} \tag{2.3.3}$$

The third term tends to zero as $R \to \infty$ since $\|\nabla I\boldsymbol{u}\|_{L^2(\mathbb{R}^d)}$ is finite, and hence

$$\|\nabla I\boldsymbol{u}\|_{L^2(A_R)} \to 0, \text{ as } R \to \infty.$$

The first term in (2.3.3) goes to zero as $R \to \infty$ because we may compute the integral only over A_R since otherwise η is constant and then use standard finite element

[3] We use $\lesssim$ to denote $\leq C$ where C is some constant in this context.

interpolation theory on each triangle:

$$\begin{aligned}
&\|\nabla I(\eta(x/R)I\boldsymbol{u}) - \nabla(I(\eta(x/R))I\boldsymbol{u})\|^2_{L^2(B_R)} \\
&= \|\nabla I(I(\eta(x/R))I\boldsymbol{u}) - \nabla(I(\eta(x/R))I\boldsymbol{u})\|^2_{L^2(B_R)} \\
&= \|\nabla I(I(\eta(x/R))I\boldsymbol{u}) - \nabla(I(\eta(x/R))I\boldsymbol{u})\|^2_{L^2(A_R)} \\
&= \sum_{\substack{T\in\mathcal{T}_{\mathrm{a}} \\ T\cap A_R\neq\emptyset}} \|\nabla I(I(\eta(x/R))I\boldsymbol{u}) - \nabla(I(\eta(x/R))I\boldsymbol{u})\|^2_{L^2(T)} \\
&\lesssim \sum_{T\in A_R} \|\nabla^2(I(\eta(x/R))I\boldsymbol{u})\|^2_{L^2(T)} \\
&= 4\sum_{T\in A_R} \|\nabla(I\boldsymbol{u})\otimes\nabla I(\eta(x/R))\|^2_{L^2(T)} \\
&= 4\|\nabla(I\boldsymbol{u})\otimes\nabla I(\eta(x/R))\|^2_{L^2(A_R)} \lesssim \|\nabla(I\boldsymbol{u})\|^2_{L^2(A_R)} \to 0.
\end{aligned}$$

Finally, introducing the standard notation for the average value, $\frac{1}{|U|}\int_U f\,dx =: \fint_U f\,dx$, the second term in the final line of (2.3.3) may be written as

$$\begin{aligned}
\|(I\boldsymbol{u} - \fint_{A_R} I\boldsymbol{u}\,dx)\otimes\nabla(I\eta(x/R))\|_{L^2(A_R)} &\lesssim \frac{1}{R}\|(I\boldsymbol{u} - \fint_{A_R} I\boldsymbol{u}\,dx)\|_{L^2(A_R)} \\
&\lesssim \|\nabla I\boldsymbol{u}\|_{A_R} \to 0.
\end{aligned} \tag{2.3.4}$$

This completes the proof that $\Pi_R\boldsymbol{u}\to\boldsymbol{u}$. □

Because $\mathcal{E}^{\mathrm{a}}(u)$ is invariant under shifts by constants, it is also well-defined on $\boldsymbol{\mathcal{U}}$. Assumptions $\boldsymbol{V}.1-\boldsymbol{V}.4$ and the following proposition of [23,56][Theorem 2.3, Theorem 2.8] shows the energy is well defined and on this space as well.

Proposition 2.3.2. *The atomistic energy $\mathcal{E}^{\mathrm{a}}$ is continuous on $\boldsymbol{\mathcal{U}}_0$ and can be extended by continuity to $\boldsymbol{\mathcal{U}}$. This extension is four times Fréchet differentiable on $\boldsymbol{\mathcal{U}}$.*

Throughout, we denote Fréchet derivatives of energies by $\delta^k\mathcal{E}$, k indicating the order. We denote Gateaux derivatives by

$$\begin{aligned}
&\langle\delta\mathcal{E}(\boldsymbol{u}),\boldsymbol{v}\rangle, \\
&\langle\delta\mathcal{E}(\boldsymbol{u})\boldsymbol{v},\boldsymbol{w}\rangle, \\
&\delta^k\mathcal{E}(\boldsymbol{u})[\boldsymbol{v}_1,\boldsymbol{v}_2,\ldots,\boldsymbol{v}_k].
\end{aligned}$$

Let $\mathcal{R}^k := \overbrace{\mathcal{R} \times \cdots \times \mathcal{R}}^{k \text{ times}}$, $\boldsymbol{\rho} = (\rho_1, \ldots, \rho_k) \in \mathcal{R}^k$, and let $V_{\xi,\boldsymbol{\rho}}$ be the derivative of V_ξ with respect to $\boldsymbol{\rho} = (\rho_1, \rho_2, \ldots, \rho_k)$:

$$V_{\xi,\boldsymbol{\rho}}((g_\rho)_{\rho\in\mathcal{R}}) = \frac{\partial^k V_\xi((g_\rho)_{\rho\in\mathcal{R}})}{\partial g_{\rho_1} \partial g_{\rho_2} \cdots \partial g_{\rho_k}}.$$

Then the derivatives of the energy are given by

$$\begin{aligned}
\langle \delta\mathcal{E}^{\mathrm{a}}(\boldsymbol{u}), \boldsymbol{v}\rangle &= \sum_\xi \sum_{\rho\in\mathcal{R}} V_{\xi,\rho}(D\boldsymbol{u}) \cdot D_\rho \boldsymbol{v} \\
\langle \delta\mathcal{E}^{\mathrm{a}}(\boldsymbol{u})\boldsymbol{v}, \boldsymbol{w}\rangle &= \sum_\xi \sum_{\rho,\tau\in\mathcal{R}} [D_\rho \boldsymbol{v}]^\top V_{\xi,\rho\tau}(D\boldsymbol{u})[D_\tau \boldsymbol{w}] \\
\delta^k\mathcal{E}^{\mathrm{a}}(\boldsymbol{u})[\boldsymbol{v}_1, \boldsymbol{v}_2, \ldots, \boldsymbol{v}_k] &= \sum_\xi \sum_{\boldsymbol{\rho}\in\mathcal{R}^k} V_{\xi,\boldsymbol{\rho}}(D\boldsymbol{u})[D_{\rho_1}\boldsymbol{v}_1, D_{\rho_2}\boldsymbol{v}_2, \ldots, D_{\rho_k}\boldsymbol{v}_k].
\end{aligned}$$

Finally, we arrive at the full, atomistic problem that we wish to approximate:

$$\boldsymbol{u}^\infty = \operatorname*{arg\,min}_{\boldsymbol{u}\in\boldsymbol{\mathcal{U}}} \mathcal{E}^{\mathrm{a}}(\boldsymbol{u}), \tag{2.3.5}$$

where arg min represents the set of local minimizers and the superscript "∞" is used throughout to indicate the *exact atomistic* solution displacement field defined on the infinite lattice $\mathsf{F}\mathbb{Z}^d$. The fact that we are minimizing over equivalence classes effectively enforces a boundary condition[4] $u(\xi) \sim$ constant for $\xi \to \infty$.

The Euler-Lagrange equation corresponding to the minimization problem (2.3.5) is

$$\langle \delta\mathcal{E}^{\mathrm{a}}(\boldsymbol{u}^\infty), \boldsymbol{v}\rangle = 0 \quad \forall \boldsymbol{v} \in \boldsymbol{\mathcal{U}}_0. \tag{2.3.6}$$

We make the following assumption regarding the local minima of (2.3.6).

Assumption A. *There exists a local minimum, $\boldsymbol{u}^\infty \in \boldsymbol{\mathcal{U}}$, of $\mathcal{E}^{\mathrm{a}}(\boldsymbol{u})$ and a real number $\gamma_{\mathrm{a}} > 0$ such that*

$$\gamma_{\mathrm{a}} \|\nabla I\boldsymbol{v}\|^2_{L^2(\mathbb{R}^d)} \le \langle \delta^2\mathcal{E}^{\mathrm{a}}(\boldsymbol{u}^\infty)\boldsymbol{v}, \boldsymbol{v}\rangle \quad \forall \boldsymbol{v} \in \boldsymbol{\mathcal{U}}_0. \tag{2.3.7}$$

The condition (2.3.7) ensures that the atomistic solution is strongly stable and is critical for the analysis. It can be interpreted as saying that perturbations of the lattice will increase the energy [31, 32].

[4] This technique is also useful in establishing well-posedness results for linear elliptic systems on all of $\mathbb{R}^d$ [55].

2.3.1 Specific Examples of Defect Configurations

With the abstract mathematical framework in place to analyze defects, we pause briefly and give two concrete examples of how specific defects can be modeled. A *vacancy* defect is a point defect that results when an atom is removed from the lattice, see Figure 2.3(a). If the vacancy is placed at the origin, then all atoms within the interaction range of the origin will have a modified site potential which accounts for this missing atom. For example, in the case of a pair potential, ϕ, where the internal potential energy is given as a sum over pairs of atoms, the homogeneous site potential could be

$$V(Du(\xi)) = \sum_{\rho\in\mathcal{R}} \phi(D_\rho u(\xi)).$$

For atoms $\xi \in (0+\mathcal{R})$, the site potential would be

$$V_\xi(Du(\xi)) = \sum_{\rho\in\mathcal{R}:\rho+\xi\neq 0} \phi(D_\rho u(\xi)), \quad V_0(Du) = 0,$$

and the total energy would remain

$$\mathcal{E}^{\mathrm{a}}(u) = \sum_{\xi\in\mathcal{L}} V_\xi(Du(\xi)).$$

If instead the potential was given by the embedded atom method [14], which has been highly useful in modeling metals, then the homogeneous site potential is of the form

$$V(Du(\xi)) = \sum_{\rho\in\mathcal{R}} \phi(D_\rho u(\xi)) + G\left(\sum_{\rho\in\mathcal{R}} \varrho(D_\rho u(\xi))\right),$$

where ϕ is again a pair potential, ϱ is a function designed to account for electron charge density, and G is an embedding function that gives the cost of embedding an atom in an electron environment described by ϱ [14]. The first pair potential term in this case is handled exactly as it was before, and the embedding term is handled similarly by removing the interactions associated with the origin.

Another example of a defect is an impurity where an atom of a different species is located at a lattice site as shown in Figure 2.3(b). In this case, there will be a second pair potential ϕ_{01} which will be the pair potential used for interactions between atoms of species 0 and 1. Thus, for atoms $\xi \in (0+\mathcal{R})$, the site potential would be

$$V_\xi(Du(\xi)) = \phi_{01}(u(0)-u(\xi)) + \sum_{\rho\in\mathcal{R}:\rho+\xi\neq 0} \phi(D_\rho u(\xi)), \quad V_0(Du) = \sum_{\rho\in\mathcal{R}} \phi_{01}(D_\rho u(0)),$$

and the homogeneous site potential would remain unchanged.

(a) A simple vacancy at the origin.. (b) A simple impurity at the origin.

Figure 2.3: Point defects in two dimensions.

These defects and several more defects including interstitials (an extra atom) are considered in [23].

2.4 Regularity and Decay of the Atomistic Solution

For point and line defects, solutions of (2.3.6) decay algebraically in their elastic far fields [23, 63]. We quantify the rates of decay using a smooth nodal interpolant of a lattice function, $u : \mathcal{L} \to \mathbb{R}^d$, which we denote by $\tilde{I}u \in W^{3,\infty}_{\rm loc}(\mathbb{R}^d)$. Its existence follows from [37, Lemma 2.1], which we state below. We refer to [37] for the proof. A simplified, one-dimensional result can be found in [42].

Lemma 2.4.1. *There exists a unique operator $\tilde{I} : \mathcal{U} \to \mathrm{C}^{2,1}(\mathbb{R}^d)$ such that for all $\xi \in \mathcal{L}$, (i) $\tilde{I}u$ is multiquintic (i.e., biquintic in the case $d = 2$ and triquintic in the case $d = 3$) in each cell $\xi + \mathsf{F}(0,1)^d$, (ii) $\tilde{I}u(\xi) = u(\xi)$, and (iii) for all multiindices $|\alpha| \leq 2$, $\partial^\alpha \tilde{I}u(\xi) = D^{\rm nn}_\alpha u(\xi)$ where $D^{\rm nn}_\alpha$ is defined by*

$$
\begin{aligned}
D^{{\rm nn},0}_i u(\xi) &:= u(\xi),\\
D^{{\rm nn},1}_i u(\xi) &:= \frac{1}{2}(u(\xi + \mathsf{F}e_i) - u(\xi - \mathsf{F}e_i)) \quad (e_i \text{ is the } i\text{th standard basis vector}),\\
D^{{\rm nn},2}_i u(\xi) &:= u(\xi + \mathsf{F}e_i) - 2u(\xi) + u(\xi - \mathsf{F}e_i),\\
D^{\rm nn}_\alpha u(\xi) &:= D^{{\rm nn},|\alpha_1|}_1 \cdots D^{{\rm nn},|\alpha_d|}_d u(\xi).
\end{aligned}
$$

Furthermore,

$$\|\nabla^j \tilde{I}u\|_{L^2(\xi+\mathsf{F}(0,1)^d)} \lesssim \|D^j u\|_{\ell^2(\xi+\mathsf{F}\{-1,0,1,2\}^d)} \quad \textit{for} \quad j=1,2,3,^{5} \tag{2.4.1}$$

where

$$\begin{aligned} D^j u(\xi) &= \left(D_{\rho_1} D_{\rho_2} \cdots D_{\rho_j} u(\xi)\right)_{(\rho_1,\rho_2,\ldots,\rho_j)\in\mathcal{R}^j}, \\ \|D^j u\|^2_{\ell^2(A)} &:= \sum_{\xi\in A} \sup_{(\rho_1,\rho_2,\ldots,\rho_j)\in\mathcal{R}^j} |D_{\rho_1} D_{\rho_2} \cdots D_{\rho_j} u(\xi)|^2. \end{aligned}$$

The uniqueness assertion of Lemma 2.4.1 and the condition that $\partial^\alpha \tilde{I}u(\xi) = D^{\mathrm{nn}}_\alpha u(\xi)$ for all $\xi \in \mathcal{L}$ imply that for any constant vector field, $u(\xi) \equiv c \in \mathbb{R}^d$, $\tilde{I}u = c$. Thus $\tilde{I}$ is well defined as an operator from $\boldsymbol{\mathcal{U}}$ to $\boldsymbol{\mathcal{U}}$ with $\tilde{I}\boldsymbol{u} := \left\{\tilde{I}u : u \in \boldsymbol{u}\right\}$. From (2.4.1) and it easily follows that

$$\|\nabla \tilde{I}\boldsymbol{u}\|_{L^2(\mathbb{R}^d)} \lesssim \|\nabla I\boldsymbol{u}\|_{L^2(\mathbb{R}^d)}.$$

The following theorem provides a sharp estimate on the algebraic decay of the minimizers for point defects only.

Theorem 2.4.2 (Regularity of a point defect)**.** *The local minimum, $\boldsymbol{u}^\infty$, of (2.3.5) satisfies*

$$\left|\nabla^j \tilde{I}\boldsymbol{u}^\infty(x)\right| \lesssim |x|^{1-j-d} \quad \textit{for } j=1,2,3 \quad x\in\mathbb{R}^d, \tag{2.4.2}$$

$$\left|\nabla I\boldsymbol{u}^\infty(x)\right| \lesssim |x|^{-d} \quad \textit{for } x\in\mathbb{R}^d. \tag{2.4.3}$$

Proof. Theorem 3.1 and Lemma 3.5 of [23] imply

$$\left|D^j \boldsymbol{u}^\infty(\xi)\right| \lesssim |\xi|^{1-j-d} \quad \text{for } j=1,2,3.$$

This, along with the local estimate (2.4.1) of $\tilde{I}$ implies (2.4.2).

An analogous local estimate,

$$\|\nabla Iu\|_{L^2(\xi+\mathsf{F}(0,1)^d)} \lesssim \|Du\|_{\ell^2(\xi+\mathsf{F}\{-1,0,1,2\}^d)},$$

implies (2.4.3). □

[5] *In this context, the modified Vinogradov notation $A \lesssim B$ means there is a constant C such that $A \le CB$ where C may depend on the dimension d. After introducing the relevant approximation parameters for the AtC method, we will explicitly state what the constant C is allowed to depend upon.*

2.5 Reduction to a Finite Dimensional Problem

One possible simple way of solving (2.3.5) would be a simple Galerkin projection by truncating the support of the admissible functions to a regular polygon or polyhedron Ω of diameter N whose boundary is comprised of a union of edges of $\mathcal{T}_{\rm a}$. The truncated displacement space would be

$$\boldsymbol{\mathcal{U}}_\Omega := \left\{ \boldsymbol{u} \in \boldsymbol{\mathcal{U}} : \mathrm{supp}(\nabla I\boldsymbol{u}) \subset \overline{\Omega} \right\}.$$

This is clearly finite-dimensional and is comprised precisely of all lattice functions that are constant outside of Ω (their gradients are 0). Replacing the full space $\boldsymbol{\mathcal{U}}$ by $\boldsymbol{\mathcal{U}}_\Omega$ in the minimization problem (2.3.5) then yields the finite dimensional atomistic problem

$$\boldsymbol{u}_\Omega = \operatorname*{arg\,min}_{\boldsymbol{\mathcal{U}}_\Omega} \mathcal{E}^{\rm a}(\boldsymbol{u}). \tag{2.5.1}$$

The corresponding Euler-Lagrange equation are to find $\boldsymbol{u}_\Omega \in \boldsymbol{\mathcal{U}}_\Omega$ such that

$$\langle \delta\mathcal{E}^{\rm a}(\boldsymbol{u}_\Omega), \boldsymbol{v} \rangle = \ 0 \qquad \forall \boldsymbol{v} \in \boldsymbol{\mathcal{U}}_\Omega. \tag{2.5.2}$$

The accuracy and efficiency of the truncated atomistic problem can be estimated in terms of the size of the truncated domain Ω. The following result is elementary and recorded in [23, 42].

Proposition 2.5.1. *Let Ω and N be given such that $B_N(0) \subset \Omega$ and $\Omega \subset B_{2N}(0)$. There exists N_0 such that for all $N \geq N_0$, the truncated problem* (2.5.1) *has a solution $\boldsymbol{u}_\Omega$ satisfying the estimate*

$$\|\nabla I\boldsymbol{u}_\Omega - \nabla I\boldsymbol{u}^\infty\|_{L^2(\mathbb{R}^d)} \lesssim \ N^{-d/2}.$$

Moreover, since the number of degrees of freedom in this method is equal to the number of atoms in Ω, the number of degrees of freedom is on the order of N^d. Thus, we can estimate the error in the truncation method by the number of degrees of freedom, (DoF):

$$\|\nabla I\boldsymbol{u}_\Omega - \nabla I\boldsymbol{u}^\infty\|_{L^2(\mathbb{R}^d)} \lesssim \ (\mathrm{DoF})^{-1/2}.$$

It is clear that for an AtC method to be worthwhile, the error of the method should then decay at a rate faster than $(\mathrm{DoF})^{-1/2}$. If a simple finite element method were applied

directly to the atomistic energy by choosing a finite element mesh that were not fully refined, then this estimate would remain the same since the atom positions inside each element would still have to be interpolated in order to compute the atomistic energy [73]. This leads to the need for AtC methods which have a faster rate of convergence, but thus far, there have been only four AtC methods whose errors have been rigorously established in the context of the point defect problem for general interactions in two or three dimensions. These are summarized in table below. The rates shown assume an optimal mesh and continuum region as explained in Chapter 6.

Table 2.1: Established convergence rates of various AtC Methods for a point defect

Method	Shorthand	Rate	Reference
Blended-force quasicontinuum	BQCF	$(\mathrm{DoF})^{-1/2-1/d}$	[37]
Blended-energy quasicontinuum	BQCE	$(\mathrm{DoF})^{1/2-2/d}$	[37]
Blended ghost force correction	BGFC	$(\mathrm{DoF})^{-1/2-1/d}$	[60]
Optimization-based AtC	Opt AtC	$(\mathrm{DoF})^{-1/2-1/d}$	[48] (this thesis)

Remark 2.5.2. *One can obtain improved bounds in the estimates above by introducing logarithmic factors into the analysis [37].*

The remainder of the thesis will be dedicated to establishing the rate shown for the optimization-based AtC method, but first we must introduce the continuum model.

Chapter 3

Continuum Model

3.1 Chapter Overview

Having defined the atomistic model, our next task is to define the continuum model which it will be coupled to. The continuum model used is the Cauchy-Born strain energy density, which dates back to Cauchy in the 19th century [11]. Later, Born modified the rule to be applicable to multilattices [8]. Two essential results that make the Cauchy-Born rule especially amenable to AtC algorithms are the second order accuracy of the Cauchy-Born rule [6, 34, 56, 74] for smooth deformations and the fact that atomistic stability implies Cauchy-Born stability [31, 74, 75]. Each of these results are discussed in this chapter.

3.2 Cauchy-Born Rule

At its core, the Cauchy-Born rule provides a means of linking the continuum deformation with the movement of individual atoms by assuming the atoms move as if they are points in the continuum [24]. Specifically, given a set of basis vectors, $\boldsymbol{a}_i$, for the underlying Bravais lattice and a continuum deformation gradient $\mathsf{G} \in \mathbb{R}^{d\times d}$, the Cauchy-Born rule dictates that a set of basis vectors for the deformed lattice is simply $\mathsf{G}\boldsymbol{a}_i$ [11, 24, 72]. In a similar vein, given the homogeneous site energy V from the previous section, a strain energy density functional can be defined by deforming the vectors in the interaction

range according to G:

$$W(\mathsf{G}) := \frac{1}{\det \mathsf{F}} V\big((\mathsf{G}\rho)_{\rho\in\mathcal{R}}\big).$$

Without loss of generality, we will assume $\det \mathsf{F} = 1$ in the remainder. Given a C^1 displacement field u, this becomes

$$W(\nabla u)(x) := V(\nabla_{\mathcal{R}} u)(x), \quad \text{where} \quad \nabla_{\mathcal{R}} u := (\nabla_\rho u(x))_{\rho\in\mathcal{R}}.$$

Integration of the strain energy yields the Cauchy-Born continuum energy of

$$\mathcal{E}^{\mathrm{c}}(u) := \int_{\mathbb{R}^d} W(\nabla u(x))\, dx, \tag{3.2.1}$$

which is defined for a suitable class of functions such as the homogeneous Sobolev space $\dot{W}^{1,2}(\mathbb{R}^d)$ [55]. (Observe yet again that $W(\nabla u)$ is well defined on this space due to the functional reliance on the displacement gradient). We also remark that our assumption that $V(0) = 0$ allows us to consider the energy functional (3.2.1) directly without having to resort to an energy difference functional. In this case, it is clear that $\mathcal{E}^{\mathrm{c}}(u)$ is defined for $u \in \mathrm{C}_0^\infty$ since then $W(\nabla u)$ is C^4 having support in a bounded set. Moreover, we have an analog to the atomistic regularity result also found in [56]:

Proposition 3.2.1. *The Cauchy-Born continuum energy, $\mathcal{E}^{\mathrm{c}}$, is continuous on C_0^∞ and can be extended by continuity to $\dot{W}^{1,2}(\mathbb{R}^d)$. This extension is four times Fréchet differentiable on $\dot{W}^{1,2}(\mathbb{R}^d)$.*

Recalling our ultimate goal of coupling the atomistic and Cauchy-Born models, we will use the Cauchy-Born rule far from the defect core because in the absence of defects it provides a second-order accurate approximation for smoothly decaying elastic fields [7, 74]. The advantage of the Cauchy-Born energy (3.2.1) over the atomistic energy (2.3.1) is that a finite element method can efficiently approximate the local minima of the Cauchy-Born energy by using a much coarser mesh than the atomistic mesh, $\mathcal{T}_{\mathrm{a}}$.

Proposition 3.2.1 allows us to consider the continuum problem of

$$\boldsymbol{u}^{\mathrm{cb}} = \operatorname*{arg\,min}_{\boldsymbol{u}\in\dot{W}^{1,2}(\mathbb{R}^d)} \mathcal{E}^{\mathrm{c}}(\boldsymbol{u}). \tag{3.2.2}$$

3.3 Consistency and Stability of the Cauchy-Born Energy

The minimization problem (3.2.2) is not alone sufficient to model defects because, in particular, it requires a homogeneous site potential $V_\xi \equiv V$. However, since the motivation behind an AtC method is to only use the continuum model away from the defect, we can heuristically justify using the Cauchy-Born continuum energy provided it is a good approximation on the defect-free infinite lattice. We collect the requisite results here, but as we are only using these as a heuristic justification, we shall only state the results and refer to the proofs in the literature. In this section, and this section alone, we assume $V_\xi \equiv V$ for all ξ.

The first result is that stability of the atomistic model implies stability of the Cauchy-Born model [31, 74, 75]. Following [31], define

$$\gamma_{\text{per}} := \inf_{\substack{v \in \boldsymbol{\mathcal{U}}_0 \\ \|\nabla Iv\|_{L^2(\mathbb{R}^d)}=1}} \langle \delta^2 \mathcal{E}^{\text{a}}(0)v, v\rangle.$$

As previously mentioned, the lattice is stable provided $\gamma_{\text{per}} > 0$ (per is short for perfect lattice). Furthermore, we have from [31, 56]

Proposition 3.3.1 (Atomistic Stability Implies Cauchy-Born Stability)**.** *With γ_{per} defined above,*

$$\langle \delta^2 \mathcal{E}^{\text{c}}(0)v, v\rangle \geq \gamma_{\text{per}} \|\nabla v\|^2_{L^2(\mathbb{R}^d)}, \quad \forall v \in \dot{W}^{1,2}(\mathbb{R}^d).$$

The second result provides an estimate on the internal forces. It is a negative norm estimate on the difference between the atomistic and continuum variations and is due to [56].

Proposition 3.3.2. *Let ζ be a finite element hat function which is 1 at the origin and 0 at all other points in the lattice. For $u \in \dot{W}^{1,2}(\mathbb{R}^d)$ with $\nabla^2 u \in L^2(\mathbb{R}^d)$ and $\nabla^3 u \in L^2(\mathbb{R}^d)$,*

$$\langle \delta\mathcal{E}^{\text{a}}(u), \zeta * v\rangle - \langle \delta\mathcal{E}^{\text{c}}(u), v\rangle \lesssim \left(\|\nabla^3 u\|_{L^2(\mathbb{R}^d)} + \|\nabla^2 u\|^2_{L^4(\mathbb{R}^d)}\right) \cdot \|\nabla Iv\|_{L^2(\mathbb{R}^d)} \quad \forall v \in \boldsymbol{\mathcal{U}}_0.$$

Remark 3.3.3. *The fact that $\zeta * v$ is used as the test function in the atomistic variation allows an atomistic definition of stress to be defined and has been critical to the analysis of AtC methods [56]. It is key to the proof of Theorem 4.3.8 below.*

The estimate in Proposition 3.3.2 is commonly referred to as a second order estimate. The reason it is second order is that if we introduce an interatomic spacing, ϵ and scaled variables

$$\check{\xi} = \epsilon\xi,\ \check{x} = \epsilon x,\ \check{u}(\check{\xi}) = \epsilon u(\epsilon^{-1}\check{\xi}),\ \text{and}\ \check{u}(\check{x}) = \epsilon u(\epsilon^{-1}\check{x})$$

along with the scaled finite difference operator $D_{\epsilon\rho}\check{u}(\check{\xi}) := \frac{\check{u}(\check{\xi}+\epsilon\rho)-\check{u}(\check{\xi})}{\epsilon}$ and scaled atomistic energy

$$\check{\mathcal{E}}^{\mathrm{a}}(\check{u}) := \epsilon^d \sum_{\check{\xi}\in\epsilon\mathcal{L}} V\big((D_{\epsilon\rho}\check{u}(\check{\xi}))_{\rho\in\mathcal{R}}\big),$$

a simple change of variables yields

$$\langle \delta\check{\mathcal{E}}^{\mathrm{a}}(\check{u}), \check{\zeta} * \check{v}\rangle - \langle \delta\mathcal{E}^{\mathrm{c}}(\check{u}), \check{v}\rangle \lesssim\ \epsilon^2 \left(\|\nabla^3\check{u}\|_{L^2(\mathbb{R}^d)} + \|\nabla^2\check{u}\|^2_{L^4(\mathbb{R}^d)}\right)\cdot \|\nabla I\check{v}\|_{L^2(\mathbb{R}^d)}.$$

Just as in the atomistic case, we can introduce a truncated domain Ω, impose a finite element mesh, $\mathcal{T}_h$ on Ω, and then use the finite element method to solve finite dimensional problem. This will be postponed until Section 4.3 when we introduce a "restricted" continuum problem on a domain which does not include the defect.

We have now reached the point where we can describe the optimization-based atomistic-to-continuum coupling algorithm.

Chapter 4

Formulation of Optimization-Based AtC

4.1 Chapter Overview

With the prerequisite knowledge of the fully atomistic problem and Cauchy-Born continuum problem acquired, we are now in a position to introduce the optimization-based algorithm. This is based on the ideas of virtual controls [26, 28] where two models are coupled by formulating individual subproblems for each model on subdomains that either overlap or intersect in a lower dimensional manifold. In either case, an artificial boundary is created on the interior of the original domain as in Figure 4.1, where Ω_1 and Ω_2 overlap creating two artificial boundaries, Γ_1 and Γ_2. We then think of solving these subproblems subject to some unknown or virtual boundary conditions being placed on the newly created artificial boundaries. Denoting the solutions to these problems abstractly by u_1 and u_2, an optimization problem is formulated by minimizing $\|u_1 - u_2\|$, where the norm must be chosen to give a well-posed problem. This can be contrasted to the well-known Schwarz alternating methods where the models are sequentially solved with each solution being fed into the next as the unknown boundary condition. A survey of the Schwarz procedure to solve atomistic-to-continuum couplings is given in [62] for much simpler (linear or one-dimensional) problems than the multidimensional point defect problem considered here.

In this chapter, we apply the virtual control method to yield what we call the

optimization-based atomistic-to-continuum coupling. We take the two models to be "restricted" atomistic and continuum problems respectively. The norm we choose is the H^1 seminorm (which is actually a norm on the spaces we will consider). Our first task in Section 4.2 is to describe the domain decomposition procedure. Then we detail the atomistic and continuum subproblems and prove regularity results concerning the existence of solutions to these subproblems in Section 4.3. We conclude the chapter with the fully defined optimization-based AtC method and a statement of the main existence theorem and error estimate.

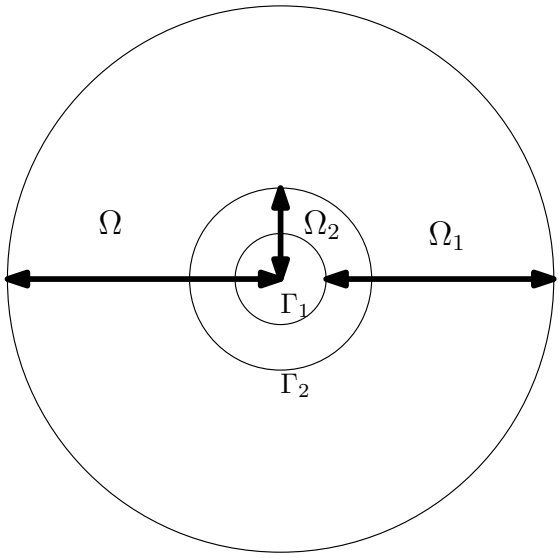

Figure 4.1: An example splitting Ω into Ω_1 and Ω_2 where different models could be used on Ω_1 and Ω_2. This creates artificial boundaries Γ_1 and Γ_2 in the interior of Ω.

4.2 Domain Selection

To describe our AtC approach we consider a configuration comprised of a finite domain Ω, a defect core $\Omega_{\text{core}} \subset \Omega$, and atomistic and continuum subdomains $\Omega_{\text{a}}, \Omega_{\text{c}} \subset \Omega$. We briefly describe the general idea behind the domain construction before going into the full technical details. Intuitively, the defect core, Ω_{core}, should be chosen large enough so that all atoms near the defect are included in this set. We then choose an atomistic domain, Ω_{a}, whose size is on the same order of magnitude as the defect core region.

Finally, we truncate the infinite lattice to a finite lattice with a domain Ω as was done in Section 2.5 and set $\Omega_{\rm c} := \Omega \backslash \Omega_{\rm core}$. The "size" of Ω should be much larger than that of $\Omega_{\rm a}$. The reason for having both an atomistic region and defect region is so that the atomistic and continuum regions overlap in a region, $\Omega_{\rm o}$, that does not contain the defect core: $\Omega_{\rm o} := \Omega_{\rm a} \backslash \Omega_{\rm core}$.

For the formulation and implementation of our method, the above construction is sufficient. However, the analysis of our AtC method requires several technical assumptions on these domains' relative sizes to one another as well as minimal regularity results on the domain boundaries so we now outline a very specific selection.

The domains are defined by first selecting a domain Ω_0 so that (i) it contains all ξ for which $V_\xi \not\equiv V$; (ii) its boundary, $\partial\Omega_0$, is Lipschitz, and (iii) $\partial\Omega_0$ is a union of edges from $\mathcal{T}_{\rm a}$. The domains $\Omega_{\rm core}, \Omega_{\rm a}$, and Ω will be defined as multiples of Ω_0 so Ω_0 provides the essential shape of these domains. [1] We choose integers $R_{\rm core} \geq 1$ and $\psi_{\rm a} \geq 4$ and set $\Omega_{\rm core} = R_{\rm core}\Omega_0$ and $\Omega_{\rm a} = \psi_{\rm a}\Omega_{\rm core}$ with the requirement that $(\psi_{\rm a} - 1)r_{\rm core} \geq 4r_{\rm cut}$, where $r_{\rm core}$ is the radii of the largest circle centered at the origin contained in $\Omega_{\rm core}$. The quantity $(\psi_{\rm a} - 1)r_{\rm core}$ is roughly a measure of the width of $\Omega_{\rm a}\backslash\Omega_{\rm core}$, which is an "annular" type region of a shape prescribed by Ω_0. See Figure 4.2 for an illustration.

Next, we select an integer $R_\Omega > R_{\rm core} \cdot \psi_{\rm a}$ and set $\Omega = R_\Omega\Omega_0$ whilst requiring that the radii of the largest circle centered at the origin contained in Ω, denoted by $r_{\rm c}$, satisfies $r_{\rm c}/r_{\rm core} = r_{\rm core}^\kappa$ for some integer $\kappa \geq 1$. The continuum domain is then defined by $\Omega_{\rm c} := \Omega\backslash\Omega_{\rm core}$. We also define the "annular" overlap region $\Omega_{\rm o} := \Omega_{\rm a}\backslash\Omega_{\rm core}$ and an "extended" overlap region $\Omega_{\rm o,ex} := (2\psi_{\rm a}\Omega_{\rm core})\backslash\Omega_{\rm core}$. See Figure 4.3 for an example, although it is not to scale.

The requirement that $(\psi_{\rm a} - 1)r_{\rm core} \geq 4r_{\rm cut}$ can now be interpreted as requiring the overlap "width" to be twice the size of the maximum interaction range allowed by the site potential. The purpose of $\Omega_{\rm o,ex}$ is to have a domain of definition common to both continuum functions defined on $\Omega_{\rm c}$ and atomistic functions defined on $\Omega_{\rm a}$ which extends just beyond $\Omega_{\rm o}$; it will be used explicitly only in the analysis of Section 5.4. Finally, the

[1] From a practical point of view, this provides a restriction on how the domains are chosen. However, we emphasize that this restriction is done for convenience of the error analysis and not the implementation of the AtC method. This restriction could be relaxed by considering families of domains with Lipschitz constants in a bounded region.

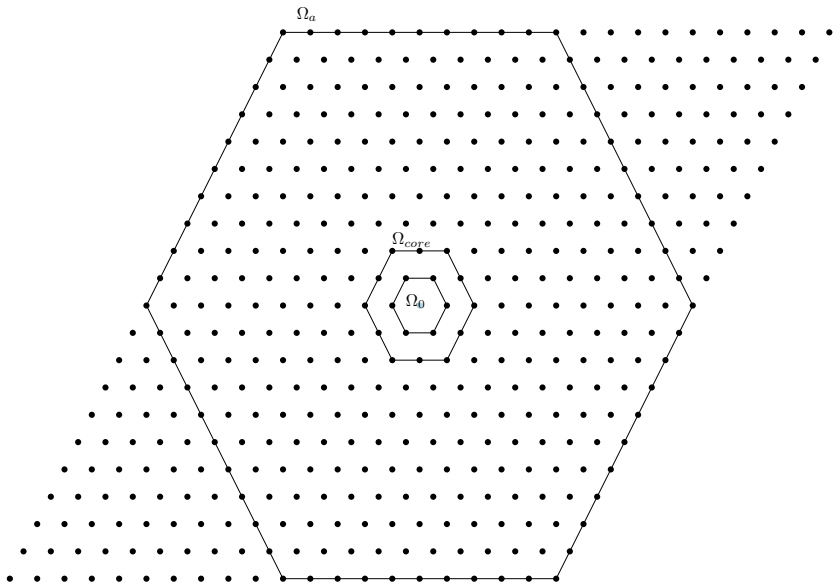

Figure 4.2: An example of the domain selection process on a lattice. Here we consider the (unwise) choice of $r_{\text{cut}} = 1$ with $\Omega_0, \Omega_{\text{core}}$, and Ω_{a} shown. We have chosen simply $R_{\text{core}} = 2$, $\psi_{\text{a}} = 5$, and $r_{\text{core}} = 1$ so that the criterion $4 = (\psi_{\text{a}} - 1)r_{\text{core}} \geq 4r_{\text{cut}} = 4$ is satisfied.

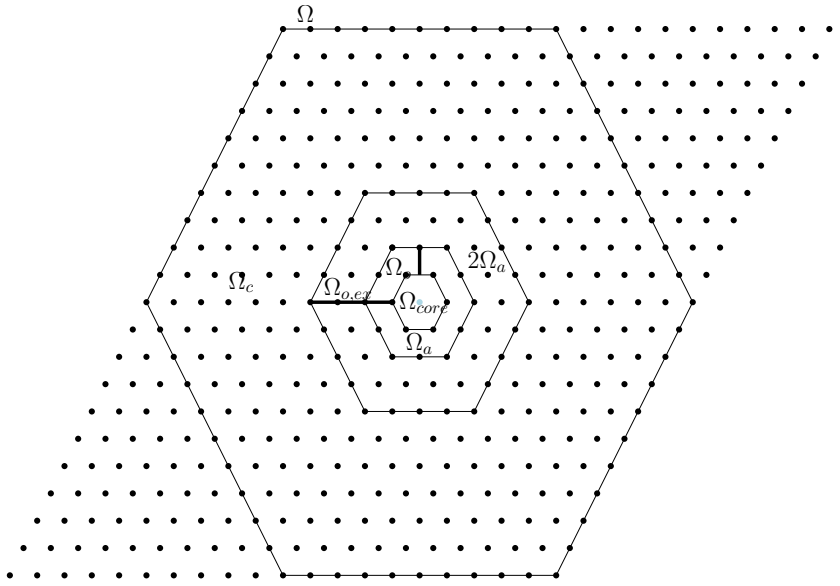

Figure 4.3: Illustration of the domains $\Omega, \Omega_{\text{c}}, \Omega_{\text{o}}$, and $\Omega_{\text{o,ex}}$. Note the atomistic and core regions are not to scale.

requirement that $r_c/r_{core} = r_{core}^{\kappa}$ for some integer $\kappa \geq 1$ can be interpreted as forcing the continuum domain to be much larger in size than the atomistic region, which should indeed be the case if we are to reap the benefits of an AtC method.

We also define the domain "size" parameters

$$R_a := R_{core} \cdot \psi_a \quad \text{and} \quad R_c := \frac{1}{2}\text{Diam}(\Omega_c),$$

and let r_a, and r_c be the radii of the largest circles inscribed in Ω_a and Ω respectively.[2]

The atomic lattices associated with the new domains are

$$\mathcal{L}_t := \mathcal{L} \cap \Omega_t \quad \text{where} \quad t = a, c, o, core,$$

and their atomistic interiors are

$$\mathcal{L}_t^{\circ} := \{\xi \in \mathcal{L}_t : \xi - \rho \in \mathcal{L}_t \quad \forall \rho \in \mathcal{R}\}.$$

Thus, $\mathcal{L}_t^{\circ}$ is the set of $\xi \in \mathcal{L}_t$ whose neighbors $\xi + \mathcal{R}$ are also in $\mathcal{L}_t$. The atomistic interiors of the interiors are $\mathcal{L}_t^{\circ\circ} = (\mathcal{L}_t^{\circ})^{\circ}$ while the atomistic boundary of $\mathcal{L}_t$ is

$$\partial_a \mathcal{L}_t := \mathcal{L}_t \backslash \mathcal{L}_t^{\circ\circ}.$$

See Figure 4.4 for an illustration of $\Omega_a^{\circ\circ}$ (open circles) and $\partial_a \mathcal{L}_a$ (solid squares) for the case $\mathcal{R} = \{\pm e_1, \pm e_2\}$ and $\mathcal{L} = \mathbb{Z}^2$.

Remark 4.2.1. *Throughout the paper we state results involving a parameter R_{core}^* such that if $R_{core} \geq R_{core}^*$, then a solution to a specific problem defined on the domains constructed above will be guaranteed to exist. Because $R_c \gg R_{core}$ by virtue of $r_c/r_{core} = r_{core}^{\kappa}$, this will automatically ensure that $R_c \gg R_{core}^*$ as well. These results always assume AtC domain configurations constructed according to the above guidelines. Furthermore, when stating inequalities, we will use modified Vinogradov notation, $A \lesssim B$ in lieu of $A \leq C \cdot B$, where $C > 0$ is a constant. This constant may only depend upon $\Omega_0, d, R_{core}^*, r_{cut}$, ψ_a, and an additional constant, β, introduced in Section 4.3 as the minimum angle of a finite element mesh.*

[2] We define r_c as the inner radii of Ω since Ω_c has a hole at the defect core and hence does not have an inscribed circle.

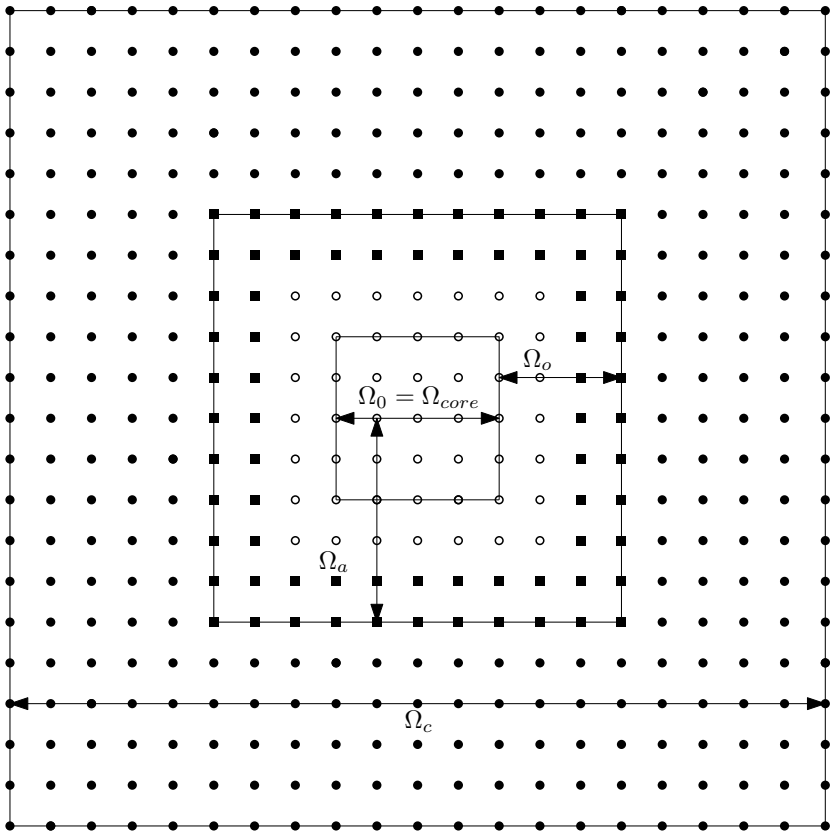

Figure 4.4: An example AtC configuration in two dimensions. The set $\Omega_{\rm a}^{\circ\circ}$ is shown as open circles. The solid squares show $\partial_{\rm a}\mathcal{L}_{\rm a}$ for the case $\mathcal{R} = \{\pm e_1, \pm e_2\}$. In this simple case, we have $R_{\rm core} = 1$ so $\Omega_0 = \Omega_{\rm core}$.

4.3 Atomistic and Continuum Subproblems

Restricted Atomistic Problem

The basis for defining an atomistic problem restricted to $\Omega_{\rm a}$ are the Euler-Lagrange equations (2.5.2). By requiring $\boldsymbol{u}_\Omega \in \boldsymbol{\mathcal{U}}_\Omega$, we are effectively imposing Dirichlet boundary conditions (in the sense of equivalence classes) for the variational problem by requiring the function to be constant outside Ω. Accordingly, we will define a restricted atomistic problem by also specifying Dirichlet boundary conditions on the atomistic boundary, $\partial_{\rm a}\mathcal{L}_{\rm a}$.

The admissible displacement space for this problem is $\boldsymbol{\mathcal{U}}^{\rm a} := \mathcal{U}^{\rm a}/\mathbb{R}^d$ where

$$\mathcal{U}^{\rm a} := \left\{ u^{\rm a} : \mathcal{L}_{\rm a} \to \mathbb{R}^d \right\}.$$

The elements of $\boldsymbol{\mathcal{U}}^{\rm a}$ are equivalence classes, $\boldsymbol{u}^{\rm a}$, of lattice functions on $\mathcal{L}_{\rm a}$ differing by a constant $c \in \mathbb{R}^d$. We again use I to denote the piecewise linear interpolant of a lattice function on $\mathcal{L}_{\rm a}$ and endow $\boldsymbol{\mathcal{U}}^{\rm a}$ with the norm $\|\nabla I \boldsymbol{u}^{\rm a}\|_{L^2(\Omega_{\rm a})}$. We then define a restricted atomistic energy functional on $\boldsymbol{\mathcal{U}}^{\rm a}$ via

$$\tilde{\mathcal{E}}^{\rm a}(\boldsymbol{u}^{\rm a}) := \sum_{\xi \in \mathcal{L}_{\rm a}^\circ} V_\xi(D\boldsymbol{u}^{\rm a}(\xi)).$$

We seek to minimize $\tilde{\mathcal{E}}^{\rm a}(\boldsymbol{u}^{\rm a})$ over $\boldsymbol{\mathcal{U}}^{\rm a}$ subject to Dirichlet boundary conditions on $\partial_{\rm a}\mathcal{L}_{\rm a}$. The set of all possible boundary values is the quotient space $\boldsymbol{\Lambda}^{\rm a} := \Lambda^{\rm a}/\mathbb{R}^d$, where

$$\Lambda^{\rm a} := \left\{ \lambda_{\rm a} : \partial_{\rm a}\mathcal{L}_{\rm a} \to \mathbb{R}^d \right\}.$$

Elements of $\boldsymbol{\Lambda}^{\rm a}$ are denoted again by $\lambda_{\rm a}$ (without boldface). Thus, the restricted atomistic problem reads

$$\boldsymbol{u}^{\rm a} = \operatorname*{arg\,min}_{\boldsymbol{\mathcal{U}}^{\rm a}} \tilde{\mathcal{E}}^{\rm a}(\boldsymbol{w}^{\rm a}) \quad \text{subject to} \quad \boldsymbol{u}^{\rm a} = \lambda_{\rm a} \quad \text{on} \quad \partial_{\rm a}\mathcal{L}_{\rm a}. \tag{4.3.1}$$

We refer to $\lambda_{\rm a}$ as a *virtual atomistic control* using the terminology of [26]. They are virtual because $\partial_{\rm a}\mathcal{L}_{\rm a}$ is an artificial rather than a physical boundary. They are controls because by varying $\lambda_{\rm a}$ we can "control" the solutions of (4.3.1).

The Euler-Lagrange equation for (4.3.1) is to find $\boldsymbol{u}^{\rm a} \in \boldsymbol{\mathcal{U}}^{\rm a}$ such that

$$\begin{aligned} \langle \delta\tilde{\mathcal{E}}^{\rm a}(\boldsymbol{u}^{\rm a}), \boldsymbol{v}^{\rm a} \rangle &= 0 \quad \forall \boldsymbol{v}^{\rm a} \in \boldsymbol{\mathcal{U}}^{\rm a}_0, \\ \boldsymbol{u}^{\rm a} &= \lambda_{\rm a} \quad \text{on} \quad \partial_{\rm a}\mathcal{L}_{\rm a}, \end{aligned} \tag{4.3.2}$$

where the space of atomistic test functions, $\boldsymbol{\mathcal{U}}_0^{\mathrm{a}} := \mathcal{U}_0^{\mathrm{a}}/\mathbb{R}^d$, is the quotient space of

$$\mathcal{U}_0^{\mathrm{a}} := \left\{ u^{\mathrm{a}} \in \mathcal{U}^{\mathrm{a}} : \exists\, c \in \mathbb{R}^d,\, u^{\mathrm{a}}|_{\partial_{\mathrm{a}}\mathcal{L}_{\mathrm{a}}} = c \right\}.$$

Because $\boldsymbol{v}^{\mathrm{a}} \in \boldsymbol{\mathcal{U}}_0^{\mathrm{a}}$ is constant on $\partial_{\mathrm{a}}\mathcal{L}_{\mathrm{a}}$, it can be extended by the same constant to be defined on all of $\mathcal{L}$, and the extended function, which we still denote by $\boldsymbol{v}^{\mathrm{a}}$, will belong to $\boldsymbol{\mathcal{U}}_0$ since the support of the gradient will remain bounded. We now utilize [23, (2.5) in Lemma 2.1]:

Proposition 4.3.1. *For $\xi \in \mathcal{L}$ and $u \in \mathcal{U}$,*

$$|D_\rho u(\xi)| \lesssim \|\nabla u\|_{L^\infty(B_{|\rho|(\xi)})} \quad \textit{and} \quad \sum_{\xi\in\mathcal{L}} \sup_{\rho\in\mathcal{R}} |D_\rho u(\xi)|^2 \lesssim \|\nabla u\|_{L^2(\mathbb{R}^d)}. \tag{4.3.3}$$

Since $\boldsymbol{v}^{\mathrm{a}}$ is constant on $\partial_{\mathrm{a}}\mathcal{L}_{\mathrm{a}}$, this proposition implies

$$\sum_{\xi\in\mathcal{L}_{\mathrm{a}}^\circ} \sup_{\rho\in\mathcal{R}} |D_\rho \boldsymbol{v}^{\mathrm{a}}|^2 = \sum_{\xi\in\mathcal{L}} \sup_{\rho\in\mathcal{R}} |D_\rho \boldsymbol{v}^{\mathrm{a}}|^2 \lesssim \|\nabla I\boldsymbol{v}^{\mathrm{a}}\|_{L^2(\mathbb{R}^d)}^2 = \|\nabla I\boldsymbol{v}^{\mathrm{a}}\|_{L^2(\Omega_{\mathrm{a}})}^2 \quad \forall \boldsymbol{v}^{\mathrm{a}} \in \boldsymbol{\mathcal{U}}_0^{\mathrm{a}}. \tag{4.3.4}$$

Moreover, this same extension process allows us to deduce, from Propostion 2.3.2, that

Theorem 4.3.2. *The restricted energy functional $\tilde{\mathcal{E}}^{\mathrm{a}}$ is four times Fréchet differentiable on $\boldsymbol{\mathcal{U}}^{\mathrm{a}}$, and each derivative is uniformly bounded in the parameter R_{core}. In particular, $\delta^2\tilde{\mathcal{E}}^{\mathrm{a}}$ is Lipschitz continuous on $\boldsymbol{\mathcal{U}}^{\mathrm{a}}$ with Lipschitz bound independent of R_{core}.*

Proof. The fact that the energy is four times Fréchet differentiable on $\boldsymbol{\mathcal{U}}^{\mathrm{a}}$ is clear since it is a finite sum of C^4 functions. For boundedness, we use the expressions for derivatives

of the atomistic energy given in Chapter 2.

$$\begin{aligned}
\delta^k\tilde{\mathcal{E}}^{\mathrm{a}}(\boldsymbol{u})[\boldsymbol{v}_1,\boldsymbol{v}_2,\dots,\boldsymbol{v}_k] = &\sum_{\xi}\sum_{\boldsymbol{\rho}\in\mathcal{R}^k} V_{\xi,\boldsymbol{\rho}}(D\boldsymbol{u}(\xi))[D_{\rho_1}\boldsymbol{v}_1(\xi), D_{\rho_2}\boldsymbol{v}_2(\xi),\dots,D_{\rho_k}\boldsymbol{v}_k(\xi)] \\
\lesssim &\sum_{\xi}\sum_{\boldsymbol{\rho}\in\mathcal{R}^k} M_k|D_{\rho_1}\boldsymbol{v}_1(\xi)|\cdot|D_{\rho_2}\boldsymbol{v}_2(\xi)|\cdots|D_{\rho_k}\boldsymbol{v}_k(\xi)| \\
\lesssim &\|\nabla I\boldsymbol{v}_3\|_{L^2(\mathbb{R}^d)}\cdots\|\nabla I\boldsymbol{v_k}\|_{L^2(\mathbb{R}^d)}\sum_{\xi}\sum_{\rho,\tau\in\mathcal{R}}|D_\rho\boldsymbol{v}_1(\xi)|\cdot|D_\tau\boldsymbol{v}_2(\xi)| \\
\lesssim &\|\nabla I\boldsymbol{v}_3\|_{L^2(\mathbb{R}^d)}\cdots\|\nabla I\boldsymbol{v_k}\|_{L^2(\mathbb{R}^d)}\sum_{\xi}\sup_{\rho\in\mathcal{R}}|D_\rho\boldsymbol{v}_1(\xi)|\cdot\sup_{\tau\in\mathcal{R}}|D_\tau\boldsymbol{v}_2(\xi)| \\
\leq &\|\nabla I\boldsymbol{v}_3\|_{L^2(\mathbb{R}^d)}\cdots\|\nabla I\boldsymbol{v_k}\|_{L^2(\mathbb{R}^d)}\left\{\sum_{\xi}\sup_{\rho\in\mathcal{R}}|D_\rho\boldsymbol{v}_1(\xi)|^2\right\}^{1/2}\left\{\sum_{\xi}\sup_{\tau\in\mathcal{R}}|D_\tau\boldsymbol{v}_2(\xi)|^2\right\}^{1/2} \\
\lesssim &\|\nabla I\boldsymbol{v}_1\|_{L^2(\mathbb{R}^d)}\|\nabla I\boldsymbol{v}_2\|_{L^2(\mathbb{R}^d)}\|\nabla I\boldsymbol{v}_3\|_{L^2(\mathbb{R}^d)}\cdots\|\nabla I\boldsymbol{v_k}\|_{L^2(\mathbb{R}^d)}.
\end{aligned}$$

□

Given the exact solution $\boldsymbol{u}^\infty$, we will later require solving (4.3.2) where we take $\lambda_{\mathrm{a}} = \boldsymbol{u}^\infty|_{\partial_{\mathrm{a}}\mathcal{L}_{\mathrm{a}}}$. To do that, first set $\boldsymbol{u}^\infty_{\mathrm{a}} := \boldsymbol{u}^\infty|_{\mathcal{L}_{\mathrm{a}}}$ and identify $\boldsymbol{v}^{\mathrm{a}} \in \boldsymbol{\mathcal{U}}^{\mathrm{a}}_0$ as an element of $\boldsymbol{\mathcal{U}}_0$ (via extension by a constant). Then we have

$$\begin{aligned}
\left\langle\delta\tilde{\mathcal{E}}^{\mathrm{a}}(\boldsymbol{u}^\infty_{\mathrm{a}}),\boldsymbol{v}^{\mathrm{a}}\right\rangle = &\sum_{\xi\in\mathcal{L}^\circ_{\mathrm{a}}}\sum_{\rho\in\mathcal{R}} V_{\xi,\rho}(D\boldsymbol{u}^\infty_{\mathrm{a}}(\xi))\cdot D_\rho v^{\mathrm{a}}(\xi) \\
= &\sum_{\xi\in\mathcal{L}}\sum_{\rho\in\mathcal{R}} V_{\xi,\rho}(D\boldsymbol{u}^\infty(\xi))\cdot D_\rho v^{\mathrm{a}}(\xi) \quad \text{since } D_\rho v^{\mathrm{a}}(\xi) \text{ is zero on } \mathcal{L}\backslash\mathcal{L}^\circ_{\mathrm{a}} \\
= &\left\langle\delta\mathcal{E}^{\mathrm{a}}(\boldsymbol{u}^\infty),\boldsymbol{v}^{\mathrm{a}}\right\rangle = 0.
\end{aligned}$$

The final equality holds since $\boldsymbol{u}^\infty$ solves the Euler Lagrange equations (2.3.6). Similarly, Assumption A implies

$$\gamma_{\mathrm{a}}\|\nabla I\boldsymbol{v}^{\mathrm{a}}\|^2_{L^2(\Omega_{\mathrm{a}})} = \gamma_{\mathrm{a}}\|\nabla I\boldsymbol{v}^{\mathrm{a}}\|^2_{L^2(\mathbb{R}^d)} \leq \left\langle\delta^2\mathcal{E}^{\mathrm{a}}(\boldsymbol{u}^\infty_{\mathrm{a}})\boldsymbol{v}^{\mathrm{a}},\boldsymbol{v}^{\mathrm{a}}\right\rangle = \left\langle\delta^2\tilde{\mathcal{E}}^{\mathrm{a}}(\boldsymbol{u}^\infty)\boldsymbol{v}^{\mathrm{a}},\boldsymbol{v}^{\mathrm{a}}\right\rangle. \quad (4.3.5)$$

Hence the solution to (4.3.2) for $\lambda_{\mathrm{a}} = \boldsymbol{u}^\infty|_{\partial_{\mathrm{a}}\mathcal{L}_{\mathrm{a}}}$ is precisely $\boldsymbol{u}^\infty_{\mathrm{a}} := \boldsymbol{u}^\infty|_{\mathcal{L}_{\mathrm{a}}}$. To avoid unnecessary notation, we will often drop the subscript and just write $\boldsymbol{u}^\infty$ as the solution to this problem. It is not immediately clear whether the restricted atomistic problem has a solution for a given virtual control λ_{a}, but we further identify in Section 5.3.1 a class of λ_{a} for which the problem (4.3.2) does possess a solution.

Restricted Continuum

We define the continuum subproblem analogously by using the Euler-Lagrange equations corresponding to minimizing the Cauchy-Born energy (3.2.1). In addition to the atomistic mesh, $\mathcal{T}_{\rm a}$, that covers $\Omega_{\rm a}$ and $\Omega_{\rm c}$, we introduce a continuum partition, $\mathcal{T}_h$, of $\Omega_{\rm c}$. We use $\mathcal{T}_h$ to define an admissible continuum finite element displacement space. Let $\mathcal{N}_h$ be the nodes of $\mathcal{T}_h$. We call a continuum mesh *fully resolved* over a domain U if for each $T \in \mathcal{T}_h$ with $T \subset U$, we have $T \in \mathcal{T}_{\rm a}$ and vice versa. In other words, the continuum and atomistic mesh coincide over U. Further define

$$h_T := \mathrm{Diam}(T), \quad \text{and} \quad h(x) := \sup_{\{T \in \mathcal{T}_h : x \in T\}} h_T.$$

For example, if x is a vertex of a triangle, then $h(x)$ is the largest diameter of the triangles which share this vertex. Our error estimates require the following assumptions on $\mathcal{T}_h$.

Assumption B. *The continuum mesh, $\mathcal{T}_h$, satisfies*

E.1 *The continuum mesh is fully resolved on $\Omega_{\rm o,ex}$.*

E.2 *Nodes in $\mathcal{N}_h$ are also nodes of $\mathcal{T}_{\rm a}$.*

E.3 *The elements $T \in \mathcal{T}_h$ satisfy a minimum angle condition for some fixed $\beta > 0$.*

E.4 *The mesh size function $h(x)$ satisfies $|h(x)| \lesssim (|x|/R_{\rm core})^{\frac{1+d}{1+d/2}}$. (This condition will be shown optimal in Section 6.3.)*

We will also need the inner and outer continuum boundaries defined as

$$\Gamma_{\rm core} := \partial\Omega_{\rm core} \quad \text{and} \quad \Gamma_{\rm c} := \partial\Omega_{\rm c} \backslash \Gamma_{\rm core},$$

respectively.

Our analysis uses two families of interpolants. The first family comprises the standard piecewise linear interpolants

$$\begin{aligned} I_h u \in \mathcal{P}^1(\mathcal{T}_h), \quad I_h u(\zeta) = u(\zeta) \quad \forall \zeta \in \mathcal{N}_h, \\ I u \in \mathcal{P}^1(\mathcal{T}_{\rm a}), \quad I u(\xi) = u(\xi) \quad \forall \xi \in \mathcal{L}, \end{aligned}$$

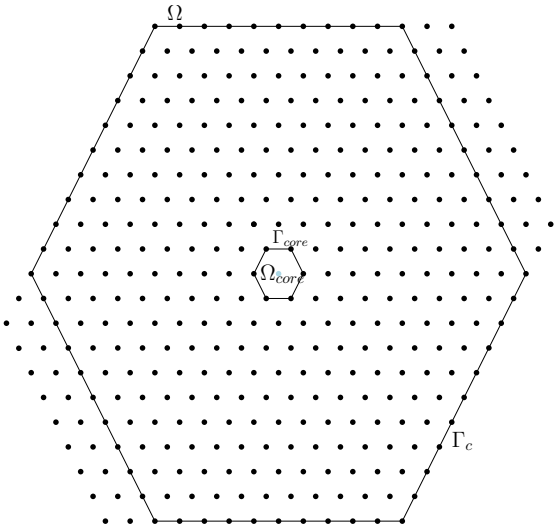

Figure 4.5: Illustration of the inner continuum boundary, Γ_{core}, and outer continuum boundary, Γ_{c}.

defined on the finite element mesh $\mathcal{T}_h$ and the atomistic mesh $\mathcal{T}_{\text{a}}$, respectively. The second family comprises Scott-Zhang (quasi-)interpolants [9,64] which we denote by S_{a}, $S_{\text{a},n}$, and $S_{h,n}$. The first, S_{a}, is defined on Ω_{c} with the atomistic mesh, $\mathcal{T}_{\text{a}}$; the second, $S_{\text{a},n}$ is defined on a domain $\tilde{\Omega}_{\text{a}}$ with a mesh $\tilde{\mathcal{T}}_{\text{a},n} = \epsilon_n \mathcal{T}_{\text{a}}$ for some $\epsilon_n > 0$; and finally, $S_{h,n}$ is defined on a domain $\tilde{\Omega}_{\text{c}}$ with mesh $\tilde{\mathcal{T}}_{h,n} = \epsilon_n \mathcal{T}_h$. (We refer to Section 5.4.1 for the precise definition of these domains.) We recall that for a given domain V, a mesh partition $\mathcal{T}$, and a function $f \in H^1(V)$, the Scott-Zhang interpolant Sf has the following four properties [9, Chapter 4]:

P.1 (Projection) $Sf = f$ for all $f \in \mathcal{P}^1(\mathcal{T})$.

P.2 (Preservation of Homogeneous Boundary Conditions) If f is constant on the boundary, ∂V, of a set V, then so is Sf.[3]

P.3 (Stability of seminorm) $\|\nabla Sf\|_{L^2(V)} \lesssim \|\nabla f\|_{L^2(V)}$ - the implied constant depending upon the shape regularity constant, or minimum angle of the mesh $\mathcal{T}$.

P.4 (Interpolation Error for S) $\|Sf - f\|_{L^2(V)} \lesssim \max_{T \in \mathcal{T}} \text{Diam}(T) \|\nabla f\|_{L^2(V)}$.

[3] The Scott-Zhang interpolant is formally introduced to preserve zero boundary conditions but that fact combined with the projection property imply the result for any constant boundary condition.

The space of admissible continuum displacements is $\boldsymbol{\mathcal{U}}_h^{\mathrm{c}} := \mathcal{U}_h^{\mathrm{c}}/\mathbb{R}^d$, where

$$\mathcal{U}_h^{\mathrm{c}} := \left\{ u^{\mathrm{c}} \in \mathrm{C}^0(\Omega_{\mathrm{c}}) : u^{\mathrm{c}}|_T \in \mathcal{P}^1(T) \;\; \forall T \in \mathcal{T}_h,\, \exists\, K \in \mathbb{R}^d,\, u^{\mathrm{c}} = K \;\text{ on } \Gamma_{\mathrm{c}} \right\}.$$

Thus, we are considering piecewise linear finite elements. The norm on this space is $\|\nabla \boldsymbol{u}^{\mathrm{c}}\|_{L^2(\Omega_{\mathrm{c}})}$. Similar to the definition of $\boldsymbol{\mathcal{U}}_\Omega$, we require the elements of $\boldsymbol{\mathcal{U}}_h^{\mathrm{c}}$ to be constant on the *outer* continuum boundary Γ_{c}, which enables their extension to infinity by a constant. We do not place such a requirement on the *inner* continuum boundary because Γ_{core} is an artificial boundary. There we will employ *virtual continuum* boundary controls belonging to the space $\boldsymbol{\Lambda}^{\mathrm{c}} := \Lambda^{\mathrm{c}}/\mathbb{R}^d$ where

$$\Lambda^{\mathrm{c}} := \left\{ \lambda_{\mathrm{c}} : \mathcal{N}_h \cap \Gamma_{\mathrm{core}} \to \mathbb{R}^d \right\}.$$

Since Γ_{core} represents a curve comprised of a union of edges in the finite element mesh, we can define the piecewise linear interpolant of $\lambda_{\mathrm{c}} \in \Lambda_{\mathrm{c}}$ with respect to $\mathcal{N}_h \cap \Gamma_{\mathrm{core}}$ by $I\lambda_{\mathrm{c}}(\xi) = \lambda_{\mathrm{c}}(\xi)$ for all $\xi \in \mathcal{N}_h \cap \Gamma_{\mathrm{core}}$. Again, if λ_{c} is constant on Γ_{core}, then $I\lambda_{\mathrm{c}}$ is as well so that this operator is well defined on $\boldsymbol{\Lambda}^{\mathrm{c}}$. Henceforth, we will always identify elements of $\boldsymbol{\Lambda}^{\mathrm{c}}$ with their piecewise linear interpolant on Γ_{core} without explicitly using I.

The restricted continuum energy functional on $\boldsymbol{\mathcal{U}}_h^{\mathrm{c}}$ is then simply given by integrating the Cauchy-Born strain energy density from Chapter 3 over Ω_{c}. Since this strain energy density is a function of the displacement gradient and since the displacement gradient is constant on each simplex T, the restricted continuum energy is

$$\tilde{\mathcal{E}}^{\mathrm{c}}(\boldsymbol{u}^{\mathrm{c}}) := \int_{\Omega_{\mathrm{c}}} W(\nabla \boldsymbol{u}^{\mathrm{c}}(x))\, dx = \sum_{T \in \mathcal{T}_h} W(\nabla \boldsymbol{u}^{\mathrm{c}}|_T)\, |T|\,,$$

where $|T|$ represents the volume of the simplex T. Given $\lambda_{\mathrm{c}} \in \boldsymbol{\Lambda}^{\mathrm{c}}$, we then consider the following restricted continuum problem

$$\boldsymbol{u}^{\mathrm{c}} = \operatorname*{arg\,min}_{\boldsymbol{\mathcal{U}}_h^{\mathrm{c}}} \tilde{\mathcal{E}}^{\mathrm{c}}(\boldsymbol{w}^{\mathrm{c}}) \quad \text{such that} \quad \boldsymbol{u}^{\mathrm{c}} = \lambda_{\mathrm{c}} \quad \text{on} \quad \Gamma_{\mathrm{core}}. \tag{4.3.6}$$

An appropriate space of test functions for (4.3.6) is $\boldsymbol{\mathcal{U}}_{h,0}^{\mathrm{c}} := \mathcal{U}_{h,0}^{\mathrm{c}}/\mathbb{R}^d$, where

$$\mathcal{U}_{h,0}^{\mathrm{c}} := \left\{ u^{\mathrm{c}} \in \mathcal{U}_h^{\mathrm{c}} : \exists\, K \in \mathbb{R}^d, u^{\mathrm{c}}|_{\Gamma_{\mathrm{core}}} = K \right\}.$$

We note that this space requires functions to be constant on both Γ_{core} and Γ_{c}, but these constants may differ.

Thus, the Euler-Lagrange equation for (4.3.6) is to find $\boldsymbol{u}^{\mathrm{c}} \in \boldsymbol{\mathcal{U}}_h^{\mathrm{c}}$ such that

$$\begin{aligned} \langle \delta\tilde{\mathcal{E}}^{\mathrm{c}}(\boldsymbol{u}^{\mathrm{c}}), \boldsymbol{v}^{\mathrm{c}} \rangle &= 0 \quad \forall \boldsymbol{v}^{\mathrm{c}} \in \boldsymbol{\mathcal{U}}_{h,0}^{\mathrm{c}}, \\ \boldsymbol{u}^{\mathrm{c}} &= \lambda_{\mathrm{c}} \quad \text{on} \quad \Gamma_{\mathrm{core}}. \end{aligned} \tag{4.3.7}$$

The following lemma is an analogue of Theorem 4.3.2.

Lemma 4.3.3. *The restricted continuum energy functional $\tilde{\mathcal{E}}^{\mathrm{c}}$ is four times continuously Fréchet differentiable on $\boldsymbol{\mathcal{U}}_h^{\mathrm{c}}$ with derivatives bounded uniformly in the parameter R_{c}. Moreover, $\delta^2\tilde{\mathcal{E}}^{\mathrm{c}}$ is Lipschitz continuous with Lipschitz bound independent of R_{c}.*

Continuum Error

This section estimates the error between the restricted continuum solution obtained by solving the continuum problem with exact atomistic boundary data (i.e. $\lambda_{\mathrm{c}} = u^{\infty}|_{\Gamma_{\mathrm{core}}}$) and the exact atomistic solution restricted to Ω_{c}. Naturally, the error is estimated only on Ω_{c}. We refer to this error as the *continuum error*. Since there are no defects present here, we expect from the discussion in Section 3.3 that the Cauchy-Born rule is second order accurate. But because we utilize piecewise linear finite elements, we should expect the continuum error to only be a *first* order accurate in the sense of the scaling at the end of Section 3.3.

We will first define an operator which maps functions in $\boldsymbol{\mathcal{U}}$ to functions in $\boldsymbol{\mathcal{U}}_h^{\mathrm{c}}$. Applying this operator to $\boldsymbol{u}^{\infty}$ will yield a representation of the atomistic solution in $\boldsymbol{\mathcal{U}}_h^{\mathrm{c}}$ which can be inserted into the variational equation (4.3.7) to obtain the consistency error.

To this end, let η be a smooth bump function equal to 1 on $B_{3/4}(0)$ and vanishing off of $B_1(0)$. Given $R > 0$ and an annulus $A_R := B_R \backslash B_{3/4R}$, we follow [23, 37] to define an operator $T_R : \boldsymbol{\mathcal{U}} \to \boldsymbol{\mathcal{U}}_\Omega$ according to

$$T_R\boldsymbol{u}(x) = \eta(x/R)\big(\tilde{I}\boldsymbol{u} - \fint_{A_R} \tilde{I}\boldsymbol{u}\, dx\big).$$

We then set

$$\Pi_h\boldsymbol{u} = I_h\left((T_{r_{\mathrm{c}}}\boldsymbol{u})\,|_{\Omega_{\mathrm{c}}}\right).$$

(Note these are not the same operators as those defined in the proof of Proposition 2.3.1 because we are now using a smooth interpolant and A_R is defined as an annulus here.)

We will use $\Pi_h \boldsymbol{u}^\infty$ in (4.3.7) to obtain the consistency error. The following lemma estimates the error of this operator over $\Omega_{\rm c}$. We note that the proof below is standard and is similar to, e.g., [55, Lemma 2.1] and Proposition 2.3.1. An analogous result is stated in [37, Lemma 4.4], but our result varies slightly in that we use a different interpolant and are stating the estimate over $\Omega_{\rm c}$. Since $r_{\rm core} \lesssim R_{\rm core} \lesssim r_{\rm core}$ and $r_{\rm c} \lesssim R_{\rm c} \lesssim r_{\rm c}$, the estimates in terms of $R_{\rm core}$ and $R_{\rm c}$ can be phrased in terms of $r_{\rm core}$ and $r_{\rm c}$ and vice versa.

Lemma 4.3.4. *Let Π_h and $\tilde{I}$ be as defined above, and recall the definition of $\boldsymbol{u}^\infty$ as the global atomistic solution. Then*

$$\|\nabla \Pi_h \boldsymbol{u}^\infty - \nabla \tilde{I} \boldsymbol{u}^\infty\|_{L^2(\Omega_{\rm c})} \lesssim R_{\rm core}^{-d/2-1} + R_{\rm c}^{-d/2}. \tag{4.3.8}$$

Proof. Recalling the definition $\Pi_h = I_h T_{r_{\rm c}}$, we first estimate the error by using the triangle inequality

$$\|\nabla I_h T_{r_{\rm c}} \boldsymbol{u}^\infty - \nabla \tilde{I} \boldsymbol{u}^\infty\|_{L^2(\Omega_{\rm c})} \leq \|\nabla I_h T_{r_{\rm c}} \boldsymbol{u}^\infty - \nabla T_{r_{\rm c}} \boldsymbol{u}^\infty\|_{L^2(\Omega_{\rm c})} + \|\nabla T_{r_{\rm c}} \boldsymbol{u}^\infty - \nabla \tilde{I} \boldsymbol{u}^\infty\|_{L^2(\Omega_{\rm c})}. \tag{4.3.9}$$

We can easily estimate the second term immediately above just as in [55, Lemma 2.1]:

$$\begin{aligned}
&\|\nabla T_{r_{\rm c}} \boldsymbol{u}^\infty - \nabla \tilde{I} \boldsymbol{u}^\infty\|_{L^2(\Omega_{\rm c})} \\
&= \big\| \tfrac{1}{r_{\rm c}} \nabla \eta(x/r_{\rm c}) \big(\tilde{I} \boldsymbol{u}^\infty - \fint_{A_{r_{\rm c}}} \tilde{I} \boldsymbol{u}^\infty \, dx \big) + [\eta(x/r_{\rm c}) - 1] \nabla \tilde{I} \boldsymbol{u}^\infty \big\|_{L^2(\Omega_{\rm c})} \\
&\lesssim \frac{1}{r_{\rm c}} \big\| \nabla \eta(x/r_{\rm c}) \big(\tilde{I} \boldsymbol{u}^\infty - \fint_{A_{r_{\rm c}}} \tilde{I} \boldsymbol{u}^\infty \, dx \big) \big\|_{L^2(A_{r_{\rm c}})} + \|(\eta(x/r_{\rm c}) - 1) \nabla \tilde{I} \boldsymbol{u}^\infty\|_{L^2(\mathbb{R}^d \setminus B_{3r_{\rm c}/4})} \\
&\lesssim \|\nabla \tilde{I} \boldsymbol{u}^\infty\|_{L^2(A_{r_{\rm c}})} + \|\nabla \tilde{I} \boldsymbol{u}^\infty\|_{L^2(\mathbb{R}^d \setminus B_{3r_{\rm c}/4})} \lesssim \|\nabla \tilde{I} \boldsymbol{u}^\infty\|_{L^2(\mathbb{R}^d \setminus B_{3r_{\rm c}/4})}.
\end{aligned}$$

In the first inequality, we have used the fact that $\nabla \eta(x/r_{\rm c})$ vanishes off $A_{r_{\rm c}}$ to place the norm over $A_{r_{\rm c}}$. In the second inequality, we have merely applied the Poincaré inequality and L^∞ boundedness of $(\eta(x/r_{\rm c}) - 1)$. Employing the decay rates in Theorem 2.4.2, we obtain

$$\|\nabla T_{r_{\rm c}} \boldsymbol{u}^\infty - \nabla \tilde{I} \boldsymbol{u}^\infty\|_{L^2(\Omega_{\rm c})} \lesssim R_{\rm c}^{-d/2}. \tag{4.3.10}$$

Similarly, the first term of (4.3.9) can be estimated by using standard finite element approximation results for smooth functions, the definition of $T_{r_{\rm c}}$, the fact that $h/r_{\rm c} \leq 1$,

the Poincaré inequality, and L^∞ boundedness of $(\nabla\eta)(x/r_{\rm c})$:

$$\begin{aligned}
\|\nabla I_h T_{r_{\rm c}}\boldsymbol{u}^\infty - \nabla T_{r_{\rm c}}\boldsymbol{u}^\infty\|_{L^2(\Omega_{\rm c})} \lesssim\ & \|h\nabla^2 T_{r_{\rm c}}\boldsymbol{u}^\infty\|_{L^2(\Omega_{\rm c})} \\
=\ & \big\|h\nabla^2\big(\eta(x/r_{\rm c})(\tilde{I}\boldsymbol{u}^\infty - \fint_{A_{r_{\rm c}}}\tilde{I}\boldsymbol{u}^\infty\,dx)\big)\big\|_{L^2(\Omega_{\rm c})} \\
\lesssim\ & \frac{1}{r_{\rm c}}\big\|(h/r_{\rm c})\nabla^2\eta(x/r_{\rm c})(\tilde{I}\boldsymbol{u}^\infty - \fint_{A_{r_{\rm c}}}\tilde{I}\boldsymbol{u}^\infty\,dx)\big\|_{L^2(A_{r_{\rm c}})} + \|h\nabla\tilde{I}\boldsymbol{u}^\infty\otimes\nabla(\eta(x/r_{\rm c}))\|_{L^2(A_{r_{\rm c}})} \\
& + \|h\eta(x/r_{\rm c})\nabla^2\tilde{I}\boldsymbol{u}^\infty\|_{L^2(\Omega_{\rm c})} \\
\lesssim\ & \|\nabla\tilde{I}\boldsymbol{u}^\infty\|_{L^2(A_{r_{\rm c}})} + \frac{1}{r_{\rm c}}\|h\nabla\tilde{I}\boldsymbol{u}^\infty\|_{L^2(A_{r_{\rm c}})} + \|h\nabla^2\tilde{I}\boldsymbol{u}^\infty\|_{L^2(\Omega_{\rm c})} \\
\lesssim\ & \|\nabla\tilde{I}\boldsymbol{u}^\infty\|_{L^2(A_{r_{\rm c}})} + \|h\nabla^2\tilde{I}\boldsymbol{u}^\infty\|_{L^2(\Omega_{\rm c})}.
\end{aligned}$$

A straightforward application of the regularity estimates in Theorem 2.4.2 and the conditions on $h(x)$ in Assumption B give

$$\|\nabla I_h T_{r_{\rm c}}\boldsymbol{u}^\infty - \nabla T_{r_{\rm c}}\boldsymbol{u}^\infty\|_{L^2(\Omega_{\rm c})} \lesssim\ R_{\rm c}^{-d/2} + R_{\rm core}^{-d/2-1}. \tag{4.3.11}$$

Combining (4.3.10) and (4.3.11) and keeping only the leading order terms yields (4.3.8). □

Lemma 4.3.6 below provides information about the stability of the Hessian of $\tilde{\mathcal{E}}^{\rm c}$ evaluated at $\Pi_h\boldsymbol{u}^\infty$. To prove it, we will borrow yet another proposition from [23, Proposition 2.6] which states that stability of the defect configuration, $\boldsymbol{u}^\infty$, is enough to imply stability of the reference state with the homogeneous site potential.

Proposition 4.3.5. *For $\boldsymbol{u}\in\boldsymbol{\mathcal{U}}$ define*

$$\mathcal{E}^{\rm a}_{\rm hom}(\boldsymbol{u}) := \sum_{\xi\in\mathbb{Z}^d} V(D\boldsymbol{u}).$$

Under Assumption A,

$$\langle\delta^2\mathcal{E}^{\rm a}_{\rm hom}(\boldsymbol{0})\boldsymbol{v},\boldsymbol{v}\rangle \geq \gamma_{\rm a}\|\nabla I\boldsymbol{v}\|^2_{L^2(\mathbb{R}^d)} \quad \forall\boldsymbol{v}\in\boldsymbol{\mathcal{U}}_0.$$

Lemma 4.3.6. *There exists $R^*_{\rm core}>0$ and $\gamma_{\rm c}>0$ such that for all $R_{\rm core}\geq R^*_{\rm core}$ (and all continuum partitions $\mathcal{T}_h$ satisfying the requirements of Section 4.3 and $\boldsymbol{E}.1-\boldsymbol{E}.3$),*

$$\gamma_{\rm c}\|\nabla\boldsymbol{v}^{\rm c}\|^2_{L^2(\Omega_{\rm c})} \leq\ \big\langle\delta^2\tilde{\mathcal{E}}^{\rm c}(\Pi_h\boldsymbol{u}^\infty)\boldsymbol{v}^{\rm c},\boldsymbol{v}^{\rm c}\big\rangle \quad \forall\boldsymbol{v}^{\rm c}\in\boldsymbol{\mathcal{U}}^{\rm c}_{h,0}.$$

Proof. Since atomistic stability implies Cauchy-Born stability, Proposition 3.3.1 and Proposition 4.3.5 imply

$$\langle \delta^2 \mathcal{E}^{\mathrm{c}}(0)\boldsymbol{v}, \boldsymbol{v}\rangle \geq \gamma_{\mathrm{a}} \|\nabla \boldsymbol{v}\|^2_{L^2(\mathbb{R}^d)} \qquad \forall v \in H^1_0(\mathbb{R}^d).$$

Furthermore, extending $\boldsymbol{v}^{\mathrm{c}} \in \mathcal{U}^{\mathrm{c}}_{h,0}$ by a constant to all of $\mathbb{R}^d$ yields

$$\begin{aligned}
\langle \delta^2 \tilde{\mathcal{E}}^{\mathrm{c}}(\Pi_h \boldsymbol{u}^\infty)\boldsymbol{v}^{\mathrm{c}}, \boldsymbol{v}^{\mathrm{c}}\rangle &= \langle \delta^2 \tilde{\mathcal{E}}^{\mathrm{c}}(\Pi_h \boldsymbol{u}^\infty)\boldsymbol{v}^{\mathrm{c}}, \boldsymbol{v}^{\mathrm{c}}\rangle - \langle \delta^2 \mathcal{E}^{\mathrm{c}}(\boldsymbol{0})\boldsymbol{v}^{\mathrm{c}}, \boldsymbol{v}^{\mathrm{c}}\rangle + \langle \delta^2 \mathcal{E}^{\mathrm{c}}(\boldsymbol{0})\boldsymbol{v}^{\mathrm{c}}, \boldsymbol{v}^{\mathrm{c}}\rangle \\
&\geq -\big|\langle \delta^2 \tilde{\mathcal{E}}^{\mathrm{c}}(\Pi_h \boldsymbol{u}^\infty)\boldsymbol{v}^{\mathrm{c}}, \boldsymbol{v}^{\mathrm{c}}\rangle - \langle \delta^2 \mathcal{E}^{\mathrm{c}}(\boldsymbol{0})\boldsymbol{v}^{\mathrm{c}}, \boldsymbol{v}^{\mathrm{c}}\rangle\big| + \langle \delta^2 \mathcal{E}^{\mathrm{c}}(\boldsymbol{0})\boldsymbol{v}^{\mathrm{c}}, \boldsymbol{v}^{\mathrm{c}}\rangle \\
&\geq -\big|\langle \delta^2 \tilde{\mathcal{E}}^{\mathrm{c}}(\Pi_h \boldsymbol{u}^\infty)\boldsymbol{v}^{\mathrm{c}}, \boldsymbol{v}^{\mathrm{c}}\rangle - \langle \delta^2 \mathcal{E}^{\mathrm{c}}(\boldsymbol{0})\boldsymbol{v}^{\mathrm{c}}, \boldsymbol{v}^{\mathrm{c}}\rangle\big| + \gamma_{\mathrm{a}} \|\nabla \boldsymbol{v}^{\mathrm{c}}\|^2_{L^2(\Omega_{\mathrm{c}})}
\end{aligned}$$

if and only if

$$\begin{aligned}
&\langle \delta^2 \tilde{\mathcal{E}}^{\mathrm{c}}(\Pi_h \boldsymbol{u}^\infty)\boldsymbol{v}^{\mathrm{c}}, \boldsymbol{v}^{\mathrm{c}}\rangle - \gamma_{\mathrm{a}} \|\nabla \boldsymbol{v}^{\mathrm{c}}\|^2_{L^2(\Omega_{\mathrm{c}})} \\
&\geq -\big|\langle \delta^2 \tilde{\mathcal{E}}^{\mathrm{c}}(\Pi_h \boldsymbol{u}^\infty)\boldsymbol{v}^{\mathrm{c}}, \boldsymbol{v}^{\mathrm{c}}\rangle - \langle \delta^2 \mathcal{E}^{\mathrm{c}}(\boldsymbol{0})\boldsymbol{v}^{\mathrm{c}}, \boldsymbol{v}^{\mathrm{c}}\rangle\big| \\
&= -\Big| \int_{\Omega_{\mathrm{c}}} \sum_{\rho,\tau \in \mathcal{R}} [\nabla_\rho \boldsymbol{v}^{\mathrm{c}}]^\top [V_{,\rho\tau}(\nabla_{\mathcal{R}} \Pi_h \boldsymbol{u}^\infty) - V(\boldsymbol{0})][\nabla_\tau \boldsymbol{v}^{\mathrm{c}}]\, dx\Big| \\
&\gtrsim -\|\nabla \Pi_h \boldsymbol{u}^\infty\|_{L^\infty(\Omega_{\mathrm{c}})} \Big| \int_{\Omega_{\mathrm{c}}} |\nabla \boldsymbol{v}^{\mathrm{c}}| \cdot |\nabla \boldsymbol{v}^{\mathrm{c}}|\, dx\Big| \\
&\geq -\|\nabla \Pi_h \boldsymbol{u}^\infty\|_{L^\infty(\Omega_{\mathrm{c}})} \cdot \|\nabla \boldsymbol{v}^{\mathrm{c}}\|^2_{L^2(\Omega_{\mathrm{c}})},
\end{aligned} \tag{4.3.12}$$

where we have employed Lipschitz continuity of the second derivatives of V.

Next,

$$\begin{aligned}
&\|\nabla \Pi_h \boldsymbol{u}^\infty\|_{L^\infty(\Omega_{\mathrm{c}})} \\
&\leq \|\nabla T_{r_{\mathrm{c}}} \boldsymbol{u}^\infty\|_{L^\infty(\Omega_{\mathrm{c}})} \\
&= \big\|\nabla\big[\eta(x/r_{\mathrm{c}})\big(\tilde{I}\boldsymbol{u} - \fint_{A_{r_{\mathrm{c}}}} \tilde{I}\boldsymbol{u}\, dx\big)\big]\big\|_{L^\infty(\Omega_{\mathrm{c}})} \\
&= \big\|\big(\tilde{I}\boldsymbol{u} - \fint_{A_{r_{\mathrm{c}}}} \tilde{I}\boldsymbol{u}\, dx\big) \otimes \nabla(\eta(x/r_{\mathrm{c}})) + \eta(x/r_{\mathrm{c}})\nabla\big(\tilde{I}\boldsymbol{u} - \fint_{A_{r_{\mathrm{c}}}} \tilde{I}\boldsymbol{u}\, dx\big)\big\|_{L^\infty(\Omega_{\mathrm{c}})} \\
&\leq \big\|\nabla(\eta(x/r_{\mathrm{c}}))\big(\tilde{I}\boldsymbol{u} - \fint_{A_{r_{\mathrm{c}}}} \tilde{I}\boldsymbol{u}\, dx\big)\big\|_{L^\infty(A_{r_{\mathrm{c}}})} + \big\|\eta(x/r_{\mathrm{c}})\nabla\big(\tilde{I}\boldsymbol{u} - \fint_{A_{r_{\mathrm{c}}}} \tilde{I}\boldsymbol{u}\, dx\big)\big\|_{L^\infty(\Omega_{\mathrm{c}})} \\
&\lesssim \frac{1}{r_{\mathrm{c}}}\big\|\big(\tilde{I}\boldsymbol{u} - \fint_{A_{r_{\mathrm{c}}}} \tilde{I}\boldsymbol{u}\, dx\big)\big\|_{L^\infty(A_{r_{\mathrm{c}}})} + \|\nabla \tilde{I}\boldsymbol{u}\|_{L^\infty(\Omega_{\mathrm{c}})} \\
&\lesssim \|\nabla \tilde{I}\boldsymbol{u}\|_{L^\infty(A_{r_{\mathrm{c}}})} + \|\nabla \tilde{I}\boldsymbol{u}\|_{L^\infty(\Omega_{\mathrm{c}})} \\
&\lesssim \|\nabla \tilde{I}\boldsymbol{u}\|_{L^\infty(\Omega_{\mathrm{c}})}.
\end{aligned}$$

Using this result in (4.3.12) together with the decay estimates (2.4.2) yields

$$\begin{aligned}\langle \delta^2\tilde{\mathcal{E}}^{\mathrm{c}}(\Pi_h \boldsymbol{u}^\infty)\boldsymbol{v}^{\mathrm{c}}, \boldsymbol{v}^{\mathrm{c}}\rangle - \gamma_{\mathrm{a}}\|\nabla \boldsymbol{v}^{\mathrm{c}}\|^2_{L^2(\Omega_{\mathrm{c}})} &\gtrsim -\|\nabla \tilde{I}\boldsymbol{u}^\infty\|_{L^\infty(\Omega_{\mathrm{c}})}\|\nabla \boldsymbol{v}^{\mathrm{c}}\|^2_{L^2(\Omega_{\mathrm{c}})} \\ &\gtrsim -(R_{\mathrm{core}})^{-d}\|\nabla \boldsymbol{v}^{\mathrm{c}}\|^2_{L^2(\Omega_{\mathrm{c}})}.\end{aligned}$$

Denoting the implied constant in the inequality by $C > 0$, this can be written as

$$\langle \delta^2\tilde{\mathcal{E}}^{\mathrm{c}}(\Pi_h \boldsymbol{u}^\infty)\boldsymbol{v}^{\mathrm{c}}, \boldsymbol{v}^{\mathrm{c}}\rangle \geq \big(-C(R_{\mathrm{core}})^{-d} + \gamma_{\mathrm{a}}\big)\|\nabla \boldsymbol{v}^{\mathrm{c}}\|^2_{L^2(\Omega_{\mathrm{c}})}.$$

Choosing R^*_{core} such that $-C(R^*_{\mathrm{core}})^{-d} + \gamma_{\mathrm{a}} \geq \gamma_{\mathrm{a}}/2$ completes the proof with $\gamma_{\mathrm{c}} := \gamma_{\mathrm{a}}/2$. □

In order to prove there exists a solution to the restricted continuum problem given exact atomistic boundary data, we rely on the following quantitative version of the inverse function theorem [30, 42, 50]. It is the standard tool in proving error estimates for AtC methods and will be used again in this thesis. The idea of the proof behind estimating the continuum error is essentially the proof needed to prove the second order accuracy of the Cauchy-Born rule alluded to earlier.

Theorem 4.3.7 (Inverse Function Theorem)**.** *Let X and Y be Banach spaces with $f : X \to Y$ a continuously differentiable function on an open set U containing x_0. Let $y_0 = f(x_0)$ with $\|y_0\|_Y < \eta$. Furthermore, suppose that $\delta f(x_0)$ is invertible, $\|\delta f(x_0)^{-1}\|_{\mathcal{L}(Y,X)} < \sigma$, $B_{2\eta\sigma}(x_0) \subset U$, δf is Lipschitz continuous on $B_{2\eta\sigma}(x_0)$ with Lipschitz constant L, and $2L\eta\sigma^2 < 1$. Then there exists a unique continuously differentiable function $g : B_\eta(y_0) \to B_{2\eta\sigma}(x_0)$ such that*

$$g(y_0) = x_0 \quad \textit{and} \quad f(g(y)) = y \quad \forall y \in B_\eta(y_0)\,.$$

In particular, there exists $\bar{x} = g(0) \in X$ such that $f(\bar{x}) = 0$ and

$$\|g(y_0) - g(0)\|_X = \|x_0 - \bar{x}\|_X < 2\eta\sigma.$$

We now linearize the continuum Euler-Lagrange equations (4.3.7) about $\Pi_h \boldsymbol{u}^\infty$ and apply the inverse function theorem to deduce the following theorem concerning existence of the solution to the restricted continuum problem given exact atomistic boundary data.

Theorem 4.3.8 (Continuum Error)**.** *Let* $\lambda_{\mathrm{c}}^{\infty} := \boldsymbol{u}^{\infty}|_{\Gamma_{\mathrm{core}}}$. *There exists* $R_{\mathrm{core}}^{*} > 0$ *such that for all* $R_{\mathrm{core}} \geq R_{\mathrm{core}}^{*}$, *the variational problem*

$$\langle \delta\tilde{\mathcal{E}}^{\mathrm{c}}(\boldsymbol{u}), \boldsymbol{v}^{\mathrm{c}} \rangle = 0 \quad \forall \boldsymbol{v}^{\mathrm{c}} \in \boldsymbol{\mathcal{U}}_{h,0}^{\mathrm{c}} \quad \textit{subject to} \quad \boldsymbol{u} = \lambda_{\mathrm{c}}^{\infty} \quad \textit{on} \quad \Gamma_{\mathrm{core}}, \tag{4.3.13}$$

has a solution $\boldsymbol{u}^{\mathrm{con}}$ *such that*

$$\|\nabla \boldsymbol{u}^{\mathrm{con}} - \nabla I\boldsymbol{u}^{\infty}\|_{L^2(\Omega_{\mathrm{c}})} \lesssim R_{\mathrm{core}}^{-d/2-1} + R_{\mathrm{c}}^{-d/2}. \tag{4.3.14}$$

Furthermore, there exists γ_{c}' *such that*

$$\left\langle \delta^2\tilde{\mathcal{E}}^{\mathrm{c}}(\boldsymbol{u}^{\mathrm{con}})\boldsymbol{v}^{\mathrm{c}}, \boldsymbol{v}^{\mathrm{c}} \right\rangle \geq \gamma_{\mathrm{c}}' \|\nabla \boldsymbol{v}^{\mathrm{c}}\|_{L^2(\Omega_{\mathrm{c}})}^2. \tag{4.3.15}$$

Proof. The proof uses ideas from [37, 56]. We employ Theorem 4.3.7 by linearizing $f = \delta\tilde{\mathcal{E}}^{\mathrm{c}}(\cdot)$ about $x_0 = \Pi_h \boldsymbol{u}^{\infty}$. Let R_{core}^{*} be as in Lemma 4.3.6. Then $\delta^2\tilde{\mathcal{E}}^{\mathrm{c}}(\Pi_h \boldsymbol{u}^{\infty})^{-1}$ exists and is bounded by γ_{c}^{-1} for all $R_{\mathrm{core}} \geq R_{\mathrm{core}}^{*}$. Moreover, $\delta^2\tilde{\mathcal{E}}^{\mathrm{c}}$ is Lipschitz continuous by Lemma 4.3.3. It remains to estimate the dual norm of the residual

$$\sup_{\boldsymbol{v}^{\mathrm{c}} \in \boldsymbol{\mathcal{U}}_{h,0}^{\mathrm{c}}, \boldsymbol{v}^{\mathrm{c}} \neq \boldsymbol{0}} \frac{\langle \delta\tilde{\mathcal{E}}^{\mathrm{c}}(\Pi_h \boldsymbol{u}^{\infty}), \boldsymbol{v}^{\mathrm{c}} \rangle}{\|\boldsymbol{v}^{\mathrm{c}}\|_{L^2(\Omega_{\mathrm{c}})}}. \tag{4.3.16}$$

This estimate requires an atomistic version of the stress. Following [56], let $\zeta(x)$ be the nodal basis function at the origin of the atomistic partition $\mathcal{T}_{\mathrm{a}}$, i.e., $\zeta(0) = 1$ and $\zeta(\xi) = 0$ for $0 \neq \xi \in \mathbb{Z}^d$. This allows us to write the interpolant of a lattice function v as $Iv(x) = \sum_{\xi \in \mathbb{Z}^d} v(\xi)\zeta(x - \xi)$. Further define the "quasi-interpolant," v^{*}, by

$$v^{*}(x) := (Iv * \zeta)(x),$$

and note that $v^{*} \in W_{\mathrm{loc}}^{3,\infty}$ [53, 56]. Letting $\chi_{\xi,\rho}(x) := \int_0^1 \zeta(\xi + t\rho - x)\, dt$, the atomistic stress, $\mathsf{S}^{\mathrm{a}}(\boldsymbol{u}, x)$, is then defined by

$$\int_{\mathbb{R}^d} \mathsf{S}^{\mathrm{a}}(\boldsymbol{u}, x) : \nabla I\boldsymbol{v}\, dx := \langle \delta\mathcal{E}^{\mathrm{a}}(\boldsymbol{u}), \boldsymbol{v}^{*} \rangle = \int_{\mathbb{R}^d} \sum_{\xi \in \mathbb{Z}^d} \sum_{\rho \in \mathcal{R}} \chi_{\xi,\rho} V_{\xi,\rho}(D\boldsymbol{u}) \otimes \rho : \nabla I\boldsymbol{v}\, dx. \tag{4.3.17}$$

See [37, 56] for further details.

We now estimate the dual norm of the residual (4.3.16). Fix an element $\boldsymbol{v}^{\mathrm{c}} \in \boldsymbol{\mathcal{U}}_{h,0}^{\mathrm{c}}$, and assume it has been extended to all of $\mathbb{R}^d$. Let $\boldsymbol{w}^{\mathrm{c}} = S_{\mathrm{a}}\boldsymbol{v}^{\mathrm{c}}$ where S_{a} is the Scott-Zhang interpolant onto $\mathcal{T}_{\mathrm{a}}$. Note that $I\boldsymbol{w}^{\mathrm{c}} = IS_{\mathrm{a}}\boldsymbol{v}^{\mathrm{c}} = S_{\mathrm{a}}\boldsymbol{v}^{\mathrm{c}}$ for these choices.

We now subtract $0 = \langle \delta\mathcal{E}^{\mathrm{a}}(\boldsymbol{u}^\infty), \boldsymbol{w}^{\mathrm{c},*}\rangle$ from the numerator of (4.3.16):

$$\begin{aligned}
&\langle \delta\tilde{\mathcal{E}}^{\mathrm{c}}(\Pi_h \boldsymbol{u}^\infty), \boldsymbol{v}^{\mathrm{c}}\rangle \\
&= \langle \delta\tilde{\mathcal{E}}^{\mathrm{c}}(\Pi_h \boldsymbol{u}^\infty), \boldsymbol{v}^{\mathrm{c}}\rangle - \langle \delta\mathcal{E}^{\mathrm{a}}(\boldsymbol{u}^\infty), \boldsymbol{w}^{\mathrm{c},*}\rangle \\
&= \langle \delta\tilde{\mathcal{E}}^{\mathrm{c}}(\Pi_h \boldsymbol{u}^\infty) - \delta\tilde{\mathcal{E}}^{\mathrm{c}}(\tilde{I}\boldsymbol{u}^\infty), \boldsymbol{v}^{\mathrm{c}}\rangle + \langle \delta\tilde{\mathcal{E}}^{\mathrm{c}}(\tilde{I}\boldsymbol{u}^\infty), \boldsymbol{v}^{\mathrm{c}} - S_{\mathrm{a}}\boldsymbol{v}^{\mathrm{c}}\rangle \\
&\quad + (\langle \delta\tilde{\mathcal{E}}^{\mathrm{c}}(\tilde{I}\boldsymbol{u}^\infty), S_{\mathrm{a}}\boldsymbol{v}^{\mathrm{c}}\rangle - \langle \delta\mathcal{E}^{\mathrm{a}}(\boldsymbol{u}^\infty), \boldsymbol{w}^{\mathrm{c},*}\rangle) \\
&=: E_1 + E_2 + E_3.
\end{aligned}$$

The term E_1 can be easily estimated:

$$\begin{aligned}
\langle \delta\tilde{\mathcal{E}}^{\mathrm{c}}(\Pi_h \boldsymbol{u}^\infty) - \delta\tilde{\mathcal{E}}^{\mathrm{c}}(\tilde{I}\boldsymbol{u}^\infty), \boldsymbol{v}^{\mathrm{c}}\rangle &\lesssim \|\nabla\Pi_h \boldsymbol{u}^\infty - \nabla\tilde{I}\boldsymbol{u}^\infty\|_{L^2(\Omega_{\mathrm{c}})}\|\nabla\boldsymbol{v}^{\mathrm{c}}\|_{L^2(\Omega_{\mathrm{c}})} \\
&\lesssim (R_{\mathrm{core}}^{-d/2-1} + R_{\mathrm{c}}^{-d/2})\|\nabla\boldsymbol{v}^{\mathrm{c}}\|_{L^2(\Omega_{\mathrm{c}})} \quad \text{by Lemma 4.3.4.}
\end{aligned}$$

Below we will make use of the notation

$$\begin{aligned}
\langle \delta\tilde{\mathcal{E}}^{\mathrm{c}}(\Pi_h \boldsymbol{u}^\infty), w\rangle &= \int_{\Omega_{\mathrm{c}}} \sum_{\rho\in\mathcal{R}} V_\rho(\nabla_{\mathcal{R}}\Pi_h \boldsymbol{u}^\infty)\cdot\nabla_\rho w \\
&= \int_{\Omega_{\mathrm{c}}} \sum_{\rho\in\mathcal{R}} (V_\rho(\nabla_{\mathcal{R}}\Pi_h \boldsymbol{u}^\infty)\otimes\rho) : \nabla w \\
&:= \int_{\Omega_{\mathrm{c}}} W'(\nabla\Pi_h \boldsymbol{u}^\infty) : \nabla w
\end{aligned}$$

for an arbitrary $w \in H^1(\Omega_{\mathrm{c}})$.

We now estimate E_2 by integrating by parts

$$\begin{aligned}
\langle \delta\tilde{\mathcal{E}}^{\mathrm{c}}(\tilde{I}\boldsymbol{u}^\infty), \boldsymbol{v}^{\mathrm{c}} - S_{\mathrm{a}}\boldsymbol{v}^{\mathrm{c}}\rangle &= \int_{\Omega_{\mathrm{c}}} W'(\nabla\tilde{I}\boldsymbol{u}^\infty) : \nabla(\boldsymbol{v}^{\mathrm{c}} - S_{\mathrm{a}}\boldsymbol{v}^{\mathrm{c}}) \\
&= \int_{\Omega_{\mathrm{c}}} \mathrm{div}(W'(\nabla\tilde{I}\boldsymbol{u}^\infty))\cdot(\boldsymbol{v}^{\mathrm{c}} - S_{\mathrm{a}}\boldsymbol{v}^{\mathrm{c}}) \\
&\le \|\mathrm{div}(W'(\nabla\tilde{I}\boldsymbol{u}^\infty))\|_{L^2(\Omega_{\mathrm{c}})}\cdot\|\boldsymbol{v}^{\mathrm{c}} - S_{\mathrm{a}}\boldsymbol{v}^{\mathrm{c}}\|_{L^2(\Omega_{\mathrm{c}})} \\
&\lesssim \|\nabla^2\tilde{I}\boldsymbol{u}^\infty\|_{L^2(\Omega_{\mathrm{c}})}\|\nabla\boldsymbol{v}^{\mathrm{c}}\|_{L^2(\Omega_{\mathrm{c}})}, \\
&\lesssim R_{\mathrm{core}}^{-d/2-1}\|\nabla\boldsymbol{v}^{\mathrm{c}}\|_{L^2(\Omega_{\mathrm{c}})},
\end{aligned}$$

where we have used the chain rule, bounded the second derivatives of $\tilde{I}\boldsymbol{u}^\infty$ by the quantity $\|\nabla^2\tilde{I}\boldsymbol{u}^\infty\|_{L^2(\Omega_{\mathrm{c}})}$, utilized the interpolation estimate **P.4** for S_{a}, and applied the decay rates of Theorem 2.4.2.

We estimate E_3 by observing

$$\begin{aligned} E_3 = &\int_{\Omega_{\mathrm{c}}} W'(\nabla \tilde{I}\boldsymbol{u}^\infty) : \nabla S_{\mathrm{a}}\boldsymbol{v}^{\mathrm{c}} - \int_{\Omega_{\mathrm{c}}} \mathsf{S}^{\mathrm{a}}(\boldsymbol{u}^\infty, x) : \nabla I\boldsymbol{w}^{\mathrm{c}} \\ = &\int_{\Omega_{\mathrm{c}}} \big(W'\big(\nabla \tilde{I}\boldsymbol{u}^\infty\big) - \mathsf{S}^{\mathrm{a}}(\boldsymbol{u}^\infty, x)\big) : \nabla S_{\mathrm{a}}\boldsymbol{v}^{\mathrm{c}}. \\ \leq &\ \|W'(\nabla \tilde{I}\boldsymbol{u}^\infty) - \mathsf{S}^{\mathrm{a}}(\boldsymbol{u}^\infty, x)\|_{L^2(\Omega_{\mathrm{c}})} \|\nabla S_{\mathrm{a}}\boldsymbol{v}^{\mathrm{c}}\|_{L^2(\Omega_{\mathrm{c}})} \\ \leq &\ \|W'(\nabla \tilde{I}\boldsymbol{u}^\infty) - \mathsf{S}^{\mathrm{a}}(\boldsymbol{u}^\infty, x)\|_{L^2(\Omega_{\mathrm{c}})} \|\nabla \boldsymbol{v}^{\mathrm{c}}\|_{L^2(\Omega_{\mathrm{c}})}, \end{aligned}$$

where in the last step we used the stability of the Scott-Zhang interpolant **P.3**. One may then modify the arguments in [56, Lemma 4.5, Equations (4.22)–(4.24)] to prove that[4]

$$E_3 \lesssim \ (\|\nabla^3 \tilde{I}\boldsymbol{u}^\infty\|_{L^2(\Omega_{\mathrm{c}})} + \|\nabla^2 \tilde{I}\boldsymbol{u}^\infty\|^2_{L^4(\Omega_{\mathrm{c}})}) \|\boldsymbol{v}^{\mathrm{c}}\|_{L^2(\Omega_{\mathrm{c}})},$$

and using the regularity theorem, Theorem 2.4.2, shows $E_3 \lesssim \ R_{\mathrm{core}}^{-d/2-2} \|\boldsymbol{v}^{\mathrm{c}}\|_{L^2(\Omega_{\mathrm{c}})}$.

Combining the bounds on E_1, E_2, and E_3 and keeping only the leading order terms yields the residual estimate

$$\sup_{\boldsymbol{v}^{\mathrm{c}} \in \mathcal{U}_h^{\mathrm{c}}, \boldsymbol{v}^{\mathrm{c}} \neq \boldsymbol{0}} \frac{\langle \delta \tilde{\mathcal{E}}^{\mathrm{c}}(\Pi_h \boldsymbol{u}^\infty), \boldsymbol{v}^{\mathrm{c}} \rangle}{\|\boldsymbol{v}^{\mathrm{c}}\|_{L^2(\Omega_{\mathrm{c}})}} \lesssim \ R_{\mathrm{core}}^{-d/2-1} + R_{\mathrm{c}}^{-d/2}. \tag{4.3.18}$$

Because the residual can be made as small as needed and because $\delta^2 \mathcal{E}^{\mathrm{c}}$ is both Lipschitz and invertible, the inverse function theorem then implies the existence of $\boldsymbol{u}^{\mathrm{con}}$ satisfying (4.3.13) and

$$\|\nabla \boldsymbol{u}^{\mathrm{con}} - \nabla \Pi_h \boldsymbol{u}^\infty\|_{L^2(\Omega_{\mathrm{c}})} \lesssim \ R_{\mathrm{core}}^{-d/2-1} + R_{\mathrm{c}}^{-d/2}. \tag{4.3.19}$$

To prove (4.3.14), observe that

$$\begin{aligned} \|\nabla \boldsymbol{u}^{\mathrm{con}} - \nabla I\boldsymbol{u}^\infty\|_{L^2(\Omega_{\mathrm{c}})} \leq \ &\|\nabla \boldsymbol{u}^{\mathrm{con}} - \nabla \Pi_h \boldsymbol{u}^\infty\|_{L^2(\Omega_{\mathrm{c}})} + \|\nabla \Pi_h \boldsymbol{u}^\infty - \nabla \tilde{I}\boldsymbol{u}^\infty\|_{L^2(\Omega_{\mathrm{c}})} \\ &+ \|\nabla \tilde{I}\boldsymbol{u}^\infty - \nabla I\boldsymbol{u}^\infty\|_{L^2(\Omega_{\mathrm{c}})}. \end{aligned}$$

Hence, combining (4.3.19) and Lemma 4.3.4 yields

$$\|\nabla \boldsymbol{u}^{\mathrm{con}} - \nabla I\boldsymbol{u}^\infty\|_{L^2(\Omega_{\mathrm{c}})} \lesssim \ R_{\mathrm{core}}^{-d/2-1} + R_{\mathrm{c}}^{-d/2} + \|\nabla \tilde{I}\boldsymbol{u}^\infty - \nabla I\boldsymbol{u}^\infty\|_{L^2(\Omega_{\mathrm{c}})}. \tag{4.3.20}$$

[4] The difference is that our choice of $\tilde{I}u$ is not the same as the smooth interpolant used there. Observe this is exactly the second-order form of the error for the Cauchy-Born rule we should suspect.

Since $\tilde{I}\boldsymbol{u}^\infty$ is in $H^2(\Omega_{\rm c})$ and $I\boldsymbol{u}^\infty = I(\tilde{I}\boldsymbol{u}^\infty)$, standard finite element approximation theory and the decay estimates in Theorem 2.4.2 give

$$\|\nabla\tilde{I}\boldsymbol{u}^\infty - \nabla I\boldsymbol{u}^\infty\|_{L^2(\Omega_{\rm c})} = \|\nabla\tilde{I}\boldsymbol{u}^\infty - \nabla I(\tilde{I}\boldsymbol{u}^\infty)\|_{L^2(\Omega_{\rm c})} \lesssim \|\nabla^2\tilde{I}\boldsymbol{u}^\infty\|_{L^2(\Omega_{\rm c})} \lesssim R_{\rm core}^{-d/2-1}. \tag{4.3.21}$$

The last inequalities (4.3.20) and (4.3.21) imply the desired estimate (4.3.14).

To prove the inequality (4.3.15), note that

$$\begin{aligned}\left\langle \delta^2\tilde{\mathcal{E}}(\boldsymbol{u}^{\rm con})\boldsymbol{v}^{\rm c}, \boldsymbol{v}^{\rm c}\right\rangle &= \left\langle \left(\delta^2\tilde{\mathcal{E}}(\boldsymbol{u}^{\rm con}) - \delta^2\tilde{\mathcal{E}}(\Pi_h\boldsymbol{u}^\infty)\right)\boldsymbol{v}^{\rm c}, \boldsymbol{v}^{\rm c}\right\rangle + \left\langle \delta^2\tilde{\mathcal{E}}(\Pi_h\boldsymbol{u}^\infty)\boldsymbol{v}^{\rm c}, \boldsymbol{v}^{\rm c}\right\rangle \\ &\gtrsim -\|\nabla\boldsymbol{u}^{\rm con} - \nabla\Pi_h\boldsymbol{u}^\infty\|_{L^2(\Omega_{\rm c})}\|\nabla v^{\rm c}\|^2_{L^2(\Omega_{\rm c})} + \gamma_{\rm c}\|\nabla v^{\rm c}\|^2_{L^2(\Omega_{\rm c})} \\ &\gtrsim (\gamma_{\rm c} - R_{\rm core}^{-d/2-1} - R_{\rm c}^{-d/2})\|\nabla v^{\rm c}\|^2_{L^2(\Omega_{\rm c})}.\end{aligned}$$

Choosing an appropriate $R^*_{\rm core}$ and $\gamma'_{\rm c}$ completes the proof. □

Finally, we formally introduce the optimization-based AtC method.

4.4 AtC Method

We couple the restricted atomistic and continuum subproblems by minimizing their mismatch on the overlap region. We measure the mismatch by the H^1 seminorm of the difference between the continuum solution and the finite element interpolant of the atomistic solution. The reason the H^1 seminorm is chosen is because this is a norm on the space of atomistic and continuum displacements and is the natural norm on which the energies are defined (recall they are both invariant under addition by constants). Our AtC problem for $d = 2, 3$ is therefore stated as finding $(u^{\rm a}, u^{\rm c}) \in \mathcal{U}^{\rm a}\times\mathcal{U}^{\rm c}_h$, $(\lambda_{\rm a}, \lambda_{\rm c}) \in \Lambda^{\rm a} \times \Lambda^{\rm c}$ that solve the following constrained optimization problem:

$$\min_{\{u^{\rm a},u^{\rm c},\lambda^{\rm a},\lambda^{\rm c}\}} \|\nabla Iu^{\rm a} - \nabla u^{\rm c}\|_{L^2(\Omega_{\rm o})} \quad \text{subject to}$$
$$\left\{ \begin{array}{l} \langle \delta\tilde{\mathcal{E}}^{\rm a}(u^{\rm a}), v^{\rm a}\rangle = 0 \quad \forall v^{\rm a} \in \mathcal{U}^{\rm a}_0 \\ \qquad\qquad u^{\rm a} = \lambda_{\rm a} \quad \text{on } \partial_{\rm a}\mathcal{L}_{\rm a} \end{array} \right. ; \left\{ \begin{array}{c} \langle \delta\tilde{\mathcal{E}}^{\rm c}(u^{\rm c}), v^{\rm c}\rangle = 0 \quad \forall v^{\rm c} \in \mathcal{U}^{\rm c}_{h,0} \\ u^{\rm c} = 0 \ \text{ on } \Gamma_{\rm c} \quad \text{and} \quad u^{\rm c} = \lambda_{\rm c} \ \text{ on } \Gamma_{\rm core} \end{array} \right. ;$$
$$\left\{ \int_{\Omega_{\rm o}} (Iu^{\rm a} - u^{\rm c})\, dx = 0 \right. , \tag{4.4.1}$$

where we recall that $\lambda_{\rm a}$ and $\lambda_{\rm c}$ represent the artificial, virtual controls on the boundaries, $\partial_{\rm a}\mathcal{L}_{\rm a}$ and $\Gamma_{\rm core}$. Observe that this is formulated on the spaces $\mathcal{U}^{\rm a} \times \mathcal{U}^{\rm c}_h$ and $\Lambda^{\rm a} \times$

Λ^{c} (not on equivalence classes yet) so the added constraint $\int_{\Omega_{\mathrm{o}}} (Iu^{\mathrm{a}} - u^{\mathrm{c}})\, dx = 0$ is needed since the optimization functional is invariant under addition by constants. The formulation (4.4.1) is introduced for its amenability to a numerical implementation as discussed in Chapter 6. It was previously used in a numerical implementation by the author in [47].

Remark 4.4.1. *For $d = 1$, there is a slight variation owing to the fact that the overlap region is disconnected. In this case, there are two integral constraints*

$$\int_{\Omega_{\mathrm{o}} \cap \mathbb{R}^+} (Iu^{\mathrm{a}} - u^{\mathrm{c}})\, dx = 0, \quad \textit{and} \quad \int_{\Omega_{\mathrm{o}} \cap \mathbb{R}^-} (Iu^{\mathrm{a}} - u^{\mathrm{c}})\, dx = 0,$$

where $\mathbb{R}^+$ is the set of positive reals and $\mathbb{R}^-$ the set of negative reals.

Alternatively, we may pose the AtC problem on quotient spaces:

$$\min_{\{\boldsymbol{u}^{\mathrm{a}}, \boldsymbol{u}^{\mathrm{c}}, \lambda^{\mathrm{a}}, \lambda^{\mathrm{c}}\}} \|\nabla I\boldsymbol{u}^{\mathrm{a}} - \nabla \boldsymbol{u}^{\mathrm{c}}\|_{L^2(\Omega_{\mathrm{o}})} \quad \text{subject to}$$
$$\begin{cases} \langle \delta\tilde{\mathcal{E}}^{\mathrm{a}}(\boldsymbol{u}^{\mathrm{a}}), \boldsymbol{v}^{\mathrm{a}} \rangle = 0 \quad \forall \boldsymbol{v}^{\mathrm{a}} \in \boldsymbol{\mathcal{U}}_0^{\mathrm{a}} \\ \boldsymbol{u}^{\mathrm{a}} = \lambda_{\mathrm{a}} \quad \text{on } \partial_{\mathrm{a}}\boldsymbol{\mathcal{L}}_{\mathrm{a}} \end{cases}, \quad \begin{cases} \langle \delta\tilde{\mathcal{E}}^{\mathrm{c}}(\boldsymbol{u}^{\mathrm{c}}), \boldsymbol{v}^{\mathrm{c}} \rangle = 0 \quad \forall \boldsymbol{v}^{\mathrm{c}} \in \boldsymbol{\mathcal{U}}_{h,0}^{\mathrm{c}} \\ \boldsymbol{u}^{\mathrm{c}} = \lambda_{\mathrm{c}} \quad \text{on} \quad \Gamma_{\mathrm{core}} \end{cases} . \tag{4.4.2}$$

It is easy to see that (4.4.1) and (4.4.2) are equivalent in the sense that every minimizer, $(u^{\mathrm{a}}, u^{\mathrm{c}}, \lambda_{\mathrm{a}}, \lambda_{\mathrm{c}})$, of the former generates an equivalence class, $(\boldsymbol{u}^{\mathrm{a}}, \boldsymbol{u}^{\mathrm{c}}, \lambda_{\mathrm{a}}, \lambda_{\mathrm{c}})$, that is a minimizer of the latter and vice versa. Indeed, if $(u^{\mathrm{a}}, u^{\mathrm{c}}, \lambda_{\mathrm{a}}, \lambda_{\mathrm{c}})$ solves (4.4.1) then for all $(v^{\mathrm{a}}, v^{\mathrm{c}}, \mu_{\mathrm{a}}, \mu_{\mathrm{c}})$ that solve the variational constraints,

$$\|\nabla I\boldsymbol{u}^{\mathrm{a}} - \nabla \boldsymbol{u}^{\mathrm{c}}\|_{L^2(\Omega_{\mathrm{o}})} = \|\nabla I u^{\mathrm{a}} - \nabla u^{\mathrm{c}}\|_{L^2(\Omega_{\mathrm{o}})} \leq \|\nabla I v^{\mathrm{a}} - \nabla v^{\mathrm{c}}\|_{L^2(\Omega_{\mathrm{o}})} = \|\nabla I\boldsymbol{v}^{\mathrm{a}} - \nabla \boldsymbol{v}^{\mathrm{c}}\|_{L^2(\Omega_{\mathrm{o}})}.$$

Thus, $(\boldsymbol{u}^{\mathrm{a}}, \boldsymbol{u}^{\mathrm{c}}, \lambda_{\mathrm{a}}, \lambda_{\mathrm{c}})$ is a minimizer of (4.4.2). The reverse statement follows from an analogous argument by noting the average value constraint and Dirichlet boundary condition on Γ_{c} furnish explicit equivalence class representatives. Specifically, if $(\boldsymbol{u}^{\mathrm{a}}, \boldsymbol{u}^{\mathrm{c}}, \lambda_{\mathrm{a}}, \lambda_{\mathrm{c}})$ solves (4.4.2), then let λ_{c} and u^{c} be the equivalence class representatives such that $u^{\mathrm{c}} = 0$ on Γ_{c}. Next choose u^{a} and λ_{a} such that $\int_{\Omega_{\mathrm{o}}} (Iu^{\mathrm{a}} - u^{\mathrm{c}})\, dx = 0$ is satisfied. Similar to before, we have

$$\|\nabla I u^{\mathrm{a}} - \nabla u^{\mathrm{c}}\|_{L^2(\Omega_{\mathrm{o}})} = \|\nabla I\boldsymbol{u}^{\mathrm{a}} - \nabla \boldsymbol{u}^{\mathrm{c}}\|_{L^2(\Omega_{\mathrm{o}})} \leq \|\nabla I\boldsymbol{v}^{\mathrm{a}} - \nabla \boldsymbol{v}^{\mathrm{c}}\|_{L^2(\Omega_{\mathrm{o}})} = \|\nabla I v^{\mathrm{a}} - \nabla v^{\mathrm{c}}\|_{L^2(\Omega_{\mathrm{o}})}.$$

For notational clarity we have omitted the class of admissible $\{u^{\mathrm{a}}, u^{\mathrm{c}}, \lambda_{\mathrm{a}}, \lambda_{\mathrm{c}}\}$ over which the minimization is taken in order to introduce the AtC formulation before

addressing additional technical details. In Section 5.3.1, we specify this class to be $\boldsymbol{\mathcal{U}}^{\mathrm{a}} \times \boldsymbol{\mathcal{U}}_h^{\mathrm{c}} \times V^{\mathrm{a}} \times V^{\mathrm{c}}$, where V^{a} and V^{c} are subsets of $\boldsymbol{\Lambda}^{\mathrm{a}}$ and $\boldsymbol{\Lambda}^{\mathrm{c}}$.

The reason we have introduced two equivalent formulations is that (4.4.2) is more convenient for the analysis so we will study the existence of AtC solutions $(\boldsymbol{u}_{\mathrm{a}}^{\mathrm{atc}}, \boldsymbol{u}_{\mathrm{c}}^{\mathrm{atc}})$ in quotient spaces. Meanwhile, the first formulation (4.4.1) is, as mentioned, more convenient for implementing. Our main result establishes the optimization problem is well-posed and furnishes a broken norm error estimate.

Theorem 4.4.2 (Existence and Error Estimate)**.** *Let* $\boldsymbol{u}_{\mathrm{a}}^{\infty} := \boldsymbol{u}^{\infty}|_{\mathcal{L}_{\mathrm{a}}}$ *and* $\boldsymbol{u}_{\mathrm{c}}^{\infty} := \boldsymbol{u}^{\infty}|_{\mathcal{L}_{\mathrm{c}}}$. *There exists* R_{core}^{*} *such that for all* $R_{\mathrm{core}} \geq R_{\mathrm{core}}^{*}$*, the minimization problem* (4.4.2) *has a solution* $(\boldsymbol{u}_{\mathrm{a}}^{\mathrm{atc}}, \boldsymbol{u}_{\mathrm{c}}^{\mathrm{atc}}, \lambda_{\mathrm{a}}^{\mathrm{atc}}, \lambda_{\mathrm{c}}^{\mathrm{atc}})$ *and*

$$\|\nabla \left(I\boldsymbol{u}_{\mathrm{a}}^{\mathrm{atc}} - I\boldsymbol{u}_{\mathrm{a}}^{\infty}\right)\|_{L^2(\Omega_{\mathrm{a}})}^2 + \|\nabla \left(\boldsymbol{u}_{\mathrm{c}}^{\mathrm{atc}} - I\boldsymbol{u}_{\mathrm{c}}^{\infty}\right)\|_{L^2(\Omega_{\mathrm{c}})}^2 \lesssim \; R_{\mathrm{core}}^{-d-2} + R_{\mathrm{c}}^{-d}. \tag{4.4.3}$$

The primary objective of the next chapter is to prove this result.

Chapter 5

Error Analysis of Optimization-Based AtC

5.1 Chapter Overview

This chapter provides the proof of Theorem 4.4.3. It is an involved process with several steps. We will switch to an equivalent reduced space formulation of (4.4.2) and apply the inverse function theorem. Applying the inverse function theorem requires regularity of the mappings taking virtual boundary controls λ_{a} and λ_{c} to solutions u^{a} and u^{c} of the restricted atomistic and continuum subproblems (4.3.2) and (4.3.7) respectively. These results are collected in Section 5.3.1. We subsequently prove consistency, stability, and an existence result and error estimate. These proofs rely on an essential norm equivalence result which is postponed until Section 5.4. It is similar in spirit to results obtained for coupling two linear PDEs in [17, 18, 26, 46] but substantially more difficult since we are dealing with a nonlinear *and* nonlocal atomistic model.

Throughout this chapter, we assume that $d = 2, 3$ due to the previously mentioned fact that the overlap region and continuum region become disconnected in $\mathbb{R}$. In effect, this gives two continuum problems to consider. One can either modify the analysis presented here or use explicit computations which are only available in one dimension. The latter approach was taken in the author's work [46]. We numerically verify that the results do in fact hold in one dimension in Chapter 6.

5.2 Reduced space formulation of the AtC problem

Given arbitrary $\lambda_{\rm a} \in \mathbf{\Lambda^a}$ and $\lambda_{\rm c} \in \mathbf{\Lambda^c}$, it is unclear whether the atomistic problem (4.3.1) and continuum problem (4.3.6) have solutions. In this section, we endow $\mathbf{\Lambda}^{\rm a}$ and $\mathbf{\Lambda}^{\rm c}$ with norms and show that there exist neighborhoods $V^{\rm a}$ in $\mathbf{\Lambda}^{\rm a}$ and $V^{\rm c}$ in $\mathbf{\Lambda}^{\rm c}$ respectively for which these problems do have solutions. These solutions define mappings from the spaces of boundary controls to atomistic and continuum displacements and are denoted by $\boldsymbol{U}^{\rm a} : V^{\rm a} \to \boldsymbol{\mathcal{U}}^{\rm a}$ and $\boldsymbol{U}^{\rm c} : V^{\rm c} \to \boldsymbol{\mathcal{U}}^{\rm c}_h$, respectively. They will be proven to exist in Theorems 5.3.2 and 5.3.4.

Using these mappings, we can write the states $u^{\rm a}$ and $u^{\rm c}$ from (4.4.2) as functions of $\lambda_{\rm a}$ and $\lambda_{\rm c}$ and obtain an equivalent unconstrained minimization problem in terms of the virtual controls only:

$$\left(\lambda_{\rm a}^{\rm atc}, \lambda_{\rm c}^{\rm atc}\right) = \underset{(\lambda_{\rm a},\lambda_{\rm c})\in V^{\rm a}\times V^{\rm c}}{\arg\min} J(\lambda_{\rm a}, \lambda_{\rm c}), \tag{5.2.1}$$

where J is defined as

$$J\left(\lambda_{\rm a}, \lambda_{\rm c}\right) = \frac{1}{2}\|\nabla I\boldsymbol{U}^{\rm a}(\lambda_{\rm a}) - \nabla \boldsymbol{U}^{\rm c}(\lambda_{\rm c})\|^2_{L^2(\Omega_{\rm o})}.$$

The Euler-Lagrange equation of (5.2.1) is given by

$$\langle \delta J(\lambda_{\rm a}, \lambda_{\rm c}), (\mu_{\rm a}, \mu_{\rm c})\rangle \;=\; 0, \quad \forall (\mu_{\rm a}, \mu_{\rm c}) \in \mathbf{\Lambda}^{\rm a} \times \mathbf{\Lambda}^{\rm c}, \tag{5.2.2}$$

and using $(\cdot,\cdot)_{L^2(\Omega_{\rm o})}$ to denote the L^2 inner product, the first variation of J is

$$\langle \delta J(\lambda_{\rm a}, \lambda_{\rm c}), (\mu_{\rm a}, \mu_{\rm c})\rangle = \left(\nabla\left(I\boldsymbol{U}^{\rm a}(\lambda_{\rm a}) - \boldsymbol{U}^{\rm c}(\lambda_{\rm c})\right), \nabla\left(I\delta\boldsymbol{U}^{\rm a}(\lambda_{\rm a})[\mu_{\rm a}] - \delta\boldsymbol{U}^{\rm c}(\lambda_{\rm c})[\mu_{\rm c}]\right)\right)_{L^2(\Omega_{\rm o})}.$$

In terms of the mappings $\boldsymbol{U}^{\rm a}$ and $\boldsymbol{U}^{\rm c}$, the AtC error in (4.4.3) assumes the form

$$\|\nabla\big(I\boldsymbol{U}^{\rm a}(\lambda_{\rm a}^{\rm atc}) - I\boldsymbol{u}_{\rm a}^{\infty}\big)\|^2_{L^2(\Omega_{\rm a})} + \|\nabla\big(\boldsymbol{U}^{\rm c}(\lambda_{\rm c}^{\rm atc}) - I\boldsymbol{u}_{\rm c}^{\infty}\big)\|^2_{L^2(\Omega_{\rm c})}. \tag{5.2.3}$$

Analyzing (5.2.3) requires several problem-dependent norms, and solutions of linearized problems on $\Omega_{\rm a}$ and $\Omega_{\rm c}$ define these norms. Set $\lambda_{\rm a}^{\infty} := \boldsymbol{u}^{\infty}|_{\partial_{\rm a}\mathcal{L}_{\rm a}}$, and let $\delta\boldsymbol{U}^{\rm a}(\lambda_{\rm a}^{\infty})[\cdot] : \mathbf{\Lambda^a} \to \mathcal{U}^{\rm a}$ be the solution to the linearized problem[1]

$$\begin{aligned} \left\langle \delta^2\tilde{\mathcal{E}}^{\rm a}(\boldsymbol{U}^{\rm a}(\lambda_{\rm a}^{\infty}))\delta\boldsymbol{U}^{\rm a}(\lambda_{\rm a}^{\infty})[\mu_{\rm a}], \boldsymbol{v}^{\rm a}\right\rangle &= \;0 \quad \forall \boldsymbol{v}^{\rm a} \in \boldsymbol{\mathcal{U}}^{\rm a}_0, \\ \delta\boldsymbol{U}^{\rm a}(\lambda_{\rm a}^{\infty})[\mu_{\rm a}] &= \;\mu_{\rm a} \quad \text{on } \partial_{\rm a}\mathcal{L}_{\rm a}. \end{aligned} \tag{5.2.4}$$

[1] Later we show that $\boldsymbol{U}^{\rm a}$ is differentiable, and $\delta\boldsymbol{U}^{\rm a}(\lambda_{\rm a}^{\infty})[\cdot]$ is the Gateaux derivative of $\boldsymbol{U}^{\rm a}$ at $\lambda_{\rm a}^{\infty}$, which justifies this usage of notation.

Similarly, let $\delta \boldsymbol{U}^{\mathrm{c}}(\lambda_{\mathrm{c}}^{\infty})[\cdot] : \boldsymbol{\Lambda}^{\mathbf{c}} \to \mathcal{U}^{\mathrm{c}}$ be the solution to a continuum problem linearized about $\boldsymbol{u}^{\mathrm{con}}$ (recall the definition of $\boldsymbol{u}^{\mathrm{con}}$ from Theorem 4.3.8):

$$\begin{aligned} \left\langle \delta^2 \tilde{\mathcal{E}}^{\mathrm{c}}(\boldsymbol{u}^{\mathrm{con}}) \delta \boldsymbol{U}^{\mathrm{c}}(\lambda_{\mathrm{c}}^{\infty})[\mu_{\mathrm{c}}], \boldsymbol{v}^{\mathrm{c}} \right\rangle &= 0 \quad \forall \boldsymbol{v}^{\mathrm{c}} \in \boldsymbol{\mathcal{U}}_{h,0}^{\mathrm{c}}, \\ \delta \boldsymbol{U}^{\mathrm{c}}(\lambda_{\mathrm{c}}^{\infty})[\mu_{\mathrm{c}}] &= \mu_{\mathrm{c}} \quad \text{on} \quad \Gamma_{\mathrm{core}}. \end{aligned}$$

Because these are both linear problems and both $\delta^2 \tilde{\mathcal{E}}^{\mathrm{c}}(\boldsymbol{u}^{\mathrm{con}})$ and $\delta^2 \tilde{\mathcal{E}}^{\mathrm{a}}(\boldsymbol{U}^{\mathrm{a}}(\lambda_{\mathrm{a}}^{\infty}))$ have been shown to be coercive, it follows that

$$\|\mu_{\mathrm{a}}\|_{\boldsymbol{\Lambda}^{\mathrm{a}}} := \|\nabla I \delta \boldsymbol{U}^{\mathrm{a}}(\lambda_{\mathrm{a}}^{\infty})[\mu_{\mathrm{a}}]\|_{L^2(\Omega_{\mathrm{a}})} \quad \text{and} \quad \|\mu_{\mathrm{c}}\|_{\boldsymbol{\Lambda}^{\mathrm{c}}} := \|\nabla \delta \boldsymbol{U}^{\mathrm{c}}(\lambda_{\mathrm{c}}^{\infty})[\mu_{\mathrm{c}}]\|_{L^2(\Omega_{\mathrm{c}})}$$

define norms on $\boldsymbol{\Lambda}^{\mathrm{a}}$ and $\boldsymbol{\Lambda}^{\mathrm{c}}$. Meanwhile, their sum

$$\|(\mu_{\mathrm{a}}, \mu_{\mathrm{c}})\|_{\mathrm{err}}^2 := \|\mu_{\mathrm{a}}\|_{\boldsymbol{\Lambda}^{\mathrm{a}}}^2 + \|\mu_{\mathrm{c}}\|_{\boldsymbol{\Lambda}^{\mathrm{c}}}^2, \tag{5.2.5}$$

is a norm on $\boldsymbol{\Lambda}^{\mathrm{a}} \times \boldsymbol{\Lambda}^{\mathrm{c}}$. In Section 5.4 we shall prove

$$\|(\mu_{\mathrm{a}}, \mu_{\mathrm{c}})\|_{\mathrm{op}} := \|\nabla \left(I \delta \boldsymbol{U}^{\mathrm{a}}(\lambda_{\mathrm{a}}^{\infty})[\mu_{\mathrm{a}}] - \delta \boldsymbol{U}^{\mathrm{c}}(\lambda_{\mathrm{c}}^{\infty})[\mu_{\mathrm{c}}] \right) \|_{L^2(\Omega_{\mathrm{o}})}$$

is a norm equivalent to $\|\cdot\|_{\mathrm{err}}$ from (5.2.5). We state this result below for further reference within this section but postpone the proof.

Theorem 5.2.1 (Norm Equivalence)**.** *There exists $R_{\mathrm{core}}^* > 0$ such that for all $R_{\mathrm{core}} \geq R_{\mathrm{core}}^*$,*

$$\|\cdot\|_{\mathrm{op}} \lesssim \|\cdot\|_{\mathrm{err}} \lesssim \|\cdot\|_{\mathrm{op}}. \tag{5.2.6}$$

5.3 The Inverse Function Theorem framework

Our goal now is to apply the inverse function theorem to show that the first order optimality condition (5.2.2) for (5.2.1) has a solution. We apply the inverse function theorem, Theorem 4.3.7, with $f = \delta J$ and $X = \boldsymbol{\Lambda}^{\mathrm{a}} \times \boldsymbol{\Lambda}^{\mathrm{c}}$ equipped with the $\|\cdot\|_{\mathrm{op}}$ norm. To fulfill the hypotheses of the inverse function theorem, we must show there exist L, η, σ such that

$$\begin{aligned} \sup_{(\lambda_{\mathrm{a}}, \lambda_{\mathrm{c}}) \text{ near } (\lambda_{\mathrm{a}}^{\infty}, \lambda_{\mathrm{c}}^{\infty})} \|\delta^3 J(\lambda_{\mathrm{a}}, \lambda_{\mathrm{c}})\| \leq L\,, \quad & \|\delta J(\lambda_{\mathrm{a}}^{\infty}, \lambda_{\mathrm{c}}^{\infty})\| \leq \eta, \\ \text{and} \quad & \|(\delta^2 J(\lambda_{\mathrm{a}}^{\infty}, \lambda_{\mathrm{c}}^{\infty}))^{-1}\| \leq \sigma. \end{aligned}$$

Each of these results requires differentiability of the functional, J, which in turn requires differentiability of the functions $\boldsymbol{U}^{\mathrm{a}}$ and $\boldsymbol{U}^{\mathrm{c}}$. We prove the necessary differentiability results and boundedness of the third derivative of J in Section 5.3.1. The second bound above is a consistency error estimate and is proven in Section 5.3.2 while the final estimate is a stability result proven in Section 5.3.3.

5.3.1 Regularity

We use the following version of the implicit function theorem to obtain existence and regularity results for $\boldsymbol{U}^{\mathrm{a}}$ and $\boldsymbol{U}^{\mathrm{c}}$. The theorem may be obtained by adapting the proof of the implicit function theorem in [30] to Banach spaces and by tracking the constants involved. For the sake of completion, we provide a sketch of this tracking procedure in Section A.2 of Appendix A based on standard references [30, 44].

Theorem 5.3.1 (Implicit Function Theorem)**.** *Let X, Y, and Z be Banach spaces with $U \subset X \times Y$ an open set. Let $f : X \times Y \to Z$ be continuously differentiable with $(x_0, y_0) \in U$ satisfying $f(x_0, y_0) = 0$. Suppose that $\delta_y f(x_0, y_0) : Y \to Z$ is a bounded, invertible linear transformation with $\left\|(\delta_y f(x_0, y_0))^{-1}\right\| =: \theta$. Also set $\phi := \|\delta_x f(x_0, y_0)\|$ and*

$$\sigma := \max\{1 + \theta\phi, \theta\}.$$

If there exists η such that

1. *$B_{2\eta\sigma}((x_0, y_0)) \subset U$,*
2. *$\|\delta f(x_1, y_1) - \delta f(x_2, y_2)\| \leq \frac{1}{2\eta\sigma^2}\|(x_1, y_1) - (x_2, y_2)\|$ for all $(x_1, y_1), (x_2, y_2) \in B_{2\eta\sigma}((x_0, y_0))$,*

then there is a unique continuously differentiable function $g : B_\eta(x_0) \to B_{2\eta\sigma}(y_0)$ such that $g(x_0) = y_0$ and $f(x, g(x)) = 0$ for all $x \in B_\eta(x_0)$. The derivative of g is

$$\delta g(x) = -\left[\delta_y f(x, g(x))^{-1}\right]\left[\delta_x f(x, g(x))\right].$$

Moreover, if f is C^k, then g is C^k, derivatives of g can be bounded in terms of derivatives of f and $\delta_y f(x, g(x))^{-1}$, and there is a uniform bound on δg.

Theorem 5.3.2 (Regularity of $\boldsymbol{U}^{\mathrm{a}}$)**.** *Under the site potential assumptions* $\boldsymbol{V}.1-\boldsymbol{V}.4$ *and Assumption A, there exists* $R^*_{\mathrm{core}}>0$ *such that for all* $R_{\mathrm{core}}\geq R^*_{\mathrm{core}}$*, there exists an open ball* V^{a} *centered at* $\lambda^\infty_{\mathrm{a}}$ *in* $\boldsymbol{\Lambda}^{\mathrm{a}}$ *and a mapping* $\boldsymbol{U}^{\mathrm{a}}:V^{\mathrm{a}}\to\boldsymbol{\mathcal{U}}^{\mathrm{a}}$ *such that* $\boldsymbol{U}^{\mathrm{a}}(\lambda_{\mathrm{a}})$ *solves* (4.3.1)*. The mapping is* C^3*, the radius of* V^{a} *is independent of* R_{core}*,* U^{a} *is Lipschitz continuous, and derivatives of* $\boldsymbol{U}^{\mathrm{a}}$ *at* $\lambda^\infty_{\mathrm{a}}$ *are also bounded uniformly in* $R_{\mathrm{core}}\geq R^*_{\mathrm{core}}$*.*

Proof. We apply Theorem 5.3.1 with $X=\boldsymbol{\Lambda}^{\mathrm{a}}$, $Y=\boldsymbol{\mathcal{U}}^{\mathrm{a}}_0$, $Z=(\boldsymbol{\mathcal{U}}^{\mathrm{a}}_0)^*$, $U=X\times Y$, and

$$f\left(\lambda_{\mathrm{a}},\boldsymbol{v}^{\mathrm{a}}\right):=\delta\tilde{\mathcal{E}}^{\mathrm{a}}\left(h\left(\lambda_{\mathrm{a}},\boldsymbol{v}^{\mathrm{a}}\right)\right),$$

where h is an auxiliary function $X\times Y\to\boldsymbol{\mathcal{U}}^{\mathrm{a}}$ defined by (recall $\delta\boldsymbol{U}^{\mathrm{a}}(\lambda^\infty_{\mathrm{a}})[\mu^{\mathrm{a}}]$ is defined to solve (5.2.4))

$$h\left(\lambda_{\mathrm{a}},\boldsymbol{v}^{\mathrm{a}}\right)=\boldsymbol{v}^{\mathrm{a}}+\boldsymbol{u}^\infty_{\mathrm{a}}+\delta\boldsymbol{U}^{\mathrm{a}}(\lambda^\infty_{\mathrm{a}})\left[\lambda_{\mathrm{a}}-\lambda^\infty_{\mathrm{a}}\right].$$

Because h is affine, f is C^k provided that $\tilde{\mathcal{E}}^{\mathrm{a}}$ is C^{k+1} on $\boldsymbol{\mathcal{U}}^{\mathrm{a}}$. Hence, Theorem 4.3.2 implies f is C^3. For the point (x_0,y_0), we take the point $(\lambda^\infty_{\mathrm{a}},\mathbf{0})$ so that $h\left(x_0,y_0\right)=\boldsymbol{u}^\infty_{\mathrm{a}}$. The chain rule shows

$$\delta_y f(x_0,y_0)=\ \delta^2\tilde{\mathcal{E}}^{\mathrm{a}}\left(h\left(x_0,y_0\right)\right)\circ\delta_y h\left(x_0,y_0\right).$$

In conjunction with $\delta_y h\left(x_0,y_0\right)[\boldsymbol{v}^{\mathrm{a}}]=\boldsymbol{v}^{\mathrm{a}}$, it follows that $\delta_y f(x_0,y_0):Y\to Z$ is given by

$$\langle\delta_y f(x_0,y_0)\boldsymbol{v}^{\mathrm{a}},\boldsymbol{w}^{\mathrm{a}}\rangle=\ \langle\delta^2\tilde{\mathcal{E}}^{\mathrm{a}}\left(\boldsymbol{u}^\infty_{\mathrm{a}}\right)\boldsymbol{v}^{\mathrm{a}},\boldsymbol{w}^{\mathrm{a}}\rangle.$$

Since both $\boldsymbol{v}^{\mathrm{a}}$ and $\boldsymbol{w}^{\mathrm{a}}$ are elements of $\boldsymbol{\mathcal{U}}^{\mathrm{a}}_0$, they can be extended by a constant to all of $\mathbb{Z}^d$ while keeping the gradient norms of $I\boldsymbol{v}^{\mathrm{a}}$ and $I\boldsymbol{w}^{\mathrm{a}}$ the same. Then using Assumption A, we find

$$\begin{aligned}\langle\delta_y f(x_0,y_0)\boldsymbol{v}^{\mathrm{a}},\boldsymbol{v}^{\mathrm{a}}\rangle=\ \langle\delta^2\tilde{\mathcal{E}}^{\mathrm{a}}\left(\boldsymbol{u}^\infty_{\mathrm{a}}\right)\boldsymbol{v}^{\mathrm{a}},\boldsymbol{v}^{\mathrm{a}}\rangle=\ \langle\delta^2\mathcal{E}^{\mathrm{a}}\left(\boldsymbol{u}^\infty\right)\boldsymbol{v}^{\mathrm{a}},\boldsymbol{v}^{\mathrm{a}}\rangle&\geq\ \gamma_{\mathrm{a}}\|\nabla I\boldsymbol{v}^{\mathrm{a}}\|^2_{L^2(\mathbb{R}^d)}\\&=\ \gamma_{\mathrm{a}}\|\nabla I\boldsymbol{v}^{\mathrm{a}}\|^2_{L^2(\Omega_{\mathrm{a}})}.\end{aligned}$$

This shows $\delta_y f(x_0,y_0)$ is coercive, and consequently, $\delta_y f(x_0,y_0)^{-1}$ exists with norm bounded by $\theta:=\gamma_{\mathrm{a}}^{-1}$. Using again the chain rule, we obtain

$$\delta_x f(x_0,y_0)=\delta^2\tilde{\mathcal{E}}^{\mathrm{a}}\left(h\left(x_0,y_0\right)\right)\circ\delta_x h\left(x_0,y_0\right)=0$$

so that $\phi=\|\delta_x f(x_0,y_0)\|=0$.

Next, observe that h is Lipschitz on its entire domain with Lipschitz constant 1 because

$$h\left(\lambda_{\mathrm{a}}, \boldsymbol{v}^{\mathrm{a}}\right) - h(\mu_{\mathrm{a}}, \boldsymbol{w}^{\mathrm{a}}) = \ \boldsymbol{v}^{\mathrm{a}} - \boldsymbol{w}^{\mathrm{a}} + \delta \boldsymbol{U}^{\mathrm{a}}(\lambda_{\mathrm{a}}^{\infty})[\lambda_{\mathrm{a}}] + \delta \boldsymbol{U}^{\mathrm{a}}(\lambda_{\mathrm{a}}^{\infty})[\mu_{\mathrm{a}}].$$

Moreover, $\delta^2 \tilde{\mathcal{E}}^{\mathrm{a}}$ is Lipschitz with some Lipschitz constant M, as guaranteed by Theorem 4.3.2. As a result, δf is Lipschitz with Lipschitz constant M. Now we may choose η small enough so that $\frac{1}{2\eta\sigma^2} \geq M$, which means both conditions (1) and (2) in the statement of implicit function theorem are fulfilled. This allows us to deduce the existence of a unique implicit function $g : B_{\eta}(\lambda_{\mathrm{a}}^{\infty}) \to B_{2\eta\sigma}(\mathbf{0})$, which we use to define a mapping $\boldsymbol{U}^{\mathrm{a}}$ via

$$\boldsymbol{U}^{\mathrm{a}}(\lambda_{\mathrm{a}}) = h\left(\lambda_{\mathrm{a}}, g(\lambda_{\mathrm{a}})\right) = g(\lambda_{\mathrm{a}}) + \boldsymbol{u}_{\mathrm{a}}^{\infty} + \delta \boldsymbol{U}^{\mathrm{a}}(\lambda_{\mathrm{a}}^{\infty}) \left[\lambda_{\mathrm{a}} - \lambda^{\infty}\right].$$

With this definition, we have

$$\begin{aligned} 0 = \ & f\left(\lambda_{\mathrm{a}}, g(\lambda_{\mathrm{a}})\right) = \delta \tilde{\mathcal{E}}^{\mathrm{a}}\left(h\left(\lambda_{\mathrm{a}}, g(\lambda_{\mathrm{a}})\right)\right) \\ = \ & \delta \tilde{\mathcal{E}}^{\mathrm{a}}\left(\boldsymbol{U}^{\mathrm{a}}(\lambda_{\mathrm{a}})\right). \end{aligned}$$

Since f is C^3, the implicit function theorem ensures g is also C^3. Thus $\boldsymbol{U}^{\mathrm{a}}$ is C^3. The radius of V^{a} is η, which is clearly independent of R_{core}, and the uniform bounds on the derivatives of $\boldsymbol{U}^{\mathrm{a}}$ follow by noting derivatives of f correspond to derivatives of the restricted atomistic energy (which is uniformly bounded by Theorem 4.3.2) and using the final remark in the statement of the implicit function theorem. □

Remark 5.3.3. *We note that the Gateaux derivative, $\delta \boldsymbol{U}^{\mathrm{a}}(\lambda_{\mathrm{a}})[\mu_{\mathrm{a}}]$, of $\boldsymbol{U}^{\mathrm{a}}$ at λ_{a} in the direction of μ_{a} solves the problem*

$$\begin{aligned} \langle \delta^2 \tilde{\mathcal{E}}^{\mathrm{a}}(\boldsymbol{U}^{\mathrm{a}}(\lambda_{\mathrm{a}})) \delta \boldsymbol{U}^{\mathrm{a}}(\lambda_{\mathrm{a}})[\mu_{\mathrm{a}}], \boldsymbol{v}^{\mathrm{a}} \rangle = \ & 0 \quad \forall \boldsymbol{v}^{\mathrm{a}} \in \boldsymbol{\mathcal{U}}_0^{\mathrm{a}}, \\ \delta \boldsymbol{U}^{\mathrm{a}}(\lambda_{\mathrm{a}})[\mu_{\mathrm{a}}] = \ & \mu_{\mathrm{a}} \quad \text{on} \quad \partial_{\mathrm{a}} \mathcal{L}_{\mathrm{a}}, \end{aligned}$$

thus justifying our usage of notation in the proof.

With only minor modifications, the proof of Theorem 5.3.2 can be adapted to establish the regularity of $\boldsymbol{U}^{\mathrm{c}}$.

Theorem 5.3.4 (Regularity of $\boldsymbol{U}^{\mathrm{c}}$)**.** *There exists $R_{\mathrm{core}}^{*} > 0$ such that for all $R_{\mathrm{core}} \geq R_{\mathrm{core}}^{*}$, there exists an open ball V^{c} centered at $\lambda_{\mathrm{c}}^{\infty}$ in $\boldsymbol{\Lambda}^{\mathrm{c}}$ and a mapping $\boldsymbol{U}^{\mathrm{c}} : V^{\mathrm{c}} \to \boldsymbol{\mathcal{U}}^{\mathrm{c}}$*

such that $\boldsymbol{U}^{\mathrm{c}}(\lambda_{\mathrm{c}})$ *solves* (4.3.6)*, and the mapping is* C^3*. The mapping* U^{c} *is Lipschitz continuous, the derivatives of* $\boldsymbol{U}^{\mathrm{c}}$ *at* $\lambda_{\mathrm{c}}^{\infty}$ *are bounded independently in* R_{core}*, and the radius of* V^{c} *is independent of* R_{core}*.*

The proof of Theorem 4.4.2 containing our main existence result and error estimate in turn relies on a stability result that enables the application of the inverse function theorem. This stability result requires the following auxiliary lemma which is a simple consequence of the triangle inequality and continuity of $\boldsymbol{U}^{\mathrm{a}}$ and $\boldsymbol{U}^{\mathrm{c}}$.

Lemma 5.3.5. *There exists* R_{core}^{*} *such that for all* $R_{\mathrm{core}} \geq R_{\mathrm{core}}^{*}$ *and all* $\mu_{\mathrm{a}}, \nu_{\mathrm{a}} \in \boldsymbol{\Lambda}^{\mathrm{a}}$ *and all* $\mu_{\mathrm{c}}, \nu_{\mathrm{c}} \in \boldsymbol{\Lambda}^{\mathrm{c}}$*,*

$$\|\nabla \left(I\delta^2 \boldsymbol{U}^{\mathrm{a}}(\lambda_{\mathrm{a}}^{\infty})[\mu_{\mathrm{a}}, \nu_{\mathrm{a}}] - \delta^2 \boldsymbol{U}^{\mathrm{c}}(\lambda_{\mathrm{c}}^{\infty})[\mu_{\mathrm{c}}, \nu_{\mathrm{c}}]\right) \|_{L^2(\Omega_{\mathrm{o}})} \lesssim \ \|(\mu_{\mathrm{a}}, \mu_{\mathrm{c}})\|_{\mathrm{op}} \cdot \|(\nu_{\mathrm{a}}, \nu_{\mathrm{c}})\|_{\mathrm{op}}. \tag{5.3.1}$$

Proof. The triangle inequality implies

$$\begin{aligned} &\|\nabla \left(I\delta^2 \boldsymbol{U}^{\mathrm{a}}(\lambda_{\mathrm{a}}^{\infty})[\mu_{\mathrm{a}}, \nu_{\mathrm{a}}] - \delta^2 \boldsymbol{U}^{\mathrm{c}}(\lambda_{\mathrm{c}}^{\infty})[\mu_{\mathrm{c}}, \nu_{\mathrm{c}}]\right) \|_{L^2(\Omega_{\mathrm{o}})} \\ &\qquad \leq \ \|\nabla I\delta^2 \boldsymbol{U}^{\mathrm{a}}(\lambda_{\mathrm{a}}^{\infty})[\mu_{\mathrm{a}}, \nu_{\mathrm{a}}]\|_{L^2(\Omega_{\mathrm{a}})} + \|\nabla \delta^2 \boldsymbol{U}^{\mathrm{c}}(\lambda_{\mathrm{c}}^{\infty})[\mu_{\mathrm{c}}, \nu_{\mathrm{c}}]\|_{L^2(\Omega_{\mathrm{c}})}. \end{aligned} \tag{5.3.2}$$

We then utilize Theorems 5.3.2 and 5.3.4 to obtain an upper bound on Hessian of the atomistic mapping:

$$\|\nabla I\delta^2 \boldsymbol{U}^{\mathrm{a}}(\lambda_{\mathrm{a}}^{\infty})[\mu_{\mathrm{a}}, \nu_{\mathrm{a}}]\|_{L^2(\Omega_{\mathrm{a}})} \lesssim \ \|\mu_{\mathrm{a}}\|_{\boldsymbol{\Lambda}^{\mathrm{a}}} \cdot \|\nu_{\mathrm{a}}\|_{\boldsymbol{\Lambda}^{\mathrm{a}}}, \tag{5.3.3}$$

and a similar bound for the Hessian of the continuum mapping:

$$\|\delta^2 \boldsymbol{U}^{\mathrm{c}}(\lambda_{\mathrm{c}}^{\infty})[\mu_{\mathrm{c}}, \nu_{\mathrm{c}}]\|_{L^2(\Omega_{\mathrm{c}})} \lesssim \ \|\mu_{\mathrm{c}}\|_{\boldsymbol{\Lambda}^{\mathrm{c}}} \cdot \|\nu_{\mathrm{c}}\|_{\boldsymbol{\Lambda}^{\mathrm{c}}}. \tag{5.3.4}$$

Inequalities (5.3.3)–(5.3.4) may in turn be used to bound the right hand side of (5.3.2) and further applying the norm equivalence theorem, Theorem 5.2.1, yeilds

$$\begin{aligned} &\|\nabla \left(I\delta^2 \boldsymbol{U}^{\mathrm{a}}(\lambda_{\mathrm{a}}^{\infty})[\mu_{\mathrm{a}}, \nu_{\mathrm{a}}] - \delta^2 \boldsymbol{U}^{\mathrm{c}}(\lambda_{\mathrm{c}}^{\infty})[\mu_{\mathrm{c}}, \nu_{\mathrm{c}}]\right) \|_{L^2(\Omega_{\mathrm{o}})} \\ &\qquad \lesssim \ \|\mu_{\mathrm{a}}\|_{\boldsymbol{\Lambda}^{\mathrm{a}}} \cdot \|\nu_{\mathrm{a}}\|_{\boldsymbol{\Lambda}^{\mathrm{a}}} + \|\mu_{\mathrm{c}}\|_{\boldsymbol{\Lambda}^{\mathrm{c}}} \cdot \|\nu_{\mathrm{c}}\|_{\boldsymbol{\Lambda}^{\mathrm{c}}} \\ &\qquad \leq \ \left(\|\mu_{\mathrm{a}}\|_{\boldsymbol{\Lambda}^{\mathrm{a}}} + \|\mu_{\mathrm{c}}\|_{\boldsymbol{\Lambda}^{\mathrm{c}}}\right) \left(\|\nu_{\mathrm{a}}\|_{\boldsymbol{\Lambda}^{\mathrm{a}}} + \|\nu_{\mathrm{c}}\|_{\boldsymbol{\Lambda}^{\mathrm{c}}}\right) \\ &\qquad \lesssim \ \|(\mu_{\mathrm{a}}, \mu_{\mathrm{c}})\|_{\mathrm{op}} \cdot \|(\nu_{\mathrm{a}}, \nu_{\mathrm{c}})\|_{\mathrm{op}}. \end{aligned}$$

□

We proceed to establish regularity of the objective functional J.

Theorem 5.3.6 (Regularity of J)**.** *Let V^{a} and V^{c} be the neighborhoods of $\lambda_{\mathrm{a}}^{\infty}$ and $\lambda_{\mathrm{c}}^{\infty}$ in $\mathbf{\Lambda}^{\mathrm{a}}$ and $\mathbf{\Lambda}^{\mathrm{c}}$ on which $\boldsymbol{U}^{\mathrm{a}}$ and $\boldsymbol{U}^{\mathrm{c}}$ are C^3. Then J is C^3 on $V^{\mathrm{a}} \times V^{\mathrm{c}}$ and its ℓ^{th} derivatives can be bounded by derivatives of $\boldsymbol{U}^{\mathrm{a}}$ and $\boldsymbol{U}^{\mathrm{c}}$ of order at most ℓ.*

Proof. Theorems 5.3.2–5.3.4 guarantee that $\boldsymbol{U}^{\mathrm{a}}$ and $\boldsymbol{U}^{\mathrm{c}}$ are C^3 on V^{a} and V^{c}. Moreover, the interpolant, I, is a linear operator so $\lambda^{\mathrm{a}} \mapsto I\boldsymbol{U}^{\mathrm{a}}(\lambda^{\mathrm{a}})$ will also be C^3 on V^{a}. The assertion of the theorem then follows from the fact that $J = \|\nabla I\boldsymbol{U}^{\mathrm{a}}(\lambda_{\mathrm{a}}) - \nabla \boldsymbol{U}^{\mathrm{c}}(\lambda_{\mathrm{c}})\|^2_{L^2(\Omega_{\mathrm{o}})}$ is a composition of a C^3 quadratic form and the C^3 functions $I\boldsymbol{U}^{\mathrm{a}}(\lambda^{\mathrm{a}})$ and $\boldsymbol{U}^{\mathrm{c}}(\lambda^{\mathrm{c}})$. □

5.3.2 Consistency

The consistency error measures the extent to which the exact atomistic solution, $\boldsymbol{u}^{\infty}$, fails to satisfy the approximate problem, which in this case is the unconstrained formulation (5.2.1) in terms of virtual controls. Thus, we seek an upper bound for $\delta J(\lambda_{\mathrm{a}}^{\infty}, \lambda_{\mathrm{c}}^{\infty})$ in the operator norm induced by $\|\cdot\|_{\mathrm{op}}$:

$$\begin{aligned}&\|\delta J(\lambda_{\mathrm{a}}^{\infty}, \lambda_{\mathrm{c}}^{\infty})\|_{\mathrm{op}^*} \\ &\quad = \sup_{\|(\mu_{\mathrm{a}},\mu_{\mathrm{c}})\|_{\mathrm{op}}=1} \left| \left(\nabla \left(I\boldsymbol{U}^{\mathrm{a}}(\lambda_{\mathrm{a}}^{\infty}) - \boldsymbol{U}^{\mathrm{c}}(\lambda_{\mathrm{c}}^{\infty})\right), \nabla \left(I\delta\boldsymbol{U}^{\mathrm{a}}(\lambda_{\mathrm{a}}^{\infty})[\mu_{\mathrm{a}}] - \delta\boldsymbol{U}^{\mathrm{c}}(\lambda_{\mathrm{c}}^{\infty})[\mu_{\mathrm{c}}]\right)\right)_{L^2(\Omega_{\mathrm{o}})} \right|.\end{aligned} \tag{5.3.5}$$

Theorem 5.3.7 (Consistency Error)**.** *There exists $R_{\mathrm{core}}^{*} > 0$ such that for all $R_{\mathrm{core}} \geq R_{\mathrm{core}}^{*}$, we have*

$$\|\delta J(\lambda_{\mathrm{a}}^{\infty}, \lambda_{\mathrm{c}}^{\infty})\|_{\mathrm{op}^*} \lesssim R_{\mathrm{core}}^{-d/2-1} + R_{\mathrm{c}}^{-d/2}. \tag{5.3.6}$$

Proof. Applying the Cauchy-Schwarz inequality to (5.3.5) yields

$$\begin{aligned}\|\delta J(\lambda_{\mathrm{a}}^{\infty}, \lambda_{\mathrm{c}}^{\infty})\|_{\mathrm{op}^*} \leq & \sup_{\|(\mu_{\mathrm{a}},\mu_{\mathrm{c}})\|_{\mathrm{op}}=1} \|\nabla \left(I\boldsymbol{U}^{\mathrm{a}}(\lambda_{\mathrm{a}}^{\infty}) - \boldsymbol{U}^{\mathrm{c}}(\lambda_{\mathrm{c}}^{\infty})\right)\|_{L^2(\Omega_{\mathrm{o}})} \cdot \\ & \qquad \|\nabla \left(I\delta\boldsymbol{U}^{\mathrm{a}}(\lambda_{\mathrm{a}}^{\infty})[\mu_{\mathrm{a}}] - \delta\boldsymbol{U}^{\mathrm{c}}(\lambda_{\mathrm{c}}^{\infty})[\mu_{\mathrm{c}}]\right)\|_{L^2(\Omega_{\mathrm{o}})} \\ = & \|\nabla \left(I\boldsymbol{U}^{\mathrm{a}}(\lambda_{\mathrm{a}}^{\infty}) - \boldsymbol{U}^{\mathrm{c}}(\lambda_{\mathrm{c}}^{\infty})\right)\|_{L^2(\Omega_{\mathrm{o}})}.\end{aligned}$$

Note that $\lambda_{\mathrm{a}}^{\infty}$ and $\lambda_{\mathrm{c}}^{\infty}$ are traces of the exact atomistic solution, and so

$$\|\nabla \left(I\boldsymbol{U}^{\mathrm{a}}(\lambda_{\mathrm{a}}^{\infty}) - \boldsymbol{U}^{\mathrm{c}}(\lambda_{\mathrm{c}}^{\infty})\right)\|_{L^2(\Omega_{\mathrm{o}})} = \|\nabla I\boldsymbol{u}_{\mathrm{a}}^{\infty} - \nabla \boldsymbol{u}^{\mathrm{con}}\|_{L^2(\Omega_{\mathrm{o}})},$$

is the simply the continuum error made by replacing the atomistic model with the continuum model on $\Omega_{\rm o}$. Thus, estimate (5.3.6) follows directly from inequality (4.3.14) in Theorem 4.3.8 which estimated the continuum error. □

5.3.3 Stability

In this section we prove that the bilinear form $\langle \delta^2 J(\lambda_{\rm a}^\infty, \lambda_{\rm c}^\infty)\cdot,\cdot\rangle$ is coercive.

Theorem 5.3.8. *There exists $R_{\rm core}^*$ such that for each $R_{\rm core} \geq R_{\rm core}^*$*

$$\langle \delta^2 J(\lambda_{\rm a}^\infty, \lambda_{\rm c}^\infty)(\mu_{\rm a},\mu_{\rm c}),(\mu_{\rm a},\mu_{\rm c})\rangle \geq \tfrac{1}{2}\|(\mu_{\rm a},\mu_{\rm c})\|_{\rm op}^2, \quad \forall (\mu_{\rm a},\mu_{\rm c}) \in \mathbf{\Lambda}^{\rm a}\times\mathbf{\Lambda}^{\rm c}.$$

Proof. The Hessian of J is given by

$$\begin{aligned}\langle \delta^2 J(\lambda_{\rm a}^\infty, \lambda_{\rm c}^\infty)(\mu_{\rm a},\mu_{\rm c}),(\mu_{\rm a},\mu_{\rm c})\rangle = \ & \|\nabla\left(I\delta \boldsymbol{U}^{\rm a}(\lambda_{\rm a}^\infty)[\mu_{\rm a}] - \delta\boldsymbol{U}^{\rm c}(\lambda_{\rm c}^\infty)[\mu_{\rm c}]\right)\|_{L^2(\Omega_{\rm o})}^2 \\ & + \left(\nabla\left(I\boldsymbol{U}^{\rm a}(\lambda_{\rm a}^\infty) - \boldsymbol{U}^{\rm c}(\lambda_{\rm c}^\infty)\right), \nabla\left(I\delta^2\boldsymbol{U}^{\rm a}(\lambda_{\rm a}^\infty)[\mu_{\rm a},\mu_{\rm a}] - \delta^2\boldsymbol{U}^{\rm c}(\lambda_{\rm c}^\infty)[\mu_{\rm c},\mu_{\rm c}]\right)\right)_{L^2(\Omega_{\rm o})}.\end{aligned}$$

Using the definition of $\|\cdot\|_{\rm op}$, this is equivalent to

$$\begin{aligned}\langle \delta^2 J(\lambda_{\rm a}^\infty, \lambda_{\rm c}^\infty)(\mu_{\rm a},\mu_{\rm c}),(\mu_{\rm a},\mu_{\rm c})\rangle = & \|(\mu_{\rm a},\mu_{\rm c})\|_{\rm op}^2 \\ & + \left(\nabla\left(I\boldsymbol{U}^{\rm a}(\lambda_{\rm a}^\infty) - \boldsymbol{U}^{\rm c}(\lambda_{\rm c}^\infty)\right), \nabla\left(I\delta^2\boldsymbol{U}^{\rm a}(\lambda_{\rm a}^\infty)[\mu_{\rm a},\mu_{\rm a}] - \delta^2\boldsymbol{U}^{\rm c}(\lambda_{\rm c}^\infty)[\mu_{\rm c},\mu_{\rm c}]\right)\right)_{L^2(\Omega_{\rm o})}.\end{aligned}$$

Lemma 5.3.5 implies the existence of $R_{\rm core}^{*,1}$ and $C_{\rm stab}$ such that for all $R_{\rm core} \geq R_{\rm core}^{*,1}$,

$$\|\nabla\left(I\delta^2\boldsymbol{U}^{\rm a}(\lambda_{\rm a}^\infty)[\mu_{\rm a},\mu_{\rm a}] - \delta^2\boldsymbol{U}^{\rm c}(\lambda_{\rm c}^\infty)[\mu_{\rm c},\mu_{\rm c}]\right)\|_{L^2(\Omega_{\rm o})} \leq C_{\rm stab}\|(\mu_{\rm a},\mu_{\rm c})\|_{\rm op}^2.$$

We then have that

$$\begin{aligned}& \left(\nabla\left(I\boldsymbol{U}^{\rm a}(\lambda_{\rm a}^\infty) - \boldsymbol{U}^{\rm c}(\lambda_{\rm c}^\infty)\right), \nabla\left(I\delta^2\boldsymbol{U}^{\rm a}(\lambda_{\rm a}^\infty)[\mu_{\rm a},\mu_{\rm a}] - \delta^2\boldsymbol{U}^{\rm c}(\lambda_{\rm c}^\infty)[\mu_{\rm c},\mu_{\rm c}]\right)\right)_{L^2(\Omega_{\rm o})} \\ \geq \ & -\|\nabla\left(I\boldsymbol{U}^{\rm a}(\lambda_{\rm a}^\infty) - \boldsymbol{U}^{\rm c}(\lambda_{\rm c}^\infty)\right)\|_{L^2(\Omega_{\rm o})}\cdot \\ & \qquad \|\nabla\left(I\delta^2\boldsymbol{U}^{\rm a}(\lambda_{\rm a}^\infty)[\mu_{\rm a},\mu_{\rm a}] - \delta^2\boldsymbol{U}^{\rm c}(\lambda_{\rm c}^\infty)[\mu_{\rm c},\mu_{\rm c}]\right)\|_{L^2(\Omega_{\rm o})} \\ \geq \ & -C_{\rm stab}\|\nabla\left(I\boldsymbol{U}^{\rm a}(\lambda_{\rm a}^\infty) - \boldsymbol{U}^{\rm c}(\lambda_{\rm c}^\infty)\right)\|_{L^2(\Omega_{\rm o})}\cdot\|(\mu_{\rm a},\mu_{\rm c})\|_{\rm op}^2.\end{aligned}$$

This implies

$$\begin{aligned}& \langle \delta^2 J(\lambda_{\rm a}^\infty, \lambda_{\rm c}^\infty)(\mu_{\rm a},\mu_{\rm c}),(\mu_{\rm a},\mu_{\rm c})\rangle \\ \geq \ & \|(\mu_{\rm a},\mu_{\rm c})\|_{\rm op}^2 - C_{\rm stab}\|\nabla\left(I\boldsymbol{U}^{\rm a}(\lambda_{\rm a}^\infty) - \boldsymbol{U}^{\rm c}(\lambda_{\rm c}^\infty)\right)\|_{L^2(\Omega_{\rm o})}\cdot\|(\mu_{\rm a},\mu_{\rm c})\|_{\rm op}^2 \\ = \ & \left(1 - C_{\rm stab}\|\nabla\left(I\boldsymbol{U}^{\rm a}(\lambda_{\rm a}^\infty) - \boldsymbol{U}^{\rm c}(\lambda_{\rm c}^\infty)\right)\|_{L^2(\Omega_{\rm o})}\right)\|(\mu_{\rm a},\mu_{\rm c})\|_{\rm op}^2,\end{aligned}$$

where we recall $\|\nabla\left(I\boldsymbol{U}^{\mathrm{a}}(\lambda_{\mathrm{a}}^{\infty})-\boldsymbol{U}^{\mathrm{c}}(\lambda_{\mathrm{c}}^{\infty})\right)\|_{L^2(\Omega_{\mathrm{o}})}$ is the continuum error. By Theorem 4.3.8, there exists $R_{\mathrm{core}}^{*,2}$ such that for all $R_{\mathrm{core}} \geq R_{\mathrm{core}}^{*,2}$,

$$\left(1 - C_{\mathrm{stab}}\|\nabla\left(I\boldsymbol{U}^{\mathrm{a}}(\lambda_{\mathrm{a}}^{\infty})-\boldsymbol{U}^{\mathrm{c}}(\lambda_{\mathrm{c}}^{\infty})\right)\|_{L^2(\Omega_{\mathrm{o}})}\right) \geq 1/2.$$

Taking $R_{\mathrm{core}}^{*} = \max\left\{R_{\mathrm{core}}^{*,1}, R_{\mathrm{core}}^{*,2}\right\}$ completes the proof. □

5.3.4 Error Estimate

We have now proven J is C^3 on $V^{\mathrm{a}} \times V^{\mathrm{c}}$, a consistency estimate in Theorem 5.3.7, and a stability result in Theorem 5.3.3. This allows us to use the inverse function theorem to prove the following theorem which estimates the error of the optimization-based AtC made in terms of the virtual controls, λ_{a} and λ_{c}. After this, we prove our main error result, Theorem 4.4.2.

Theorem 5.3.9. *There exists $R_{\mathrm{core}}^{*} > 0$ such that for all $R_{\mathrm{core}} \geq R_{\mathrm{core}}^{*}$, the reduced space problem* (5.2.1) *has a solution $(\lambda_{\mathrm{a}}^{\mathrm{atc}}, \lambda_{\mathrm{c}}^{\mathrm{atc}})$, such that*

$$\|(\lambda_{\mathrm{a}}^{\infty}, \lambda_{\mathrm{c}}^{\infty}) - (\lambda_{\mathrm{a}}^{\mathrm{atc}}, \lambda_{\mathrm{c}}^{\mathrm{atc}})\|_{\mathrm{op}} \lesssim \; R_{\mathrm{core}}^{-d/2-1} + R_{\mathrm{c}}^{-d/2}. \tag{5.3.7}$$

Proof. We apply the inverse function theorem, Theorem 4.3.7, with $f = \delta J$, $X = \boldsymbol{\Lambda}^{\mathrm{a}} \times \boldsymbol{\Lambda}^{\mathrm{c}}$ endowed with the norm $\|\cdot\|_{\mathrm{op}}$, $Y = (\boldsymbol{\Lambda}^{\mathrm{a}} \times \boldsymbol{\Lambda}^{\mathrm{c}})^*$ endowed with the dual norm $\|\cdot\|_{\mathrm{op}^*}$, and $x_0 = (\lambda_{\mathrm{a}}^{\infty}, \lambda_{\mathrm{c}}^{\infty})$. Let R_{core}^{*} be the maximum of the R_{core}^{*} guaranteed to exist in Theorems 5.3.2, 5.3.4, 5.3.7 and, 5.3.8. Noting that $\|f(x_0)\|_{\mathrm{op}^*}$ is the consistency error defined in Section 5.3.2, Theorem 5.3.7, implies the bound

$$\|f(x_0)\|_{\mathrm{op}^*} \lesssim R_{\mathrm{core}}^{-d/2-1} + R_{\mathrm{c}}^{-d/2} =: \eta.$$

Observe also that $\delta f(x_0) = \delta^2 J(\lambda_{\mathrm{a}}^{\infty}, \lambda_{\mathrm{c}}^{\infty})$ and that the existence of a coercivity constant, $\sigma := 1/2$, from Section 5.3.3 implies $\|\delta f(x_0)^{-1}\| < \sigma^{-1} = 2$.

Furthermore, Theorems 5.3.2 and 5.3.4 provide constants η_{a} and η_{c} such that $\boldsymbol{U}^{\mathrm{a}}$ and $\boldsymbol{U}^{\mathrm{c}}$ are C^3 on $B_{\eta_{\mathrm{a}}}(\lambda_{\mathrm{a}}^{\infty})$ and $B_{\eta_{\mathrm{c}}}(\lambda_{\mathrm{c}}^{\infty})$ respectively. By Theorem 5.3.6, $\delta^3 J$ is bounded by derivatives of $\boldsymbol{U}^{\mathrm{a}}$ and $\boldsymbol{U}^{\mathrm{c}}$ of order at most 3. Furthermore, Theorems 5.3.2 and 5.3.4 state that derivatives of $\boldsymbol{U}^{\mathrm{a}}$ and $\boldsymbol{U}^{\mathrm{c}}$ are uniformly bounded in R_{core}. We may therefore conclude that the third derivative of J is also uniformly bounded in $R_{\mathrm{core}} \geq R_{\mathrm{core}}^{*}$. This implies $\delta f = \delta^2 J$ is Lipschitz on $B_{\eta_{\mathrm{a}}}(\lambda_{\mathrm{a}}^{\infty}) \times B_{\eta_{\mathrm{c}}}(\lambda_{\mathrm{c}}^{\infty})$ with a Lipschitz constant that we denote by L.

The bound $2L\eta(2)^2 < 1$ holds since the consistency error η may be made small for R^*_{core} large enough. Analogously, $B_{4\eta}(\lambda_{\text{a}}^\infty, \lambda_{\text{c}}^\infty) \subset B_{\eta_{\text{a}}}(\lambda_{\text{a}}^\infty) \times B_{\eta_{\text{c}}}(\lambda_{\text{c}}^\infty)$ for small enough η. Theorem 4.3.7, can now be invoked to deduce the existence of a minimizer, $(\lambda_{\text{a}}^{\text{atc}}, \lambda_{\text{c}}^{\text{atc}}) \in B_{4\eta}(\lambda_{\text{a}}^\infty, \lambda_{\text{c}}^\infty)$, of J, satisfying the stated bounds (5.3.7). □

We now provide a proof of Theorem 4.4.2, which is our main result.

Proof of Theorem 4.4.2. Let R^*_{core} be the maximum of the R^*_{core} from Theorem 5.3.9 and Theorem 5.2.1 so there exists $(\lambda_{\text{a}}^{\text{atc}}, \lambda_{\text{c}}^{\text{atc}})$ satisfying (5.3.7). Furthermore,

$$\left(\boldsymbol{U}^{\text{a}}(\lambda_{\text{a}}^{\text{atc}}), \boldsymbol{U}^{\text{c}}(\lambda_{\text{c}}^{\text{atc}}), \lambda_{\text{a}}^{\text{atc}}, \lambda_{\text{c}}^{\text{atc}}\right)$$

solves the constrained minimization problem (4.4.2). Hence setting $\boldsymbol{u}_{\text{a}}^{\text{atc}} = \boldsymbol{U}^{\text{a}}(\lambda_{\text{a}}^{\text{atc}})$ and $\boldsymbol{u}_{\text{c}}^{\text{atc}} = \boldsymbol{U}^{\text{c}}(\lambda_{\text{c}}^{\text{atc}})$, we obtain

$$\begin{aligned}
&\|\nabla\left(I\boldsymbol{u}_{\text{a}}^\infty - I\boldsymbol{u}_{\text{a}}^{\text{atc}}\right)\|^2_{L^2(\Omega_{\text{a}})} + \|\nabla\left(I\boldsymbol{u}_{\text{c}}^\infty - \boldsymbol{u}_{\text{c}}^{\text{atc}}\right)\|^2_{L^2(\Omega_{\text{c}})} \\
&= \|\nabla I\left(\boldsymbol{u}^\infty - \boldsymbol{U}^{\text{a}}(\lambda_{\text{a}}^{\text{atc}})\right)\|^2_{L^2(\Omega_{\text{a}})} + \|\nabla\left(I\boldsymbol{u}^\infty - \boldsymbol{U}^{\text{c}}(\lambda_{\text{c}}^{\text{atc}})\right)\|^2_{L^2(\Omega_{\text{c}})} \\
&\lesssim \|\nabla I\left(\boldsymbol{U}^{\text{a}}(\lambda_{\text{a}}^\infty) - \boldsymbol{U}^{\text{a}}(\lambda_{\text{a}}^{\text{atc}})\right)\|^2_{L^2(\Omega_{\text{a}})} + \|\nabla\left(I\boldsymbol{u}^\infty - \boldsymbol{U}^{\text{c}}(\lambda_{\text{c}}^\infty)\right)\|^2_{L^2(\Omega_{\text{c}})} \\
&\quad + \|\nabla\left(\boldsymbol{U}^{\text{c}}(\lambda_{\text{c}}^\infty) - \boldsymbol{U}^{\text{c}}(\lambda_{\text{c}}^{\text{atc}})\right)\|^2_{L^2(\Omega_{\text{c}})}.
\end{aligned}$$

The second term above is the continuum error. To handle the remaining terms, we recall that $\boldsymbol{U}^{\text{a}}$ and $\boldsymbol{U}^{\text{c}}$ are Lipschitz on $B_{\eta_{\text{a}}}(\lambda_{\text{a}}^\infty)$ and $B_{\eta_{\text{c}}}(\lambda_{\text{c}}^\infty)$ by virtue of $\delta\boldsymbol{U}^{\text{a}}$ and $\delta\boldsymbol{U}^{\text{c}}$ being uniformly bounded on these sets (see Lemma A.2.4 in the Appendix). Then, using norm-equivalence (5.2.6), Theorem 4.3.8 and Theorem 5.3.9 yields

$$\begin{aligned}
&\|\nabla\left(I\boldsymbol{u}^\infty - I\boldsymbol{u}_{\text{a}}^{\text{atc}}\right)\|^2_{L^2(\Omega_{\text{a}})} + \|\nabla\left(I\boldsymbol{u}^\infty - \boldsymbol{u}_{\text{c}}^{\text{atc}}\right)\|^2_{L^2(\Omega_{\text{c}})} \\
&\quad\lesssim \|\nabla I\left(\boldsymbol{U}^{\text{a}}(\lambda_{\text{a}}^\infty) - \boldsymbol{U}^{\text{a}}(\lambda_{\text{a}}^{\text{atc}})\right)\|^2_{L^2(\Omega_{\text{a}})} + \|\nabla\left(I\boldsymbol{u}^\infty - \boldsymbol{U}^{\text{c}}(\lambda_{\text{c}}^\infty)\right)\|^2_{L^2(\Omega_{\text{c}})} \\
&\qquad + \|\nabla\left(\boldsymbol{U}^{\text{c}}(\lambda_{\text{c}}^\infty) - \boldsymbol{U}^{\text{c}}(\lambda_{\text{c}}^{\text{atc}})\right)\|^2_{L^2(\Omega_{\text{c}})} \\
&\quad\lesssim \|\lambda_{\text{a}}^\infty - \lambda_{\text{a}}^{\text{atc}}\|^2_{\boldsymbol{\Lambda}^{\text{a}}} + \|\nabla\left(I\boldsymbol{u}^\infty - \boldsymbol{U}^{\text{c}}(\lambda_{\text{c}}^\infty)\right)\|^2_{L^2(\Omega_{\text{c}})} + \|\lambda_{\text{c}}^\infty - \lambda_{\text{c}}^{\text{atc}}\|^2_{\boldsymbol{\Lambda}^{\text{c}}} \\
&\quad= \|(\lambda_{\text{a}}^\infty, \lambda_{\text{c}}^\infty) - (\lambda_{\text{a}}^{\text{atc}}, \lambda_{\text{c}}^{\text{atc}})\|^2_{\text{err}} + \|\nabla\left(I\boldsymbol{u}^\infty - \boldsymbol{U}^{\text{c}}(\lambda_{\text{c}}^\infty)\right)\|^2_{L^2(\Omega_{\text{c}})} \\
&\quad\lesssim \|(\lambda_{\text{a}}^\infty, \lambda_{\text{c}}^\infty) - (\lambda_{\text{a}}^{\text{atc}}, \lambda_{\text{c}}^{\text{atc}})\|^2_{\text{op}} + \|\nabla\left(I\boldsymbol{u}^\infty - \boldsymbol{U}^{\text{c}}(\lambda_{\text{c}}^\infty)\right)\|^2_{L^2(\Omega_{\text{c}})} \lesssim R_{\text{core}}^{-d-2} + R_{\text{c}}^{-d}.
\end{aligned}$$

□

5.4 Norm Equivalence

The main result of this section is the norm equivalence result stated in Theorem 5.2.1. The author's previous work [46] has established a similar norm equivalence in a simplified setting involving linear equations in one dimension. The proofs in [46] rely on an explicit characterization of the properties of the atomistic and continuum solutions and cannot be extended to the nonlinear or higher dimensional case. For continuum problems, related results exist in the context of overlapping and non-overlapping heterogeneous domain decomposition of partial differential equations via virtual controls in, for example [26]. The recent work [18] provides an alternative setting for coupling various fluid flow problems in which the problem subdomains overlap, but the objective is defined by measuring the difference in solutions only on the interface parts of the overlap region. Their paper shows that the discretized version of the cost functional is a norm on the virtual control space.

The proof of the lower bound, $\|(\mu_{\rm a},\mu_{\rm c})\|_{\rm op} \lesssim \|(\mu_{\rm a},\mu_{\rm c})\|_{\rm err}$, is clear since

$$\begin{aligned}\|(\mu_{\rm a},\mu_{\rm c})\|_{\rm op} = &\ \|\nabla\left(I\delta\boldsymbol{U}^{\rm a}(\lambda_{\rm a}^{\infty})[\mu_{\rm a}] - \delta\boldsymbol{U}^{\rm c}(\lambda_{\rm c}^{\infty})[\mu_{\rm c}]\right)\|_{L^2(\Omega_{\rm o})}\\ \leq &\ \|\nabla I\delta\boldsymbol{U}^{\rm a}(\lambda_{\rm a}^{\infty})[\mu_{\rm a}]\|_{L^2(\Omega_{\rm a})} + \|\nabla\delta\boldsymbol{U}^{\rm c}(\lambda_{\rm c}^{\infty})[\mu_{\rm c}]\|_{L^2(\Omega_{\rm c})}\\ \lesssim &\ \|(\mu_{\rm a},\mu_{\rm c})\|_{\rm err},\end{aligned}$$

so we focus only on the upper equivalence bound. We recall that the finite element mesh $\mathcal{T}_h$ is subject to a minimum angle condition for some $\beta > 0$ and state a precise version of the right inequality in Theorem 5.2.1.

Theorem 5.4.1. *There exists $C, R^*_{\rm core} > 0$ such that for all domains $\Omega_{\rm a}, \Omega_{\rm c}$, and meshes $\mathcal{T}_h$ constructed according to the guidelines of Section 4.2 (in particular $\psi_{\rm a}R_{\rm core} = R_{\rm a}$) with $R_{\rm core} \geq R^*_{\rm core}$, we have*

$$\|(\mu_{\rm a},\mu_{\rm c})\|_{\rm err} \leq C\|(\mu_{\rm a},\mu_{\rm c})\|_{\rm op} \quad \forall(\mu_{\rm a},\mu_{\rm c}) \in \boldsymbol{\Lambda}^{\rm a}\times\boldsymbol{\Lambda}^{\rm c}. \tag{5.4.1}$$

Equivalently, for all $(\boldsymbol{w}^{\rm a},\boldsymbol{w}^{\rm c}) \in \boldsymbol{\mathcal{U}}^{\rm a}\times\boldsymbol{\mathcal{U}}^{\rm c}_h$ such that

$$\langle\delta^2\tilde{\mathcal{E}}^{\rm a}(\boldsymbol{u}_{\rm a}^{\infty})\boldsymbol{w}^{\rm a},\boldsymbol{v}^{\rm a}\rangle = 0 \quad \forall\boldsymbol{v}^{\rm a}\in\boldsymbol{\mathcal{U}}^{\rm a}_0 \qquad \textit{and} \tag{5.4.2}$$

$$\langle\delta^2\tilde{\mathcal{E}}^{\rm c}(\boldsymbol{u}^{\rm con})\boldsymbol{w}^{\rm c},\boldsymbol{v}^{\rm c}\rangle = 0 \quad \forall\boldsymbol{v}^{\rm c}\in\boldsymbol{\mathcal{U}}^{\rm c}_{h,0} \tag{5.4.3}$$

we have

$$\|\nabla I\boldsymbol{w}^{\mathrm{a}}\|^2_{L^2(\Omega_{\mathrm{a}})} + \|\nabla \boldsymbol{w}^{\mathrm{c}}\|^2_{L^2(\Omega_{\mathrm{c}})} \leq C\|\nabla \left(I\boldsymbol{w}^{\mathrm{a}} - \boldsymbol{w}^{\mathrm{c}}\right)\|^2_{L^2(\Omega_{\mathrm{o}})}. \tag{5.4.4}$$

Equivalence of (5.4.1) and (5.4.4) follows directly from definitions of $\|\cdot\|_{\mathrm{err}}$, $\|\cdot\|_{\mathrm{op}}$, $\boldsymbol{U}^{\mathrm{a}}$, and $\boldsymbol{U}^{\mathrm{c}}$.

In Section 5.4.1 we show that proving Theorem 5.4.1 reduces to proving the following result

Theorem 5.4.2. *There exists $0 < c < 1$ and $R^*_{\mathrm{core}} > 0$ such that for all domains $\Omega_{\mathrm{a}}, \Omega_{\mathrm{c}}$ and meshes $\mathcal{T}_h$ satisfying the requirements of Section 4.2 with $R_{\mathrm{core}} \geq R^*_{\mathrm{core}}$,*

$$\sup_{\boldsymbol{w}^{\mathrm{a}},\boldsymbol{w}^{\mathrm{c}}\neq\boldsymbol{0}} \frac{(\nabla I\boldsymbol{w}^{\mathrm{a}}, \nabla \boldsymbol{w}^{\mathrm{c}})_{L^2(\Omega_{\mathrm{o}})}}{\|\nabla(I\boldsymbol{w}^{\mathrm{a}})\|_{L^2(\Omega_{\mathrm{o}})}\|\nabla \boldsymbol{w}^{\mathrm{c}}\|_{L^2(\Omega_{\mathrm{o}})}} \leq c,$$

for all $(\boldsymbol{w}^{\mathrm{a}}, \boldsymbol{w}^{\mathrm{c}}) \in \boldsymbol{\mathcal{U}}^{\mathrm{a}} \times \boldsymbol{\mathcal{U}}^{\mathrm{c}}_h$ such that

$$\langle \delta^2\tilde{\mathcal{E}}^{\mathrm{a}}(\boldsymbol{u}^{\infty}_{\mathrm{a}})\boldsymbol{w}^{\mathrm{a}}, \boldsymbol{v}^{\mathrm{a}}\rangle = 0 \quad \forall \boldsymbol{v}^{\mathrm{a}} \in \boldsymbol{\mathcal{U}}^{\mathrm{a}}_0,$$
$$\langle \delta^2\tilde{\mathcal{E}}^{\mathrm{c}}(\boldsymbol{u}^{\mathrm{con}})\boldsymbol{w}^{\mathrm{c}}, \boldsymbol{v}^{\mathrm{c}}\rangle = 0 \quad \forall \boldsymbol{v}^{\mathrm{c}} \in \boldsymbol{\mathcal{U}}^{\mathrm{c}}_{h,0}.$$

We prove Theorem 5.4.2 in Section 5.4.2 by using extension results due to Stein and Burenkov in [71] and [10]. These are written for reference as Theorems A.1.1–A.1.2 in the appendix. The theorem due to Burenkov is an extension result that preserves the seminorm, and this will allow us to bound solutions to the atomistic and continuum subproblems in terms of the solutions over Ω_{o}.

5.4.1 Reduction

Before proving Theorem 5.4.2 in Section 5.4.2, we show that Theorem 5.4.2 does indeed imply the assertion of Theorem 5.4.1. The first step is to bound solutions of the atomistic and continuum problems in terms of their values over the overlap region. We shall argue by contradiction using scaled versions of (5.4.2) and (5.4.3). We distinguish objects in the scaled domain by using a tilde accent, i.e. $\tilde{\mathcal{L}}_{\mathrm{a},n} = \epsilon_n \mathcal{L}_{\mathrm{a},n}$.

In each proof, we will consider sequences $R^*_{\mathrm{core},n} \to \infty$ and $R_{\mathrm{c},n} \to \infty$ with

$$R_{\mathrm{c},n}/R^*_{\mathrm{core},n} \to \infty$$

and with corresponding domains $\Omega_{\mathrm{a},n}, \Omega_{\mathrm{c},n}$, etc. and lattices $\mathcal{L}_{\mathrm{a},n}, \mathcal{L}_{\mathrm{c},n}$, etc. Given $\boldsymbol{w}^{\mathrm{a}}_n$ and $\boldsymbol{w}^{\mathrm{c}}_n$, we will then set $\varepsilon_n = 1/R_{\mathrm{core},n}$, and scale by ε_n to obtain functions $\tilde{\boldsymbol{w}}^{\mathrm{c}}_n(\varepsilon_n x) =$

$\varepsilon_n \boldsymbol{w}_n^{\mathrm{c}}(x)$ and $\tilde{\boldsymbol{w}}_n^{\mathrm{a}}(\varepsilon_n x) = \varepsilon_n \boldsymbol{w}_n^{\mathrm{a}}(x)$. Thus, each $\tilde{\boldsymbol{w}}_n^{\mathrm{a}}$ is defined on $\tilde{\mathcal{L}}_{\mathrm{a},n} = \epsilon_n \mathcal{L}_{\mathrm{a},n}$. Note also that the domains $\tilde{\Omega}_{\mathrm{core}} := \epsilon_n \Omega_{\mathrm{core},n}$ and $\tilde{\Omega}_{\mathrm{a}}$ have fixed radii of 1 and ψ_{a} respectively. The domains in the sequence $\{\tilde{\Omega}_{\mathrm{c},n}\}_{n=1}^{\infty}$ have fixed inner boundaries, but their outer boundaries tend to infinity since $R_{\mathrm{c},n}/R_{\mathrm{core},n}^{*} \to \infty$. Because each $\boldsymbol{w}_n^{\mathrm{c}}$ is constant on the outer boundary of $\Omega_{\mathrm{c},n}$, we may extend each of them outside of this region to infinity to obtain scaled functions $\tilde{\boldsymbol{w}}_n^{\mathrm{c}}$ defined on $\tilde{\Omega}_{\mathrm{c}} := \mathbb{R}^n \backslash \tilde{\Omega}_{\mathrm{core}}$. Using this notation, we also define $\tilde{\mathcal{L}}_n := \epsilon_n \mathcal{L}$.

The functions $\tilde{\boldsymbol{w}}_n^{\mathrm{a}}$ and $\tilde{\boldsymbol{w}}_n^{\mathrm{c}}$ now satisfy scaled versions of (5.4.2) and (5.4.3) in which the interpolants and displacement spaces are parametrized by n in the obvious manner: $\tilde{\boldsymbol{\mathcal{U}}}_n^{\mathrm{a}}, \tilde{\boldsymbol{\mathcal{U}}}_{0,n}^{\mathrm{a}}, \tilde{\boldsymbol{\mathcal{U}}}_{h,n}^{\mathrm{c}}$, and $\tilde{\boldsymbol{\mathcal{U}}}_{h,0,n}^{\mathrm{c}}$. For clarity, we introduce several new notations. We define scaled finite differences and finite difference stencils for $\xi \in \tilde{\mathcal{L}}_n$ and $\rho \in \mathcal{R}$ by

$$D_{\epsilon_n \rho} \tilde{\boldsymbol{u}}(\xi) = \frac{\tilde{\boldsymbol{u}}(\xi + \epsilon_n \rho) - \tilde{\boldsymbol{u}}(\xi)}{\epsilon_n} \quad \text{and} \quad D_{\epsilon_n} \tilde{\boldsymbol{u}}(\xi) = \left(D_{\epsilon_n \rho} \tilde{\boldsymbol{u}}(\xi)\right)_{\rho \in \mathcal{R}}.$$

The discrete norm (4.3.4) scales to

$$\|D_{\epsilon_n} \tilde{\boldsymbol{v}}\|_{\ell^2_{\epsilon_n}(\tilde{\mathcal{L}}^{\circ}_{\mathrm{a},n})}^2 = \epsilon_n^d \sum_{\xi \in \tilde{\mathcal{L}}^{\circ}_{\mathrm{a},n}} \sup_{\rho \in \mathcal{R}} |D_{\epsilon_n \rho} \tilde{\boldsymbol{v}}|^2,$$

for which we still possess the estimate

$$\|D_{\epsilon_n} \tilde{\boldsymbol{v}}\|_{\ell^2_{\epsilon_n}(\tilde{\mathcal{L}}^{\circ}_{\mathrm{a},n})} \lesssim \|\nabla I_n \tilde{\boldsymbol{v}}\|_{L^2(\tilde{\Omega}_{\mathrm{a},n})}.$$

The function $\tilde{\boldsymbol{w}}_n^{\mathrm{a}}$ satisfies the following scaled variational equation:

$$\begin{aligned} \epsilon_n^d \sum_{\xi \in \tilde{\mathcal{L}}^{\circ}_{\mathrm{a},n}} \sum_{\rho,\tau \in \mathcal{R}} & [D_{\epsilon_n \rho} \tilde{\boldsymbol{w}}_n^{\mathrm{a}}(\xi)]^{\top} V_{\xi,\rho\tau}(D_{\epsilon_n} \tilde{\boldsymbol{u}}_{\mathrm{a},n}^{\infty}(\xi))[D_{\epsilon_n \tau} \tilde{\boldsymbol{v}}^{\mathrm{a}}(\xi)] \\ & \equiv \epsilon_n^d \sum_{\xi \in \tilde{\mathcal{L}}^{\circ}_{\mathrm{a},n}} V_{\xi}''(D_{\epsilon_n} \tilde{\boldsymbol{u}}_{\mathrm{a},n}^{\infty}(\xi)) : D_{\epsilon_n} \tilde{\boldsymbol{w}}_n^{\mathrm{a}} : D_{\epsilon_n} \tilde{\boldsymbol{v}}^{\mathrm{a}} = 0 \quad \forall \tilde{\boldsymbol{v}}^{\mathrm{a}} \in \tilde{\boldsymbol{\mathcal{U}}}_{0,n}^{\mathrm{a}}, \end{aligned} \tag{5.4.5}$$

where we define the : notation through the equality above.

It will be extremely useful to express (5.4.5) as an integral for those $\tilde{\boldsymbol{v}}^{\mathrm{a}}$ such that $D_{\epsilon_n} \tilde{\boldsymbol{v}}^{\mathrm{a}}$ vanishes on $\tilde{\mathcal{L}}_{\mathrm{a},n} \backslash \tilde{\mathcal{L}}^{\circ}_{\mathrm{a},n}$ and $D_{\epsilon_n} \tilde{\boldsymbol{v}}^{\mathrm{a}}$ vanishes where $V_{\xi} \neq V$. This requires an additional tool. The cell, ς_{ξ}, based on $\xi \in \tilde{\mathcal{L}}_n$ is

$$\varsigma_{\xi} := \mathsf{F}\left\{x \in \mathbb{R}^d : 0 \leq x_i - \xi_i < \epsilon_n, i = 1, \ldots, d\right\}.$$

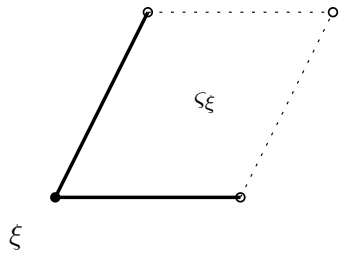

Figure 5.1: An example of ς_ξ. The boundaries are formed by the Bravais lattice basis vectors given by the columns of F. The solid lines are included in the set, while the dotted lines are not.

An example is shown pictured in Figure 5.1.

Let $\bar{I}_n$ be a piecewise constant interpolation operator defined by

$$\bar{I}_n f(x) := f(\xi) \quad \text{where } x \in \varsigma_\xi.$$

Then for such a $\tilde{\boldsymbol{v}}^{\mathrm{a}}$,

$$\begin{aligned}
&\epsilon_n^d \sum_{\xi \in \tilde{\mathcal{L}}^{\circ}_{\mathrm{a},n}} V''_\xi(D_{\epsilon_n}\tilde{\boldsymbol{u}}^{\infty}_{\mathrm{a},n}(\xi)) : D_{\epsilon_n}\tilde{\boldsymbol{w}}^{\mathrm{a}}_n(\xi) : D_{\epsilon_n}\tilde{\boldsymbol{v}}^{\mathrm{a}}(\xi) \\
&\quad = \sum_{\xi \in \tilde{\mathcal{L}}^{\circ}_{\mathrm{a},n}} V''_\xi(D_{\epsilon_n}\tilde{\boldsymbol{u}}^{\infty}_{\mathrm{a},n}(\xi)) : D_{\epsilon_n}\tilde{\boldsymbol{w}}^{\mathrm{a}}_n(\xi) : D_{\epsilon_n}\tilde{\boldsymbol{v}}^{\mathrm{a}}(\xi)\, \mathrm{vol}(\varsigma_\xi \cap \tilde{\Omega}_{\mathrm{a}}) \\
&\quad = \sum_{\xi \in \tilde{\mathcal{L}}_{\mathrm{a},n}} V''_\xi(D_{\epsilon_n}\tilde{\boldsymbol{u}}^{\infty}_{\mathrm{a},n}(\xi)) : D_{\epsilon_n}\tilde{\boldsymbol{w}}^{\mathrm{a}}_n(\xi) : D_{\epsilon_n}\tilde{\boldsymbol{v}}^{\mathrm{a}}(\xi)\, \mathrm{vol}(\varsigma_\xi \cap \tilde{\Omega}_{\mathrm{a}}) \\
&\quad = \int_{\tilde{\Omega}_{\mathrm{a}}} \bar{I}_n V''(D_{\epsilon_n}\tilde{\boldsymbol{u}}^{\infty}_{\mathrm{a},n}(x)) : \bar{I}_n D_{\epsilon_n}\tilde{\boldsymbol{w}}^{\mathrm{a}}_n(x) : \bar{I}_n D_{\epsilon_n}\tilde{\boldsymbol{v}}^{\mathrm{a}}(x)\, dx.
\end{aligned} \tag{5.4.6}$$

Observe that we have replaced V''_ξ with V'' in the integral since $D_{\epsilon_n}\tilde{\boldsymbol{v}}^{\mathrm{a}}$ is assumed to vanish whenever $V \neq V_\xi$.

Similarly, $\tilde{\boldsymbol{w}}^{\mathrm{c}}_n$ satisfies an analogous scaled version of (5.4.7):

$$\begin{aligned}
\int_{\tilde{\Omega}_{\mathrm{c},n}} \sum_{\rho,\tau \in \mathcal{R}} [\nabla_\rho \tilde{\boldsymbol{w}}^{\mathrm{c}}_n]^\top [V''_{,\rho\tau}(\nabla_{\mathcal{R}}\tilde{\boldsymbol{u}}^{\mathrm{con}}_n)][\nabla_\tau \tilde{\boldsymbol{v}}^{\mathrm{c}}]\, dx \equiv & \int_{\tilde{\Omega}_{\mathrm{c},n}} W''(\nabla\tilde{\boldsymbol{u}}^{\mathrm{con}}_n) : \nabla\tilde{\boldsymbol{w}}^{\mathrm{c}}_n : \nabla\tilde{\boldsymbol{v}}^{\mathrm{c}}_n\, dx \\
&= 0 \quad \forall \tilde{\boldsymbol{v}}^{\mathrm{c}} \in \tilde{\boldsymbol{\mathcal{U}}}^{\mathrm{c}}_{h,0,n}.
\end{aligned} \tag{5.4.7}$$

Further define the fourth order tensor, $\mathbb{C} = W''(\mathbf{0})$.

The next lemma bounds solutions of the atomistic and continuum problems in terms of their values over the overlap region. It can be considered an analog of an elliptic regularity result for the linearized atomistic and continuum operators.

Lemma 5.4.3. *Suppose that* $\boldsymbol{w}^{\mathrm{a}}$ *and* $\boldsymbol{w}^{\mathrm{c}}$ *are such that equations* (5.4.2) *and* (5.4.3) *hold. Then there exists* $R^*_{\mathrm{core}} > 0$ *such that*

$$\|\nabla I\boldsymbol{w}^{\mathrm{a}}\|_{L^2(\Omega_{\mathrm{a}})} \lesssim \|\nabla I\boldsymbol{w}^{\mathrm{a}}\|_{L^2(\Omega_{\mathrm{o}})} \qquad \textit{and} \tag{5.4.8}$$

$$\|\nabla \boldsymbol{w}^{\mathrm{c}}\|_{L^2(\Omega_{\mathrm{c}})} \lesssim \|\nabla \boldsymbol{w}^{\mathrm{c}}\|_{L^2(\Omega_{\mathrm{o}})}, \tag{5.4.9}$$

for all domains $\Omega_{\mathrm{a}}, \Omega_{\mathrm{c}}$ *and continuum meshes* $\mathcal{T}_h$ *constructed according to the guidelines of Section 4.2 with* $R_{\mathrm{core}} \geq R^*_{\mathrm{core}}$.

Proof. Assume that (5.4.8)–(5.4.9) do not hold. Then, there exists a sequence $R^*_{\mathrm{core},n} \to \infty$, with corresponding sequences $R_{\mathrm{core,n}} \geq R^*_{\mathrm{core},n}$, $R_{\mathrm{c},n}$, $\Omega_{\mathrm{a},n}, \Omega_{\mathrm{c},n}$, $\mathcal{T}_{h,n}$, $\boldsymbol{w}^{\mathrm{c}}_n$ and $\boldsymbol{w}^{\mathrm{a}}_n$, such that $R_{\mathrm{core},n} \to \infty$, $R_{\mathrm{c},n} \to \infty$, $R_{\mathrm{c},n}/R_{\mathrm{core,n}} = R^{\kappa}_{\mathrm{core,n}} \to \infty$ with

$$\frac{\|\nabla I_n \boldsymbol{w}^{\mathrm{a}}_n\|_{L^2(\Omega_{\mathrm{a},n})}}{\|\nabla I_n \boldsymbol{w}^{\mathrm{a}}_n\|_{L^2(\Omega_{\mathrm{o},n})}} \to \infty, \qquad \frac{\|\nabla \boldsymbol{w}^{\mathrm{c}}_n\|_{L^2(\Omega_{\mathrm{c},n})}}{\|\nabla \boldsymbol{w}^{\mathrm{c}}_n\|_{L^2(\Omega_{\mathrm{o},n})}} \to \infty. \tag{5.4.10}$$

After scaling the lattice, the domains, and the functions by $\epsilon_n := \frac{1}{R_{\mathrm{core,n}}}$ and using the notation introduced in this section, we find from (5.4.10) that

$$\frac{\|\nabla I_n \tilde{\boldsymbol{w}}^{\mathrm{a}}_n\|_{L^2(\tilde{\Omega}_{\mathrm{a}})}}{\|\nabla I_n \tilde{\boldsymbol{w}}^{\mathrm{a}}_n\|_{L^2(\tilde{\Omega}_{\mathrm{o}})}} \to \infty. \tag{5.4.11}$$

Extend $I_n \tilde{\boldsymbol{w}}^{\mathrm{a}}_n|_{\tilde{\Omega}_{\mathrm{o}}}$ to $\mathbb{R}^d$ using the extension operator R from Theorem A.1.2. This operator "preserves" seminorms so we have

$$\|\nabla(R(I_n \tilde{\boldsymbol{w}}^{\mathrm{a}}_n|_{\tilde{\Omega}_{\mathrm{o}}}))\|_{L^2(\tilde{\Omega}_{\mathrm{a}})} \leq C(\tilde{\Omega}_{\mathrm{o}}) \|\nabla I_n \tilde{\boldsymbol{w}}^{\mathrm{a}}_n\|_{L^2(\tilde{\Omega}_{\mathrm{o}})}.$$

Moreover, $R(I_n \tilde{\boldsymbol{w}}^{\mathrm{a}}_n|_{\tilde{\Omega}_{\mathrm{o}}}) = I_n \tilde{\boldsymbol{w}}^{\mathrm{a}}_n$ on $\partial_{\mathrm{a}}\tilde{\mathcal{L}}_{\mathrm{a}}$. Let $S_{\mathrm{a},n}$ be the Scott-Zhang interpolant operator from $H^1(\tilde{\Omega}_{\mathrm{a}})$ to

$$\left\{ u \in \mathrm{C}(\tilde{\Omega}_{\mathrm{a}}) : u|_\tau \in \mathcal{P}_1(\tau) \quad \forall \tau \in \tilde{\mathcal{T}}_{\mathrm{a},n} \right\}.$$

Then $S_{\mathrm{a},n} R(I_n \tilde{\boldsymbol{w}}^{\mathrm{a}}_n|_{\tilde{\Omega}_{\mathrm{o}}})$ defines an atomistic function in $\boldsymbol{\mathcal{U}}^{\mathrm{a}}_n$, which is equal to $\tilde{\boldsymbol{w}}^{\mathrm{a}}_n$ on $\partial_{\mathrm{a}}\tilde{\mathcal{L}}_{\mathrm{a},n}$ since $R(I_n \tilde{\boldsymbol{w}}^{\mathrm{a}}_n|_{\tilde{\Omega}_{\mathrm{o}}})$ is piecewise linear on $\tilde{\Omega}_{\mathrm{o}}$ and due to the projection property

of $S_{\mathrm{a},n}$. This implies that $\tilde{\boldsymbol{z}}_n^{\mathrm{a}} := S_{\mathrm{a},n}R(I_n\tilde{\boldsymbol{w}}_n^{\mathrm{a}}|_{\tilde{\Omega}_{\mathrm{o}}})|_{\tilde{\Omega}_{\mathrm{a}}} - \tilde{\boldsymbol{w}}_n^{\mathrm{a}} \in \tilde{\boldsymbol{\mathcal{U}}}_{0,n}^{\mathrm{a}}$ and that $\tilde{\boldsymbol{z}}_n^{\mathrm{a}}$ solves the problem

$$\langle \delta^2\tilde{\mathcal{E}}_n^{\mathrm{a}}(\tilde{\boldsymbol{u}}_{\mathrm{a},n}^{\infty})\tilde{\boldsymbol{z}}_n^{\mathrm{a}}, \tilde{\boldsymbol{v}}_n^{\mathrm{a}}\rangle = \langle \delta^2\tilde{\mathcal{E}}^{\mathrm{a}}(\boldsymbol{u}_{\mathrm{a}}^{\infty})S_{\mathrm{a},n}R(I_n\tilde{\boldsymbol{w}}_n^{\mathrm{a}}|_{\tilde{\Omega}_{\mathrm{o}}})|_{\tilde{\Omega}_{\mathrm{a}}}, \tilde{\boldsymbol{v}}_n^{\mathrm{a}}\rangle \quad \forall \tilde{\boldsymbol{v}}_n^{\mathrm{a}} \in \tilde{\boldsymbol{\mathcal{U}}}_{0,n}^{\mathrm{a}}.$$

Thus, taking $\tilde{\boldsymbol{v}}_n^{\mathrm{a}} = \tilde{\boldsymbol{z}}_n^{\mathrm{a}}$, using (4.3.5), and the stability of the Scott-Zhang interpolant (see **P.3** in Section 4.3 or [9, Theorem 4.8.16]), we see that

$$\begin{aligned}\|\nabla I_n\tilde{\boldsymbol{z}}_n^{\mathrm{a}}\|_{L^2(\tilde{\Omega}_{\mathrm{a}})} \lesssim \|\nabla S_{\mathrm{a},n}R(I_n\tilde{\boldsymbol{w}}_n^{\mathrm{a}}|_{\tilde{\Omega}_{\mathrm{o}}})|_{\tilde{\Omega}_{\mathrm{a}}}\|_{L^2(\tilde{\Omega}_{\mathrm{a}})} &\lesssim \|\nabla R(I_n\tilde{\boldsymbol{w}}_n^{\mathrm{a}}|_{\tilde{\Omega}_{\mathrm{o}}})\|_{L^2(\tilde{\Omega}_{\mathrm{a}})} \\ &\leq C(\tilde{\Omega}_{\mathrm{o}})\|\nabla I_n\tilde{\boldsymbol{w}}_n^{\mathrm{a}}\|_{L^2(\tilde{\Omega}_{\mathrm{o}})}.\end{aligned}$$

The final bound follows from the boundedness of the extension operator due to Burenkov [10] detailed in Theorem A.1.2. This and the definition of $\boldsymbol{z}_n^{\mathrm{a}}$ imply

$$\|\nabla S_{\mathrm{a},n}R(I_n\tilde{\boldsymbol{w}}_n^{\mathrm{a}}|_{\tilde{\Omega}_{\mathrm{o}}})|_{\tilde{\Omega}_{\mathrm{a}}} - \nabla I_n\tilde{\boldsymbol{w}}_n^{\mathrm{a}}\|_{L^2(\tilde{\Omega}_{\mathrm{a}})} \lesssim C(\tilde{\Omega}_{\mathrm{o}})\|\nabla I_n\tilde{\boldsymbol{w}}_n^{\mathrm{a}}\|_{L^2(\tilde{\Omega}_{\mathrm{o}})},$$

which further leads to

$$\begin{aligned}\|\nabla I_n\tilde{\boldsymbol{w}}_n^{\mathrm{a}}\|_{L^2(\tilde{\Omega}_{\mathrm{a}})} &\lesssim C(\tilde{\Omega}_{\mathrm{o}})\|\nabla I_n\tilde{\boldsymbol{w}}_n^{\mathrm{a}}\|_{L^2(\tilde{\Omega}_{\mathrm{o}})} + \|\nabla R(I_n\tilde{\boldsymbol{w}}_n^{\mathrm{a}}|_{\tilde{\Omega}_{\mathrm{o}}})\|_{L^2(\tilde{\Omega}_{\mathrm{a}})} \\ &\leq 2C(\tilde{\Omega}_{\mathrm{o}})\|\nabla I_n\tilde{\boldsymbol{w}}_n^{\mathrm{a}}\|_{L^2(\tilde{\Omega}_{\mathrm{o}})},\end{aligned}$$

a contradiction to (5.4.11). This establishes (5.4.8).

A similar argument utilizing the Scott-Zhang interpolant on $\tilde{\Omega}_{\mathrm{c}}$ with mesh $\tilde{\mathcal{T}}_{h,n}$ yields (5.4.9). □

Finally, we show that the norm equivalence theorem, Theorem 5.4.1, is a consequence of Theorem 5.4.2, a strong Cauchy-Schwarz inequality.

Proof of Theorem 5.4.1. According to Lemma 5.4.3, if $\boldsymbol{w}^{\mathrm{a}}$ and $\boldsymbol{w}^{\mathrm{c}}$ satisfy both equations (5.4.2) and (5.4.3) then,

$$\|\nabla I\boldsymbol{w}^{\mathrm{a}}\|_{L^2(\Omega_{\mathrm{a}})}^2 + \|\nabla\boldsymbol{w}^{\mathrm{c}}\|_{L^2(\Omega_{\mathrm{c}})}^2 \lesssim \|\nabla I\boldsymbol{w}^{\mathrm{a}}\|_{L^2(\Omega_{\mathrm{o}})}^2 + \|\nabla\boldsymbol{w}^{\mathrm{c}}\|_{L^2(\Omega_{\mathrm{o}})}^2.$$

Consequently, to prove (5.4.4) in Theorem 5.4.1 it suffices to show that

$$\|\nabla(I\boldsymbol{w}^{\mathrm{a}})\|_{L^2(\Omega_{\mathrm{o}})}^2 + \|\nabla\boldsymbol{w}^{\mathrm{c}}\|_{L^2(\Omega_{\mathrm{o}})}^2 \lesssim \|\nabla(I\boldsymbol{w}^{\mathrm{a}} - \boldsymbol{w}^{\mathrm{c}})\|_{L^2(\Omega_{\mathrm{o}})}^2.$$

This result is a direct consequence of Theorem 5.4.2 since

$$\begin{aligned}
\|\nabla(I\boldsymbol{w}^{\mathrm{a}}-\boldsymbol{w}^{\mathrm{c}})\|^2_{L^2(\Omega_{\mathrm{o}})} &= \|\nabla I\boldsymbol{w}^{\mathrm{a}}\|^2_{L^2(\Omega_{\mathrm{o}})}+\|\nabla\boldsymbol{w}^{\mathrm{c}}\|^2_{L^2(\Omega_{\mathrm{o}})}-2\left(\nabla I\boldsymbol{w}^{\mathrm{a}},\nabla\boldsymbol{w}^{\mathrm{c}}\right)_{L^2(\Omega_{\mathrm{o}})}\\
&\geq \|\nabla I\boldsymbol{w}^{\mathrm{a}}\|^2_{L^2(\Omega_{\mathrm{o}})}+\|\nabla\boldsymbol{w}^{\mathrm{c}}\|^2_{L^2(\Omega_{\mathrm{o}})}-2c\|\nabla I\boldsymbol{w}^{\mathrm{a}}\|_{L^2(\Omega_{\mathrm{o}})}\|\nabla\boldsymbol{w}^{\mathrm{c}}\|_{L^2(\Omega_{\mathrm{o}})}\\
&\geq \|\nabla I\boldsymbol{w}^{\mathrm{a}}\|^2_{L^2(\Omega_{\mathrm{o}})}+\|\nabla\boldsymbol{w}^{\mathrm{c}}\|^2_{L^2(\Omega_{\mathrm{o}})}-c\|\nabla I\boldsymbol{w}^{\mathrm{a}}\|^2_{L^2(\Omega_{\mathrm{o}})}-c\|\nabla\boldsymbol{w}^{\mathrm{c}}\|^2_{L^2(\Omega_{\mathrm{o}})}\\
&= (1-c)\big(\|\nabla I\boldsymbol{w}^{\mathrm{a}}\|^2_{L^2(\Omega_{\mathrm{o}})}+\|\nabla\boldsymbol{w}^{\mathrm{c}}\|^2_{L^2(\Omega_{\mathrm{o}})}\big).
\end{aligned}$$

□

It remains to prove Theorem 5.4.2. For clarity, we break the proof into several intermediate steps.

5.4.2 Proof of Theorem 5.4.2

The proof is by contradiction and is derived from the following statement.

Statement 1. *There exist sequences*

$$R^*_{\mathrm{core},n}\to\infty, R_{\mathrm{core},n}\to\infty, R_{\mathrm{c},n}\to\infty, R_{\mathrm{c},n}/R_{\mathrm{core,n}}\to\infty;$$

a corresponding sequence of grids $\mathcal{T}_{h,n}$ with a minimum angle at least β; and corresponding sequences $\boldsymbol{w}^{\mathrm{c}}_n$, $\boldsymbol{w}^{\mathrm{a}}_n$ satisfying

$$\begin{aligned}
\langle\delta^2\tilde{\mathcal{E}}^{\mathrm{a}}(\boldsymbol{u}^{\infty}_{\mathrm{a}})\boldsymbol{w}^{\mathrm{a}},\boldsymbol{v}^{\mathrm{a}}\rangle &= 0 \quad \forall\boldsymbol{v}^{\mathrm{a}}\in\boldsymbol{\mathcal{U}}^{\mathrm{a}}_0,\\
\langle\delta^2\tilde{\mathcal{E}}^{\mathrm{c}}(\boldsymbol{u}^{\mathrm{con}})\boldsymbol{w}^{\mathrm{c}},\boldsymbol{v}^{\mathrm{c}}\rangle &= 0 \quad \forall\boldsymbol{v}^{\mathrm{c}}\in\boldsymbol{\mathcal{U}}^{\mathrm{c}}_{h,0},
\end{aligned}$$

such that

$$\frac{(\nabla I\boldsymbol{w}^{\mathrm{a}}_n,\nabla\boldsymbol{w}^{\mathrm{c}}_n)_{L^2(\Omega_{\mathrm{o}})}}{\|\nabla(I\boldsymbol{w}^{\mathrm{a}}_n)\|_{L^2(\Omega_{\mathrm{o}})}\|\nabla\boldsymbol{w}^{\mathrm{c}}_n\|_{L^2(\Omega_{\mathrm{o}})}}\to 1. \tag{5.4.12}$$

We will show (5.4.12) yields a contradiction in four steps. In the first step, we will again scale the lattice by $\varepsilon_n = 1/R_{\mathrm{core},n}$ to define sequences of functions $\tilde{\boldsymbol{w}}^{\mathrm{a}}_n$, having a common domain of definition—$\tilde{\Omega}_{\mathrm{a}}$—and $\tilde{\boldsymbol{w}}^{\mathrm{c}}_n$, having a common domain of definition—$\tilde{\Omega}_{\mathrm{c}}$. These are bounded sequences so this will allow us to extract weak limits of these sequences. The second step is to show these limits satisfy the homogeneous Cauchy-Born equation. In the third step, we show weak convergence, combined with satisfying atomistic and finite element equations, implies the limit and inner product commute.

This will yield a contradiction in the final, fourth step of the proof where we use the fact that the inner product of a weakly convergent and strongly convergent pair of sequences converges strongly to the inner product of the limit.

Step 1:

Recall that we use the tilde accent for objects on the scaled domains. Let I_n be the piecewise interpolant onto the lattice $\tilde{\mathcal{L}}_n$, and normalize $\tilde{\boldsymbol{w}}_n^{\mathrm{a}}$ and $\tilde{\boldsymbol{w}}_n^{\mathrm{c}}$ to functions $\bar{\boldsymbol{w}}_n^{\mathrm{a}}$ and $\bar{\boldsymbol{w}}_n^{\mathrm{c}}$ such that

$$\|\nabla I_n \bar{\boldsymbol{w}}_n^{\mathrm{a}}\|_{L^2(\tilde{\Omega}_{\mathrm{o}})} = 1, \quad \text{and} \quad \|\nabla \bar{\boldsymbol{w}}_n^{\mathrm{c}}\|_{L^2(\tilde{\Omega}_{\mathrm{o}})} = 1.$$

Due to this property and our hypothesis (5.4.12), we have that

$$(\nabla I_n \bar{\boldsymbol{w}}_n^{\mathrm{a}}, \nabla \bar{\boldsymbol{w}}_n^{\mathrm{c}})_{L^2(\tilde{\Omega}_{\mathrm{o}})} \to 1. \tag{5.4.13}$$

Moreover, $\nabla I_n \bar{\boldsymbol{w}}_n^{\mathrm{a}}$ is a bounded sequence in $L^2(\tilde{\Omega}_{\mathrm{a}})$ since

$$\begin{aligned} \|\nabla I_n \bar{\boldsymbol{w}}_n^{\mathrm{a}}\|_{L^2(\tilde{\Omega}_{\mathrm{a}})} = & \ \|\nabla I_n \tilde{\boldsymbol{w}}_n^{\mathrm{a}}\|_{L^2(\tilde{\Omega}_{\mathrm{a}})} / \|\nabla I_n \tilde{\boldsymbol{w}}_n^{\mathrm{a}}\|_{L^2(\tilde{\Omega}_{\mathrm{o}})} \\ \lesssim & \ \|\nabla I_n \tilde{\boldsymbol{w}}_n^{\mathrm{a}}\|_{L^2(\tilde{\Omega}_{\mathrm{o}})} / \|\nabla I_n \tilde{\boldsymbol{w}}_n^{\mathrm{a}}\|_{L^2(\tilde{\Omega}_{\mathrm{o}})} = 1, \end{aligned}$$

after using a scaled version of Lemma 5.4.3. Similarly, $\nabla \bar{\boldsymbol{w}}_n^{\mathrm{c}}$ is bounded in $L^2(\tilde{\Omega}_{\mathrm{c}})$. Meanwhile, $\bar{\boldsymbol{w}}_n^{\mathrm{a}}$ and $\bar{\boldsymbol{w}}_n^{\mathrm{c}}$ will still satisfy the variational equalities (5.4.5) and (5.4.7) by linearity.

For each n, we let $\bar{w}_n^{\mathrm{a}}$ (without boldface) be the element in the equivalence class of $\bar{\boldsymbol{w}}_n^{\mathrm{a}}$ such that $I_n \bar{w}_n^{\mathrm{a}}$ has mean value 0 over $\tilde{\Omega}_{\mathrm{a}}$. The resulting sequence is bounded in $H^1(\tilde{\Omega}_{\mathrm{a}})$ and so it has a weakly convergent subsequence, which we denote again by $I_n \bar{w}_n^{\mathrm{a}}$. Let $\bar{w}_0^{\mathrm{a}} \in H^1(\tilde{\Omega}_{\mathrm{a}})$ be the weak limit. By the compactness of the embedding $H^1(\tilde{\Omega}_{\mathrm{a}}) \subset L^2(\tilde{\Omega}_{\mathrm{a}})$ it follows that $I_n \bar{w}_n^{\mathrm{a}} \to \bar{w}_0^{\mathrm{a}}$ in $L^2(\tilde{\Omega}_{\mathrm{a}})$. Similarly, the functions $\bar{\boldsymbol{w}}_n^{\mathrm{c}}$ form a bounded sequence on the Hilbert space (cf. [55]),

$$\boldsymbol{W}^{1,2}(\tilde{\Omega}_{\mathrm{c}}) := \left\{ u^{\mathrm{c}} \in H^1_{\mathrm{loc}}(\tilde{\Omega}_{\mathrm{c}}) : \nabla u^{\mathrm{c}} \in L^2(\tilde{\Omega}_{\mathrm{c}}) \right\} / \mathbb{R}^d.$$

Thus, we can extract a weakly convergent subsequence, still denoted by $\bar{\boldsymbol{w}}_n^{\mathrm{c}}$, with limit $\bar{\boldsymbol{w}}_0^{\mathrm{c}} \in \boldsymbol{W}^{1,2}(\tilde{\Omega}_{\mathrm{c}})$, i.e, $\bar{\boldsymbol{w}}_n^{\mathrm{c}} \rightharpoonup \bar{\boldsymbol{w}}_0^{\mathrm{c}}$ in $\boldsymbol{W}^{1,2}(\tilde{\Omega}_{\mathrm{c}})$.

Let $\bar{w}_n^{\mathrm{c}}$ and $\bar{w}_0^{\mathrm{c}}$ (without boldface) be equivalence class elements having zero mean over $\tilde{\Omega}_{\mathrm{o,ex}}$. Then $\bar{w}_n^{\mathrm{c}}$ is bounded in $H^1(\tilde{\Omega}_{\mathrm{o,ex}})$ and converges weakly to some $\bar{w}^{\mathrm{c}} \in$

$H^1(\tilde{\Omega}_{\rm o,ex})$. But since $\bar{\boldsymbol{w}}^{\rm c}_n \rightharpoonup \bar{\boldsymbol{w}}^{\rm c}_0$ in $\boldsymbol{W}^{1,2}(\tilde{\Omega}_{\rm c})$ we must have $\nabla \bar{w}^{\rm c} = \nabla \bar{w}^{\rm c}_0$ on $\tilde{\Omega}_{\rm o,ex}$ so the two functions differ almost everywhere by a constant on $\tilde{\Omega}_{\rm o,ex}$. Since both $\bar{w}^{\rm c}_0$ and $\bar{w}^{\rm c}$ have mean value 0 over $\tilde{\Omega}_{\rm o,ex}$, the two functions are in fact equal on $\tilde{\Omega}_{\rm o,ex}$. Thus $\bar{w}^{\rm c}_n$ converges weakly to $\bar{w}^{\rm c}_0$ in $H^1(\tilde{\Omega}_{\rm o,ex})$. The strong convergence $\bar{w}^{\rm c}_n \to \bar{w}^{\rm c}_0$ in $L^2(\tilde{\Omega}_{\rm o,ex})$ then follows from the compactness of the embedding $H^1(\tilde{\Omega}_{\rm o,ex}) \hookrightarrow L^2(\tilde{\Omega}_{\rm o,ex})$.

In summary, we have established the following result.

Lemma 5.4.4. *There exist sequences $\bar{w}^{\rm a}_n$ with $I_n \bar{w}^{\rm a}_n \in H^1(\tilde{\Omega}_{\rm a})$ and $\bar{w}^{\rm c}_n \in L^2_{\rm loc}(\tilde{\Omega}_{\rm c})$ and with $\nabla \bar{w}^{\rm c}_n \in L^2(\tilde{\Omega}_{\rm c})$ which satisfy the variational equalities* (5.4.5) *and* (5.4.7) *and functions $\bar{w}^{\rm a}_0 \in H^1(\tilde{\Omega}_{\rm a})$ and $\bar{w}^{\rm c}_0 \in \boldsymbol{W}^{1,2}(\tilde{\Omega}_{\rm c})$ such that*

$$I_n \bar{w}^{\rm a}_n \rightharpoonup \bar{w}^{\rm a}_0 \quad \textit{in} \quad H^1(\tilde{\Omega}_{\rm a}), \qquad I_n \bar{w}^{\rm a}_n \to \bar{w}^{\rm a}_0 \quad \textit{in} \quad L^2(\tilde{\Omega}_{\rm a}), \tag{5.4.14}$$

$$\bar{w}^{\rm c}_n \rightharpoonup \bar{w}^{\rm c}_0 \quad \textit{in} \quad H^1(\tilde{\Omega}_{\rm o,ex}), \qquad \bar{w}^{\rm c}_n \to \bar{w}^{\rm c}_0 \quad \textit{in} \quad L^2(\tilde{\Omega}_{\rm o,ex}). \tag{5.4.15}$$

Step 2:

Theorem 5.4.5. *The functions $\bar{w}^{\rm a}_0$ and $\bar{\boldsymbol{w}}^{\rm c}_0$ satisfy the linear, homogeneous Cauchy-Born elasticity equations in weak form:*

$$\int_{\tilde{\Omega}_{\rm a}} (\mathbb{C} : \nabla \bar{w}^{\rm a}_0) : \nabla v = 0 \quad \forall v \in H^1_0(\tilde{\Omega}_{\rm a}), \tag{5.4.16}$$

$$\int_{\tilde{\Omega}_{\rm c}} (\mathbb{C} : \nabla \bar{\boldsymbol{w}}^{\rm c}_0) : \nabla v = 0 \quad \forall v \in H^1_0(\tilde{\Omega}_{\rm c}). \tag{5.4.17}$$

We break the proof into several lemmas. We start with the atomistic case (5.4.16), where special care must be exercised near the defect at the origin.

Lemma 5.4.6. *Let $\tilde{N}$ be any neighborhood of the origin with $\tilde{N} \subset \tilde{\Omega}_{\rm a}$ and set $\tilde{\Omega}' := \tilde{\Omega}_{\rm a} \backslash \tilde{N}$. Then $\bar{w}^{\rm a}_0$ satisfies*

$$\int_{\tilde{\Omega}'} (\mathbb{C} : \nabla \bar{w}^{\rm a}_0) : \nabla v = 0 \quad \forall v \in H^1_0\big(\tilde{\Omega}'\big). \tag{5.4.18}$$

The key result in proving Lemma 5.4.6 is the auxiliary Lemma 5.4.7. In the proof, we use the standard notation $\subset\subset$ to denote compact subsets. The proof uses a diagonalizing argument and draws upon ideas related to weak convergence of difference quotients, see e.g. [25].

Lemma 5.4.7. *Let U be a bounded domain in $\mathbb{R}^d$ whose boundary is Lipschitz and a union of edges of $\mathcal{T}_{\mathrm{a}}$. Take a domain $U_1 \subset\subset U$, and suppose v_n is piecewise linear with respect to $\tilde{\mathcal{L}}_n = \epsilon_n \mathcal{L}$ and $v_n \rightharpoonup v_0$ in $H^1(U)$ for some $v_0 \in H^1(U)$. Then for $r \in \mathcal{R}$, $\bar{I}_n D_{\varepsilon_n r} v_n \rightharpoonup \nabla_r v_0$ in $L^2(U_1)$.*

Proof of Lemma 5.4.7. We prove the lemma for $v_0 = 0$ and then reduce the case $v_0 \neq 0$ to this setting.

Case 1 ($v_0 = 0$). Take $\varphi \in \mathrm{C}_0^\infty(U_1)$, and note since $v_n \rightharpoonup 0$ in $H^1(U)$, $v_n \to 0$ strongly in $L^2(U)$. For n large enough, we may choose $\tilde{\mathcal{L}}_{n,1} \subset \tilde{\mathcal{L}}_n$ such that $U_1 \subset \bigcup_{\xi \in \tilde{\mathcal{L}}_{n,1}} \varsigma_\xi \subset U$. We think of $\tilde{\mathcal{L}}_{n,1}$ as a lattice associated with U_1. Applying Taylor's Theorem with the notation $\mathrm{conv}(\xi, x)$ representing the convex hull of ξ and x produces

$$
\begin{aligned}
&\limsup_{n\to\infty} \left|(\bar{I}_n D_{\varepsilon_n r} v_n, \varphi)_{L^2(U_1)}\right| \\
&= \limsup_{n\to\infty} \left| \int_{U_1} \bar{I}_n D_{\varepsilon_n r} v_n(x) \varphi(x)\, dx \right| = \limsup_{n\to\infty} \left| \sum_{\xi \in \tilde{\mathcal{L}}_{n,1}} \int_{\varsigma_\xi \cap U_1} \bar{I}_n D_{\varepsilon_n r} v_n(x) \varphi(x)\, dx \right| \\
&= \limsup_{n\to\infty} \left| \sum_{\xi \in \tilde{\mathcal{L}}_{n,1}} \int_{\varsigma_\xi \cap U_1} D_{\varepsilon_n r} v_n(\xi)(\varphi(\xi) + \nabla\varphi(\tau_{\xi,x})(x-\xi))\, dx \right| \text{for } \tau_{\xi,x} \in \mathrm{conv}(\xi, x) \\
&\leq \limsup_{n\to\infty} \underbrace{\left| \sum_{\xi \in \tilde{\mathcal{L}}_{n,1}} \int_{\varsigma_\xi \cap U_1} D_{\varepsilon_n r} v_n(\xi) \varphi(\xi)\, dx \right|}_{T_1} \\
&\qquad + \limsup_{n\to\infty} \underbrace{\left| \sum_{\xi \in \tilde{\mathcal{L}}_{n,1}} \int_{\varsigma_\xi \cap U_1} D_{\varepsilon_n r} v_n(\xi) \nabla\varphi(\tau_{\xi,x})(x-\xi)\, dx \right|}_{T_2}.
\end{aligned}
\tag{5.4.19}
$$

Since we are taking limits, we assume throughout that $\epsilon_n < \mathrm{dist}(U_1, \partial U)$ so that the expressions above are well defined. We first estimate T_2 by bounding $|x - \xi| \leq \varepsilon_n$ and $|\nabla\varphi(\tau_{\xi,x})| \leq \|\nabla\varphi\|_{L^\infty(U_1)} \lesssim 1$:

$$
\begin{aligned}
T_2 \lesssim \varepsilon_n \sum_{\xi \in \tilde{\mathcal{L}}_{n,1}} \int_{\varsigma_\xi \cap U_1} |D_{\varepsilon_n r} v_n(\xi)| dx &= \varepsilon_n \sum_{\xi \in \tilde{\mathcal{L}}_{n,1}} |D_{\varepsilon_n r} v_n(\xi)| \mathrm{vol}(\varsigma_\xi \cap U_1) \\
&\leq \varepsilon_n |r|\, \|\nabla v_n\|_{L^1(U)} \lesssim \varepsilon_n \|\nabla v_n\|_{L^2(U)}.
\end{aligned}
$$

Note that here the bound $\sum_{\xi \in \tilde{\mathcal{L}}_{n,1}} |D_{\varepsilon_n r} v_n(\xi)| \mathrm{vol}(\varsigma_\xi \cap U_1) \leq |r|\, \|\nabla v_n\|_{L^1(U)}$ follows from

a local bound $|D_{\varepsilon_n r} v_n(\xi)| \leq \int_0^1 |\nabla_r v_n(\xi + \varepsilon_n r t)|\, dt$ for sufficiently small ε_n. Since $\|\nabla v_n\|_{L^2(U)}$ are bounded (as a consequence of $v_n \rightharpoonup v_0$ in H^1), we have that $T_2 \lesssim \varepsilon_n \to 0$.

To estimate T_1, we shift the finite difference operator onto $\varphi(\xi)\mathrm{vol}\,(\varsigma_\xi \cap U_1)$ using summation by parts, use the product rule for difference quotients (see (5.4.2)), and recall that $\varphi \in \mathrm{C}_0^\infty(U_1)$:

$$\begin{aligned}
T_1 &= \sum_{\xi \in \tilde{\mathcal{L}}_{n,1}} D_{\varepsilon_n r} v_n(\xi) \varphi(\xi) \mathrm{vol}\,(\varsigma_\xi \cap U_1) = -\sum_{\xi \in \tilde{\mathcal{L}}_{n,1}} v_n(\xi) D_{-\varepsilon_n r}(\varphi(\xi)\mathrm{vol}\,(\varsigma_\xi \cap U_1)) \\
&= -\sum_{\xi \in \tilde{\mathcal{L}}_{n,1}} v_n(\xi)(D_{-\varepsilon_n r}(\varphi(\xi))\mathrm{vol}\,(\varsigma_\xi \cap U_1) + \varphi(\xi - \epsilon_n r) D_{-\varepsilon_n r}\mathrm{vol}\,(\varsigma_\xi \cap U_1)) \\
&= -\sum_{\xi \in \tilde{\mathcal{L}}_{n,1}} v_n(\xi) D_{-\varepsilon_n r}(\varphi(\xi))\mathrm{vol}\,(\varsigma_\xi \cap U_1) \\
&\leq \Big(\sum_{\xi \in \tilde{\mathcal{L}}_{n,1}} |v_n(\xi)|^2 \mathrm{vol}\,(\varsigma_\xi \cap U_1) \Big)^{1/2} \Big(\sum_{\xi \in \tilde{\mathcal{L}}_{n,1}} |D_{-\varepsilon_n r}\varphi(\xi)|^2 \mathrm{vol}\,(\varsigma_\xi \cap U_1) \Big)^{1/2} \\
&\lesssim \|\bar{I}_n v_n\|_{L^2(U_1)} \|\nabla I_n \varphi\|_{L^2(U)} \lesssim \|\bar{I}_n v_n\|_{L^2(U_1)}, \qquad (5.4.20)
\end{aligned}$$

where in the last step we used that the smoothness of φ implies that $\|\nabla I_n \varphi\|_{L^2(U)}$ converges to $\|\nabla \varphi\|_{L^2(U)} \lesssim 1$.

We now wish to bound $\|\bar{I}_n v_n\|_{L^2(U_1)}$ by $\|v_n\|_{L^2(U)}$. Consider the cell ς_ξ and take T to be a micro-simplex of $\tilde{\mathcal{T}}_{\mathrm{a},n} = \epsilon_n \mathcal{T}_\mathrm{a}$ such that ξ is a vertex of T and $T \subset \varsigma_\xi$. Further let $\mathcal{N}(T)$ be the nodes of T and let $\hat{T}$ be a reference simplex with nodes $\mathcal{N}(\hat{T})$. If $\hat{f}$ is the pullback of a function f on T, then

$$\begin{aligned}
\|\bar{I}_n v_n\|_{L^2(\varsigma_\xi)} = \epsilon_n^{d/2} \cdot |v_n(\xi)| \lesssim\ |T|^{1/2} \sup_{\zeta \in \mathcal{N}(T)} |v_n(\zeta)| &= |T|^{1/2} \sup_{\hat{\zeta} \in \mathcal{N}(\hat{T})} |\hat{v}_n(\hat{\zeta})| \\
&\lesssim |T|^{1/2} \|\hat{v}_n\|_{L^2(\hat{T})} \lesssim \|v_n\|_{L^2(T)}.
\end{aligned}$$

Summing over all $\xi \in \tilde{\mathcal{L}}_{n,1}$ gives

$$\|\bar{I}_n v_n\|_{L^2(U_1)} \leq \|v_n\|_{L^2(U)},$$

Because v_n converges weakly to 0 in $H^1(U)$, v_n converges strongly to 0 in $L^2(U)$. This shows that $T_1 \to 0$ which, together with $T_2 \to 0$, yields

$$\limsup_{n \to \infty} \left| (\bar{I}_n D_{\varepsilon_n r} v_n, \varphi)_{L^2(U_1)} \right| = 0.$$

We can use similar computations to those in our estimate of T_2, in particular, the local bound $|D_{\varepsilon_n r} v_n(\xi)|^2 \leq \int_0^1 |\nabla_r v_n(\xi + \varepsilon_n r t)|^2 dt$, to conclude that $\|\bar{I}_n D_{\varepsilon_n r} v_n\|_{L^2(U_1)} \lesssim \|v_n\|_{L^2(U)}$. Then using boundedness of $\bar{I}_n D_{\varepsilon_n r} v_n$ and density of smooth functions in $L^2(U)$ allows us to deduce $\bar{I}_n D_{\varepsilon_n r} v_n \rightharpoonup 0$.

Case 2 ($v_0 \neq 0$). We reduce this case to the previous one by using a diagonalizing argument to find a sequence of piecewise linear comparison functions which converge weakly to v_0 and then applying the previous case to the difference of the comparison sequence and original sequence.

The hypotheses on U imply we may take $v_{0,j} \in \mathrm{C}^\infty(U)$ such that

$$\|v_{0,j} - v_0\|_{H^1(U)} \leq 1/j. \tag{5.4.21}$$

Since $v_{0,j}$ is smooth, for any fixed j, $I_n v_{0,j} \to v_{0,j}$ in $H^1(U)$. Similarly,

$$D_{\epsilon_n r} v_{0,j} \to \nabla_r v_{0,j} \quad \text{uniformly in } x \in U_1 \text{ as } \epsilon_n \to 0.$$

Hence $D_{\epsilon_n r} v_{0,j} \to \nabla_r v_{0,j}$ in $L^2(U_1)$. Furthermore,

$$\begin{aligned}
&\|\bar{I}_n D_{\epsilon_n r} v_{0,j} - D_{\epsilon_n r} v_{0,j}\|^2_{L^2(U_1)} = \int_{U_1} |\bar{I}_n D_{\epsilon_n r} v_{0,j} - D_{\epsilon_n r} v_{0,j}|^2 \, dx \\
&= \sum_{\xi \in \tilde{\mathcal{L}}_{n,1}} \int_{\varsigma_\xi \cap U_1} |D_{\epsilon_n r} v_{0,j}(\xi) - D_{\epsilon_n r} v_{0,j}(x)|^2 \, dx \\
&= \sum_{\xi \in \tilde{\mathcal{L}}_{n,1}} \int_{\varsigma_\xi \cap U_1} |D_{\epsilon_n r} \nabla v_{0,j}(\tau_{\xi,x})(\xi - x)|^2 \, dx \quad \text{for some } \tau_{\xi,x} \in \mathrm{conv}(\xi, x) \\
&\lesssim \epsilon_n^2 \sum_{\xi \in \tilde{\mathcal{L}}_{n,1}} \int_{\varsigma_\xi \cap U_1} |D_{\epsilon_n r} \nabla v_{0,j}(\tau_{\xi,x})|^2 \, dx \lesssim \epsilon_n^2 \|\nabla^2 v_{0,j}\|^2_{L^2(U)} \to 0 \quad \text{as } n \to \infty.
\end{aligned}$$

Thus, as $n \to \infty$, we have that

$$\begin{aligned}
&\|\bar{I}_n D_{\varepsilon_n r} v_{0,j} - \nabla_r v_{0,j}\|_{L^2(U_1)} \\
&\leq \|\bar{I}_n D_{\varepsilon_n r} v_{0,j} - D_{\varepsilon_n r} v_{0,j}\|_{L^2(U_1)} + \|D_{\varepsilon_n r} v_{0,j} - \nabla_r v_{0,j}\|_{L^2(U_1)} \to 0.
\end{aligned} \tag{5.4.22}$$

This and $I_n v_{0,j} \to v_{0,j}$ as $n \to \infty$ in $H^1(U)$ imply that for any j there exists N_j (which can be chosen such that N_j strictly increases to infinity as j goes to ∞) such that

$$\|I_n v_{0,j} - v_{0,j}\|_{H^1(U)} \leq 1/j \quad \forall n \geq N_j, \tag{5.4.23}$$

$$\|\bar{I}_n D_{\varepsilon_n r} v_{0,j} - \nabla_r v_{0,j}\|_{L^2(U_1)} \leq 1/j \quad \forall n \geq N_j. \tag{5.4.24}$$

Hence we choose a sequence J_n by letting $J_n := j$ whenever $N_j \leq n < N_{j+1}$ (and $J_n = 1$ for $n < N_1$). It is easy to see that $J_n \to \infty$ as $n \to \infty$; hence equations (5.4.21), (5.4.23), and (5.4.24) give

$$\|I_n v_{0,J_n} - v_0\|_{H^1(U)} \leq \|I_n v_{0,J_n} - v_{0,J_n}\|_{H^1(U)} + \|v_{0,J_n} - v_0\|_{H^1(U)} \leq 2/J_n \to 0, \tag{5.4.25}$$

$$\begin{aligned}\|\bar{I}_n D_{\varepsilon_n r} v_{0,J_n} - \nabla_r v_0\|_{L^2(U_1)} &\leq \|\bar{I}_n D_{\varepsilon_n r} v_{0,J_n} - \nabla_r v_{0,J_n}\|_{L^2(U_1)} + \|\nabla_r v_{0,J_n} - \nabla_r v_0\|_{L^2(U_1)} \\ &\lesssim 2/J_n \to 0.\end{aligned} \tag{5.4.26}$$

The functions $\hat{v}_n := I_n v_{0,J_n}$ will serve as our comparison functions. Observe $v_n - \hat{v}_n$ converges weakly to zero in $H^1(U)$ by (5.4.25) and our hypothesis that v_n converges weakly to v_0. Case 1 then implies

$$\bar{I}_n D_{\varepsilon_n r} v_n - \bar{I}_n D_{\varepsilon_n r} \hat{v}_n \rightharpoonup 0 \quad \text{in} \quad L^2(U_1). \tag{5.4.27}$$

But a straightforward calculation shows

$$\bar{I}_n D_{\varepsilon_n r} \hat{v}_n = \bar{I}_n D_{\varepsilon_n r} I_n v_{0,J_n} = \bar{I}_n D_{\varepsilon_n r} v_{0,J_n},$$

and (5.4.26) states that $\bar{I}_n D_{\varepsilon_n r} v_{0,J_n}$ converges strongly, whence weakly, to $\nabla_r v_0$ in $L^2(U_1)$. This, along with (5.4.27), means

$$\bar{I}_n D_{\varepsilon_n r} v_n \rightharpoonup \nabla_r v_0 \quad \text{in} \quad L^2(U_1).$$

□

Remark 5.4.8. *With only minor modifications to the proof, the statement of the theorem remains true if weak convergence is replaced with strong convergence. For the $v_0 = 0$ case, one only needs to replace φ with $\bar{I}_n D_{\varepsilon_n r} v_n$ and carry out simplified computations while the $v_0 \neq 0$ case can then be proven almost verbatim by replacing weak convergence with strong convergence.*

Proof of Lemma 5.4.6. First, notice that it is enough to test (5.4.18) with $v \in \mathrm{C}_0^\infty(\tilde{\Omega}_\mathrm{a} \setminus \tilde{N})$, i.e., for $\mathrm{supp}(v) \subset\subset \tilde{\Omega}_\mathrm{a}$, $0 \notin \mathrm{supp}(v)$. Take a domain Ω_1 such that $\mathrm{supp}(v) \subset \Omega_1 \subset \subset \tilde{\Omega}_\mathrm{a}$. Because $I_n \bar{w}_n^\mathrm{a} \rightharpoonup \bar{w}_0^\mathrm{a}$ on $H^1(\tilde{\Omega}_\mathrm{a})$ by (5.4.14), Lemma 5.4.7 implies

$$\bar{I}_n D_{\epsilon_n r} \bar{w}_n^\mathrm{a} \rightharpoonup \nabla_r \bar{w}_0^\mathrm{a} \quad \text{in } L^2(\Omega_1) \quad \text{for all} \quad r \in \mathcal{R}. \tag{5.4.28}$$

Since v has compact support inside $\tilde{\Omega}_{\rm a} \setminus \tilde{N}$, $D_{\epsilon_n \rho} v(\xi)$ vanishes on $\tilde{\mathcal{L}}_{{\rm a},n} \backslash \tilde{\mathcal{L}}^{\circ}_{{\rm a},n}$ for all n large enough and $\rho \in \mathcal{R}$. We may therefore rewrite (5.4.5) with $\bar{w}^{\rm a}_n$ using the integral formulation introduced in (5.4.6)

$$0 = \int_{\tilde{\Omega}_{\rm a}} \bar{I}_n V''_\xi(D_{\epsilon_n} \tilde{\boldsymbol{u}}^\infty_{{\rm a},n}) : \bar{I}_n D_{\epsilon_n} \bar{w}^{\rm a}_n : \bar{I}_n D_{\epsilon_n} v \, dx. \tag{5.4.29}$$

Because v is smooth, a calculation analogous to (5.4.22) implies

$$\bar{I}_n D_{\epsilon_n r} v \to \nabla_r v \quad \text{in } L^2(\Omega_1) \text{ for all } r \in \mathcal{R}. \tag{5.4.30}$$

According to estimate (2.4.3) of Theorem 2.4.2, the local minimum, $\boldsymbol{u}^\infty$, of $\mathcal{E}^{\rm a}$ satisfies

$$|\nabla I \boldsymbol{u}^\infty(x)| \lesssim |x|^{-d} \quad \text{for } x \notin \Omega_{\rm core}.$$

After scaling the lattice by ϵ_n we get a sequence of global solutions $\tilde{\boldsymbol{u}}^\infty_n(\xi) = \epsilon_n \boldsymbol{u}^\infty(\xi/\epsilon_n)$ for $\xi \in \tilde{\mathcal{L}}_n$. Thus, for $x \neq 0$ and large enough n there holds $x \notin \epsilon_n \Omega_{\rm core}$. Since $d > 1$ it follows that

$$|\nabla(I_n \tilde{\boldsymbol{u}}^\infty_n(x))| = |(\nabla I_n \boldsymbol{u}^\infty_n)(x/\epsilon_n)| \lesssim |x/\epsilon_n|^{-d} = \epsilon_n^d \, |x|^{-d} \to 0$$

uniformly in $x \in \tilde{\Omega}_{\rm a} \backslash \tilde{N}$ as $\epsilon_n \to 0$. This also implies

$$|\bar{I}_n D_{\epsilon_n} \tilde{\boldsymbol{u}}^\infty_{{\rm a},n}(x)| \to 0 \qquad \text{uniformly as } \epsilon_n \to 0 \text{ on } \tilde{\Omega}_{\rm a} \backslash \tilde{N};$$

whence

$$\bar{I}_n V''(D_{\epsilon_n} \tilde{\boldsymbol{u}}^\infty_{{\rm a},n}(x)) = V''(\bar{I}_n D_{\epsilon_n} \tilde{\boldsymbol{u}}^\infty_{{\rm a},n}(x)) \to V''(\boldsymbol{0}) \quad \text{uniformly as } \epsilon_n \to 0 \text{ on } \tilde{\Omega}_{\rm a} \backslash \tilde{N}.$$

Hence, taking the limit of (5.4.29), and using (5.4.28), (5.4.30), and the fact that the "dual pairing" (:) of a weakly convergent and a strongly convergent sequence converges to the dual pairing of the limits, we obtain

$$\begin{aligned} 0 &= \lim_{n\to\infty} \int_{\tilde{\Omega}_{\rm a}} \bar{I}_n V''(D_{\epsilon_n} \tilde{\boldsymbol{u}}^\infty_{\rm a}) : \bar{I}_n D_{\epsilon_n} \bar{w}^{\rm a}_n : \bar{I}_n D_{\epsilon_n} v \, dx \\ &= \lim_{n\to\infty} \int_{\tilde{\Omega}_{\rm a}} \bar{I}_n V''(D_{\epsilon_n} \tilde{\boldsymbol{u}}^\infty_{\rm a}) : \bar{I}_n D_{\epsilon_n} v : \bar{I}_n D_{\epsilon_n} \bar{w}^{\rm a}_n \, dx \\ &= \int_{\tilde{\Omega}_{\rm a}} V''(\boldsymbol{0}) : \nabla_{\mathcal{R}} \bar{w}^{\rm a}_0 : \nabla_{\mathcal{R}} v \, dx = \int_{\tilde{\Omega}_{\rm a}} \mathbb{C} : \nabla \bar{w}^{\rm a}_0 : \nabla v \, dx. \end{aligned}$$

□

Proof of Theorem 5.4.5. We first prove the atomistic case (5.4.16), followed by the continuum case (5.4.17).

Proof of (5.4.16). By density, it suffices to prove the theorem for $v \in \mathrm{C}_0^\infty(\tilde{\Omega}_\mathrm{a})$. Let η be a standard mollifier on a unit ball with $\eta_R(x) = \frac{1}{R^d}\eta(x/R)$ its extension to a ball of radius R. Let

$$\chi_R(x) = \begin{cases} 1 & \text{if} \quad |x| < 2R, \\ 0 & \text{if} \quad |x| \geq 2R, \end{cases}$$

and define the smooth bump function

$$\varphi_R(x) := (\eta_R * \chi_R)(x).$$

Recall that $\varphi_R(x)$ is of class C^∞ and satisfies

$$0 \leq \varphi_R(x) \leq 1, \quad \text{and} \quad \begin{cases} \varphi_R(x) = 1 & \text{for} \quad |x| < R, \\ \varphi_R(x) = 0 & \text{for} \quad |x| \geq 3R. \end{cases}$$

Thus, $v - \varphi_R v$ is smooth and vanishes on $B_R(0)$. By Lemma 5.4.6,

$$\begin{aligned} 0 = & \int_{\tilde{\Omega}_\mathrm{a}\setminus B_R(0)} \mathbb{C} : \nabla \bar{w}_0^\mathrm{a} : \nabla(v - \varphi_R v)\, dx = \int_{\tilde{\Omega}_\mathrm{a}} \mathbb{C} : \nabla \bar{w}_0^\mathrm{a} : \nabla(v - \varphi_R v)\, dx \\ = & \int_{\tilde{\Omega}_\mathrm{a}} \mathbb{C} : \nabla \bar{w}_0^\mathrm{a} : \nabla v\, dx - \int_{\tilde{\Omega}_\mathrm{a}} \mathbb{C} : \nabla \bar{w}_0^\mathrm{a} : \nabla(\varphi_R v)\, dx \\ = & \int_{\tilde{\Omega}_\mathrm{a}} \mathbb{C} : \nabla \bar{w}_0^\mathrm{a} : \nabla v\, dx - \int_{B_{3R}(0)} \mathbb{C} : \nabla \bar{w}_0^\mathrm{a} : \nabla(\varphi_R v)\, dx. \end{aligned}$$

This implies

$$\int_{\tilde{\Omega}_\mathrm{a}} \mathbb{C} : \nabla \bar{w}_0^\mathrm{a} : \nabla v\, dx = \int_{B_{3R}(0)} \mathbb{C} : \nabla \bar{w}_0^\mathrm{a} : \nabla(\varphi_R v)\, dx. \tag{5.4.31}$$

Also note

$$\Big| \int_{B_{3R}(0)} \mathbb{C} : \nabla \bar{w}_0^\mathrm{a} : \nabla(\varphi_R v)\, dx \Big| \leq \ \|\mathbb{C} : \nabla \bar{w}_0^\mathrm{a}\|_{L^2(B_{3R}(0))} \|\nabla(\varphi_R v)\|_{L^2(B_{3R}(0))}. \tag{5.4.32}$$

Moreover,

$$\begin{aligned} \|\nabla(\varphi_R v)\|_{L^2(B_{3R}(0))} \leq & \ \|\varphi_R \nabla v\|_{L^2(B_{3R}(0))} + \big\|v \nabla \varphi_R^\top\big\|_{L^2(B_{3R}(0))} \\ \leq & \ \|\nabla v\|_{L^2(B_{3R}(0))} + \|v\|_{L^2(B_{3R}(0))} \|\nabla \varphi_R\|_{L^2(B_{3R}(0))}. \end{aligned} \tag{5.4.33}$$

Furthermore,

$$\begin{aligned}
\|\nabla\varphi_R\|^2_{L^2(B_{3R}(0))} &= \sum_{i=1}^{d}\int_{L^2(B_{3R}(0))}\big|\tfrac{\partial\varphi_R}{\partial x_i}\big|^2\,dx = \sum_{i=1}^{d}\int_{L^2(B_{3R}(0))}\big|\tfrac{\partial\eta_R}{\partial x_i}*\chi_R\big|^2\,dx\\
&= \sum_{i=1}^{d}\big\|\tfrac{\partial\eta_R}{\partial x_i}*\chi_R\big\|^2_{L^2(B_{3R}(0))} \le \sum_{i=1}^{d}\big\|\tfrac{\partial\eta_R}{\partial x_i}\big\|^2_{L^1(B_{3R}(0))}\|\chi_R\|^2_{L^2(B_{3R}(0))} \text{ Young's Inequality}\\
&= \sum_{i=1}^{d}\Big(\int_{B_{3R}(0)}\big|\tfrac{\partial\eta_R}{\partial x_i}\,dx\big|\Big)^2\cdot\Big(\int_{B_{3R}(0)}|\chi_R|^2\,dx\Big)\\
&\le \sum_{i=1}^{d}\Big(\int_{B_{3R}(0)}\big|\tfrac{1}{R^{d+1}}\tfrac{\partial\eta}{\partial x_i}(x/R)\big|\,dx\Big)^2\cdot\Big(\int_{B_{3R}(0)}1\,dx\Big)\\
&= \sum_{i=1}^{d}\Big(\int_{B_3(0)}\big|\tfrac{1}{R}\tfrac{\partial\eta}{\partial x_i}(x)\big|\,dx\Big)^2\cdot\Big(\textstyle\int_{B_{3R}(0)}1\,dx\Big)\lesssim R^{d-2}.
\end{aligned}$$

Thus for $d\ge 3, \|\nabla\varphi_R\|_{L^2(B_{3R}(0))}\to 0$ and for $d=2$, $\|\nabla\varphi_R\|_{L^2(B_{3R}(0))}$ is uniformly bounded in R. Since v is fixed, $\|v\|_{L^2(B_{3R}(0))}\to 0$ as $R\to 0$ and taking $R\to 0$ in (5.4.32) and using (5.4.31) and (5.4.33) shows

$$\begin{aligned}
\Big|\int_{\tilde\Omega_{\rm a}}\mathbb{C}:\nabla\bar w_0^{\rm a}:\nabla v\Big| &= \lim_{R\to 0}\Big|\int_{B_{3R}(0)}\mathbb{C}:\nabla\bar w_0^{\rm a}:\nabla(\varphi_R v)\Big|\\
&\le \lim_{R\to 0}\|\mathbb{C}:\nabla\bar w_0^{\rm a}\|_{L^2(B_{3R}(0))}\big(\|\nabla v\|_{L^2(B_{3R}(0))}+\|v\|_{L^2(B_{3R}(0))}\|\nabla\varphi_R\|_{L^2(B_{3R}(0))}\big) = 0
\end{aligned}$$

so long as $d\ge 2$, which proves (5.4.16).[2]

Proof of (5.4.17). We prove (5.4.17)) for $v\in \mathrm{C}_0^\infty(\tilde\Omega_{\rm c})$. Interpolation of v on each finite element grid $\tilde{\mathcal{T}}_{h,n}=\epsilon_n\mathcal{T}_{h,n}$ yields a sequence, $v_n^{\rm c}$, of piecewise linear functions with respect to $\tilde{\mathcal{T}}_{h,n}$. Let $V\subset\subset\tilde\Omega_{\rm c}$ be a bounded set such that the support of v and all but finitely many $v_n^{\rm c}$ are compactly contained in V. Then for all but finitely many n,

$$0=\int_{\tilde\Omega_{{\rm c},n}}W''(\nabla\tilde{\boldsymbol{u}}_n^{\rm con}):\nabla\bar{\boldsymbol{w}}_n^{\rm c}:\nabla v_n^{\rm c}\,dx=\int_V W''(\nabla\tilde{\boldsymbol{u}}_n^{\rm con}):\nabla\bar{\boldsymbol{w}}_n^{\rm c}:\nabla v_n^{\rm c}\,dx.$$

[2] This portion of the proof fails for the $d=1$ case, which has the special property that the atomistic region becomes disconnected when a neighborhood of the origin is deleted and that the overlap region is disconnected. Additional notation and effort is required to do this so we do not pursue it further.

Taking limits of both sides produces

$$\begin{aligned} 0 = & \lim_{n\to\infty} \int_V W''(\nabla \tilde{\boldsymbol{u}}_n^{\mathrm{con}}) : \nabla \bar{\boldsymbol{w}}_n^{\mathrm{c}} : \nabla v_n^{\mathrm{c}}\, dx \\ = & \lim_{n\to\infty} \int_V \left(W''(\nabla \tilde{\boldsymbol{u}}_n^{\mathrm{con}}) - W''(\nabla I_n \tilde{\boldsymbol{u}}_n^{\infty})\right) : \nabla \bar{\boldsymbol{w}}_n^{\mathrm{c}} : \nabla v_n^{\mathrm{c}}\, dx \\ & + \lim_{n\to\infty} \int_V W''(\nabla I_n \tilde{\boldsymbol{u}}_n^{\infty}) : \nabla \bar{\boldsymbol{w}}_n^{\mathrm{c}} : \nabla v_n^{\mathrm{c}}\, dx. \end{aligned} \tag{5.4.34}$$

Observe

$$\begin{aligned} & \lim_{n\to\infty} \int_V \left(W''(\nabla \tilde{\boldsymbol{u}}_n^{\mathrm{con}}) - W''(\nabla I_n \tilde{\boldsymbol{u}}_n^{\infty})\right) : \nabla \bar{\boldsymbol{w}}_n^{\mathrm{c}} : \nabla v_n^{\mathrm{c}}\, dx \\ & \qquad \lesssim \lim_{n\to\infty} \epsilon_n \|\nabla \tilde{\boldsymbol{u}}_n^{\mathrm{con}} - \nabla I_n \tilde{\boldsymbol{u}}_n^{\infty}\|_{L^2(V)} \|\nabla \bar{\boldsymbol{w}}_n^{\mathrm{c}}\|_{L^2(V)} \|\nabla v_n^{\mathrm{c}}\|_{L^2(V)} = 0, \end{aligned}$$

due to Lipschitz continuity of W, due to scaling the estimate in Theorem 4.3.8 that estimates the continuum error, and due to boundedness of $\nabla \bar{\boldsymbol{w}}_n^{\mathrm{c}}$ and ∇v_n^{c}. Hence, (5.4.34) simplifies to

$$0 = \lim_{n\to\infty} \int_V W''(\nabla I_n \tilde{\boldsymbol{u}}_n^{\infty}) : \nabla \bar{\boldsymbol{w}}_n^{\mathrm{c}} : \nabla v_n^{\mathrm{c}}\, dx.$$

Reasoning as in the end of the proof of Lemma 5.4.6, $W''(\nabla I_n \tilde{\boldsymbol{u}}_n^{\infty})$ converges uniformly to $W''(\mathbf{0})$ on V while ∇v_n^{c} converges strongly to ∇v in $H^1(V)$. The functions $\bar{\boldsymbol{w}}_n^{\mathrm{c}}$ converge weakly to $\bar{w}_0^{\mathrm{c}}$ in $\boldsymbol{W}^{1,2}(\tilde{\Omega}_{\mathrm{c}})$, and thus, we have the inner produce of a strongly and weakly convergent sequence again:

$$0 = \lim_{n\to\infty} \int_V W''(\nabla I_n \tilde{\boldsymbol{u}}_n^{\infty}) : \nabla \bar{\boldsymbol{w}}_n^{\mathrm{c}} : \nabla v_n^{\mathrm{c}}\, dx = \int_V \mathbb{C} : \nabla \bar{\boldsymbol{w}}_0^{\mathrm{c}} : \nabla v\, dx = \int_{\tilde{\Omega}_{\mathrm{c}}} \mathbb{C} : \nabla \bar{\boldsymbol{w}}_0^{\mathrm{c}} : \nabla v\, dx.$$

□

Step 3:

With the convergence properties of Step 1 and limiting equations of Step 2, we shall prove

Theorem 5.4.9. *Let $\bar{w}_n^{\mathrm{a}}$ and $\bar{w}_n^{\mathrm{c}}$ be as defined in Step 1. Then*

$$\left(\nabla I_n \bar{w}_n^{\mathrm{a}}, \nabla \bar{w}_n^{\mathrm{c}}\right)_{L^2(\tilde{\Omega}_{\mathrm{o}})} \to \left(\nabla \bar{w}_0^{\mathrm{a}}, \nabla \bar{w}_0^{\mathrm{c}}\right)_{L^2(\tilde{\Omega}_{\mathrm{o}})}. \tag{5.4.35}$$

Proof of Theorem 5.4.9. Split $\tilde{\Omega}_{\mathrm{o}}$ into an inner part, A_1, and an outer part, A_2 such that $\tilde{\Omega}_{\mathrm{o}} = A_1 \cup A_2$ and A_1 and A_2 have disjoint interiors as in Figure 5.2. Specifically, let $\lfloor x \rfloor$ be the greatest integer less than or equal to x and set

$$\begin{aligned} A_1 &:= (\lfloor \psi_{\mathrm{a}}/2 \rfloor \tilde{\Omega}_{\mathrm{core}}) \backslash \tilde{\Omega}_{\mathrm{core}}, \\ A_2 &:= \tilde{\Omega}_{\mathrm{o}} \backslash A_1. \end{aligned}$$

We prove in Lemma 5.4.10 below that

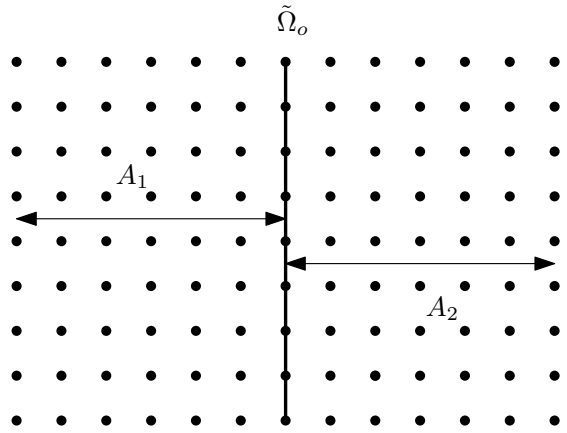

Figure 5.2: An example decomposition of a portion of $\tilde{\Omega}_{\mathrm{o}}$ into A_1 and A_2.

$$\|\nabla (\bar{w}_n^{\mathrm{c}} - \bar{w}_0^{\mathrm{c}}) \|_{L^2(A_2)} \to 0$$

and in Lemma 5.4.11 that

$$\left\|\nabla \left(I_n \bar{w}_n^{\mathrm{a}} - \bar{w}_0^{\mathrm{a}}\right)\right\|_{L^2(A_1)} \to 0.$$

Using these two strong convergence results along with the weak convergence properties of Lemma 5.4.4—namely, $\nabla \bar{w}_n^{\mathrm{c}} \rightharpoonup \bar{w}_0^{\mathrm{c}}$ on A_1 and $\nabla I_n \bar{w}_n^{\mathrm{a}} \rightharpoonup \bar{w}_0^{\mathrm{a}}$ on A_2—yields

$$\begin{aligned} \left(\nabla I_n \bar{w}_n^{\mathrm{a}}, \nabla \bar{w}_n^{\mathrm{c}}\right)_{L^2(\tilde{\Omega}_{\mathrm{o}})} &= \left(\nabla I_n \bar{w}_n^{\mathrm{a}}, \nabla \bar{w}_n^{\mathrm{c}}\right)_{L^2(A_1)} + \left(\nabla I_n \bar{w}_n^{\mathrm{a}}, \nabla \bar{w}_n^{\mathrm{c}}\right)_{L^2(A_2)} \\ &\to (\nabla \bar{w}_0^{\mathrm{a}}, \nabla \bar{w}_0^{\mathrm{c}})_{L^2(A_1)} + (\nabla \bar{w}_0^{\mathrm{a}}, \nabla \bar{w}_0^{\mathrm{c}})_{L^2(A_2)} = (\nabla \bar{w}_0^{\mathrm{a}}, \nabla \bar{w}_0^{\mathrm{c}})_{L^2(\tilde{\Omega}_{\mathrm{o}})}. \end{aligned} \tag{5.4.36}$$

□

In the preceding theorem, we have made reference to the following lemma, which we now prove.

Lemma 5.4.10. *Let $\bar{w}_n^{\mathrm{c}}$ and $\bar{w}_0^{\mathrm{c}}$ be as defined in Lemma 5.4.4. Then*

$$\|\nabla\left(\bar{w}_n^{\mathrm{c}} - \bar{w}_0^{\mathrm{c}}\right)\|_{L^2(A_2)} \to 0. \tag{5.4.37}$$

Proof. We let η be a smooth bump function with compact support in $\tilde{\Omega}_{\mathrm{o,ex}}$ and equal to 1 on A_2. Our starting point in proving (5.4.37) will be to define $z_n := \bar{w}_n^{\mathrm{c}} - \bar{w}_0^{\mathrm{c}}$ and bound $\|\nabla z_n\|_{L^2(A_2)} \leq \|\nabla(\eta z_n)\|_{L^2(\tilde{\Omega}_{\mathrm{o,ex}})}$. Then we shall prove $\|\nabla(\eta z_n)\|_{L^2(\tilde{\Omega}_{\mathrm{o,ex}})} \to 0$.[3]

Note that $z_n \rightharpoonup 0$ in $H^1(\tilde{\Omega}_{\mathrm{o,ex}})$ by the definition of z_n and (5.4.15). As a simple corollary, $\eta z_n \rightharpoonup 0$ in $H^1(\tilde{\Omega}_{\mathrm{o,ex}})$, and therefore a short calculation implies $\nabla(\eta z_n) \rightharpoonup 0$ in $L^2(\tilde{\Omega}_{\mathrm{o,ex}})$. Since ηz_n can be extended by 0 to all of $\mathbb{R}^d$, coercivity of the continuum Hessian (4.3.15) gives us

$$\begin{aligned}\|\nabla z_n\|_{L^2(A_2)}^2 \leq \|\nabla(\eta z_n)\|_{L^2(\tilde{\Omega}_{\mathrm{o,ex}})}^2 &\lesssim \int_{\tilde{\Omega}_{\mathrm{o,ex}}} W''(\nabla \tilde{\boldsymbol{u}}_n^{\mathrm{con}}) : \nabla(\eta z_n) : \nabla(\eta z_n)\, dx \\ = \int_{\tilde{\Omega}_{\mathrm{o,ex}}} W''(\nabla \tilde{\boldsymbol{u}}_n^{\mathrm{con}}) : \nabla(\eta \bar{w}_n^{\mathrm{c}}) : \nabla(\eta z_n)\, dx &- \int_{\tilde{\Omega}_{\mathrm{o,ex}}} W''(\nabla \tilde{\boldsymbol{u}}_n^{\mathrm{con}}) : \nabla(\eta \bar{w}_0^{\mathrm{c}}) : \nabla(\eta z_n)\, dx\end{aligned} \tag{5.4.38}$$

Taking the limit of (5.4.38) and using that $\nabla(\eta z_n) \rightharpoonup 0$ weakly in $L^2(\tilde{\Omega}_{\mathrm{o,ex}})$ while $W''(\nabla \tilde{\boldsymbol{u}}_n^{\mathrm{con}}) \to W''(0)$ strongly in $L^\infty(\tilde{\Omega}_{\mathrm{o,ex}})$ yields

$$\lim_{n\to\infty} \|\nabla z_n\|_{L^2(A_2)}^2 \lesssim \lim_{n\to\infty} \int_{\tilde{\Omega}_{\mathrm{o,ex}}} W''(\nabla \tilde{\boldsymbol{u}}_n^{\mathrm{con}}) : \nabla(\eta \bar{w}_n^{\mathrm{c}}) : \nabla(\eta z_n)\, dx.$$

[3] Note this construction is the reason we defined the extended overlap region $\tilde{\Omega}_{\mathrm{o,ex}}$; we need η to be one on A_2 and decay to zero on $\tilde{\Omega}_{\mathrm{o,ex}}$.

We hence continue to estimate

$$\begin{aligned}
&\lim_{n\to\infty} \|\nabla z_n\|^2_{L^2(A_2)}\\
&\lesssim \lim_{n\to\infty} \int_{\tilde\Omega_{\mathrm{o,ex}}} W''(\nabla \tilde{\boldsymbol{u}}_n^{\mathrm{con}}) : \nabla \bar w_n^{\mathrm{c}} : \eta \nabla(\eta z_n)\,dx\\
&\qquad + \lim_{n\to\infty} \int_{\tilde\Omega_{\mathrm{o,ex}}} W''(\nabla \tilde{\boldsymbol{u}}_n^{\mathrm{con}}) : \bar w_n^{\mathrm{c}} (\nabla\eta)^\top : \nabla(\eta z_n)\,dx\\
&= \lim_{n\to\infty} \int_{\tilde\Omega_{\mathrm{o,ex}}} W''(\nabla \tilde{\boldsymbol{u}}_n^{\mathrm{con}}) : \nabla \bar w_n^{\mathrm{c}} : \nabla(\eta^2 z_n)\,dx\\
&\qquad - \lim_{n\to\infty} \int_{\tilde\Omega_{\mathrm{o,ex}}} W''(\nabla \tilde{\boldsymbol{u}}_n^{\mathrm{con}}) : \nabla \bar w_n^{\mathrm{c}} : \eta z_n (\nabla\eta)^\top\,dx\\
&\qquad + \lim_{n\to\infty} \int_{\tilde\Omega_{\mathrm{o,ex}}} W''(\nabla \tilde{\boldsymbol{u}}_n^{\mathrm{con}}) : \bar w_n^{\mathrm{c}} (\nabla\eta)^\top : \nabla(\eta z_n)\,dx,
\end{aligned}$$

where the second limit converges to zero thanks to $z_n \to 0$ in $L^2(\tilde\Omega_{\mathrm{o,ex}})$ and $\nabla \bar w_n^{\mathrm{c}} \rightharpoonup \nabla \bar w_0^{\mathrm{c}}$ in $L^2(\tilde\Omega_{\mathrm{o,ex}})$ and the third term converges to zero because $\bar w_n^{\mathrm{c}} \to \bar w_0^{\mathrm{c}}$ and $\nabla(\eta z_n) \rightharpoonup 0$ in $L^2(\tilde\Omega_{\mathrm{o,ex}})$ (of course, both together with $W''(\nabla \tilde{\boldsymbol{u}}_n^{\mathrm{con}}) \to W''(0)$ in $L^\infty(\tilde\Omega_{\mathrm{o,ex}})$). Thus

$$\lim_{n\to\infty} \|\nabla z_n\|^2_{L^2(A_2)} \lesssim \lim_{n\to\infty} \int_{\tilde\Omega_{\mathrm{o,ex}}} W''(\nabla \tilde{\boldsymbol{u}}_n^{\mathrm{con}}) : \nabla \bar w_n^{\mathrm{c}} : \nabla(\eta^2 z_n)\,dx.$$

To estimate this term, we recall each $\bar w_n^{\mathrm{c}}$ solves a variational equality of the form

$$\int_{\tilde\Omega_{\mathrm{c},n}} W''(\nabla \tilde{\boldsymbol{u}}_n^{\mathrm{con}}) : \nabla \bar w_n^{\mathrm{c}} : \nabla v^{\mathrm{c}}\,dx = 0 \quad \forall v^{\mathrm{c}} \in \tilde{\boldsymbol{\mathcal{U}}}^{\mathrm{c}}_{h,0,n}.$$

We use this equality with $v_n^{\mathrm{c}} = I_n\big(\eta^2 z_n\big) \in \tilde{\boldsymbol{\mathcal{U}}}_{h,0,n}$ to further estimate

$$\begin{aligned}
&\lim_{n\to\infty} \|\nabla z_n\|^2_{L^2(A_2)}\\
&\lesssim \lim_{n\to\infty} \int_{\tilde\Omega_{\mathrm{o,ex}}} W''(\nabla \tilde{\boldsymbol{u}}_n^{\mathrm{con}}) : \nabla \bar w_n^{\mathrm{c}} : \nabla(\eta^2 z_n)\,dx\\
&\qquad - \lim_{n\to\infty} \int_{\tilde\Omega_{\mathrm{o,ex}}} W''(\nabla \tilde{\boldsymbol{u}}_n^{\mathrm{con}}) : \nabla \bar w_n^{\mathrm{c}} : \nabla I_n(\eta^2 z_n)\,dx \qquad (5.4.39)\\
&= \lim_{n\to\infty} \int_{\tilde\Omega_{\mathrm{o,ex}}} W''(\nabla \tilde{\boldsymbol{u}}_n^{\mathrm{con}}) : \nabla \bar w_n^{\mathrm{c}} : \nabla(\eta^2 z_n - I_n(\eta^2 z_n))\,dx\\
&\lesssim \lim_{n\to\infty} \big\|\nabla(\eta^2 z_n - I_n(\eta^2 z_n))\big\|_{L^2(\tilde\Omega_{\mathrm{o,ex}})}.
\end{aligned}$$

Next,

$$\begin{aligned}
&\lim_{n\to\infty} \big\|\nabla(\eta^2 z_n - I_n(\eta^2 z_n))\big\|_{L^2(\tilde\Omega_{\mathrm{o,ex}})}\\
&\le \lim_{n\to\infty} \big\|\nabla(\eta^2 \bar w_n^{\mathrm{c}} - I_n(\eta^2 \bar w_n^{\mathrm{c}}))\big\|_{L^2(\tilde\Omega_{\mathrm{o,ex}})} + \lim_{n\to\infty} \big\|\nabla(\eta^2 \bar w_0^{\mathrm{c}} - I_n(\eta^2 \bar w_0^{\mathrm{c}}))\big\|_{L^2(\tilde\Omega_{\mathrm{o,ex}})}.
\end{aligned}$$

According to Theorem 5.4.5, the function $\bar{w}_0^{\mathrm{c}}$ satisfies a variational equality of the form

$$\int_{\tilde{\Omega}_{\mathrm{c}}} \mathbb{C} : \nabla \bar{w}_0^{\mathrm{c}} : \nabla v_0^{\mathrm{c}}\, dx = 0 \quad \forall v_0^{\mathrm{c}} \in H_0^1(\tilde{\Omega}_{\mathrm{c}}),$$

which corresponds to a linear elliptic system. From elliptic regularity, $\bar{w}_0^{\mathrm{c}}$ belongs to $H^2_{\mathrm{loc}}(\tilde{\Omega}_{\mathrm{c}})$ [27, 55]. Thus, standard finite element approximation theory implies

$$\lim_{n\to\infty} \big\|\nabla(\eta^2 \bar{w}_0^{\mathrm{c}} - I_n(\eta^2 \bar{w}_0^{\mathrm{c}}))\big\|_{L^2(\tilde{\Omega}_{\mathrm{o,ex}})} \lesssim \lim_{n\to\infty} \epsilon_n \big\|\nabla^2(\eta^2 \bar{w}_0^{\mathrm{c}})\big\|_{L^2(\tilde{\Omega}_{\mathrm{o,ex}})} = 0.$$

Finally, to show

$$\lim_{n\to\infty} \big\|\nabla\big(\eta^2 \bar{w}_n^{\mathrm{c}} - I_n(\eta^2 \bar{w}_n^{\mathrm{c}})\big)\big\|_{L^2(\tilde{\Omega}_{\mathrm{o,ex}})} = 0, \tag{5.4.40}$$

observe that $\eta^2 \bar{w}_n^{\mathrm{c}} - I_n(\eta^2 \bar{w}_n^{\mathrm{c}})$ vanishes outside a neighborhood $N_\delta \subset\subset \tilde{\Omega}_{\mathrm{o,ex}}$ of $\mathrm{supp}(\eta)$. Then

$$\begin{aligned}
\big\|\nabla\big(\eta^2 \bar{w}_n^{\mathrm{c}} - I_n(\eta^2 \bar{w}_n^{\mathrm{c}})\big)\big\|^2_{L^2(\tilde{\Omega}_{\mathrm{o,ex}})} &= \big\|\nabla\big(\eta^2 \bar{w}_n^{\mathrm{c}} - I_n(\eta^2 \bar{w}_n^{\mathrm{c}})\big)\|^2_{L^2(N_\delta)} \\
&= \int_{N_\delta} \big|\nabla\big(\eta^2 \bar{w}_n^{\mathrm{c}} - I_n(\eta^2 \bar{w}_n^{\mathrm{c}})\big)\big|^2\, dx \\
&\le \sum_{\substack{T\in\tilde{\mathcal{T}}_{\mathrm{a},n} \\ T\cap N_\delta\neq\emptyset}} \int_T \big|\nabla\big(\eta^2 \bar{w}_n^{\mathrm{c}} - I_n(\eta^2 \bar{w}_n^{\mathrm{c}})\big)\big|^2\, dx \\
&\lesssim \sum_{\substack{T\in\tilde{\mathcal{T}}_{\mathrm{a},n} \\ T\cap N_\delta\neq\emptyset}} |T|^2 \big\|\nabla^2(\eta^2 \bar{w}_n^{\mathrm{c}})\big\|^2_{L^2(T)} \\
&\lesssim \epsilon_n^{2d} \sum_{\substack{T\in\tilde{\mathcal{T}}_{\mathrm{a},n} \\ T\cap N_\delta\neq\emptyset}} \big\|\nabla^2(\eta^2 \bar{w}_n^{\mathrm{c}})\big\|^2_{L^2(T)},
\end{aligned}$$

where the last line follows from the Bramble-Hilbert lemma and scaling (cf. [9]). Because $\bar{w}_n^{\mathrm{c}}$ is piecewise linear its second derivatives vanish on all T. Using the uniform boundedness of η and its derivatives then yields

$$\big\|\nabla^2(\eta^2 \bar{w}_n^{\mathrm{c}})\big\|^2_{L^2(T)} = \int_T \big|\nabla^2(\eta^2 \bar{w}_n^{\mathrm{c}})\big|^2\, dx \lesssim \int_T |\bar{w}_n^{\mathrm{c}}|^2\, dx + \int_T |\nabla \bar{w}_n^{\mathrm{c}}|^2\, dx.$$

Choose N'_δ such that $\bigcup_{\substack{T\in\tilde{\mathcal{T}}_{\mathrm{a},n} \\ T\cap N_\delta\neq\emptyset}} \subset N'_\delta \subset\subset \tilde{\Omega}_{\mathrm{o,ex}}$ for all but finitely many n. Then for all such n,

$$\begin{aligned}
\big\|\nabla\big(\eta^2 \bar{w}_n^{\mathrm{c}} - I_n(\eta^2 \bar{w}_n^{\mathrm{c}})\big)\big\|^2_{L^2(N_\delta)} &\lesssim \epsilon_n^{2d} \sum_{\substack{T\in\tilde{\mathcal{T}}_{\mathrm{a},n} \\ T\cap N_\delta\neq\emptyset}} \int_T |\bar{w}_n^{\mathrm{c}}|^2 + |\nabla \bar{w}_n^{\mathrm{c}}|^2\, dx \\
&\lesssim \epsilon_n^{2d}\big(\|\bar{w}_n^{\mathrm{c}}\|^2_{L^2(N'_\delta)} + \|\nabla \bar{w}_n^{\mathrm{c}}\|^2_{L^2(N'_\delta)}\big).
\end{aligned}$$

Now note that $\|\bar{w}_n^{\mathrm{c}}\|_{L^2(N'_\delta)} \to \|\bar{w}_0^{\mathrm{c}}\|_{L^2(N'_\delta)}$ while $\|\nabla \bar{w}_n^{\mathrm{c}}\|_{L^2(N'_\delta)}$ is bounded since $\bar{w}_n^{\mathrm{c}}$ is weakly convergent in $H^1(N'_\delta)$. As ϵ_n goes to 0, we obtain (5.4.40). Inserting (5.4.40) into (5.4.39) proves the theorem.

□

Our second task is to prove the atomistic version of Lemma 5.4.10 over A_1.

Lemma 5.4.11. *Let $\bar{w}_n^{\mathrm{a}}$ and $\bar{w}_0^{\mathrm{a}}$ be as defined in Lemma 5.4.4. Then*

$$\left\|\nabla\left(I_n \bar{w}_n^{\mathrm{a}} - \bar{w}_0^{\mathrm{a}}\right)\right\|_{L^2(A_1)} \to 0. \tag{5.4.41}$$

Proof. As in previous case, $\bar{w}_0^{\mathrm{a}} \in H^2_{\mathrm{loc}}(\tilde{\Omega}_{\mathrm{a}})$ so we again consider again a sequence $\hat{w}_n^{\mathrm{a}} := I_n \bar{w}_0^{\mathrm{a}}$, which converges in $H^1(A_1)$ to $\bar{w}_0^{\mathrm{a}}$. Set $X := (\lfloor \psi_{\mathrm{a}}/2 \rfloor + 1)\tilde{\Omega}_{\mathrm{core}}$, and take η to be a bump function equal to one on A_1, zero on a neighborhood of the origin, and $\mathrm{supp}(\eta) \subset\subset \mathrm{X}$, i.e. η rapidly vanishes off A_1. Note that we still possess convergence of $\hat{w}_n^{\mathrm{a}}$ to $\bar{w}_0^{\mathrm{a}}$ in $H^1(X)$. We also know $I_n \bar{w}_n^{\mathrm{a}} \rightharpoonup \bar{w}_0^{\mathrm{a}}$ in $H^1(\tilde{\Omega}_{\mathrm{a}})$ by Lemma 5.4.4 so $y_n := I_n \bar{w}_n^{\mathrm{a}} - \hat{w}_n^{\mathrm{a}}$ converges weakly to zero in $H^1(X)$.

We recall that the product rule for difference quotients involves a shift operator which we denote by T_r:

$$\begin{aligned} D_{\epsilon_n \rho}(uv)(\xi) &= (D_{\epsilon_n \rho} u)v + (T_{\epsilon_n \rho} u) D_{\epsilon_n \rho} v, \quad \text{where} \quad T_{\epsilon_n \rho} v(\xi) := v(\xi + \epsilon_n \rho), \\ T_{\epsilon_n} v(\xi) &:= (T_{\epsilon \rho} v(\xi))_{\rho \in \mathcal{R}}, \qquad\qquad\qquad \text{and} \qquad T_{\epsilon_n} u\, D_{\epsilon_n} v = (T_{\epsilon_n \rho} u\, D_{\epsilon_n \rho} v)_{\rho \in \mathcal{R}}, \end{aligned}$$

and choose a domain $\Omega_1 \subset\subset X$ such that $\mathrm{supp}(T_{\epsilon_n r}\eta) \subset\subset \Omega_1$ for all but finitely many n. Because y_n converges weakly to zero in $H^1(X)$, the conclusion of Lemma 5.4.7 asserts that

$$\bar{I}_n D_{\epsilon_n} y_n \rightharpoonup 0 \quad \text{in} \quad L^2(\Omega_1).$$

Then note that $D_{\epsilon_n r}(\eta y_n) = (T_{\epsilon_n r}\eta) D_{\epsilon_n r} y_n + y_n D_{\epsilon_n r}\eta$ and

$$\begin{aligned} \bar{I}_n((T_{\epsilon_n r}\eta) D_{\epsilon_n r} y_n) &= \bar{I}_n(T_{\epsilon_n r}\eta)\bar{I}_n(D_{\epsilon_n r} y_n), \\ \bar{I}_n(y_n D_{\epsilon_n r}\eta) &= \bar{I}_n(y_n)\bar{I}_n(D_{\epsilon_n r}\eta). \end{aligned}$$

Strong convergence of $\bar{I}_n(T_{\epsilon_n r}\eta)$ to η on $H^1(X)$ and weak convergence of $\bar{I}_n(D_{\epsilon_n r} y_n)$ to zero on Ω_1 imply weak convergence of $\bar{I}_n(T_{\epsilon_n r}\eta D_{\epsilon_n r} y_n)$ to zero on Ω_1. Moreover, using boundedness of $\bar{I}_n$ and strong $L^2(X)$ convergence of y_n to zero, we see that $\bar{I}_n(y_n)$

converges strongly to 0 so that $\bar{I}_n(y_n D_{\epsilon_n r}\eta)$ converges to zero in $L^2(\Omega_1)$. It thus follows that

$$\bar{I}_n D_{\epsilon_n r}(\eta y_n) \rightharpoonup 0 \quad \text{in} \quad L^2(\Omega_1). \tag{5.4.42}$$

Furthermore, $I_n(\eta\hat{w}_n^{\mathrm{a}}) = I_n(\eta\bar{w}_0^{\mathrm{a}})$ by the definition of $\hat{w}_n^{\mathrm{a}}$ so standard finite element approximation theory implies $I_n(\eta\hat{w}_n^{\mathrm{a}})$ converges strongly to $\eta\bar{w}_0^{\mathrm{a}}$ in $H^1(X)$. Remark 5.4.8 after Lemma 5.4.7 then asserts

$$\bar{I}_n D_{\epsilon_n r}(\eta\hat{w}_n^{\mathrm{a}}) = \bar{I}_n D_{\epsilon_n r} I_n(\eta\hat{w}_n^{\mathrm{a}}) \to \nabla_r(\eta\bar{w}_0^{\mathrm{a}}) \quad \text{in} \quad L^2(\Omega_1). \tag{5.4.43}$$

These convergence properties and the fact that each $\bar{w}_n^{\mathrm{a}}$ solves

$$0 = \sum_{\xi\in\tilde{\mathcal{L}}_{\mathrm{a},n}^{\circ}} V_\xi''(D_{\epsilon_n}\tilde{\boldsymbol{u}}_{\mathrm{a},n}^{\infty}) : D_{\epsilon_n}\bar{w}_n^{\mathrm{a}} : D_{\epsilon_n}v^{\mathrm{a}} \quad \forall v^{\mathrm{a}} \in \tilde{\boldsymbol{\mathcal{U}}}_{0,n}^{\mathrm{a}} \tag{5.4.44}$$

will be used later in the proof.

From coercivity of the atomistic Hessian in (2.3.7),

$$\begin{aligned}\|\nabla I_n y_n\|_{L^2(A_1)}^2 \lesssim \|\nabla I_n(\eta y_n)\|_{L^2(X)}^2 &\lesssim \langle \delta^2\tilde{\mathcal{E}}^{\mathrm{a}}(\tilde{\boldsymbol{u}}_{\mathrm{a},n}^{\infty})(\eta y_n), (\eta y_n)\rangle \\ &= \sum_{\xi\in\tilde{\mathcal{L}}_{\mathrm{a},n}^{\circ}} V_\xi''(D_{\epsilon_n}\tilde{\boldsymbol{u}}_{\mathrm{a},n}^{\infty}) : D_{\epsilon_n}(\eta y_n) : D_{\epsilon_n}(\eta y_n).\end{aligned}$$

We now employ the integral formulation (5.4.6), which is valid since η rapidly vanishes off A_1 and due to the choice of A_1. Taking limits of the inequality immediately above produces

$$\begin{aligned}&\lim_{n\to\infty} \|\nabla I_n y_n\|_{L^2(A_1)}^2 \\ &\lesssim \lim_{n\to\infty} \int_{\tilde{\Omega}_{\mathrm{a}}} \bar{I}_n V''(D_{\epsilon_n}\tilde{\boldsymbol{u}}_{\mathrm{a},n}^{\infty}) : \bar{I}_n D_{\epsilon_n}(\eta y_n) : \bar{I}_n D_{\epsilon_n}(\eta y_n)\, dx \\ &= \lim_{n\to\infty} \int_{\tilde{\Omega}_{\mathrm{a}}} \bar{I}_n V''(D_{\epsilon_n}\tilde{\boldsymbol{u}}_{\mathrm{a},n}^{\infty}) : \bar{I}_n D_{\epsilon_n}(\eta\bar{w}_n^{\mathrm{a}}) : \bar{I}_n D_{\epsilon_n}(\eta y_n)\, dx \\ &\quad - \lim_{n\to\infty} \int_{\tilde{\Omega}_{\mathrm{a}}} \bar{I}_n V''(D_{\epsilon_n}\tilde{\boldsymbol{u}}_{\mathrm{a},n}^{\infty}) : \bar{I}_n D_{\epsilon_n}(\eta\hat{w}_n^{\mathrm{a}}) : \bar{I}_n D_{\epsilon_n}(\eta y_n)\, dx.\end{aligned} \tag{5.4.45}$$

The second limit is zero after noting we may write the integral over Ω_1 (relying on how Ω_1 was chosen) and then using (5.4.43), (5.4.42), and that $\bar{I}_n V''(D_{\epsilon_n}\tilde{\boldsymbol{u}}_{\mathrm{a},n}^{\infty})$ converges to $V''(0)$ in $L^\infty(\Omega_1)$.

Returning to (5.4.45)

$$\begin{aligned}
&\lim_{n\to\infty} \|\nabla I_n y_n\|^2_{L^2(A_1)} \\
&\lesssim \lim_{n\to\infty} \int_{\tilde{\Omega}_\mathrm{a}} \bar{I}_n V''(D_{\epsilon_n}\tilde{\boldsymbol{u}}^\infty_{\mathrm{a},n}) : \bar{I}_n D_{\epsilon_n}(\eta \bar{w}^\mathrm{a}_n) : \bar{I}_n D_{\epsilon_n}(\eta y_n)\, dx \\
&= \lim_{n\to\infty} \int_{\tilde{\Omega}_\mathrm{a}} \bar{I}_n V''(D_{\epsilon_n}\tilde{\boldsymbol{u}}^\infty_{\mathrm{a},n}) : (\bar{I}_n D_{\epsilon_n}\bar{w}^\mathrm{a}_n)(\bar{I}_n T_{\epsilon_n}\eta) : \bar{I}_n D_{\epsilon_n}(\eta y_n)\, dx \\
&\quad + \lim_{n\to\infty} \int_{\tilde{\Omega}_\mathrm{a}} \bar{I}_n V''(D_{\epsilon_n}\tilde{\boldsymbol{u}}^\infty_{\mathrm{a},n}) : (\bar{I}_n \bar{w}^\mathrm{a}_n)(\bar{I}_n D_{\epsilon_n}\eta) : \bar{I}_n D_{\epsilon_n}(\eta y_n)\, dx \\
&= \lim_{n\to\infty} \int_{\tilde{\Omega}_\mathrm{a}} \bar{I}_n V''(D_{\epsilon_n}\tilde{\boldsymbol{u}}^\infty_{\mathrm{a},n}) : \bar{I}_n D_{\epsilon_n}\bar{w}^\mathrm{a}_n : \bar{I}_n D_{\epsilon_n}(\eta^2 y_n)\, dx \\
&\quad - \lim_{n\to\infty} \int_{\tilde{\Omega}_\mathrm{a}} \bar{I}_n V''(D_{\epsilon_n}\tilde{\boldsymbol{u}}^\infty_{\mathrm{a},n}) : \bar{I}_n D_{\epsilon_n}\bar{w}^\mathrm{a}_n : (\bar{I}_n D_{\epsilon_n}\eta)\bar{I}_n(\eta y_n)\, dx \\
&\quad + \lim_{n\to\infty} \int_{\tilde{\Omega}_\mathrm{a}} \bar{I}_n V''(D_{\epsilon_n}\tilde{\boldsymbol{u}}^\infty_{\mathrm{a},n}) : (\bar{I}_n \bar{w}^\mathrm{a}_n)(\bar{I}_n D_{\epsilon_n}\eta) : \bar{I}_n D_{\epsilon_n}(\eta y_n)\, dx
\end{aligned}$$

The first of these limits is zero due to (5.4.44). The second is also zero since Lemma 5.4.7 implies $\bar{I}_n D_{\epsilon_n}\bar{w}^\mathrm{a}_n$ converges weakly to $\nabla \bar{w}^\mathrm{a}_0$, since

$$\|\bar{I}_n(\eta y_n)\|_{L^2(\Omega_1)} \lesssim \|\bar{I}_n(y_n)\|_{L^2(\Omega_1)} \lesssim \|y_n\|_{L^2(X)} \to 0,$$

and since $\bar{I}_n\big(D_{\epsilon_n}\eta V''(D_{\epsilon_n}\tilde{\boldsymbol{u}}^\infty_{\mathrm{a},n})\big)$ converges to $V''(0)$ in $L^\infty(\Omega_1)$. Using this latter fact, the third limit is then zero due to (5.4.42) and $\bar{I}_n\bar{w}^\mathrm{a}_n \to \bar{w}^\mathrm{a}_0$ in $L^2(X)$.

□

Step 4:

Conclusion of Proof of Theorem 5.4.2. We assume the existence of a sequence satisfying (5.4.12), which yields sequences of normalized functions $\bar{w}^\mathrm{a}_n$ and $\bar{w}^\mathrm{c}_n$ possessing properties (5.4.14)–(5.4.15) of Lemma 5.4.4. Combining (5.4.35) of Theorem 5.4.9 with (5.4.13) resulting from Statement 1 shows

$$(\nabla \bar{w}^\mathrm{a}_0, \nabla \bar{w}^\mathrm{c}_0)_{L^2(\tilde{\Omega}_\mathrm{o})} = 1. \tag{5.4.46}$$

The weak convergence of $I_n\bar{w}^\mathrm{a}_n$ to $\bar{w}^\mathrm{a}_0$ implies that

$$\|\nabla \bar{w}^\mathrm{a}_0\|_{L^2(\tilde{\Omega}_\mathrm{o})} \le \limsup_{n\to\infty} \|\nabla \bar{w}^\mathrm{a}_n\|_{L^2(\tilde{\Omega}_\mathrm{o})} = 1,$$

and likewise we have that $\|\nabla \bar{w}_0^{\mathrm{c}}\|_{L^2(\tilde{\Omega}_{\mathrm{o}})} \leq 1$. In view of (5.4.46), it is only possible if $\|\nabla \bar{w}_0^{\mathrm{a}}\|_{L^2(\tilde{\Omega}_{\mathrm{o}})} = \|\nabla \bar{w}_0^{\mathrm{c}}\|_{L^2(\tilde{\Omega}_{\mathrm{o}})} = 1$, and therefore

$$(\nabla \bar{w}_0^{\mathrm{a}}, \nabla \bar{w}_0^{\mathrm{c}})_{L^2(\tilde{\Omega}_{\mathrm{o}})} = \|\nabla \bar{w}_0^{\mathrm{a}}\|_{L^2(\tilde{\Omega}_{\mathrm{o}})} \|\nabla \bar{w}_0^{\mathrm{c}}\|_{L^2(\tilde{\Omega}_{\mathrm{o}})}.$$

Hence $\nabla \bar{w}_0^{\mathrm{a}} = \alpha \nabla \bar{w}_0^{\mathrm{c}}$ on $\tilde{\Omega}_{\mathrm{o}}$ for some real number α implying

$$1 = (\alpha \nabla \bar{w}_0^{\mathrm{c}}, \nabla \bar{w}_0^{\mathrm{c}})_{L^2(\tilde{\Omega}_{\mathrm{o}})} = \alpha \|\nabla \bar{w}_0^{\mathrm{c}}\|^2_{L^2(\tilde{\Omega}_{\mathrm{o}})} = \alpha.$$

Thus $\nabla \bar{w}_0^{\mathrm{a}}$ and $\nabla \bar{w}_0^{\mathrm{c}}$ are equal on $\tilde{\Omega}_{\mathrm{o}}$ so $\bar{w}_0^{\mathrm{a}}$ and $\bar{w}_0^{\mathrm{c}}$ differ by a constant on $\tilde{\Omega}_{\mathrm{o}}$. Let $\hat{w}_0^{\mathrm{c}}$ be the element of the equivalence class $\bar{\boldsymbol{w}}_0^{\mathrm{c}}$ which is equal to $\bar{w}_0^{\mathrm{a}}$ on $\tilde{\Omega}_{\mathrm{o}}$. We can then define a function

$$\bar{w}_0 = \begin{cases} \bar{w}_0^{\mathrm{a}} & \text{on} \quad \tilde{\Omega}_{\mathrm{a}} \\ \hat{w}_0^{\mathrm{c}} & \text{on} \quad \tilde{\Omega}_{\mathrm{c}} \end{cases},$$

for which $\bar{w}_0 \in L^2_{\mathrm{loc}}(\mathbb{R}^d)$ and $\nabla \bar{w}_0 \in L^2(\mathbb{R}^d)$. Consequently, $\bar{w}_0$ is a global solution to the linear, homogeneous Cauchy-Born equation,

$$\int_{\mathbb{R}^d} \mathbb{C} : \nabla \bar{w}_0 : \nabla v = 0, \quad \forall v \in H^1_0(\mathbb{R}^d),$$

so that $\nabla \bar{w}_0 = 0$. We conclude that $(\nabla \bar{w}_0^{\mathrm{a}}, \nabla \bar{w}_0^{\mathrm{c}})_{L^2(\tilde{\Omega}_{\mathrm{o}})} = 0$, which contradicts (5.4.46). □

Chapter 6

Algorithm Implementation and Complexity

6.1 Chapter Overview

The optimization-based atomistic-to-continuum coupling as formulated in (4.4.1) is a constrained optimization problem. The method we advise using to numerically solve this problem is through Lagrange multipliers. This has the disadvantage of resulting in a saddle-point problem with a Lagrangian involving derivatives of the restricted atomistic and continuum energies. Thus, the first derivative of the Lagrangian will include second derivatives of the restricted energies, and the second derivative will incorporate third derivatives of the energies. Setting the first variations of the Lagrangian with respect to both the states, u^{a} and u^{c}, and the Lagrange multiplier variables, v^{a} and v^{c}, equal to zero produces a nonlinear system of equations which can be solved to yield the optimal solution of the original problem. This is dubbed a "one-shot method" [29] because we solve simultaneously for the states, adjoint variables, and controls. At the moment, this seems to be the most practical method for an implementation, though we address other possibilities in the discussion.

This chapter describes the Lagrangian functional, provides the derivation of the optimal mesh size function alluded to in Assumption B, and converts the error estimate in Theorem 4.4.2 to an estimate in terms of the computational work. We end with some simple numerical experiments in one dimension. As previously mentioned, we work with

the formulation (4.4.1) without equivalence classes. A similar rendition of this appeared in the author's paper [47].

6.2 Derivation of the Lagrangian

To obtain the Lagrangian formulation from (4.4.1), we introduce the Lagrange multipliers (adjoint variables) $v^{\mathrm{a}} \in \mathcal{U}_0^{\mathrm{a}}$ and $v^{\mathrm{c}} \in \mathcal{U}_{h,0}^{\mathrm{c}}$ for the first two constraints and a scalar multiplier $\eta \in \mathbb{R}$ for the integral constraint. Our Lagrangian functional is then

$$\begin{aligned}\Psi(u^{\mathrm{a}}, u^{\mathrm{c}}, v^{\mathrm{a}}, v^{\mathrm{c}}, \eta) = \frac{1}{2}\|\nabla I u^{\mathrm{a}} - \nabla u^{\mathrm{c}}\|^2_{L^2(\Omega_{\mathrm{o}})} \\ - \langle \delta\mathcal{E}^{\mathrm{a}}(u^{\mathrm{a}}), v^{\mathrm{a}}\rangle - \langle \delta\mathcal{E}^{\mathrm{c}}(u^{\mathrm{c}}), v^{\mathrm{c}}\rangle - \eta \int_{\Omega_{\mathrm{o}}} (I u^{\mathrm{a}} - u^{\mathrm{c}})\, dx.\end{aligned} \tag{6.2.1}$$

Finding critical points of this Lagrangian corresponds to finding zeros of the first-variations. We write this (nonlinear) system of equations as

$$\text{find } u^{\mathrm{a}},\ u^{\mathrm{c}},\ v^{\mathrm{a}},\ v^{\mathrm{c}}, \text{ and } \eta \text{ such that } \nabla\Psi(u^{\mathrm{a}}, u^{\mathrm{c}}, v^{\mathrm{a}}, v^{\mathrm{c}}, \eta) = 0, \tag{6.2.2}$$

where

$$\nabla\Psi = \left(\frac{\partial\Psi}{\partial u^{\mathrm{a}}}, \frac{\partial\Psi}{\partial u^{\mathrm{c}}}, \frac{\partial\Psi}{\partial v^{\mathrm{a}}}, \frac{\partial\Psi}{\partial v^{\mathrm{c}}}, \frac{\partial\Psi}{\partial \eta}\right)^T \tag{6.2.3}$$

We solve this system using a simple Newton iteration.

1. Choose an initial guess $\mathbf{z} = [u^{\mathrm{a}},\ u^{\mathrm{c}},\ v^{\mathrm{a}},\ v^{\mathrm{c}},\ \eta]^T$.
2. Compute $\nabla^2\Psi(\mathbf{z})\mathbf{x}$ and $\nabla\Psi(\mathbf{z})$.
3. Solve the linear equation
$$\nabla^2\Psi(\mathbf{z})\mathbf{x} = -\nabla\Psi(\mathbf{z}) \tag{6.2.4}$$
4. Define the new iterate $\mathbf{z} = \mathbf{z} + \mathbf{x}$.
5. Repeat steps 2-4 until either $\|\nabla\Psi(\mathbf{z})\| < \text{tol}$ for some small tolerance or until a maximum number of iterations has been reached.

Clearly, more sophisticated approaches are possible, but this seems to perform well in the limited testing done so far. The initial guess can be taken to be the reference configuration in the case of a point defect.

The Hessian, $\nabla^2\Psi(z)$, is of the form

$$\nabla^2\Psi = \begin{pmatrix} \frac{\partial^2\Psi}{\partial(u^{\rm a})^2} & \frac{\partial^2\Psi}{\partial u^{\rm c}\partial u^{\rm a}} & \frac{\partial^2\Psi}{\partial v^{\rm a}\partial u^{\rm a}} & \mathbf{0} & \frac{\partial^2\Psi}{\partial\eta\partial u^{\rm a}} \\ \frac{\partial^2\Psi}{\partial u^{\rm a}\partial u^{\rm c}} & \frac{\partial^2\Psi}{\partial(u^{\rm c})^2} & \mathbf{0} & \frac{\partial^2\Psi}{\partial v^{\rm c}\partial u^{\rm c}} & \frac{\partial^2\Psi}{\partial\eta\partial u^{\rm c}} \\ \frac{\partial^2\Psi}{\partial u^{\rm a}\partial v^{\rm a}} & \mathbf{0} & \mathbf{0} & \mathbf{0} & \mathbf{0} \\ \mathbf{0} & \frac{\partial^2\Psi}{\partial u^{\rm c}\partial v^{\rm c}} & \mathbf{0} & \mathbf{0} & \mathbf{0} \\ \frac{\partial^2\Psi}{\partial u^{\rm a}\partial\eta} & \frac{\partial^2\Psi}{\partial u^{\rm c}\partial\eta} & \mathbf{0} & \mathbf{0} & \mathbf{0} \end{pmatrix} =: \begin{pmatrix} \boldsymbol{A} & \boldsymbol{B}^T \\ \boldsymbol{B} & \mathbf{0} \end{pmatrix}, \tag{6.2.5}$$

which produces the structure of a saddle point problem.

6.3 Optimal Parameter Choices

Here we show that the choice of mesh size function, $h(x) = C(x)(|x|/R_{\rm core})^{\frac{1+d}{1+d/2}}$ is optimal where $C(x)$ is some function which is approximately equal to one. Recall that

$$h_T := \mathrm{Diam}(T), \quad \text{and} \quad h(x) := \sup_{\{T\in\mathcal{T}_h : x\in T\}} h_T.$$

We previously only assumed in $\boldsymbol{E}.4$ that $h(x) \lesssim (|x|/R_{\rm core})^{\frac{1+d}{1+d/2}}$, which is clearly consistent with this choice. We follow the procedure of [23,42,47,52] in deriving h, and also derive how $R_{\rm c}$ should be chosen given $R_{\rm a} = \psi_{\rm a}R_{\rm core}$ where $R_{\rm core}$ is a known quantity.

The key to obtaining the optimal parameter choices is the broken norm error estimate

$$\begin{aligned} &\|\nabla\left(I\boldsymbol{u}_{\rm a}^{\infty} - I\boldsymbol{u}_{\rm a}^{\rm atc}\right)\|_{L^2(\Omega_{\rm a})} + \|\nabla\left(I\boldsymbol{u}_{\rm c}^{\infty} - \boldsymbol{u}_{\rm c}^{\rm atc}\right)\|_{L^2(\Omega_{\rm c})} \\ &\lesssim \|\nabla\tilde{I}\boldsymbol{u}^{\infty}\|_{L^2(\mathbb{R}^d\setminus B_{3r_{\rm c}/4})} + \|h\nabla^2\tilde{I}\boldsymbol{u}^{\infty}\|_{L^2(\Omega_{\rm c})} + \left(\|\nabla^3\tilde{I}\boldsymbol{u}^{\infty}\|_{L^2(\Omega_{\rm c})} + \|\nabla^2\tilde{I}\boldsymbol{u}^{\infty}\|_{L^4(\Omega_{\rm c})}^2\right), \end{aligned} \tag{6.3.1}$$

which has actually already been proven. Indeed, if we return momentarily to the proof of Theorem 4.4.2, we saw that

$$\begin{aligned} &\|\nabla\left(I\boldsymbol{u}_{\rm a}^{\infty} - I\boldsymbol{u}_{\rm a}^{\rm atc}\right)\|_{L^2(\Omega_{\rm a})}^2 + \|\nabla\left(I\boldsymbol{u}_{\rm c}^{\infty} - \boldsymbol{u}_{\rm c}^{\rm atc}\right)\|_{L^2(\Omega_{\rm c})}^2 \\ &\lesssim \|(\lambda_{\rm a}^{\infty},\lambda_{\rm c}^{\infty}) - (\lambda_{\rm a}^{\rm atc},\lambda_{\rm c}^{\rm atc})\|_{\rm err}^2 + \|\nabla\left(I\boldsymbol{u}^{\infty} - \boldsymbol{U}^{\rm c}(\lambda_{\rm c}^{\infty})\right)\|_{L^2(\Omega_{\rm c})}^2. \end{aligned} \tag{6.3.2}$$

The second term above is the continuum error estimated in Theorem 4.3.8. However, if we return to that proof and do not use the decay estimates to bound L^p norms of $I\boldsymbol{u}^{\infty}$, then the continuum error is seen to be bounded by the quantity

$$\|\nabla\tilde{I}\boldsymbol{u}^{\infty}\|_{L^2(\mathbb{R}^d\setminus B_{3r_{\rm c}/4})} + \|h\nabla^2\tilde{I}\boldsymbol{u}^{\infty}\|_{L^2(\Omega_{\rm c})} + \left(\|\nabla^3\tilde{I}\boldsymbol{u}^{\infty}\|_{L^2(\Omega_{\rm c})} + \|\nabla^2\tilde{I}\boldsymbol{u}^{\infty}\|_{L^4(\Omega_{\rm c})}^2\right).$$

The first term in (6.3.2) was likewise estimated in Theorem 5.3.9 to be bounded by the consistency error of Section 5.3.5. But there we saw the consistency error was nothing more than the continuum error, which we just estimated immediately above. This validates the claim in (6.3.1).

The first error in this bound represents the far-field error made from truncating the infinite domain to a finite domain. The third term in parentheses is precisely the Cauchy-Born error introduced in Chapter 3, which represented a second order estimate. Note that there is no finite element coarsening error involved here so it is "pure" Cauchy-Born error. Meanwhile, the second error is exactly the finite element discretization error made by using piecewise linear finite elements. We maintain the mesh size function inside the L^2 norm in order to find the optimal mesh size function.

Our immediate goal is to derive the optimal mesh function as well as the optimal size for the continuum region. Since both the size of the continuum region and the mesh size enter the error estimate in the first two terms of (6.3.1), it will be exactly these two error terms which we will optimize to find h and R_{c}. The remaining error terms are higher order so we neglect these from here on. The rough procedure will be to fix a number of degrees of freedom (which is equal to the number of nodes in the finite element mesh) and then minimize the finite element error $\|h\nabla^2\tilde{I}\boldsymbol{u}^{\infty}\|_{L^2(\Omega_{\mathrm{c}})}$ with respect to h and R_{c}.

In order to make this problem tractable, we assume a radial mesh size function, h. Clearly, this is not realistic since we are working with polygonal objects, which is why we include $C(x)$ when we say that $h(x) = C(x)(|x|/R_{\mathrm{core}})^{\frac{1+d}{1+d/2}}$. The finite element mesh is assumed fully resolved in the atomistic region, so we need only consider the number of degrees of freedom in the continuum region. This quantity can be written as

$$\#\mathrm{DoF} \approx \sum_{\substack{T\in\mathcal{T}_h \\ T\cap\Omega_{\mathrm{o}}=\emptyset}} 1 = \sum_{\substack{T\in\mathcal{T}_h \\ T\cap\Omega_{\mathrm{o}}=\emptyset}} \frac{|T|}{|T|} \approx \int_{R_{\mathrm{a}}}^{R_{\mathrm{c}}} \frac{1}{h^d} r^{d-1}\, dr,$$

where $X \approx Y$ indicates that X and Y are equal up to a multiplicative constant.

Recalling the decay estimate $|\nabla^j\tilde{I}\bar{u}(x)| \sim |x|^{1-d-j}$ for $|x|$ large enough (and in

particular all $x \in \Omega_c$), we have

$$\begin{aligned} \|h\nabla^2 \tilde{I}\boldsymbol{u}^\infty\|^2_{L^2(\Omega_c\setminus\Omega_o)} &\lesssim \int_{R_a}^{R_c} h^2 r^{-2-2d} r^{d-1}\, dr = \int_{R_a}^{R_c} h^2 r^{-3-d}\, dr \\ \|\nabla \tilde{I}\boldsymbol{u}^\infty\|^2_{L^2(\mathbb{R}^d\setminus B_{3r_c/4})} &\lesssim \|\nabla \tilde{I}\boldsymbol{u}^\infty\|^2_{L^2(\mathbb{R}^d\setminus B_{3R_c/4})} \lesssim \int_{R_c}^{\infty} r^{-2d} r^{d-1}\, dr \\ &= \int_{R_c}^{\infty} r^{-d-1}\, dr. \end{aligned}$$

We only consider the first error over $\Omega_c\setminus\Omega_o$ since the remaining contribution over Ω_o cannot be optimized since the mesh is assumed fully resolved on Ω_o. Using these estimates for the error, we attempt to solve the following optimization problem for R_c and h:

$$\begin{aligned} &\text{minimize} \int_{R_a}^{R_c} h^2 r^{-3-d}\, dr + \int_{R_c}^{\infty} r^{-d-1}\, dr \\ &\text{subject to} \quad \begin{cases} \#\text{DoF} = \int_{R_a}^{R_c} \frac{1}{h^d} r^{d-1}\, dr = C, \\ h(R_a) = 1. \end{cases} \end{aligned}$$

Here, C is a fixed constant. We introduce a Lagrange multiplier, ν, for the degree of freedom constraint and take the variation of

$$\int_{R_a}^{R_c} h^2 r^{-3-d}\, dr + \int_{R_c}^{\infty} r^{-d-1}\, dr + \nu\Big(\int_{R_a}^{R_c} \frac{1}{h^d} r^{d-1}\, dr - C\Big)$$

with respect to h in the direction p where p is an L^2 function. Setting the result equal to zero produces

$$0 = 2\int_{R_a}^{R_c} hpr^{-3-d}\, dr - d\nu \int_{R_a}^{R_c} \frac{p}{h^{d+1}} r^{d-1}\, dr = \int_{R_a}^{R_c} pr^{-3-d}(2h - d\nu \frac{r^{2d+2}}{h^{d+1}})\, dr.$$

Since p is arbitrary, this forces the final integrand to be zero so

$$h = \frac{d\nu}{2}\frac{r^{2d+2}}{h^{d+1}} \quad \text{if and only if} \quad h = \left(\frac{d\nu}{2}\right)^{1/(d+2)} r^{\frac{2d+2}{d+2}}$$

if and only if

$$h = \left(\frac{d\nu}{2}\right)^{1/(d+2)} r^{\frac{2d+2}{d+2}} = \left(\frac{d\nu}{2}\right)^{1/(d+2)} r^{\frac{1+d}{1+d/2}}.$$

Up to the constant factor, this was exactly the choice indicated in Section 4.3. From the second constraint, $h(R_a) = 1$, we have

$$1 = \left(\frac{d\nu}{2}\right)^{1/(d+2)} R_a^{\frac{1+d}{1+d/2}}$$

which gives simply

$$\left(\frac{d\nu}{2}\right)^{1/(d+2)} = R_{\mathrm{a}}^{-\frac{1+d}{1+d/2}},$$

and finally

$$h(r) = \left(\frac{r}{R_{\mathrm{a}}}\right)^{\frac{1+d}{1+d/2}}.$$

Likewise, differentiating

$$\int_{R_{\mathrm{a}}}^{R_{\mathrm{c}}} h^2 r^{-3-d}\,dr + \int_{R_{\mathrm{c}}}^{\infty} r^{-d-1}\,dr + \nu\Big(\int_{R_{\mathrm{a}}}^{R_{\mathrm{c}}} \frac{1}{h^d} r^{d-1}\,dr - C\Big)$$

with respect to R_{c} in the direction S_{c} and setting the result equal to zero yields

$$\begin{aligned} 0 = &\ S_{\mathrm{c}} h(R_{\mathrm{c}})^2 R_{\mathrm{c}}^{-3-d} - S_{\mathrm{c}} R_{\mathrm{c}}^{-d-1} + S_{\mathrm{c}}\nu \frac{1}{h(R_{\mathrm{c}})^d} R_{\mathrm{c}}^{d-1} \\ = &\ S_{\mathrm{c}} \left(h(R_{\mathrm{c}})^2 R_{\mathrm{c}}^{-3-d} + \nu \frac{1}{h(R_{\mathrm{c}})^d} R_{\mathrm{c}}^{d-1} - R_{\mathrm{c}}^{-d-1} \right). \end{aligned}$$

Since S_{c} is arbitrary, the term inside the parentheses must be zero, and we write this as

$$R_{\mathrm{c}}^{-d-1} = h(R_{\mathrm{c}})^2 R_{\mathrm{c}}^{-3-d} + \nu \frac{1}{h(R_{\mathrm{c}})^d} R_{\mathrm{c}}^{d-1}.$$

Using the previously derived expressions for h and ν, this implies

$$\begin{aligned} R_{\mathrm{c}}^{-d-1} = &\ R_{\mathrm{c}}^{\frac{2+2d}{1+d/2}-3-d} R_{\mathrm{a}}^{-\frac{2+2d}{1+d/2}} + \nu R_{\mathrm{c}}^{-\frac{d+d^2}{1+d/2}+d-1} R_{\mathrm{a}}^{\frac{d+d^2}{1+d/2}} \\ = &\ R_{\mathrm{c}}^{-\frac{d^2+d+2}{d+2}} R_{\mathrm{a}}^{-\frac{2+2d}{1+d/2}} + \frac{2}{d} R_{\mathrm{a}}^{-\frac{(1+d)(d+2)}{1+d/2}+\frac{d+d^2}{1+d/2}} R_{\mathrm{c}}^{-\frac{d^2+d+2}{d+2}} \\ = &\ R_{\mathrm{c}}^{-\frac{d^2+d+2}{d+2}} R_{\mathrm{a}}^{-\frac{2+2d}{1+d/2}} + \frac{2}{d} R_{\mathrm{a}}^{-\frac{2+2d}{1+d/2}} R_{\mathrm{c}}^{-\frac{d^2+d+2}{d+2}} \\ = &\ \left(1+\frac{2}{d}\right) R_{\mathrm{c}}^{-\frac{d^2+d+2}{d+2}} R_{\mathrm{a}}^{-\frac{2+2d}{1+d/2}} \end{aligned}$$

We can solve this latter relation for R_{c} in terms of R_{a}:

$$R_{\mathrm{c}} \eqsim R_{\mathrm{a}}^{\frac{1+d}{d/2}},$$

and we have now found both the optimal mesh and optimal choice for R_{c} to minimize the error of our method.

Next, we convert the error bound to be in terms of the computational work, or number of degrees of freedom, (#DoF). The number of degrees of freedom is simply

equal to the number of degrees of freedom in the atomistic region plus the number in the continuum region:

$$\begin{aligned}
\#\text{DoF} &\eqsim R_{\mathrm{a}}^d + \int_{R_{\mathrm{a}}}^{R_{\mathrm{c}}} \left((r/R_{\mathrm{a}})^{\frac{1+d}{1+d/2}} \right)^{-d} r^{d-1}\, dr \\
&= R_{\mathrm{a}}^d + R_{\mathrm{a}}^{\frac{d(1+d)}{1+d/2}} \int_{R_{\mathrm{a}}}^{R_{\mathrm{c}}} r^{\frac{-d(1+d)}{1+d/2}+d-1}\, dr \\
&= R_{\mathrm{a}}^d + R_{\mathrm{a}}^{\frac{d(1+d)}{1+d/2}} \frac{1}{\frac{-d(1+d)}{1+d/2}+d} \left(R_{\mathrm{c}}^{\frac{-d(1+d)}{1+d/2}+d} - R_{\mathrm{a}}^{\frac{-d(1+d)}{1+d/2}+d} \right) \\
&= R_{\mathrm{a}}^d + \frac{1}{\frac{-d(1+d)}{1+d/2}+d} \left(R_{\mathrm{a}}^{\frac{d(1+d)}{1+d/2}} R_{\mathrm{a}}^{(\frac{1+d}{d/2})(\frac{-d(1+d)}{1+d/2}+d)} - R_{\mathrm{a}}^d \right) \\
&= R_{\mathrm{a}}^d + \frac{1}{\frac{-d(1+d)}{1+d/2}+d} (1 - R_{\mathrm{a}}^d) \eqsim R_{\mathrm{a}}^d - \frac{d+2}{d^2}.
\end{aligned} \tag{6.3.3}$$

We will ignore the constant factor here since R_{a}^d is far greater than this quantity.

Recall yet again the fundamental error estimate of Theorem 4.4.2

$$\|\nabla \left(I\boldsymbol{u}_{\mathrm{a}}^{\mathrm{atc}} - I\boldsymbol{u}_{\mathrm{a}}^{\infty} \right)\|_{L^2(\Omega_{\mathrm{a}})}^2 + \|\nabla \left(\boldsymbol{u}_{\mathrm{c}}^{\mathrm{atc}} - I\boldsymbol{u}_{\mathrm{c}}^{\infty} \right)\|_{L^2(\Omega_{\mathrm{c}})}^2 \lesssim R_{\mathrm{core}}^{-d-2} + R_{\mathrm{c}}^{-d}, \tag{6.3.4}$$

and the fact that $R_{\mathrm{a}} = \psi_{\mathrm{a}} R_{\mathrm{core}}$ so that $R_{\mathrm{a}} \eqsim R_{\mathrm{core}}$. We have just shown that $R_{\mathrm{c}} = R_{\mathrm{a}}^{\frac{1+d}{d/2}}$ is an optimal choice to minimize the error and $\#\text{DoF} \eqsim R_{\mathrm{a}}^d$. Substituting these facts into (6.3.4) gives

$$\begin{aligned}
\|\nabla \left(I\boldsymbol{u}_{\mathrm{a}}^{\mathrm{atc}} - I\boldsymbol{u}_{\mathrm{a}}^{\infty} \right)\|_{L^2(\Omega_{\mathrm{a}})}^2 + \|\nabla \left(\boldsymbol{u}_{\mathrm{c}}^{\mathrm{atc}} - I\boldsymbol{u}_{\mathrm{c}}^{\infty} \right)\|_{L^2(\Omega_{\mathrm{c}})}^2 &\lesssim R_{\mathrm{a}}^{-d-2} + R_{\mathrm{a}}^{-d-2} \\
&= (\#\text{DoF})^{\frac{-d-2}{d}}.
\end{aligned}$$

This means that if we double the number of degrees of freedom in the problem (or double the amount of work used), the error will be halved in two dimensions and cut by slightly less than half in three dimensions. As shown in Table 2.1, this decay rate matches the optimal known rate among AtC methods.

Remark 6.3.1. *If instead of a point defect, we assumed a more general condition that the elastic fields of the defect decay as*

$$|\nabla^j \tilde{I}\boldsymbol{u}^{\infty}(x)| \lesssim |x|^{1-\gamma-j} \quad \textit{for all } x \textit{ outside the core defect region,}$$

then the above proof could easily be adopted to show that the optimal mesh size function and continuum diameters are

$$h(x) = (|x|/R_{\rm a})^{\frac{1+\gamma}{1+d/2}}, \quad R_{\rm c} \eqsim R_{\rm a}^{\frac{1+\gamma}{\gamma-d/2}}, \quad \textit{provided } 2\gamma - d > 0. \textit{ [47]}$$

The error estimate in terms of the degrees of freedom then becomes

$$\|\nabla \left(I\boldsymbol{u}_{\rm a}^{\rm atc} - I\boldsymbol{u}_{\rm a}^{\infty}\right)\|_{L^2(\Omega_{\rm a})}^2 + \|\nabla \left(\boldsymbol{u}_{\rm c}^{\rm atc} - I\boldsymbol{u}_{\rm c}^{\infty}\right)\|_{L^2(\Omega_{\rm c})}^2 \lesssim \ (\#\text{DoF})^{\frac{-2-2\gamma+d}{d}}. \qquad (6.3.5)$$

For a point defect, $\gamma = d$, and this agrees with our previous results. For a dislocation, we could take $\gamma = 1$ [23].

Practically speaking, the mesh can be constructed as long as the atomistic region is chosen to be of a sufficiently regular shape. In this case, this shape can be extended into layers which are spaced out according to h and each layer is then refined [52]. This is carried out when the atomistic region is a hexagon in two dimensions in [52]. We give an explicit algorithm in one dimension in the next section.

6.4 Numerical Experiments

In this section, we detail some rather simple numerical experiments conducted in one dimension, assuming a next-nearest neighbor Lennard-Jones pair potential model. These are reported from the author's work [47]. These same experiments have been performed for many popular AtC algorithms in [42], where the atomistic model used was the embedded atom method. We will also show how to incorporate external forces into the model and explain how a site potential is obtained. We use external forces to mimic a defect whose decay rate is characterized by $\gamma = \frac{3}{2}$ and $\gamma = 1$ as discussed in Remark 6.3.1. From the preceding section, we then expect that carrying out the optimization-based AtC algorithm with optimal mesh and optimal choice of $R_{\rm c}$ should give an error that decays as $(\#\text{DoF})^{-2}$ for $\gamma = 3/2$ and $(\#\text{DoF})^{-3/2}$ for $\gamma = 1$ (after taking square roots of (6.3.5)).

We take the lattice, $\mathcal{L}$, to simply be $\mathbb{Z}$. The Lennard-Jones pair potential is $\phi(r) := r^{-12} - 2r^{-6}$ and is shown graphed below.

We assume next-nearest neighbor interactions so that the site potential is given by

$$V(Du(\xi)) = \phi(1 + D_1 u) + \phi(2 + D_1 u - D_{-1} u) - (\phi(1) + \phi(2)) - f(\xi)u(\xi),$$

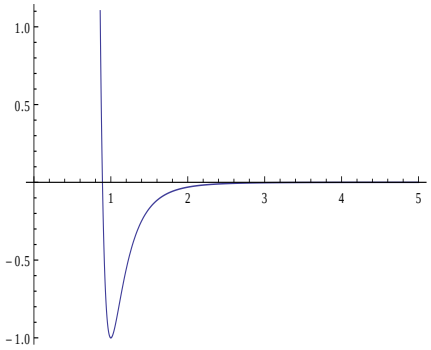

Figure 6.1: Lennard-Jones Potential.

where $f(\xi)$ is the external force at ξ. (Note that this site potential does not satisfy $V(0) = 0$ due to the external forces, but the portion of the site potential due to the Lennard-Jones potential does satisfy this.) The total atomistic energy is

$$\mathcal{E}^{\mathrm{a}}(u) = \sum_{\xi\in\mathbb{Z}} \phi(1 + D_1u(\xi)) + \phi(2 + D_1u(\xi) - D_{-1}u(\xi)) - (\phi(1) - \phi(2)) - f(\xi)u(\xi),$$

The Cauchy-Born continuum energy is

$$\mathcal{E}^{\mathrm{c}}(u) = \int_{\mathbb{R}} W(\nabla u)\,dx - \int (I_h f)u\,dx, \quad \text{where} \quad W(\mathsf{G}) = \phi(1 + \mathsf{G}) + \phi(2 + 2\mathsf{G}).$$

Here, we continue using I_h as the piecewise linear interpolant onto the finite element mesh.

In order to be able to compute the *a priori* error estimates, we will use the time-honored practice of choosing an atomistic solution which has the appropriate decay and then computing the external forces that result from it. We use the same atomistic solution as in [42]:

$$u^{\infty}(\xi) = \frac{1}{10}\left(1 + \xi^2\right)^{-\gamma/2}\xi.$$

From this solution, we compute the external forces required for u^{∞} to satisfy the Euler Lagrange equations corresponding to minimizing $\mathcal{E}^{\mathrm{a}}$. This yields

$$f(\xi) = -\frac{\partial\mathcal{E}^{\mathrm{a}}(u)}{\partial u_\xi}\Big|_{u=u^{\infty}}.$$

We introduce Lagrange multipliers for the constraints of the optimization-based algorithm and find the Lagrangian is

$$\begin{aligned}\Psi(u^{\mathrm{a}}, u^{\mathrm{c}}, v^{\mathrm{a}}, v^{\mathrm{c}}, \eta) = \frac{1}{2}\|\nabla I u^{\mathrm{a}} - \nabla u^{\mathrm{c}}\|^2_{L^2(\Omega_{\mathrm{o}})} + \langle \delta\mathcal{E}^{\mathrm{a}}(u^{\mathrm{a}}), v^{\mathrm{a}}\rangle \\ + \langle \delta\mathcal{E}^{\mathrm{c}}(u^{\mathrm{c}}), v^{\mathrm{c}}\rangle + \eta_1 \int\limits_{\Omega_{\mathrm{o}}\cap\mathbb{R}^+} (Iu^{\mathrm{a}} - u^{\mathrm{c}})\, dx + \eta_2 \int\limits_{\Omega_{\mathrm{o}}\cap\mathbb{R}^-} (Iu^{\mathrm{a}} - u^{\mathrm{c}})\, dx\end{aligned} \tag{6.4.1}$$

Here, we require two Lagrange multipliers to enforce the mean value zero condition because the overlap region is disconnected in one dimension, having a left overlap region and right overlap region.

To select the appropriate parameters, we choose R_{core} from a range of interest and construct the mesh according to the analysis of the preceding section. Namely, we set $R_{\mathrm{a}} = 2R_{\mathrm{core}}$ and recursively construct the nodes, $\mathcal{N}_h$, of the triangulation, $\mathcal{T}_h$, as follows.

1. Each $\xi \in B_{R_{\mathrm{a}}}(0)$ is chosen as a node.
2. Set $\xi = \max_{\zeta\in\mathcal{N}_h} \zeta$, and sequentially add a new node at $\pm[\xi + h(\xi)]$ where $h(\xi) := \lfloor (\xi/R_{\mathrm{a}})^{\frac{1+\gamma}{1+d/2}} \rfloor$.
3. Repeat the second step until $h(\xi) \approx \xi$, at which point we add two final nodes at $\pm R_C$.

Finally, we carry out the optimization-based AtC algorithm and calculate u^{atc} for $R_{\mathrm{core}} \in \{10, 20, 40, 80, 160\}$. As previously mentioned, we expect the error to decay as $(\#\mathrm{DoF})^{-2}$. We have plotted a log-log graph of the error involved in each of these approximations versus the number of degrees of freedom (nodes in the mesh) in Figure 6.2. The error behaves like $(\#\mathrm{DoFs})^{-2}$, exactly according to the theory.

We have also carried out the same experimental procedure for the defect parameter choice $\gamma = 1$. In Figure 6.3, we provide a plot of the strain error, $\|\nabla I u^{\infty} - \nabla I u^{\mathrm{atc}}\|_{L^2}$ versus the number of degrees of freedom. Also included is a plot of $3(\#\mathrm{DoF})^{-3/2}$, which is the expected rate of decay for $\gamma = 1$. There is once again very good asymptotic agreement.

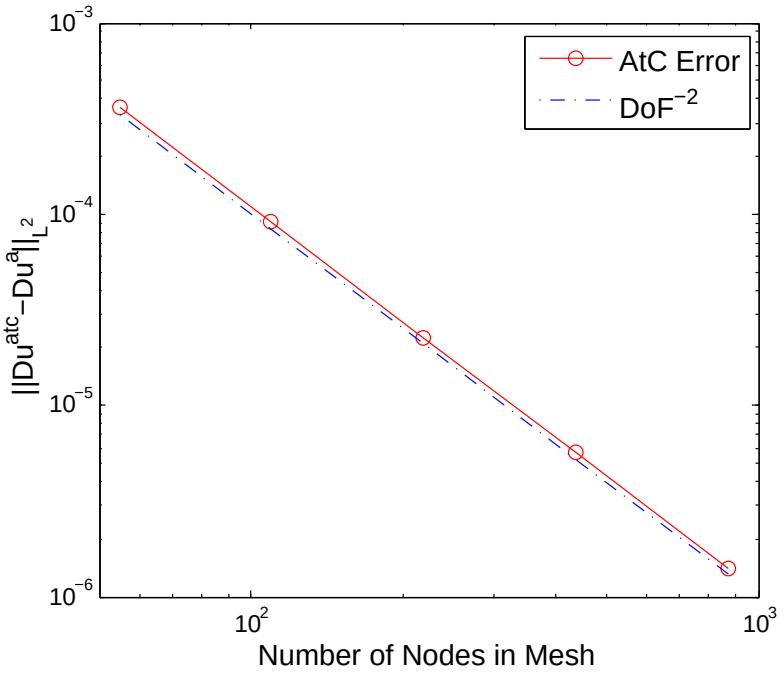

Figure 6.2: Log-Log plot of error of AtC approximation for $\gamma = 3/2$ plotted against number of degrees of freedom.

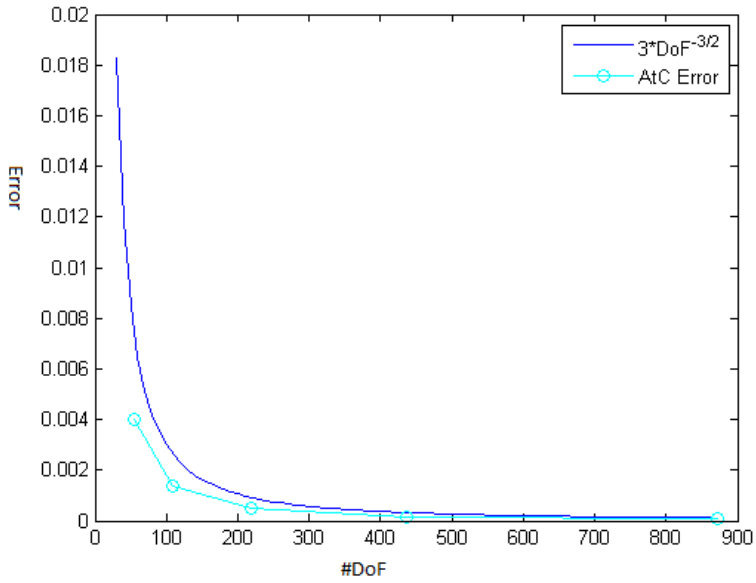

Figure 6.3: Error of AtC approximation for $\gamma = 1$ plotted against number of degrees of freedom.

Chapter 7

Discussion

A complete analysis of the optimization-based atomistic-to-continuum coupling method has been presented in the context of point defect. This method has several inherent advantages compared to previous AtC methods, but significant work also remains to implement the method in two and three dimensions. Perhaps the greatest attribute of the optimization-based approach is its robustness with respect to the specific models employed and lack of geometric restrictions in dimensions two and three. There is nothing precluding using the same algorithm to couple, for example, the recent tight-binding method of [12] with another atomistic model. In this, there are many possible avenues for further investigation. At the moment, much of the focus of other groups has been only on coupling linear problems in [15, 17, 18, 46] with the exception of the present work.

Just within the realm of atomistic-to-continuum coupling, we could consider implementing the method for more complicated defects such as dislocations where an extra line of atoms is present in the lattice. In fact, the present analysis extends almost verbatim to this case, except that the reference configuration cannot simply be taken to be the undeformed lattice, and the sharp decay estimates include a logarithmic factor [23]. Multiple defects in which there are multiple objective functionals is also a physically important application which needs further investigation as does the possibility of adaptivity. By adaptivity, we mean the ability of the algorithm to both refine the mesh in the continuum region and increase the size of the atomistic region when more accuracy is needed or to coarsen the mesh and decrease the size of the continuum region when

more efficiency is needed. Thus far, adaptivity has only been analyzed in one dimension for the original quasicontinuum method in [1, 2, 57]. The effects of adaptivity on the current method are particularly interesting since changing the atomistic and continuum region could change the overlap region and hence the optimization difference functional.

7.1 Discussion of Alternative Numerical Implementations

Perhaps the greatest drawback of the optimization-based AtC is the current lack of an efficient numerical implementation in two and three dimensions. The Lagrange multiplier approach is suitable for "single use" applications but not robust enough for wide usage. In particular, the need to compute third derivatives of the energy in order to compute the Hessian of the Lagrangian from Section 6.2 is a time-consuming process. Hard-coding the Hessian is what is currently implemented. Alternative approaches would be to use automatic differentiation tools or use Hessian-free methods.

Another alternative would be to use an iterative, descent-type method to solve the unconstrained minimization problem prior to introducing Lagrange multipliers. However, this would require computing a full gradient of the mappings $\boldsymbol{U}^{\mathrm{a}}$ and $\boldsymbol{U}^{\mathrm{c}}$ and not just directional derivatives $\delta\boldsymbol{U}^{\mathrm{a}}(\cdot)[\cdot], \delta\boldsymbol{U}^{\mathrm{c}}(\cdot)[\cdot]$. Computing the full gradients would in turn involve sampling the entire space of virtual atomistic and continuum controls. If the problem were linear, then this would be very feasible since this could be done once, but the nonlinear problem requires this to be done at each iteration after the linearization point is updated. In one dimension the computational work to do this is minimal, but this quickly escalates even in two dimensions. This process was in fact carried out in the author's one dimensional work [46] for a linear problem.

We briefly discuss what would be involved in these descent-type iterations following the basic descent algorithm of [29]. For all of these methods, we define the Lagrangian via

$$\begin{aligned}
&\mathcal{G}(\boldsymbol{u}^{\mathrm{a}}, \boldsymbol{u}^{\mathrm{c}}, \lambda_{\mathrm{a}}, \lambda_{\mathrm{c}}, \boldsymbol{v}^{\mathrm{a}}, \boldsymbol{v}^{c}, \mu_{\mathrm{a}}, \mu_{\mathrm{c}}) \\
&:= \frac{1}{2}\int_{\Omega_{\mathrm{o}}} (\nabla I\boldsymbol{u}^{\mathrm{a}} - \nabla\boldsymbol{u}^{\mathrm{c}}) : (\nabla I\boldsymbol{u}^{\mathrm{a}} - \nabla\boldsymbol{u}^{\mathrm{c}}) + \langle \delta\tilde{\mathcal{E}}^{\mathrm{a}}(\boldsymbol{u}^{\mathrm{a}}), \boldsymbol{v}^{\mathrm{a}}\rangle + \langle \delta\tilde{\mathcal{E}}^{\mathrm{c}}(\boldsymbol{u}^{\mathrm{c}}), \boldsymbol{v}^{\mathrm{c}}\rangle \\
&\quad + \langle \boldsymbol{u}^{\mathrm{a}}|_{\partial_{\mathrm{a}}\Omega_{\mathrm{a}}} - \lambda_{\mathrm{a}}, \mu_{\mathrm{a}}\rangle_{\ell^2(\partial_{\mathrm{a}}\Omega_{\mathrm{a}})} + \langle \boldsymbol{u}^{\mathrm{c}}|_{\Gamma_{\mathrm{core}}} - \lambda_{\mathrm{c}}, \mu_{\mathrm{c}}\rangle_{L^2(\Gamma_{\mathrm{core}})}.
\end{aligned}$$

We also recall that the optimization objective is

$$\mathcal{J}(\boldsymbol{u}^{\mathrm{a}}, \boldsymbol{u}^{\mathrm{c}}) := \frac{1}{2}\int_{\Omega_{\mathrm{o}}} (\nabla I\boldsymbol{u}^{\mathrm{a}} - \nabla \boldsymbol{u}^{\mathrm{c}}) : (\nabla I\boldsymbol{u}^{\mathrm{a}} - \nabla \boldsymbol{u}^{\mathrm{c}})$$
$$\mathcal{J}(\boldsymbol{U}^{\mathrm{a}}(\lambda_{\mathrm{a}}), \boldsymbol{U}^{\mathrm{c}}(\lambda_{\mathrm{c}})) := \frac{1}{2}\int_{\Omega_{\mathrm{o}}} (\nabla I\boldsymbol{U}^{\mathrm{a}}(\lambda_{\mathrm{a}}) - \nabla \boldsymbol{U}^{\mathrm{c}}(\lambda_{\mathrm{c}})) : (\nabla I\boldsymbol{U}^{\mathrm{a}}(\lambda_{\mathrm{a}}) - \nabla \boldsymbol{U}^{\mathrm{c}}(\lambda_{\mathrm{c}})),$$

and the constraints are

$$F(\boldsymbol{u}^{\mathrm{a}}, \boldsymbol{u}^{\mathrm{c}}, \lambda_{\mathrm{a}}, \lambda_{\mathrm{c}}) = \begin{pmatrix} \delta\tilde{\mathcal{E}}^{\mathrm{a}}(\boldsymbol{u}^{\mathrm{a}}) \\ \delta\tilde{\mathcal{E}}^{\mathrm{c}}(\boldsymbol{u}^{\mathrm{c}}) \\ \boldsymbol{u}_{\mathrm{a}}|_{\partial_{\mathrm{a}}\Omega_{\mathrm{a}}} - \lambda_{\mathrm{a}} \\ \boldsymbol{u}_{\mathrm{c}}|_{\Gamma_{\mathrm{core}}} - \lambda_{\mathrm{c}} \end{pmatrix} = \mathbf{0}.$$

The basic descent algorithm is [29]

1. Choose an initial guess for the virtual controls $\lambda_{\mathrm{a}}, \lambda_{\mathrm{c}}$ and solve the constraint equations to obtain $\boldsymbol{u}^{a} = \boldsymbol{U}^{\mathrm{a}}(\lambda_{\mathrm{a}})$ and $\boldsymbol{u}^{\mathrm{c}} = \boldsymbol{U}^{\mathrm{c}}(\lambda_{\mathrm{c}})$.

2. Compute the Fréchet derivative of $\mathcal{J}(\boldsymbol{U}^{\mathrm{a}}(\lambda_{\mathrm{a}}), \boldsymbol{U}^{\mathrm{c}}(\lambda_{\mathrm{c}}))$ with respect to λ_{a} and λ_{c}.

3. Compute descent directions μ_{a} and μ_{c} using the Fréchet derivative in the previous step.

4. Set $\lambda_{\mathrm{a}} = \lambda_{\mathrm{a}} + \mu_{\mathrm{a}}$ and $\lambda_{\mathrm{c}} = \lambda_{\mathrm{c}} + \mu_{\mathrm{c}}$.

The key difficulty encountered in this algorithm is the second step where the Fréchet derivative of $\mathcal{J}$ with respect to the controls must be computed. By the chain rule, this is simply

$$\frac{\partial \mathcal{J}(\boldsymbol{U}^{\mathrm{a}}(\lambda_{\mathrm{a}}), \boldsymbol{U}^{\mathrm{c}}(\lambda_{\mathrm{c}}))}{\partial \lambda_{\mathrm{a}}}|_{(\nu_{\mathrm{a}},\nu_{\mathrm{c}})} = \frac{\partial \mathcal{J}}{\partial \boldsymbol{u}^{\mathrm{a}}}|_{(\nu_{\mathrm{a}},\nu_{\mathrm{c}})} \cdot \frac{\partial \boldsymbol{U}^{\mathrm{a}}}{\partial \lambda_{\mathrm{a}}}|_{\nu_{\mathrm{a}}}.$$

A similar equation is clearly obtained by differentiating with respect to λ_{c}. We will see there are two approaches to computing this quantity through either sensitivities or adjoints.

7.1.1 Sensitivities

The sensitivity method to computing the Fréchet derivative is to differentiate the constraint equation $F(\boldsymbol{u}^{\mathrm{a}}, \boldsymbol{u}^{\mathrm{c}}, \lambda_{\mathrm{a}}, \lambda_{\mathrm{c}}) = \mathbf{0}$ with respect to λ_{a} and λ_{c}. Note that λ_{a} and λ_{c}

belong to finite dimensional spaces, and thus we will differentiate with respect to $\lambda_{\mathrm{a}}(\xi)$ where $\xi \in \partial_{\mathrm{a}}\Omega_{\mathrm{a}}$. Thus, we choose μ_{a} such $\mu_{\mathrm{a}}(\xi) = 1$ for exactly one $\xi \in \partial_{\mathrm{a}}\Omega_{\mathrm{a}}$ and $\mu_{\mathrm{a}}(\zeta) = 0$ for all $\zeta \neq \xi$ in $\partial_{\mathrm{a}}\Omega_{\mathrm{a}}$. Differentiating the constraint equation by using the chain rule on $\boldsymbol{u}^{\mathrm{a}} = \boldsymbol{U}^{\mathrm{a}}(\lambda_{\mathrm{a}})$ yields

$$\begin{pmatrix} \delta^2\tilde{\mathcal{E}}^{\mathrm{a}}(\boldsymbol{U}^{\mathrm{a}}(\lambda_{\mathrm{a}}))\delta\boldsymbol{U}^{\mathrm{a}}(\lambda_{\mathrm{a}})[\mu_{\mathrm{a}}] \\ 0 \\ (\delta\boldsymbol{U}^{\mathrm{a}}(\lambda_{\mathrm{a}})[\mu_{\mathrm{a}}])\,|_{\partial_{\mathrm{a}}\Omega_{\mathrm{a}}} - \mu_{\mathrm{a}} \\ 0 \end{pmatrix} = \boldsymbol{0}.$$

This is equivalent to solving the linear variational problem

$$\begin{aligned} \langle \delta^2\tilde{\mathcal{E}}^{\mathrm{a}}(\boldsymbol{U}^{\mathrm{a}}(\lambda_{\mathrm{a}}))\delta\boldsymbol{U}^{\mathrm{a}}(\lambda_{\mathrm{a}})[\mu_{\mathrm{a}}], \boldsymbol{w}^{\mathrm{a}}\rangle &= 0, \quad \forall \boldsymbol{w}^{\mathrm{a}} \in \boldsymbol{\mathcal{U}}_0^{\mathrm{a}} \\ \delta\boldsymbol{U}^{\mathrm{a}}(\lambda_{\mathrm{a}})[\mu_{\mathrm{a}}] &= \mu_{\mathrm{a}} \quad \text{on } \partial_{\mathrm{a}}\Omega_{\mathrm{a}}. \end{aligned}$$

Consequently, we see at each iteration that we must solve a number of linear equations which is equal to the number of atoms in $\partial_{\mathrm{a}}\Omega_{\mathrm{a}}$. In one dimension, this is tractable since the number of boundary points will be typically less than ten. However, in two dimensions and three dimensions, this quickly becomes intractable. It should be noted that if we were considering a problem with linear constraints, then these equations could be solved once, and there would be no need to solve them at each iteration. This approach was taken in the author's work [46].

7.1.2 Adjoints

The adjoint method relies upon solving the adjoint equation in order to compute the Fréchet derivative. The adjoint equation is obtained by taking the variation of the Lagrangian, $\mathcal{G}$, with respect to the states, $\boldsymbol{u}^{\mathrm{a}}$ and $\boldsymbol{u}^{\mathrm{c}}$, and setting the results equal to zero. Carrying this out (for $\boldsymbol{u}^{\mathrm{a}}$ in the direction $\boldsymbol{w}^{\mathrm{a}}$) yields the adjoint equation

$$\int_{\Omega_{\mathrm{o}}} \nabla I\boldsymbol{w}^{\mathrm{a}} \cdot (\nabla I\boldsymbol{u}^{\mathrm{a}} - \nabla\boldsymbol{u}^{\mathrm{c}}) + \langle \delta^2\tilde{\mathcal{E}}^{\mathrm{a}}(\boldsymbol{u}^{\mathrm{a}})\boldsymbol{w}^{\mathrm{a}}, \boldsymbol{v}^{\mathrm{a}}\rangle + \langle \boldsymbol{w}^{\mathrm{a}}|_{\partial_{\mathrm{a}}\Omega_{\mathrm{a}}}, \mu_{\mathrm{a}}\rangle_{\ell^2(\partial_{\mathrm{a}}\Omega_{\mathrm{a}})} = 0,$$

which can be written as finding $\boldsymbol{v}^{\mathrm{a}}$ such that

$$\begin{aligned} \langle \delta^2\tilde{\mathcal{E}}^{\mathrm{a}}(\boldsymbol{u}^{\mathrm{a}})\boldsymbol{w}^{\mathrm{a}}, \boldsymbol{v}^{\mathrm{a}}\rangle &= -\int_{\Omega_{\mathrm{o}}} \nabla I\boldsymbol{w}^{\mathrm{a}} \cdot (\nabla I\boldsymbol{u}^{\mathrm{a}} - \nabla\boldsymbol{u}^{\mathrm{c}}), \quad \forall \boldsymbol{w}^{\mathrm{a}} \in \boldsymbol{\mathcal{U}}_0^{\mathrm{a}} \\ \boldsymbol{v}^{\mathrm{a}} &= 0 \quad \text{on } \partial_{\mathrm{a}}\Omega_{\mathrm{a}}. \end{aligned}$$

If this problem can be solved efficiently, then we have the basis for a descent algorithm. This approach seems to have more promise than the previous approach since it involves solving only a single linearized equation at each iteration step.

Finding an efficient numerical implementation will be a particular focus going forward.

7.2 Multilattices

A different focus will be the extension of the optimization-based method to multilattices and in particular to two dimensional materials such as graphene. (Recall a multilattice is a material in which more than atom is present at each lattice site.) However, my current focus is on the extension of the force-based blending quasicontinuum (BQCF) method to multilattices and the bond-based energy of Shapeev [65]. A very similar process to the norm equivalence proof used in this thesis and the stability proof of [37] is required to also prove stability of the BQCF method, and this proof is very nearly complete. The bond-based energy of Shapeev [65] is unfortunately restricted to pair and bond angle potentials, but this does allow for a simple model of graphene to be included.

References

[1] M. Arndt and M. Luskin. Goal-oriented atomistic-continuum adaptivity for the quasicontinuum approximation. *International Journal for Multiscale Computational Engineering*, 5(5), 2007.

[2] M. Arndt and M. Luskin. Error estimation and atomistic-continuum adaptivity for the quasicontinuum approximation of a frenkel-kontorova model. *Multiscale Modeling & Simulation*, 7(1):147–170, 2008.

[3] S. Badia, P. Bochev, M. Gunzburger, R. Lehoucq, and M. Parks. Blending methods for coupling atomistic and continuum models. In J. Fish, editor, *Bridging the scales in science and engineering*, pages 165–186. Oxford University Press, 2009.

[4] S. Badia, M. Parks, P. Bochev, M. Gunzburger, and R. Lehoucq. On atomistic-to-continuum coupling by blending. *Multiscale Modeling & Simulation*, 7(1):381–406, 2008.

[5] P. Bauman, H. Ben Dhia, N. Elkhodja, J. Oden, and S. Prudhomme. On the application of the Arlequin method to the coupling of particle and continuum models. *Computational Mechanics*, 42:511–530, 2008.

[6] X. Blanc, C. Le Bris, and P.L. Lions. From molecular models to continuum mechanics. *Archive for Rational Mechanics and Analysis*, 164(4):341–381, 2002.

[7] X. Blanc, C. Le Bris, and P.L. Lions. Atomistic to continuum limits for computational materials science. *ESAIM: Mathematical Modelling and Numerical Analysis*, 41(2):391–426, 6 2007.

[8] M. Born and K. Huang. *Dynamical Theory of Crystal Lattices*. Clarendon Press, first edition, 1954.

[9] S. Brenner and R. Scott. *The mathematical theory of finite element methods*, volume 15. Springer, 2008.

[10] V.I. Burenkov. On extension of functions with preservation of seminorm. *Trudy Mat. Inst. Steklov.*, 172:71–85, 1985.

[11] A.L. Cauchy. De la pression ou la tension dans un systeme de points materiels. In *Exercices de Mathematiques*. 1828.

[12] H. Chen and C. Ortner. QM/MM methods for crystalline defects. Part 1: Locality of the tight binding model. *ArXiv e-prints*, 1505.05541, 2015.

[13] H. Cho, X. Yang, D Venturi, and G. Karniadakis. Algorithms for propagating uncertainty across heterogeneous domains. *preprint*, 2015.

[14] M. Daw and M. Baskes. Embedded-atom method: Derivation and application to impurities, surfaces, and other defects in metals. *Physical Review B*, 29(12):6443, 1984.

[15] M. D'Elia and P. Bochev. Optimization-based coupling of nonlocal and local diffusion models. In *2014 MRS Fall Meeting Proceedings*, 2015.

[16] J. Dieudonne. *Foundations of modern analysis*. New York: Academic Press, 1960.

[17] M. Discacciati, P. Gervasio, and A. Quarteroni. The interface control domain decomposition (icdd) method for elliptic problems. *SIAM Journal on Control and Optimization*, 51(5):3434–3458, 2013.

[18] M. Discacciati, P. Gervasio, and A. Quarteroni. Interface control domain decomposition methods for heterogeneous problems. *International Journal for Numerical Methods in Fluids*, 76(8):471–496, 2014.

[19] M. Dobson and M. Luskin. Analysis of a force-based quasicontinuum approximation. *ESAIM: Mathematical Modelling and Numerical Analysis*, 42:113–139, 0 2008.

[20] M. Dobson, M. Luskin, and C. Ortner. Sharp stability estimates for the force-based quasicontinuum approximation of homogeneous tensile deformation. *Multiscale Modeling & Simulation*, 8(3):782–802, 2010.

[21] M. Dobson, M. Luskin, and C. Ortner. Stability, instability, and error of the force-based quasicontinuum approximation. *Archive for Rational Mechanics and Analysis*, 197(1):179–202, 2010.

[22] W. E, J. Lu, and J.Z. Yang. Uniform accuracy of the quasicontinuum method. *Phys. Rev. B*, 74:214115, 2006.

[23] V. Ehrlacher, C. Ortner, and A.V. Shapeev. Analysis of Boundary Conditions for Crystal Defect Atomistic Simulations. *ArXiv e-prints*, June 2013. 1306.5334.

[24] J. Ericksen. On the cauchy-born rule. *Mathematics and Mechanics of solids*, 13(3-4):199–220, 2008.

[25] L.C. Evans. *Partial Differential Equations*. Graduate studies in mathematics. American Mathematical Society, second edition, 2010.

[26] P. Gervasio, J.L. Lions, and A. Quarteroni. Heterogeneous coupling by virtual control methods. *Numerische Mathematik*, 90(2):241–264, 2001.

[27] M. Giaquinta. *Multiple integrals in the calculus of variations and nonlinear elliptic systems*. Princeton University Press, 1983.

[28] R. Glowinski, Quang V. Dinh, and J. Periaux. Domain decomposition methods for nonlinear problems in fluid dynamics. *Computer methods in applied mechanics and engineering*, 40(1):27–109, 1983.

[29] M. D. Gunzburger. *Perspectives in Flow Control and Optimization*. Society for Industrial and Applied Mathematics, 2002.

[30] J. Hubbard and B. Hubbard. *Vector calculus, linear algebra, and differential forms : a unified approach*. Matrix Editions, fourth edition, 2009.

[31] T. Hudson and C. Ortner. On the stability of Bravais lattices and their Cauchy–Born approximations. *M2AN Math. Model. Numer. Anal.*, 46:81–110, 2012.

[32] T. Hudson and C. Ortner. Existence and stability of a screw dislocation under anti-plane deformation. *Arch. Ration. Mech. Anal.*, 213(3):887–929, 2014.

[33] B. Van Koten and M. Luskin. Analysis of energy-based blended quasi-continuum approximations. *SIAM J. Numer. Anal.*, 49(5):2182–2209, 2011.

[34] B. Van Koten and C. Ortner. Symmetries of 2-lattices and second order accuracy of the cauchy–born model. *SIAM Multiscale Modelling and Simulation*, 11:615–634, 2013.

[35] X. Li, M. Luskin, and C. Ortner. Positive definiteness of the blended force-based quasicontinuum method. *Multiscale Modeling & Simulation*, 10(3):1023–1045, 2012.

[36] X. Li, M. Luskin, C. Ortner, and A.V. Shapeev. Theory-based benchmarking of the blended force-based quasicontinuum method. *Computer Methods in Applied Mechanics and Engineering*, 268:763–781, 2014.

[37] X. Li, C. Ortner, A.V. Shapeev, and B. Van Koten. Analysis of Blended Atomistic/Continuum Hybrid Methods. *ArXiv e-prints*, April 2014. 1404.4878.

[38] Xingjie Helen Li and Mitchell Luskin. A generalized quasinonlocal atomistic-to-continuum coupling method with finite-range interaction. *IMA Journal of Numerical Analysis*, page drq049, 2011.

[39] J.L. Lions. Virtual and effective control for distributed systems and decomposition of everything. *Journal d'Analyse Mathématique*, 80:257–297, 2000.

[40] J.L. Lions and O. Pironneau. Algorithmes paralleles pour la solution de problemes aux limites. *Comptes Rendus de l'Académie des Sciences-Series I-Mathematics*, 327(11):947–952, 1998.

[41] J.L. Lions and O. Pironneau. Virtual control, replicas and decomposition of operators. *C. R. Acad. Sci. Paris*, 330(1):47–54, 2000.

[42] M. Luskin and C. Ortner. Atomistic-to-continuum coupling. *Acta Numerica*, 22:397–508, 4 2013.

[43] C. Makridakis, D. Mitsoudis, and P. Rosakis. On atomistic-to-continuum couplings without ghost forces in three dimensions. *Applied Mathematics Research eXpress*, 2014(1):87–113, 2014.

[44] J. Marsden. *Elementary classical analysis*. Freeman and Company, 1974.

[45] R. Miller and E. Tadmor. A unified framework and performance benchmark of fourteen multiscale atomistic/continuum coupling methods. *Modeling and Simulation in Materials Science and Engineering*, 17(5):053001, 2009.

[46] D. Olson, P. Bochev, M. Luskin, and A. Shapeev. An Optimization-Based Atomistic-to-Continuum Coupling Method. *SIAM J. Numer. Anal.*, 52(4):2183–2204, 2014.

[47] D. Olson, P. Bochev, M. Luskin, and A. Shapeev. Development of an optimization-based atomistic-to-continuum coupling method. In I. Lirkov, S. Margenov, and J. Waniewski, editors, *Large-Scale Scientific Computing*, volume 8353 of *Lecture Notes in Computer Science*, pages 33–44. Springer Berlin Heidelberg, 2014.

[48] D. Olson, A. Shapeev, P. Bochev, and M. Luskin. Analysis of an optimization-based atomistic-to-continuum coupling method for point defects. *ESAIM: M2AN*, 2015. To Appear.

[49] M. Ortiz, R. Phillips, and E. Tadmor. Quasicontinuum analysis of defects in solids. *Philosophical Magazine A*, 73(6):1529–1563, 1996.

[50] C. Ortner. A posteriori existence in numerical computations. *SIAM J. Numer. Anal.*, 47(4):2550–2577, 2009.

[51] C. Ortner. The role of the patch test in 2d atomistic-to-continuum coupling methods. *ESAIM Math. Model. Numer. Anal.*, 46, 2012.

[52] C. Ortner and A Shapeev. Analysis of an energy-based atomistic/continuum approximation of a vacancy in the 2d triangular lattice. *Mathematics of Computation*, 82(284):2191–2236, 2013.

[53] C. Ortner and A.V. Shapeev. Interpolants of Lattice Functions for the Analysis of Atomistic/Continuum Multiscale Methods. *ArXiv e-prints*, April 2012. 1204.3705.

[54] C. Ortner, A.V. Shapeev, and L. Zhang. (In-)stability and stabilisation of QNL-type atomistic-to-continuum coupling methods. arXiv:1308.3894, 2013.

[55] C. Ortner and E. Süli. A note on linear elliptic systems on $\mathbb{R}^d$. *ArXiv e-prints*, 2012. 1202.3970.

[56] C. Ortner and F. Theil. Justification of the Cauchy–Born approximation of elastodynamics. *Arch. Ration. Mech. Anal.*, 207:1025–1073, 2013.

[57] C. Ortner and H. Wang. A posteriori error control for a quasi-continuum approximation of a periodic chain. *IMA Journal of Numerical Analysis*, 34(3):977–1001, 2014.

[58] C. Ortner and L. Zhang. Construction and sharp consistency estimates for atomistic/continuum coupling methods with general interfaces: a 2D model problem. *SIAM J. Numer. Anal.*, 50, 2012.

[59] C. Ortner and L. Zhang. Construction and sharp consistency estimates for atomistic/continuum coupling methods with general interfaces: A two-dimensional model problem. *SIAM Journal on Numerical Analysis*, 50(6):2940–2965, 2012.

[60] C. Ortner and L. Zhang. Atomistic/continuum blending with ghost force correction. *ArXiv e-prints*, 1407.0053, 2014.

[61] C. Ortner and L. Zhang. Energy-based atomisitic-to-continuum coupling without ghost forces. *Comput. Meth. Appl. Mech. Engrg.*, 279:29–45, 2014.

[62] M. Parks, P. Bochev, and R. Lehoucq. Connecting atomistic-to-continuum coupling and domain decomposition. *SIAM J. Multiscale Model. Simul.*, 7(1):362–380, 2008.

[63] R. Phillips. *Crystals, defects and microstructures: modeling across scales*. Cambridge University Press, 2001.

[64] R. Scott and S. Zhang. Finite element interpolation of nonsmooth functions satisfying boundary conditions. *Mathematics of Computation*, 54(190):483–493, 1990.

[65] A. Shapeev, D. Olson, and M. Luskin. *Unpublished Manuscript*, 2015.

[66] A. V. Shapeev. Consistent energy-based atomistic/continuum coupling for two-body potentials in three dimensions. *SIAM J. Sci. Comput.*, 34(3):B335–B360, 2012.

[67] A.V. Shapeev. Consistent energy-based atomistic/continuum coupling for two-body potentials in one and two dimensions. *SIAM J. Multiscale Model. Simul.*, 9:905–932, 2011.

[68] V. B. Shenoy, R. Miller, E. B. Tadmor, D. Rodney, R. Phillips, and M. Ortiz. An adaptive finite element approach to atomic-scale mechanics–the quasicontinuum method. *J. Mech. Phys. Solids*, 47(3):611–642, 1999.

[69] L. Shilkrot, R. Miller, and W. Curtin. Coupled atomistic and discrete dislocation plasticity. *Physical Review Letters*, 89(2):025501, 2002.

[70] T. Shimokawa, J.J. Mortensen, J. Schiotz, and K.W. Jacobsen. Matching conditions in the quasicontinuum method: Removal of the error introduced at the interface between the coarse-grained and fully atomistic region. *Phys. Rev. B*, 69:214104, Jun 2004.

[71] E. Stein. *Singular integrals and differentiability properties of functions*, volume 2. Princeton University Press, 1970.

[72] E. Tadmor, G. Smith, N. Bernstein, and E. Kaxiras. Mixed finite element and atomistic formulation for complex crystals. *Physical Review B*, 59(1):235, 1999.

[73] B. Van Koten. *Development and Analysis of the Blended Energy-Based Quasicontinuum Method.* PhD thesis, University of Minnesota, 2012.

[74] E W. and P. Ming. Cauchy–born rule and the stability of crystalline solids: static problems. *Archive for Rational Mechanics and Analysis*, 183(2):241–297, 2007.

[75] D. Wallace. *Thermodynamics of Crystals.* Dover, 1998.

[76] S.P. Xiao and T. Belytschko. A bridging domain method for coupling continua with molecular dynamics. *Computer methods in applied mechanics and engineering*, 193(17):1645–1669, 2004.

Appendix A

Collected Theorems

A.1 Extension Theorems

In this appendix, we recall Stein's extension theorem [71] for domains with minimally smooth boundary and a modified extension operator that preserves the H^1 seminorm due to Burenkov [10].

Theorem A.1.1 (Stein's Extension Theorem)**.** *Let U be a connected, open set for which there exists $\epsilon > 0$, integers $N, M > 0$, and a sequence of open sets $U_1, U_2, \ldots$ satisfying*

1. *For each $x \in \partial U$, $B_\epsilon(x) \subset U_i$ for some i,*
2. *The intersection of more than N of the sets U_i is empty,*
3. *For each U_i, there exists a Lipschitz continuous function φ_i and domains*

$$D_i = \left\{(x', y) \in \mathbb{R}^{n+1} : y > \varphi_i(x'), \left|\varphi_i(x'_1) - \varphi_i(x'_2)\right| \leq M \left|x'_1 - x'_2\right|\right\}$$

such that

$$U_i \cap U = U_i \cap D_i.$$

Then there exists a bounded linear extension operator $E : H^1(U) \to H^1(\mathbb{R}^d)$. The bound of the extension depends upon the domain U through N, M, and ϵ.

Theorem A.1.1 can be used to prove an extension theorem with preservation of seminorm due to Burenkov [10]:

Theorem A.1.2 (Extension with preservation of seminorm)**.** *Let U be a connected, bounded open set for which there exists a bounded linear extension operator $E : H^1(U) \to H^1(\mathbb{R}^n)$ and a bounded projection operator P from $H^1(U)$ onto the constants with the property that for all $f \in H^1(U)$,*

$$\|f - Pf\|_{L^2(U)} \lesssim c(U)\|f\|_{H^1(U)}.$$

Then the operator defined by

$$R = P + E(\mathrm{id} - P)$$

is a linear extension operator with the property that

$$\|\nabla Rf\|_{L^2(U)} \leq \|E\| \left(c(U) + 1\right) \|\nabla f\|_{L^2(U)}.$$

Remark A.1.3. *We can set E to be Stein's extension operator and choose*

$$Pu = \frac{1}{|U|} \int_U u(x)\, dx.$$

In this case, $c(U)$ is the Poincare constant for the domain U.

A.2 Implicit Function Theorem

This section of the appendix is devoted to exhibiting the bounds asserted in the statements of the implicit function theorem. This will be done by tracking the constants in the proof of the implicit function theorem by using the inverse function theorem. Thus we begin with the inverse function theorem and a bound on the derivatives of the inverse function. We closely follow [30].

Theorem A.2.1 (Inverse Function Theorem)**.** *Let X and Y be Banach spaces with $f : X \to Y$ a continuously differentiable function on an open set U containing x_0. Let $y_0 = f(x_0)$ with $\|y_0\|_Y < \eta$. Furthermore, suppose that $\delta f(x_0)$ is invertible and such that $\|\delta f(x_0)^{-1}\|_{\mathcal{L}(Y,X)} < \sigma$, $B_{2\eta\sigma}(x_0) \subset U$, δf is Lipschitz continuous on $B_{2\eta\sigma}(x_0)$ with Lipschitz constant L, and $2L\eta\sigma^2 < 1$. Then there exists a unique continuously differentiable function $g : B_\eta(y_0) \to B_{2\eta\sigma}(x_0)$ such that*

$$g(y_0) = x_0 \quad \textit{and} \quad f(g(y)) = y \quad \forall y \in B_\eta(y_0)\,.$$

In particular, there exists $\bar{x} = g(0) \in X$ *such that* $f(\bar{x}) = 0$ *and*

$$\|g(y_0) - g(0)\|_X = \|x_0 - \bar{x}\|_X < 2\eta\sigma.$$

The derivative of g *is given by*

$$\delta g(y) = [\delta f(g(y))]^{-1}.$$

Lemma A.2.2 (Bounds on the inverse function)**.** *With the same hypotheses as in the inverse function theorem, for all* $x \in B_{2\eta\sigma}(x_0)$

$$\|\delta f(x)^{-1}\|_{\mathcal{L}(Y,X)} \leq 2\|\delta f(x_0)^{-1}\|_{\mathcal{L}(Y,X)}.$$

In particular, using the formula for the derivative of the inverse function

$$\|\delta g(y)\|_{\mathcal{L}(Y,X)} = [\delta f(g(y))]^{-1} \leq 2\|\delta f(x_0)^{-1}\|_{\mathcal{L}(Y,X)}.$$

Proof. Let $x \in B_{2\eta\sigma}(x_0)$ with I the identity operator on X and define

$$\begin{aligned} A :=& \ I - \delta f(x_0)^{-1} \circ \delta f(x) \\ =& \ \delta f(x_0)^{-1} \circ \delta f(x_0) - \delta f(x_0)^{-1} \circ \delta f(x) \\ =& \ \delta f(x_0)^{-1} \circ [\delta f(x_0) - \delta f(x)]. \end{aligned}$$

Thus

$$\begin{aligned} \|A\|_{\mathcal{L}(X,X)} \leq& \ \|\delta f(x_0)^{-1}\|_{\mathcal{L}(Y,X)} \cdot \|\delta f(x_0) - \delta f(x)\|_{\mathcal{L}(X,Y)} \\ \leq& \ L\|\delta f(x_0)^{-1}\|_{\mathcal{L}(Y,X)} \cdot \|x_0 - x\|_X \quad \text{by Lipschitz continuity of } \delta f \\ <& \ 2\eta\sigma L\|\delta f(x_0)^{-1}\|_{\mathcal{L}(Y,X)} \quad \text{since } x \in B_{2\eta\sigma}(x_0) \\ <& \ 2\eta\sigma^2 L \quad \text{since } \|\delta f(x_0)^{-1}\|_{\mathcal{L}(Y,X)} < \sigma \\ <& \ \frac{1}{2} \quad \text{by the hypothesis of the inverse function theorem.} \end{aligned}$$

It follows that $I - A$ is invertible with inverse given by

$$\sum_{n=0}^{\infty} A^n.$$

But note that $I - A = \delta f(x_0)^{-1} \circ \delta f(x)$ so that $\delta f(x_0)^{-1} \circ \delta f(x)$ is invertible. But $\delta f(x_0)^{-1}$ is invertible so this implies $\delta f(x)$ is invertible. Moreover,

$$\begin{aligned}[I - A]^{-1} = & \left[\delta f(x_0)^{-1}\delta f(x)\right]^{-1} \\ = & \ \delta f(x)^{-1}\delta f(x_0),\end{aligned}$$

which implies

$$\begin{aligned}\delta f(x)^{-1} = & \ [I - A]^{-1}\, \delta f(x_0)^{-1} \\ = & \left[\sum_{n=0}^{\infty} A^n\right] \delta f(x_0)^{-1}.\end{aligned}$$

Consequently,

$$\begin{aligned}\|\delta f(x)^{-1}\|_{\mathcal{L}(Y,X)} \leq & \ \|\sum_{n=0}^{\infty} A^n\|_{\mathcal{L}(X,X)} \cdot \|\delta f(x_0)^{-1}\|_{\mathcal{L}(Y,X)} \\ \leq & \ \sum_{n=0}^{\infty} \frac{1}{2^n} \cdot \|\delta f(x_0)^{-1}\|_{\mathcal{L}(Y,X)} \\ = & \ 2\|\delta f(x_0)^{-1}\|_{\mathcal{L}(Y,X)}.\end{aligned}$$

□

Theorem A.2.3 (Implicit Function Theorem)**.** *Let X, Y, and Z be Banach spaces with $U \subset X \times Y$ an open set. Let $f : X \times Y \to Z$ be continuously differentiable with $(x_0, y_0) \in U$ satisfying $f(x_0, y_0) = 0$. Suppose that $\delta_y f(x_0, y_0) : Y \to Z$ is a bounded, invertible linear transformation with $\left\|(\delta_y f(x_0, y_0))^{-1}\right\| =: \theta$. Also set $\phi := \|\delta_x f(x_0, y_0)\|$ and*

$$\sigma := \max\left\{1 + \theta\phi, \theta\right\}.$$

If there exists η such that

1. *$B_{2\eta\sigma}((x_0, y_0)) \subset U$,*
2. *$\|\delta f(x_1, y_1) - \delta f(x_2, y_2)\| \leq \frac{1}{2\eta\sigma^2}\|(x_1, y_1) - (x_2, y_2)\|$ for all $(x_1, y_1), (x_2, y_2) \in B_{2\eta\sigma}((x_0, y_0))$,*

then there is a unique continuously differentiable function $g : B_\eta(x_0) \to B_{2\eta\sigma}(y_0)$ *such that* $g(x_0) = y_0$ *and* $f(x, g(x)) = 0$ *for all* $x \in B_\eta(x_0)$*. The derivative of* g *is*

$$\delta g(x) = -\left[\delta_y f(x, g(x))^{-1}\right]\left[\delta_x f(x, g(x))\right].$$

Moreover, if f *is* C^k*, then* g *is* C^k*.*

We include a standard proof for the implicit function theorem, see e.g. [30], so that we may use the explicitly derived formula for the implicit function to obtain non-standard bounds on the implicit function in Lemma A.2.4 which are included as part of the statement of the implicit function theorem needed in Theorem 5.3.1.

Proof. Define the function $F : X \times Y \to X \times Z$ by

$$F(x, y) = (x, f(x, y))$$

so that

$$\delta F(x, y) = \begin{pmatrix} I_X & 0 \\ \delta_x f(x, y) & \delta_y f(x, y) \end{pmatrix},$$

and

$$\delta F(x, y)^{-1} = \begin{pmatrix} I_X & 0 \\ -\delta_y f(x, y)^{-1} \circ \delta_x f(x, y) & \delta_y f(x, y)^{-1} \end{pmatrix}.$$

Observe

$$\delta F(x_0, y_0)^{-1} \begin{pmatrix} u \\ v \end{pmatrix} = \begin{pmatrix} u \\ -\delta_y f(x_0, y_0)^{-1} \circ \delta_x f(x_0, y_0)u + \delta_y f(x_0, y_0)^{-1} v \end{pmatrix} \in X \times Y$$

implying

$$\begin{aligned} &\|\delta F(x, y)^{-1}(u, v)^\top\|_{X\times Z} \\ &= \|u\|_X + \| - \delta_y f(x_0, y_0)^{-1} \circ \delta_x f(x_0, y_0)u + \delta_y f(x_0, y_0)^{-1} v\|_Z \\ &\leq (1 + \|\delta_y f(x_0, y_0)^{-1}\|_{\mathcal{L}(Z,Y)} \cdot \|\delta_x f(x_0, y_0)\|_{\mathcal{L}(X,Z)})\|u\|_X + \|\delta_y f(x_0, y_0)^{-1}\|_{\mathcal{L}(Z,Y)}\|v\|_Z \\ &\leq \max\{1 + \theta\phi, \theta\}\,(\|u\|_X + \|v\|_Z) \\ &= \sigma\|(u, v)\|_{X\times Z}. \end{aligned} \tag{A.2.1}$$

Next note

$$\begin{aligned}
&\|\delta F(x_1,y_1)-\delta F(x_2,y_2)\|_{\mathcal{L}(X\times Y,X\times Z)}\\
&= \left\| \begin{pmatrix} I_X & 0 \\ \delta_x f(x_1,y_1) & \delta_y f(x_1,y_1)\end{pmatrix} - \begin{pmatrix} I_X & 0 \\ \delta_x f(x_2,y_2) & \delta_y f(x_2,y_2)\end{pmatrix} \right\|_{\mathcal{L}(X\times Y,X\times Z)}\\
&= \left\| \begin{pmatrix} 0 & 0 \\ \delta_x f(x_1,y_1)-\delta_x f(x_2,y_2) & \delta_y f(x_1,y_1)-\delta_y f(x_2,y_2)\end{pmatrix} \right\|_{\mathcal{L}(X\times Y,X\times Z)}\\
&\leq \frac{1}{2\eta\sigma^2}\|(x_1,y_1)-(x_1,y_1)\|_{X\times Y} \quad \forall\,(x_1,y_1),(x_2,y_2)\in B_{2\eta\sigma}((x_0,y_0))
\end{aligned}$$

by the second hypothesis in the statement of the implicit function theorem. The inverse function theorem then guarantees a unique continuously differentiable inverse function $G : B_\eta(x_0,0) \to B_{2\eta\sigma}((x_0,y_0))$. Define $g : B_\eta(x_0) \to B_{2\eta\sigma(y_0)}$ by

$$g(x) := \pi_Y(G(x,0)), \quad \text{where } \pi_Y \text{ is the projection operator onto } Y.$$

By the definition of an inverse function, we then have

$$(x,z) = (F\circ G)(x,z) = \big(\pi_X(G(x,z)), f(\pi_X(G(x,z)),\pi_Y(G(x,z)))\big),$$

and taking $z = 0$ produces

$$\begin{aligned}
(x,0) &= \big(\pi_X(G(x,0)), f(\pi_X(G(x,0)),\pi_Y(G(x,0)))\big)\\
&= \big(\pi_X(G(x,0)), f(\pi_X(G(x,0)), g(x))\big).
\end{aligned}$$

Therefore $x = \pi_X(G(x,0))$ only if $0 = f(x,g(x))$ for all $x \in\in B_\eta(x_0)$. The formula for the derivative is standard to derive and the regularity statements follow immediately from that. Finally, one can show that g has all desired properties of the theorem. □

Lemma A.2.4 (Bounds on implicit function)**.** *With the same hypotheses as in the statement of the implicit function theorem, for all* $x \in B_\eta(x_0)$

$$\|\delta g(x)\| \leq 2\max\left\{1+\|\delta_y f(x_0,y_0)^{-1}\|\|\delta_x f(x_0,y_0)\|, \|\delta_y f(x_0,y_0)^{-1}\|\right\}$$

Higher order derivatives of g *can also be bounded in terms of derivatives of* f *and* $\delta_y f(x,g(x))^{-1}$

Proof. From the preceding proof and the chain rule,

$$\begin{aligned}\delta g(x) &= \delta\pi_Y(G(x,0)) \circ \delta G(x,0) \\ &= \pi_Y \circ \delta G(x,0) \quad \text{since } \pi_Y \text{ is a linear operator.}\end{aligned}$$

Hence

$$\begin{aligned}\|\delta g(x)\| &\leq \|\pi_Y\|\|\delta G(x,0)\| \\ &\leq \|\delta G(x,0)\| \\ &\leq 2\|\delta F(x_0,y_0)^{-1}\| \quad \text{by Lemma A.2.2} \\ &\leq 2\sigma \quad \text{by (A.2.1)} \\ &= 2\max\left\{1 + \|\delta_y f(x_0,y_0)^{-1}\|\|\delta_x f(x_0,y_0)\|, \|\delta_y f(x_0,y_0)^{-1}\|\right\}\end{aligned}$$

The statement that higher order derivatives can be bounded in terms of derivatives of f and $\delta_y f(x,g(x))^{-1}$ follows from the formula for g, G and the fact that the mapping from $H : \mathcal{L}(X,Y) \to \mathcal{L}(Y,X)$ given by $L \mapsto L^{-1}$ is smooth and has derivative given by $\delta H(A)[B] = -A^{-1}BA^{-1}$ where $A \in \mathcal{L}(X,Y)$ and $B \in \mathcal{L}(X,Y)$ [16, 44]. □

Appendix B

List of Notation

- d — the dimension of the lattice under consideration, $d = 1, 2, 3$.
- $\mathcal{L}$ — the lattice $\mathsf{F}\mathbb{Z}^d$.
- ξ — an element of $\mathcal{L}$.
- V_ξ — the atomistic site potential.
- $\mathcal{R}$ — the interaction range.
- $\mathcal{R}^k = \overbrace{\mathcal{R} \times \cdots \times \mathcal{R}}^{k \text{ times}}$.
- ρ, τ — a generic vector in the interaction range.
- $\boldsymbol{\rho} = (\rho_1, \ldots, \rho_k) \in \mathcal{R}^k$
- $V_{\xi,\boldsymbol{\rho}}$ — derivative of V_ξ with respect to $\boldsymbol{\rho}$: $V_{\xi,\boldsymbol{\rho}}((g_\rho)_{\rho\in\mathcal{R}}) = \frac{\partial^k V_\xi}{\partial g_{\rho_1} \partial g_{\rho_2} \cdots \partial g_{\rho_k}}$.
- $|\cdot|$ — meaning depends on context: $|\cdot|$ is ℓ^2 norm of a vector, matrix, or higher order tensor, $|T|$ is area or volume of element T in a finite element partition, $|\alpha|$ is the order of a multiindex.
- $\|\cdot\|_{\ell^2(A)}$ — ℓ^2 norm over a set A. If $f : A \to \mathbb{R}^d$ is a vector-valued function, $\|f\|_{\ell^2(A)} = (\sum_{\alpha\in A} |f(\alpha)|^2)^{1/2}$.
- $B_r(\boldsymbol{y}) = \{\boldsymbol{x} \in \mathbb{R}^d : |\boldsymbol{y} - \boldsymbol{x}| \le r\}$ - Ball of radius r in $\mathbb{R}^d$

- $\bar{U}$ — closure of a domain U.
- $\mathrm{supp}(f)$ — support of a function f.
- $\mathrm{Diam}(U)$ — diameter of the set U measured with the Euclidean norm.
- $\mathrm{dist}(U, V)$ — distance between the sets U and V measured with the Euclidean norm.
- $\mathrm{conv}(x, y)$ — convex hull of x and y.
- $(\mathbb{R}^d)^{\mathcal{R}}$ — direct product of vectors with $|\mathcal{R}|$ terms.
- G — a $d \times d$ matrix.
- e_i — ith standard basis vector in $\mathbb{R}^d$.
- $^\top$ — transpose of a matrix.
- $\otimes$ — tensor product.
- ∇^j — jth Fréchet derivative of a function defined on $\mathbb{R}^d$.
- $\delta F(x)[u]$ — for a generic function F, denotes the Gateaux derivative at x in the direction u.
- ∂^α — multiindex notation for derivatives.
- $L^p(U)$ — Standard Lebesgue spaces.
- $(\cdot, \cdot)_{L^2(U)}$ — L^2 inner product over U.
- $W^{k,p}(U)$ — Standard Sobolev spaces.
- $\dot{W}^{1,2}(\mathbb{R}^d)$ — Homogeneous type Sobolev space whose elements are equivalence classes. Defined by $\left\{[f + c] \in W^{1,2}_{\mathrm{loc}}(\mathbb{R}^d) : \nabla f \in L^2(\mathbb{R}^d), c \in \mathbb{R}^d\right\}$.
- $W^{k,p}_{\mathrm{loc}}(U) = \left\{f : U \to \mathbb{R}^d | f \in W^{k,p}(V)\, \forall V \subset\subset U\right\}$.
- $H^k(U) = W^{k,2}(U)$, $H^1_0(U) = \left\{f \in H^k(U) : \mathrm{Trace}(f) = 0 \text{ on } \partial U\right\}$.
- C^k — generic space of functions that are k times differentiable.

- $\mathrm{C}^{k,1}(\bar{U}) = \big\{ f : U \to \mathbb{R}^d : \sum_{|\alpha| \leq k} \sup_{x \in \bar{U}} |\partial^\alpha f(x)| + \sum_{|\alpha|=k} \sup_{\substack{x,y \in \bar{U} \\ x \neq y}} \dfrac{|\partial^\alpha f(x) - \partial^\alpha f(y)|}{|x-y|} \big\}$.

  (Standard Lipschitz spaces).

- C_0^∞ — space of smooth functions having compact support.

- $*$ — used to denote convolution of functions.

- $\fint_U f \, dx$ — average value of f over U.

- $\mathcal{T}$ — a finite element discretization of triangles in $2D$ or tetrahedra in $3D$.

- $\mathcal{P}^1(T)$ — set of affine functions over a triangle or tetrahedron, T.

- $\mathcal{P}^1(\mathcal{T})$ — set of piecewise affine functions with respect to the discretization $\mathcal{T}$.

- h_T and $h(x)$ — finite element mesh size functions.

- I — piecewise linear interpolant onto atomistic mesh.

- I_h — piecewise linear interpolant on finite element mesh.

- $\tilde{I}$ — smooth interpolant on atomistic mesh.